Winter 1990

The Role of Small Peptides in Cancer Physiology and Chemotherapy

Bao-Ling Tsay
Old Dominion University

THE ROLE OF SMALL PEPTIDES IN CANCER PHYSIOLOGY AND CHEMOTHERAPY

BY

Bao-Ling Tsay
B.S., May 1982, National Taiwan Normal University
Taiwan, Republic of China

A Dissertation Submitted to the Faculties of
Old Dominion University
and
Eastern Virginia Medical School
in Partial Fulfillment of the
Requirements for the Degree of

Doctor of Philosophy

Biomedical Sciences

OLD DOMINION UNIVERSITY
and
EASTERN VIRGINIA MEDICAL SCHOOL
December, 1990

Approved by:

Lloyd Wolfinbarger, Jr., Ph.D. (Director)

Keith A. Carson, Ph.D.

Joseph C. Daniel, Jr., Ph.D.

George L. Wright, Jr., Ph.D.

ABSTRACT

THE ROLE OF SMALL PEPTIDES IN

CANCER PHYSIOLOGY AND CHEMOTHERAPY

Bao-Ling Tsay

Old Dominion University
and
Eastern Virginia Medical School

Director: Dr. Lloyd Wolfinbarger, Jr.

The targeting of proven anticancer drugs specifically to cancer cells would provide a unique opportunity to restrict neoplasms without damaging the cancer patient. The present research utilizes the phenomenon of illicit transport, i.e. the coupling of normally impermeant metabolites to permeant metabolites, in targeting the drug melphalan to mouse Ehrlich ascites tumor cells. The dipeptide beta-alanyl-melphalan was synthesized and tested in vitro for toxicity towards mouse Ehrlich ascites tumor cells, mouse liver cells, and mouse 3T3 embryonic cells. The parent compound, melphalan, was used as a control treatment. In addition, both melphalan and beta-alanyl-melphalan were utilized in in vivo chemotherapeutic assays to assess the efficacy of both drugs to restrict tumor cell growth in a mouse model system.

The dipeptide, beta-alanyl-melphalan, was synthesized using standard liquid synthesis procedures and assayed for purity and stability by high performance liquid chromatography. The peptide was shown to be greater than 85% pure and was significantly more stable at 37° C than melphalan, exhibiting a half-life in solution of 607.71 minutes. The half-life of melphalan under similar conditions was 105.21 minutes. The inclusion of proteins in solutions of melphalan increased the stability of this drug, providing for a half-life of 176.72 minutes. Both melphalan and beta-alanyl-melphalan were stable at 0° C.

In in vitro toxicity assays, melphalan was shown to be toxic to all three cell systems studied, whereas beta-alanyl-melphalan was toxic only towards the Ehrlich ascites tumor cells and the 3T3 fibroblast cells. The dipeptide containing melphalan was not toxic to the mouse liver cells at concentrations up to 0.1 mM. Toxicity assays included assessment of both plasma membrane permeability and cell proliferation after drug treatment. Morphological studies, using scanning and transmission electron microscopy as well as light microscopy, of treated cells corroborated the toxicity assays, revealing reduced cell numbers, aberrant cell morphologies, and cell destruction where drug treatment had been demonstrated to alter membrane integrity and/or cell proliferation was observed, i.e. beta-alanyl-melphalan treatment of mouse liver cells, cellular morphologies were demonstrated to be similar to nontreated liver cells.

In vivo chemotherapy assays, using Ehrlich ascites tumor cells injected into the abdominal cavity of mice, revealed that melphalan, at concentrations of 5 and 10 mg/kg, was an effective anticancer drug providing for T/C rations of 179 and 193 respectively. The dipeptide, beta-alanyl-melphalan, was also an effective anticancer drug, exhibiting reduced toxicity towards the tumor bearing animal when compared to the parent drug melphalan, providing for T/C rations of 152 at a drug concentration of 40 mg/kg. Neither drug had observable effects on animal activities, i.e. food and water consumption, yet significantly restricted tumor cell growth as assessed by increasing body weights and survival times of tumor bearing mice.

DEDICATION

I Would Like To Dedicate This Work To

My Parents,

Jiann-Yin and Chu-Chu Tsay,

My Mentor,

Dr. Lloyd Wolfinbarger, Jr.,

My Fiance,

Michael Adam,

Who are the most important people in my life.

ACKNOWLEDGEMENTS

I especially wish to thank Dr. Lloyd Wolfinbarger, Jr, my mentor, my fatherly advisor, and my friend, who gave me not only knowledge of scientific research, but also the valuable insight in the way of life. I owe him my greatest gratitude. I would also like to thank the other members of my dissertation committee, Dr. Keith Carson, Dr. Joseph Daniel, and Dr. George Wright, for their helpful suggestions, comments and advice on my dissertation. I also thank Dr. Sam Barranco, who supported me and allowed me total access to his laboratory on the last year of my research.

To the faculty, staff, and graduate students in the Biology Department, I extend a sincere thanks for the kindness and friendship shown to me, especially, Dr. Samuel Bieber, Dr. Paul Homsher, and Mrs. Virginia Bagley. I consider myself fortunate to have had friends who always gave me emotional support and encouragement during my graduate studies. I am especially grateful to my best friend, Dr. Jen-Ing Hwang, for her constant support and encouragement.

A special thanks also goes to my fiance, Michael Adam, who was always understanding, loving, and caring. I also wish to thank him for his technical

assistance in my electron microscopic studies.

I also would like to thank my parents, Jiann-Yin, and Chu-chu Tsay and my brothers, Gwo-Wei and Jong-Wei, without whose continual support, encouragement, and love, being here would not have been possible.

This study was funded by Dr. Samuel Gillespie, The Jeffress Trust, Sovran Bank and Sigma XI.

TABLE OF CONTENTS

LIST OF FIGURES

LIST OF TABLES

INTRODUCTION

Effective cancer chemotherapy is based on the premise that the anticancer agent can be targeted specifically to the cancer cells. One such means of targeting cells for potentially toxic compounds lies in the phenomenon of portage transport. Portage transport, first reported in a microbial cell system (*Escherichia coli*) led to the demonstration that normally impermeant amino acid analogues (which are not recognized by the more stringent amino acid transport systems) could be transported into cells when incorporated into the backbone of a peptide (Ames et al., 1973). The amino acid analogues are released, after transport, by the intense peptidase activity normally found in the cytoplasm. In efforts aimed at broadening the scope of portage transport to molecules other than amino acid analogues, Boehm (1983) and Perry (1983) described the transport of sulfhydryl containing compounds by their attachment through a disulfide bond to the cysteine residue of a di- or tripeptide (Boehm et al., 1983; Perry and Gilvarg, 1983). After transport into *Escherichia coli*, the sulfhydryl compounds are released by disulfide exchange reactions in the sulfhydryl-rich cytoplasm. Additional studies reported transport of synthetic dipeptides and oligopeptides containing nucleophilic moieties attached to the alpha carbon of a glycine residue

(Kingsbury et al., 1984). These peptides are accepted by the peptide transport systems of *Escherichia coli* and are capable of being hydrolyzed by intracellular peptidases. After releasing its amino group the alpha-substituted glycine is chemically unstable and decomposes, releasing the nucleophilic moiety. Thus, the combination of peptide transport and intracellular peptidase action results in the intracellular release of the nucleophile. These findings validated the feasibility of using side-chain attachment to facilitate portage transport by peptide transport systems of *Escherichia coli.* These types of synthetic peptides have broad applicability to the study of microbial physiology and the development of an additional class of antimicrobial agents. This form of metabolite transport relies on the ability to couple the transport of normally impermeant molecules to the transport of permeant molecules, permitting their accumulation by cells. The peptide transport systems described in microorganisms (Payne and Bell, 1977; Wolfinbarger and Marzluf, 1975a) and in mammalian cell systems (Mathews, 1975) afford a convenient means for toxic metabolite accumulation.

Studies of peptide transport in microorganisms have been important in that they have permitted both biochemical and genetic dissection of peptide and amino acid transport systems and have formed the initial basis for the prediction of separate transport mechanisms. Most organisms utilize peptides nutritionally as sources of amino acids for protein synthesis (Payne and Bell, 1977). In bacteria, primarily *Escherichia coli* which lacks extracellular peptidase activities,peptides are transported intact and hydrolyzed intracellularly. The

peptide transport systems of *Escherichia coli* have been extensively characterized and have been shown to include three distinct systems, one for dipeptides, another for oligopeptides, and a third for tripeptides (Payne and Nisbet, 1980). The dipeptide transport system appears to exhibit a requirement for the alpha-amino and alpha-carboxyl groups of structurally dissimilar dipeptides such that the residue amino acids contribute little to recognition for transport. Oligopeptides are not transported by the dipeptide transport system. Instead, oligopeptides are accumulated into bacterial cells by an oligopeptide transport system that recognizes a free alpha-amino group and the overall size of the oligopeptide, but does not require an intact alpha-carboxyl group. The tripeptide transport system appears to prefer peptides composed of amino acids with hydrophobic side chains.

The study of peptide transport in eukaryotic microorganisms has been confined primarily to yeast and *Neurospora crassa*. The ascomycetous fungus *Neurospora crassa* appears to possess only an oligopeptide transport system requiring a free alpha-amino acid group for transport (Wolfinbarger and Marzluf, 1975b). The oligopeptide transport system has a relatively wide specificity for short-chain oligopeptides but does not handle dipeptides or free amino acids. *Neurospora crassa* does not grow well on dipeptides unless they are hydrolyzed extracellularly to free amino acids nor do dipeptides compete with oligopeptides for transport. In addition, the oligopeptide transport system appears not to be able to transport peptides larger than a pentapeptide. These studies in

microorganisms have been important in that they have permitted the use of small peptides containing antimetabolites in chemotherapy. Thus, a number of research groups have shown that microbial transport can be used for delivery of cytotoxic amino acid analogues that are not transported by the more stringent amino acid transport systems (Boisvert et al., 1986).

The complexity of studying peptide transport in mammalian cell systems has restricted the utility of portage transport in vertebrate cell systems. Only three tissues have been reported to accumulate small peptides, intestinal mucosal cells (Rosen-Levin, et al, 1980; Ganapathy and Mendicino, 1981b), proximal tubule epithelial cells in kidney (Carone and Peterson, 1980; Ganapathy and Leibach, 1982a), and specific tumor cells (Christensen and Rafn, 1952). The tumor cell system is of primary interest here, but it is essential that transport of small peptides in noncancerous cell systems be considered because of the potential for toxic side effects during chemotherapy.

Research in animal cell systems has been confined primarily to studies of peptide absorption by mammalian intestine (Matthews, 1975; Scriver, et al., 1975) and kidney cortex slices (Adibi, 1977). Many of these studies have used glycine containing peptides and confirmed the presence of biochemically distinct peptide transport mechanisms in mammalian cell systems. These peptide transport systems are distinct from the amino acid transport systems also present in animal cells (Benuck, et al., 1981). The resistance of carnosine (beta-alanyl-L-histidine)

to peptidohydrolases has resulted in the use of this peptide in a large number of peptide transport studies in small intestine cell systems (Addision, et al., 1974; Matthews, et al., 1974; Adibi and Soleimanpour, 1974). Glycyl-proline also has been shown to be highly resistant to hydrolysis by the particulate fraction of small intestinal mucosal cells (Ganapathy, et al., 1980). It may be suggested that all mammalian cells possess the genetic potential for small peptide transport, but the majority of mammalian cells do not transport small peptides suggests that this genetic potential is perhaps not normally expressed. Indeed, the premise has been advanced that the role of small peptides in the hormonal mediation of cellular regulation may require that such cells not be capable of small peptide transport. Neoplastic transformation of a cell is known to relieve genetic repression of a number of genes in the cancerous cell and thus cancer cells may be capable of small peptide transport. This differential ability of cancerous and noncancerous cells to transport small peptides should provide the opportunity to synthesize small peptides with toxic amino acid analogues which, when injected into a cancerous animal, would selectively kill the cancer cells without doing significant damage to the animal (Ringrose, 1983).

Peptide transport in mammalian cell systems has been more difficult to study than in microbial systems because of large numbers of peptidohydrolytic enzymes. Tumor cells typically secrete (Holmberg, 1961; Ottoson, 1960) large numbers and levels of such enzymes and the problems experienced by Christensen and Rafn (1952) continue to complicate studies on peptide transport and indeed the role

of small peptide hormones in regulation of tumor cell physiology. Significant advances in the study of peptide transport in mammalian cells came with the introduction of brush-border membrane vesicles obtained from epithelial cells of the small intestine (Ganapathy, et al., 1984; Berteloot, 1982) and renal proximal tubules (Ganapathy, et al., 1981; Ganapathy and Leibach, 1982). The removal of small peptides from solution in both systems (intestine and kidney) and their enzymatic degradation may occur by two mechanisms: 1) transport of small peptides into the cell with intracellular hydrolysis, or 2) enzymatic cleavage of small peptides at the luminal surface with transportation of the products through resident amino acid transport systems. Membrane hydrolysis was first described in the small intestine, and an extensive literature supports this mechanism (Matthews, 1975). The intestinal brush border has a complex microvillar structure covered by a trilaminar membrane that is lined on the luminal side by the glycocalyx, a branching carbohydrate-rich network of fine filaments. The brush border is rich in hydrolytic enzymes and proteins active in transport. Brush border enzymes are hydrolases, and include disaccharidases, peptidases, and phosphatases, and those that degrade substrate outside the cell are either sequestered in the glycocalyx or attached to the external surface of the membrane with part of their molecular structure exposed to cell exterior (Alpers and Seetharam, 1977; Matthews, 1975; Ugolev, et al., 1977). Hydrolysis of peptides in the intestine occurs at several sites. Intraluminal hydrolysis occurs within the bulk phase of the fluid in the intestinal lumen (Matthews, 1975). Membrane hydrolysis occurs in the brush border by exogenous peptidases adsorbed to the

brush border glycocalyx or by hydrolases in the cell membrane (Alpers and Seetharam, 1977; Matthews, 1975; Ugoloev, et al., 1977). Intracellular hydrolysis occurs deep in the cell membrane, in the cytosol or within intracellular organelles (Josefesson, et al., 1977; Matthews, 1975; Ugolev, et al., 1977). It has been established that intraluminal and membrane hydrolysis in the intestine yields a mixture of small peptides and amino acids of which peptides predominate (Matthews, 1975). Two mechanisms are involved in the uptake of small peptides in intestine; membrane hydrolysis followed by intracellular release of amino acids, and carrier-mediated absorption of di- and tripeptides with subsequent hydrolysis in the cytoplasm (Matthews, 1975). Additional research efforts on this subject have been published (Berteloot et al., 1982; Ganapathy and Leibach, 1983; Wilson, et al., 1989). Rajendran, et al. (1987) suggested that dipeptides are transported by a Na^+-dependent, nonconcentrative, carrier-mediated process. Tripeptide transport may occur by both diffusional and carrier-mediated processes (Wilson, et al., 1989), of which the latter is not energized by a sodium or proton gradient.

The fine structure of the brush border membrane of the kidney proximal tubule is similar to that of the intestine and is also rich in hydrolytic enzymes. Functionally, both membranes have a high capacity to hydrolyze oligopeptides and reabsorb amino acids. A number of studies have shown that small peptides are hydrolyzed by peptidases associated with the renal brush border membrane and the liberated amino acids are absorbed by the Na^+-dependent, carrier-

mediated processes known to exist for free amino acids (Silbernagl, et al., 1975; Carone and Peterson, 1980). Ganapathy and coworkers (1988) reported for the first time that brush border membrane vesicles, prepared from rabbit renal cortex, possess a dipeptide system which transports intact glycyl-L-proline by a Na^+-dependent, carrier-mediated transport. Ganapathy, et al. (1988) further characterized the dipeptide transport system using L-carnosine, which has greater resistance to hydrolysis by rabbit renal brush-border membranes compared to glycyl-L-proline. L-carnosine was shown to be transported into rabbit renal brush-border membrane vesicles by a Na^+- independent mechanism. Various di- and tripeptides inhibited L-carnosine transport, whereas amino acids did not. There was no detectable hydrolysis of L-carnosine outside the vesicles and intravesicular contents showed a 30% hydrolysis of the peptide within the vesicles. Based on the observations, Ganapathy proposed a model for the transport of dipeptides across the brush-border membrane of renal epithelial cells. According to this model, transport of the intact peptide across the membrane is followed by its partial or complete hydrolysis by a membrane peptidase whose active site is on the cytoplasmic side of the membrane (Ganapathy, et al., 1982b). In a recent publication, Triruppathi, et al. (1990) investigated the transport characteristics of L-phenylalanyl-L-prolyl-L-alanine in renal brush-border membrane vesicles isolated from the Japan Fisher 344 rat. This strain has been described as genetically lacking in dipeptidyl peptidase IV activity (Watanable, et al., 1987). Dipeptidyl peptidase IV, which is one of the major renal brush-border peptidases, releases X-Pro or X-Ala type dipeptides from the amino-terminal end of large

peptides. X-Pro-Y sequence type of peptides are almost exclusively hydrolyzed by dipeptidyl peptidase IV (Watanable, et al., 1987). These investigators found that (a) Phe-Pro-Ala is not hydrolyzed by renal brush-border membrane vesicles isolated from Japan Fisher 344 rats, (b) the transport of the tripeptide is in the intact form into the vesicles, (c) transport of the tripeptide is active, is driven by an inwardly directed H^+ gradient, is electrogenic, and occurs via the tripeptide-proton symport mechanism. This report is the first direct evidence for the presence of an electrogenic tripeptide-proton symport peptide transport mechanism in renal brush-border membrane (Tiruppathi, et al., 1990).

The uptake of peptides by a free-cell neoplasm was first studied prior to 1952 by Christensen and Rafn (1952). This study measured the transport of seven peptides by Ehrlich mouse ascites carcinoma cells and human and duck erythrocytes. The peptides utilized in this study included glycyl-glycine, glycyl-glycyl-glycine, L-leucyl-glycine, L-phenylalanyl-glycine, L-tyrosyl-glycine, glutathione, and L-glutamyl-L-glutamic acid. The erythrocytes failed to take up any of these seven peptides and the neoplastic cells hydrolyzed leucyl-glycine, phenylalanyl-glycine, and tyrosyl-glycine too rapidly to permit observation of cellular uptake of unsplit peptide. Only glycyl-glycine, glycyl-glycyl-glycine, and glutamyl-L-glutamate were reported to be transported intact by the mouse carcinoma cells. The uptake of these three peptides was inferior to that of free amino acids and, in addition, the peptides were strong inhibitors of amino acid uptake without themselves being transported (Christensen and Rafn, 1952).

In a recent publication, Yagi, et al. (1988a) suggested that PTT.119 (a tripeptide; *p*-fluoro-phenylalanyl-m-bis-(2-chloroethyl)amino-L-phenylalanyl-methionine ethoxy HCl) was transported by the MJY-alpha mammary tumor and B16 melanoma cell lines via two natural pathways for amino acid transport. Covalent linkage of methionine and phenylalanine residues to the bis-(2-chloroethyl)amino-phenylalanine molecule yielded a new bifunctional alkylating agent, PTT.119 (*p*-F-Phe-m-bis-(2-chloroethyl)-amino-L-Phe-Met-ethoxy-HCl). The primary route of PTT.119 entry was the classical L system, with the ASC system accounting for approximately 5-6% of PTT.119 transport in the B16 melanoma cells. The L system in mammalian cells preferentially catalyzes the uptake of branch-chain and aromatic amino acids, i.e. leucine, isoleucine, phenylalanine and valine by a sodium-independent mechanism. The nonmetabolizable analog, 2-aminobicyclo-[2,2,1]-heptane-2-carboxylic acid (BCH), is an ideal and specific substrate for system L. System ASC is sodium-dependent and transports alanine, serine, cysteine and threonine. Alpha-aminoisobutyric acid (AIB), is the nonmetabolizable substrate typical used for system ASC analysis. Tripeptide (PTT.119) uptake by MJY-alpha mammary tumor cells occur only through system L (Yagi, et al., 1988a). Yagi et al. (1988b) also investigated the transport of PTT.119 in L1210 leukemia cells. A major amino acid transport system in L1210 cells for PTT.119 was the classic sodium-independent L system as evidenced by competitive inhibition of BCH uptake by PTT.119 in the absence of sodium. A second transport system which

was also involved in PTT.119 uptake was probably the ASC system (Yagi et al. 1988b). There are no specific substrates which allow discrimination of the ASC system. Although threonine has been reported to be highly selective for the sodium-dependent ASC system in rat HTC hepatoma cells. Yagi, et al. (1988b) suggested that the low level of PTT.119 competition with threonine in the presence of sodium indicated that the ASC system probably played a small role in PTT.119 transport in L1210 leukemia cells.

Tumor cells typically secrete large numbers of hydrolytic enzymes (Poole, 1978) and the levels of these enzymes rise in the plasma of animals as the growth of the tumor develops (Santesson, 1935). It has been known for many years that cultured tumor explants exhibit proteolytic enzyme activity (Fisher, 1946) and the suggestion that proteinases play a role in tumor invasion was made by Santesson (1935) and Fisher (1946), and prompted the meticulous studies of Sylven and Bois-Svenssen (Sylven, 1960) on the localization of enzymes in tumors. With the advent of exquisitely sensitive and specific enzyme assays, the whole field of proteolysis by tumors has advanced enormously over the last decade (Poole, 1978; Strauli, 1980; Mort, 1981).

Proteases (peptide hydrolases; peptidohydrolases) include all enzymes that cleave peptide bonds (classified by the Enzyme Commission of the International Union of Biochemistry as EC 3.4.). Peptidohydrolytic enzymes are generally considered to be divided into proteinases (endopeptidases) and peptidases

(exopeptidases). Proteinases cleave peptide bonds internally in peptides and usually cannot accommodate the charged amino- or carboxyl-terminal amino acids at the active site. Peptidases reaction is directed by the amino- or carboxyl-terminus of the peptide. Proteinases are classified to four classes (serine, cysteine, aspartic, metallo) depending on the catalytic mechanisms of their active center, which are revealed by the use of inhibitors rather than the substrates. Serine proteinases are active at neutral pH values. Serine proteinases are abundant in the body and can be active almost anywhere; hence the need for "control" systems. Most of the serine proteinase are synthesized as inactive precursors that require limited proteolysis to activate them. This provides a convenient form of enzyme for storage, as in the pancreatic zymogen granules, and also allows control systems with positive feedback, such as the activation of trypsinogen by trypsin, and "cascade" control systems as in blood coagulation factors (Davie, et al., 1979). Two similarly related serine proteinases that have been of particular interest in relation to the growth of cancer cells are plasmin and plasminogen activator (Moscatelli, et al., 1980). The plasmin formed by the activation of plasminogen by plasminogen activator may function to degrade elements of the surrounding tissue, thereby permitting invasion by tumor (Quigley, et al., 1974). A study of the correlation between malignant transformation and increased plasminogen activator synthesis or secretion in a variety of cell lines has shown that both adenomas and carcinomas have higher plasminogen activator activity levels than normal mucosa (Suzumiya, et al., 1988). The second form of control of serine proteinases is protein inhibitors.

About 10% of human plasma protein consists of serine proteinase inhibitors, the most abundant of which are alpha 1-proteinase and alpha 2-macroglobulin (Keohane, et al., 1990).

Lysosomal cysteine proteinases are active at pH 6 and unstable above pH 7. Cathepsin B is the most studied of the mammalian cysteine-proteinases. This enzyme was suggested by Sylven (1974) to be involved in cellular detachment and subsequent metastasis of tumors. Cathepsin B is a lysosomal cysteine protease that may play a role in the activation of extracellular degrading enzymes involved in the destruction of the subendothelial matrix and extravasation of metastatic tumor cells.

A cellular cysteine proteinase with properties very different from the lysosomal cysteine proteinases is the Ca^{++}-dependent proteinase first discovered in skeletal muscle (Dayton, et al., 1975) and then in brain, liver and other tissues (Puca, et al., 1977; Reville, et al., 1976; Takai, et al., 1977). This enzyme occurs in the cytoplasm, and is most active at neutral pH, in the presence of a thiol compound and calcium ions. Many studies of malignant cells or neoplastic tissue in culture have implicated cysteine proteases in the progression of malignancy (Sheahan, et al., 1989). Both cathepsin B-like and cathepsin L-like cysteine protease specific activities were significantly elevated in the carcinoma tissue. Correlation of cathepsin B-like and L-like cysteine protease activities in individuals with different stages of colorectal cancer demonstrated significantly

higher cysteine protease activities in individuals with Dukes A tumors (tumors confined to the bowel wall) than in patients with more advanced tumors (Dukes' B, C, or D tumors). These results implied an important role for cysteine proteases in the early progression of human colorectal carcinoma (Sheahan, et al., 1989). Keren and LeGrue (1988) also reported the presence of cathepsin B-like enzyme activity on the surface of tumor cell variants expressing both high and low metastatic potentials demonstrating that all tumor lines had detectable cathepsin B-like enzymes which may play a role in the activation of extracellular degrading enzymes involved in the destruction of the subendothelial matrix and extravasation of metastatic tumor cells.

Aspartic proteinases have not been identified in prokaryotes, but are present in eukaryotes. In mammalian systems, several extracellular aspartic proteinases have been well studied: the pepsins (from the gastric juice of many species), chymosin (from calf stomach), and renin (from kidney and plasma of many species). The most studied of the aspartic proteinases is pepsin, or rather the family of related pepsins responsible for the digestion of food proteins in the strongly acidic conditions of the stomach. Cathepsin D, the cathepsin first studied in detail by Anson (1940), is by far the most easily detectable lysosomal aspartic proteinase. Cathepsin D has limited action against native proteins but possesses considerable activity against denatured proteins at pH 3.5-5. The enzyme preferentially attacks peptide bonds flanked by hydrophobic amino acids, i.e. phe-phe, phe-tyr, leu-phe (von Figura and Hasilik, 1986) and it has been

proposed that cathepsin D plays a role in pathological degradation of central nervous system proteins such as myelin basic protein (Whitaker and Seyer, 1979).

Metallo-proteinases are widely distributed in prokaryotes and eukaryotes. Mammalian metallo-proteinases have been identified extracellularly, in cell membrane (plasma and endoplasmic reticulum), and in cytosol (Bond and Beynon, 1985). These extracellular enzymes include collagenases, gelatinases, and procollagen N-proteinase. These enzymes preferentially cleave peptides with hydrophobic amino acid residues (Chu and Orlowski, 1985). Neutral to slightly alkaline pH is preferred for maximal activity of the metallo-proteinases, which are also sensitive to thiols. There have been studies of collagenase in relation to a variety of tumors (Woolley, et al., 1980). Most mammalian tissue collagenases require preliminary proteolytic activation in order for activities to be detected in in vitro assays. Kao and Stern (1986) compared collagenases from breast carcinoma and human stromal cells. It is the malignant epithelial cells and not the stromal cells that are the major source of collagenolytic activity, and this activity is not dependent on an interaction between the two cell types. Maslow (1987) showed that the motility of tumor cells is enhanced by exposure to exogenous collagenase independent of its effect on collagen-containing extracellular matrix. Several studies have indicated that stromal collagens as well as the extracellular matrix glycoproteins laminin and fibronectin are chemostatic for tumor cells (Terranova and Lyall, 1986; Nekeshima, et al., 1986). Terranova, et al (1989) further examined the effect of various proteases involved in

connective tissue degradation on tumor cell motility and found that type I collagen- and type IV collagen-specific collagenases, collagen, and collagen degradation products are stimuli for the directed migration of tumor cells. They also demonstrated that other proteases, specifically plasminogen and plasminogen activator (urokinase), which are involved in collagen activation and basement membrane degradation, also influence the directed migration of tumor cells (Terranova, et al., 1989). All extracellular matrix and especially basement membranes are thought to act as barriers to the invasion of tumor cells and to be the major connective tissue obstacles for metastatic spread (Liotta, 1984). The degradation of these matrices involves the action of proteolytic enzymes, and collagenases are believed to be of major importance in the degradation of this collagen-rich material (Liotta et al., 1982). The demonstration that B16 melanoma cells with higher lung colonization potentials have greater collagen-degrading activity and that metastatic tumors alone were capable of degrading type IV collagen present only in basement membrane (Liotta et al., 1980) focused additional attention on the degrading role of collagenases in metastasis.

Many of the early studies critically reviewed by Recklies and Poole (Recklies, 1982) showed that a variety of tumors contained enzymes capable of producing connective tissue degradation and thereby facilitating invasion. The evidence that proteolytic degradation of basement membrane (BM) plays a role in invasion includes the undisputed facts that tumor cells can actively degrade BM (Liotta, 1986) or BM-related products (DiStefano, 1985) in vitro; that purified

proteases have been derived from tumor cells that degrade BM collagen (Liotta, et al., 1981); and that protease inhibitors block or partially inhibit invasion in some model systems (Liotta, et al., 1981). Based on work in Liotta's laboratory, it appears that many metastatic cells bind preferentially to basement membrane (type IV) collagen by using basement membrane laminin as a attachment protein. These cells also produce a distinct collagenase that is able to degrade basement membrane (type IV) collagen. The ability of plasma proteinase inhibitors to prevent tissue destruction is determined not only by their presence in plasma and their affinities for proteinases, but most importantly by their ability to diffuse into the extravascular space (Heimburger, 1975; Travis, 1978). A firm indication that certain plasma proteinase inhibitors play a role in protecting tissues from proteolytic attack is derived from studies of proteinase enzymes. The proteinase/plasma proteinase complexes are found at sites of tissue destruction (Ohlssin, 1976).

What role does peptide/protein transport and hydrolysis play in the growth and development of cancers? Are tumor cells resistant to regulation by peptide hormones because the tumor cells transport and/or degrade them prior to their acting? Are the peptides liberated by peptidohydrolytic enzymes useful as a nutrient in tumor cell growth? Provided tumor cells possess peptide transport systems, can we take advantage of this activity? These are the questions we were trying to answer.

The peptide transport differences elaborated among mammalian cells should provide the opportunity to synthesize small peptides containing toxic amino acid analogues which when injected into a cancerous animal should selectively kill the cancerous cells without doing significant damage to noncancerous cells. The potential for using peptides containing toxic metabolites in cancer chemotherapy was described in the early 1950's by Bergel and Stock (1954) and Larionov, et al (1955). Bergel and Stock (1954) attempted to enhance the anticancer potential of nitrogen mustard by synthesizing the bis-(2-chloroethyl)-amino-DL-phenylalanine derivative which they called melphalan. Melphalan was synthesized with the hope that the incorporation of phenylalanine, a precursor of melanin, into the molecule would give the compound some selectivity of action against melanoma. Larionov, et al. (1955) synthesized an oligopeptide of sarcolysine (3-p-bis-(2-chloroethyl) aminophenyl-D,L-alanine) and studied it for its anticancer activities. They reported that an increase in the specificity of sarcolysine for certain tumor cells resulted from substitution of the methyl group of nitrogen mustard with phenylalanine. Nyhan (1960) subsequently hypothesized that p-sarcolysine possessed dual alkylator-antimetabolite activities, since the compound specifically inhibited incorporation of amino acid precursors in tumor cells. Further, examination of the racemic mixture of p-sarcolysin revealed that the L form (melphalan or L-PAM) was the active isomer (Schmidt, 1965).

The alkylating agent HN_2 (nitrogen mustard) is transported by an active, carrier-mediated process that is shared with choline in murine L5178Y

lymphoblasts (Goldenberg, et al., 1970; Goldenberg et al., 1971). HN_2 transport was not competitively inhibited by other alkylating agents, including melphalan, chlorambucil, trenimon [2,3,5-tris(ethyleneimino)-1,4-benzoquinone], mitomycin C, and intact enzyme-activated cyclophosphamide (Goldenberg, 1975). Similarly, cyclophosphamide transport was not altered by melphalan, chlorambucil, HN_2, or isophosphamide (Goldenberg, et al., 1974). These observations indicate that uptake of several alkylating agents occurs by independent transport mechanisms (Goldenberg, 1975; Goldenberg, et al., 1974; Goldenberg, et al., 1970). Melphalan transport by L5178Y lymphoblasts was shown to be mediated by a carrier mechanism independent of that utilized by other alkylating agents (Goldenberg, et al., 1977). Vistica, et al. (1978, 1979) showed that melphalan and the amino acid leucine share a common transport system in murine L1210 leukemia cells.

The mechanism of melphalan uptake by murine LPC-1 plasmatoma cells was investigated by Goldenberg et al. (1979). Evidence indicated that melphalan uptake is an active process in that uptake of melphalan that proceeds "uphill" against a concentration gradient, is temperature- and sodium-dependent, and is inhibited by several metabolic antagonists (i.e. antimycin A, oligomycin, m-chlorophenyl carbonyl cyanide hydrazone, p-hydroxymercuribenzoate and ouabain). Other findings indicate that melphalan uptake is carrier-mediated by two separate and distinct amino acid transport carriers. Melphalan uptake by one component was inhibited by BCH, but was unaffected by Na^+ depletion, which

appeared to be mediated by system L. Melphalan uptake by the other component was Na^+-dependent, unaffected by BCH, AIB or Me-AIB, and was inhibited by alanine, serine, cysteine, phenylalanine, glutamine and leucine, suggesting an involvement of the ASC system (Goldenberg, et al., 1979).

These findings stimulated development of chemotherapeutic agents composed of synthetic peptides with cytotoxic activity due to the alkylating group and selective carrier function towards specific target cells resulting from linkage of various amino acid residues (De Barbieri, 1972). Research efforts were continued at the Instituto Sierotherapico Milanese Serafino Belfanti (I.S.M.) under the direction of Dr. De Barbieri and resulted in synthesis of hundreds of peptides, numerous publications on this subject (De Barbieri, 1983) and eventual development of a combination of the most effective peptides into a formulation known as peptichemio (De Barbieri, 1972). Reductions in growth of established tumors were observed without adverse physiologic, histologic or enzymatic alterations in principal organs and tissue of the host.

In a recent publication, De Barbieri (1983) reported on the cancerocidal activity of a synthetic tripeptide mustard p-fluoro-phenylalanyl-m-bis-(2-chloroethyl) amino-phenylalanyl-methionine ethoxy hydrochloride), PTT.119, against a broad spectrum of virulent leukemia. PTT.119 was able to induce a dose-dependent, irreversible loss of murine, primate, and human cancer cell survival in in vitro systems (De Barbieri, 1983). This work was quickly followed

by reports of research conducted in the United States on the potential for PTT.119 in killing cancer cells (Yagi et al., 1984a; 1984b). These later studies evaluated the therapeutic potential of this synthetic tripeptide by assessing the tumorigenicity of L1210 leukemia, MJY-alpha mammary tumor cells exposed to PTT.119. Treatment with physiological dosages of PTT.119 effectively reduced or completely eliminated tumorigenicity of the tumor cells.

The research to be described here represents a continuation of this effort and is divided into parts: I. Basic morphology of mouse Ehrlich ascites tumor cells, mouse liver cells, and mouse 3T3 embryonic cells to provide basic information of these three cell lines. II. Growth curves and population doubling times to provide the basic information on these three cell lines grown in cell culture. III. Peptidohydrolytic enzyme activity assays to characterize the numbers and kinds of peptidohydrolytic enzymes which are associated with mouse Ehrlich ascites tumor cells in the abdominal cavity of mice. IV. Synthesis and purification of a dipeptide (beta-alanyl-melphalan) containing the alkylating agent melphalan as the toxic antimetabolite. V. Chemical stability of melphalan and beta-alanyl-melphalan. VI. Reactivity of melphalan and beta-alanyl-melphalan toward peptidohydrolytic enzymes. VII. In vitro toxicity testing of melphalan and beta-alanyl-melphalan. VIII. In vitro survival curve testing of mammalian cells treated with melphalan and beta-alanyl-melphalan. IX. Morphological studies describing the effects of drug treatment on mouse Ehrlich ascites tumor cells and mouse liver cells (using a scanning electron microscope, a light microscope, and a

transmission electron microscope). X. In vivo chemotherapy.

The objective of research presented here was to evaluate the potential role of small peptides in cancer physiology and chemotherapy.

MATERIALS AND METHODS

CELL CULTURES. Three cell lines, mouse Ehrlich ascites tumor cells, mouse liver cells, and mouse 3T3 embryonic cells were maintained in cell culture at 37° C in a humidified incubator gassed with 4% CO_2. The culture medium was routinely changed twice a week.

Mouse Ehrlich ascites tumor cells (Tsay strain) were derived by selection culture as a substrain of an original mouse Ehrlich ascites tumor cell line, which were the generous gift of Dr. Margaret Neville, University of Colorado (Denver). This cell line (Neville) was routinely maintained by serial subculture in the abdominal cavity of CF-1 albino mice. Tumor cells were transferred from the abdominal cavity of CF-1 mice into culture flasks containing NCTC-135 medium supplemented with 10% heat-inactivated fetal bovine serum (Gibco). Contaminating red blood cells and lymphocytes were typically lost from the culture with the first media change since they fail either to attach or proliferate under these culture conditions. By repeated passage, a subline (the "Tsay" strain) was established which grew well in tissue culture and maintained the capacity to proliferate in the abdominal cavity of a CF-1 albino mouse. The

Tsay strain of mouse Ehrlich ascites tumor cells were used in all experiments described in this study.

The mouse liver cell line (ATCC CCL 9.1), obtained from the American Type Culture Collection (ATCC), was routinely cultured in NCTC-135 medium (Gibco) supplemented with 10% heat-inactivated horse serum (Gibco). Subcultures were prepared by scraping, using a sterile rubber policeman. Old medium was removed and fresh medium was added before dislodging cells from culture flasks. Cells were transferred to new flasks for subculture. The passage number of mouse liver cells utilized in the assays were p15 (initial passage number) to p20.

Balb/3T3 mouse embryonic cell line (ATCC CCL 163) obtained from the American Type Culture Collection (ATCC), was routinely cultured in Dulbecco's modified Eagle's medium (Gibco) containing 10% calf serum (Gibco). This cell line was routinely passaged (for 4 to 5 passages) by trypsinization (0.25% trypsin, 0.02% EDTA, Gibco) and split into new flasks before reaching confluence. Mouse 3T3 embryonic cells were used at passage 18 to 25 (18 was the passage number when obtained from the ATCC).

CRYOPRESERVATION OF CELL LINES. Cell cryopreservation was performed on mouse liver cells and mouse 3T3 embryonic cells. Mouse liver cells were harvested by scraping, and centrifuged at 2,000 rpm for 5 min. Cell pellets were

then resuspended in cryopreservation medium (10% horse serum and 5% dimethyl sulfoxide in NCTC-135 medium) to a cell density of approximately 5 million cells per ml. Mouse 3T3 embryonic cells were harvested using trypsin and centrifuged at 2,000 rpm for 5 minutes. Cell pellets were then resuspended in cryopreservation medium (10% calf serum and 5% dimethyl sulfoxide in Dulbecco's modified Eagle's medium) to a cell density of approximately 5 million cells per ml. Cell suspensions were dispensed as 1 ml aliquots into sterile Cryogenic vials (Corning), placed in a refrigerator (4° C) for 30 minutes, and then into a freezer (-20° C) for 60 minutes, and finally the cells were stored at -80° C.

GROWTH CURVE DETERMINATION. For all three cell lines, known numbers of exponentially growing cells were seeded into 35 mm cell culture petri dishes containing a known quantity of the appropriate medium, supplemented with 10% appropriate serum. Cell cultures were incubated in a humidified CO_2 incubator at 37° C with 4% CO_2. Twice each day, for 3 to 5 days, triplicate flasks of cells were sampled. The total cell counts were determined using a hemocytometer and plotted relative to the sample time. The length of time required for a cell population to increase by a factor of 2 is the population doubling time (T_D). The number of cells at the plateau phase (or stationary phase) of growth is the saturation density. The average population doubling times and saturation densities of the three cell lines are reported.

ANALYSIS OF INTRACELLULAR AND EXTRACELLULAR PEPTIDO-HYDROLYTIC ENZYME ACTIVITIES.

Cell Extract Preparations: Mouse Ehrlich ascites tumor cells (Tsay strain) were used in peptidohydrolytic enzyme activity assays. Mice were injected intraperitoneally with approximately 1 million cells. After 10 to 12 days, the mice were killed by cervical dislocation. The Ehrlich ascites tumor cells were then removed from the abdominal cavity of the mouse, transferred to centrifuge tubes and pelleted by centrifugation using an IEC table top centrifuge (2,000 rpm). The supernatant, which constitutes the ascites fluid, was then transferred into Oak Ridge centrifuge tubes and put on ice for further preparation of the extracellular extract. The cell pellet which contained tumor cells, red blood cells, and lymphocytes, was resuspended in hypotonic buffer (0.1 M Tris-HCl, 0.01 M NaCl, 0.0015 M $MgCl_2$, pH 7.4) and recentrifuged at 2,000 rpm for 5 minutes. The red blood cells and lymphocytes ruptured in the hypotonic buffer due to osmolarity differences and the supernatant, which contained buffer and ruptured red blood cells and lymphocytes, were discarded and replaced with fresh hypotonic buffer. This procedure was repeated until a "pure white" population of tumor cells was obtained (usually two times). The tumor cell suspension was centrifuged at 2,000 rpm for 5 minutes to pellet the tumor cells. The supernatant was discarded and replaced with Dulbecco's phosphate buffered saline (DPBS) at 1:1 (v:v; cell pellet:DPBS). The tumor cell suspension was then transferred to a tissue homogenizer (PYREX, No. 7727), and homogenized on ice for 15 strokes.

The cell homogenate was transferred into Oak Ridge centrifuge tubes and put on ice for further preparation of the intracellular extract.

The extracellular ascites fluid from the original cell suspension and the intracellular extract from the cell pellet were centrifuged separately at 14,000 rpm for 30 minutes at 4° C using a JA-17 rotor in a Beckman J2-21 refrigerated centrifuge. The supernatants (approximately 10 ml) were transferred into a dialysis membrane tubing (SPECTRAPOR, m.w. cutoff approximately 3,500) and dialyzed against 1 liter of 0.2M Tris-HCl buffer, pH 7.4, at 0° C in the cold room overnight with stirring. Protein concentrations were determined by the method of Lowry (Lowry et al. 1951) using bovine serum albumin (BSA) as a standard.

Polyacrylamide Gel Electrophoresis with in situ Staining: A separating gel of 7.5% cyanogum 41 (a mixture of 95% acrylamide and 5% N,N'-methylene-bis-acrylamide; Sigma Chem. Co.) was prepared in 35ml of 0.5M Tris-HCl buffer, pH 8.9, with 16.8 mg L-amino acid oxidase (Type I crude dried venom from *Crotalus adamanteus*, 0.48 units/mg solid. One unit will oxidatively deaminate 1.0 umole L-phenylalanine per minute at pH 6.5 and 37° C., Sigma Chem. Co.). The acrylamide solution was then degassed for 5 minutes using a cold finger probe vacuum pump. N,N,N,N'-Tetramethyl-ethylenediamine (TEMED)(105 ul) and ammonium persulfate (2.45 mg) were gently added into the degassed acrylamide/ enzyme solution, and the solution transferred into electrophoresis gel tubes (120 mm X 15 mm) using a Pasteur pipette. Distilled water was carefully applied to

the top of the gel solutions to fill the gel tube prior to polymerization. During the polymerization process the tubes were held in a vertical position in the electrophoresis unit with the bottom of each tube tightly covered with a piece of parafilm. Gel polymerization was complete in approximately 30 to 50 minutes with a clear boundary zone evident between the gel and water overlay. The upper and lower chambers of the electrophoresis unit were filled with cold electrode buffer (0.05M Tris, 0.005M glycine, pH 8.3) and the water overlay in each tube also displaced with buffer. The samples (50 *ul*), which were mixed with sucrose and tracking dye (0.4% bromophenol blue) with protein concentrations of 2 mg/ml (approximately 100 *ug*/50 *ul*/gel), were then applied to the top of gels using a PYREX disposable microsampling pipette. The electrophoresis unit was placed in the cold room and an initial constant current of 1 mAmp/gel was applied until the tracking dye entered the gels. The constant current was then increased to 3 mAmp/gel for the whole term of electrophoresis. The power source used was a Buchler 3-1500 constant power supply pack. The separation of protein samples in the gel occurred from cathode to anode. At the end of the run, 3 to 4 hours, each gel column was removed from the electrophoresis tube by rimming the tube gently with water using a syringe and cut off at the position of the tracking dye. These gels were then transferred into test tubes of the enzyme activity staining solution which contained different peptide substrates.

The staining solution was prepared by dissolving 23 mg nitro blue tetrazolium (NBT) (Sigma Chem. Co.) and 2.3 mg phenazine methylsulfate (PMS) in 140 ml

Tris-HCl buffer (0.1M, pH 7.4). The staining solution (10 ml) was transferred to individual test tubes (18 X 150 mm) and 1 mg of each peptide tested was dissolved in separate tubes to constitute the "staining solution". Individual gels were then incubated in this solution overnight in the dark at room temperature. Peptidohydrolytic enzyme activity towards a given peptide was detected by the appearance of dark blue bands on the gels. The distances of these bands were measured from the top of the gels and their relative mobilities (R_m) calculated. R_m, refers to the mobility of the peptidase of interest measured with reference to the mobility of the tracking dye where:

$$R_m = \frac{\text{distance migrated by peptidase}}{\text{distance migrated by tracking dye}}$$

SYNTHESIS OF BETA-ALANYL-MELPHALAN (BAM). Incorporation of beta-alanine and melphalan (Figure 1) was performed using traditional small peptide synthesis procedures (Stewart and Yong, 1984) to get the dipeptide beta-alanyl-melphalan (figure 2). N-tert-butoxycarbonyl-beta-alanine (BOC-beta-alanine, 10.589 g; 56 mmoles), dissolved in 80 ml methylene chloride, was added to a solution of 5.768 g (28 mmoles) dicyclohexyl-carbodimide (DCCD), which is a coupling reagent, dissolved in 240 ml methylene chloride. BOC-beta-alanine is an amino protected derivative of beta-alanine. DCCD is a coupling reagent which couples a partially protected amino acid or peptide with a free carboxyl group to a second carboxyl group protected amino acid or peptide containing a free amino group. The resulting solution was stirred at room temperature for 10 minutes

1. Structure of melphalan.

Melphalan

(4-bis-(2-Chloroethyl) amino-L-phenylalanine

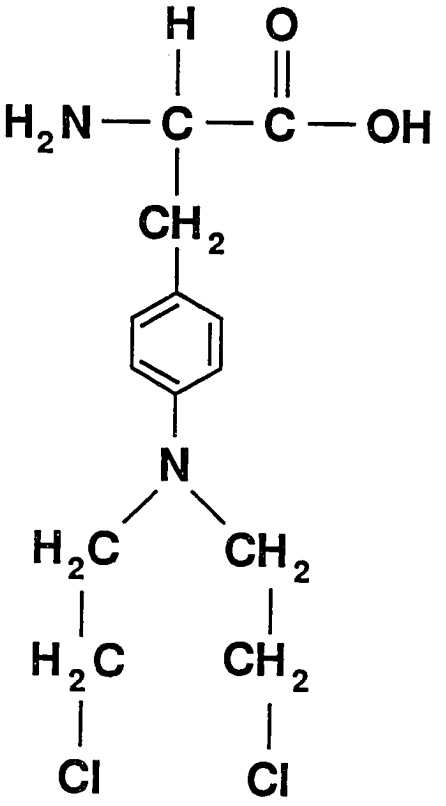

Figure 2. Structure of beta-alanyl-melphalan.

beta-alanyl-melphalan

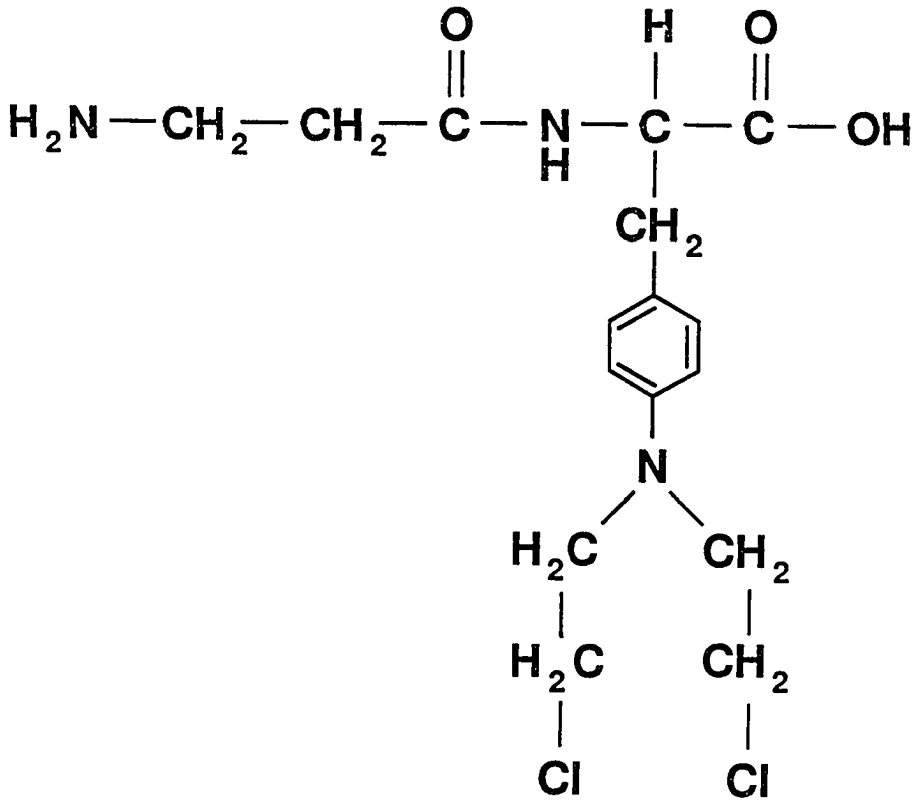

and then cooled to 4° C and held for 10 minutes. The formed precipitate was removed by filtration and washed with two 80 ml methylene chloride washes. The washes and the filtrate containing BOC-beta-alanine anhydride were combined. Melphalan (4.270 g, 14 mmoles) was slowly added with stirring to dimethylformamide (1120 ml). To this solution, after stirring 15 minutes, the methylene chloride solution of BOC-beta-alanine anhydride was slowly added. After complete addition of the BOC-beta-alanine anhydride, one ml of diisopropylethylamine was added and the stirring continued for 4 hours at room temperature. The reaction was monitored for ninhydrin positive material. All ninhydrin tests proved negative which indicated complete acylation of the amino component of melphalan.

The resulting yellow solution was evaporated under vacuum yielding a thick yellow oil. The oil was dissolved in toluene and any white insoluble material (primarily dicyclohexylurea) was filtered off. The insoluble material was washed several times with toluene and the washes were combined with the soluble filtrate. The solution was evaporated under vacuum again, yielding a yellow oil. The oil was dissolved in ethyl ether and dried under vacuum, leaving an off-white solid. This material, BOC-beta-alanyl-melphalan (3.86 g, 58% yield), was homogenous by high-performance liquid chromatography (HPLC). This form of the dipeptide was most stable for storage and was stored at -20° C. HPLC analysis involved use of a Waters' HPLC system. The columm was a Vydac (0.4 X 25 cm)(Waters, MA) and the absorbance detector was set to 210 nm. The

gradient mobile phase was 0.15 % trifluoroacetic acid in water (solvent A) and 0.15% trifluoroacetic acid in acetonitrile (solvent B). The gradient mobile phase was run at 1 ml/minute of 90% solvent A and 10% solvent B to 50% solvent A and 50% solvent B over a 20 minute interval followed by a hold at 50% solvent A and 50% solvent B for 5 minutes, then returning to 90% solvent A and 10% solvent B over a final interval of 5 minutes.

Prior to utilization in toxicity or chemotherapeutic studies, sufficient BOC-beta-alanyl-melphalan was converted to the dipeptide-HCl salt for usage over a 1 or 2 month period. For deblocking, the BOC-beta-alanyl-melphalan (1 mg) was dissolved in 250 ml trifluoroacetic acid (removes BOC group in an acidolysis reaction) and reacted at room temperature for 20 minutes. After evaporation under minimal vacuum, the resulting yellow-brown oil was ninhydrin-positive, and homogenous by HPLC. The oil was treated with a three-fold molar excess of 2N HCl with stirring at room temperature for 10 minutes. After evaporating the solution under vacuum, the resulting solid was also a yellow-brown oil. This compound was ninhydrin positive. HPLC analysis indicated this compound to be approximately 85% pure, containing two decomposition products comprising 6% and 9% , respectively, of the total "peak areas".

CHEMICAL STABILITY OF MELPHALAN AND BETA-ALANYL-MELPHALAN. Melphalan was dissolved at a concentration of 3.052 mg/ml (0.01 M) in distilled

water and beta-alanyl-melphalan was dissolved at a concentration of 4.13 mg/ml (0.01 M) in distilled water. Solutions of melphalan were made fresh and stored on ice prior to use. Degradation was investigated at different temperatures (0° C and 37° C) in water, bovine serum albumin solutions (10% and 30% in distilled water), and in NCTC-135 culture medium supplemented with 10% fetal bovine serum. In experiments on the degradation of melphalan in different solutions, 1 ml of melphalan solution was added to 4 ml of incubation medium (i.e. BSA solution, etc.). At timed intervals, 0.5 ml samples were taken and added to 1 ml of methanol. These mixtures were centrifuged in an Eppendorf Centrifuge model 5412 for 3 minutes at 12,000 rpm. The supernatants were filtered through ACRODISC CR disposable syringe filters (0.2 micron), and 10 ul of filtrate used for HPLC analysis. HPLC involved use of an ISCO (ISCO, Inc. Lincoln, NE, U.S.A.) ternary HPLC system incorporating an ISCO Model 2360 gradient programmer, an ISCO Model 2350 pump and sample injection valve, and an ISCO V^4 absorbance detector set to 254 nm (the measured Lamda max of melphalan in water is 260nm). Chromatograms were recorded on an AT Turbo computer using Isco ChemResearch computer software for data collection. The column was a C_{18} (Octadecyl) 5 um particle size, 250 X 4.5 mm, from IBM Instruments, Inc..

The mobile phase was 80% H_2O and 20% methanol for melphalan separation. The mobile phase was 60% H_2O and 40% methanol for beta-alanyl-melphalan (BAM) separation. All materials and reagents were of

HPLC grade and were filtered through a 0.8 um Millipore filter (Millipore, Bedford, MA, U.S.A.) prior to use. The flow rate of the mobile phase was 2 ml/minute.

ENZYME ASSAY. Leucine aminopeptidase assays were performed on the extracellular and intracellular extracts of mouse Ehrlich ascites tumor cells. The extracellular and intracellular extracts were prepared using the procedure mentioned earlier in the section titled Cell Extract Preparation (page 26). The cell extract (2 ml) was added to 10 ml of substrate solution (0.2, 0.4, 0.8, 1.2, 1.6, 2.0, 4.0 mM L-leucine-p-nitroanilide in 4 mM H_2SO_4) and 10 ml Tris-HCl buffer (200 mM Tris, pH 7.4) with 2 ml melphalan (in Tris-Hcl buffer; 2.5 mg/ml) or 2 ml Tris-HCl buffer as control. This extract/substrate (total 24 ml) mixture was incubated in a 37° C water bath. The aliquots (3 ml) were taken out at 0, 5, 10, 20, 30, and 60 minutes. Ice-cold distilled water (0.5 ml) was added into this 3 ml aliquot to stop the reaction and absorbance was measured at 405 nm in a Beckman Model 25 Spectrophotometer (BECKMAN, Irvine, CA, U.S.A.). Triplicate samples were taken for each assay.

ANALYSIS OF MELPHALAN AND BETA-ALANYL-MELPHALAN (BAM) TOXICITY IN CELL CULTURE. For in vitro toxicity assays, mouse Ehrlich ascites tumor cells (Tsay strain), mouse liver cells, and mouse 3T3 embryonic cells (approximately 100,000 cells) were seeded into T-25 tissue culture flasks containing 5 ml of the appropriate culture medium. The culture medium was

routinely changed twice a week. The cell cultures were incubated at 37° C for two days in a humidified CO_2 incubator. The incubation medium was then changed for fresh medium supplemented with the drug being tested. The cultures were incubated an additional 24 hours and were then harvested by trypsinization and stained using trypan blue dye exclusion (0.4% trypan blue in Dulbecco's phosphate buffered saline). The cells were counted in a hemocytometer where cells staining blue were considered metabolically "dead" and their number, added to the number of "clear" cells (i.e. living cells), equaled total cell number. The "dead" cell number was divided by the total cell number to get the % of "dead" cells which was then converted to $\log_{10}$. Each assay was done in triplicate culture flasks and 3 separate experiments.

For the cell survival study, mouse Ehrlich ascites tumor cells, mouse liver cells, and mouse 3T3 embryonic cells were seeded into T-75 tissue culture flasks with 15 ml appropriate culture medium. After 48 hours, the culture medium was changed for fresh medium supplemented with the drug being tested. After 2 hours incubation, the cells were harvested and reseeded into T-25 tissue culture flasks at a density of 100,000 cells per flask. To get the total cell number, the cells were harvested and counted at regular timed intervals. Total cell numbers from triplicate assay flasks were averaged and plotted versus time on semi-log paper to determine survival curves.

MORPHOLOGICAL STUDY DURING MELPHALAN AND BETA-ALANYL-MELPHALAN (BAM) TREATMENT. Only mouse Ehrlich ascites tumor cells and mouse liver cells were used in this study. Light microscopy, scanning (SEM), and transmission (TEM) electron microscopy were used for examination of the morphology of each cell line which was treated with anticancer drugs. For light microscopic and transmission electron microscopic study, cells were seeded into T-75 tissue culture flasks and incubated in a humidified CO_2 incubator at 37° C. Cells in the exponential growth phase were used for these experiments and were incubated in medium with the drug being tested for 2 hours. Cells were trypsinized and pelleted using a IEC table-top centrifuge (Internation Equipment Co., Needham Hights, MA, U.S.A.) at 2,000 rpm for 5 minutes. After the supernatant was removed, the cell pellets were fixed (2% glutaraldehyde in 0.1 M sodium cacodylate buffer, pH 7.4, for 1 hour at room temperature) and washed three times (10 minutes for each wash) with 0.1 M sodium cacodylate buffer. After secondary fixation (1% OsO_4 in 0.1 M sodium cacodylate buffer, pH 7.4 for 90 minutes at 4° C), the cell pellet was rinsed again three times in buffer and then dehydrated in a graded alcohol series (30%, 50%, 70%, 95% and 100%), transferred to acetone, and embedded in POLYBED (Polysciences) mixture. Sections were cut with a LKB III ultramicrotome. Thick sections were stained with Richardson stain for light microscopic examination. Thin sections were stained with 2% uranyl acetate and 0.4% lead citrate, and viewed with a Hitachi H-U 11B transmission electron microscope (Hitachi, Ltd., Tokyo, Japan).

For the scanning electron microscopic study, cells were grown on a piece of tissue culture cover slip (THERMANOX; Nunc, Inc., Naperville, IL, U.S.A.) in a Petri dish. Cells attached on the cover slip were prepared for SEM following the same fixation and dehydration procedure as described for the TEM studies. The cover slips were dried using a DCP-1 critical point dryer (Enton Accum, Inc., Cherry Hill, NJ, U.S.A.), mounted on stubs, and coated with gold/palladium using a Polaron E5200 Sputter Coater (Polaron Equipment Ltd., Cambridge, MA, U.S.A.). Cells were examined using a Cambridge Stereoscan 100 SEM (Deerfield, IL, U.S.A.).

ANALYSIS OF IN VIVO CHEMOTHERAPY. For the chemotherapy assays, mouse Ehrlich ascites tumor cells were harvested fresh from the abdominal cavity of a mouse into hypotonic buffer (8.0 g NaCl, 0.2 g KCl, 1.15 g Na_2HPO_4, 0.2 g KH_2PO_4, 0.1 g $MgCl_2$ in 1 liter glass distilled water, pH 7.4). The cells were washed with hypotonic buffer until the tumor cells were free of red blood cells and lymphocytes and then the tumor cells were transferred to DPBS and injected into the abdominal cavity of mice (approximately one million tumor cells per mouse). After 24 hours, the drug being tested was injected intraperitoneally at the desired concentration. Control mice having been injected with tumor cells received a sham injection of the solvent used to inject the drugs. Since all "drugs" tested in this study were soluble in DPBS, this solvent was utilized in all assays. Additional controls consisted of mice receiving a sham injection of DPBS, i.e. no tumor cells and the same drug treatment as the mice receiving the tumor cells.

The mice were weighed daily and their water and food consumption monitored. The survival day after injection of each mouse in the assay was recorded. The T/C ratio was the calculation of the average survival day of mice in a treatment group divided by the average survival day of mice in a control group.

RESULTS

I. Basic Morphology of Mouse Ehrlich Ascites Tumor Cell Line, Mouse Liver Cell Line and Mouse 3T3 Embryonic Cell Line:

The objective of this study was to illustrate the fundamental morphological and growth characteristics of the three cell lines grown in cell culture.

A monolayer cell culture of round (80%) and bipolar-shaped (spindle shape) cells (20%) is shown (Figure 3). Many doublet-cells are shown and two nuclei are seen in some spindle-shaped cells. Both round and spindle-shaped cells demonstrated vacuoles and sparse granularity of the cytoplasm is usually perinuclear in location. Nuclei typically appeared as round or oval in shape.

Mouse liver cells also demonstrated two types of cell morphology in monolayer culture (Figure 4). The majority of mouse liver cells were round (90%) with a few spindle-shaped cells demonstrated (10%). Cells appeared to contain a single round nucleus and granulated cytoplasm.

Figure 3. Photomicrograph of mouse Ehrlich ascites tumor cells grown in monolayer cell culture. Photograph was taken through an inverted microscope (400X).

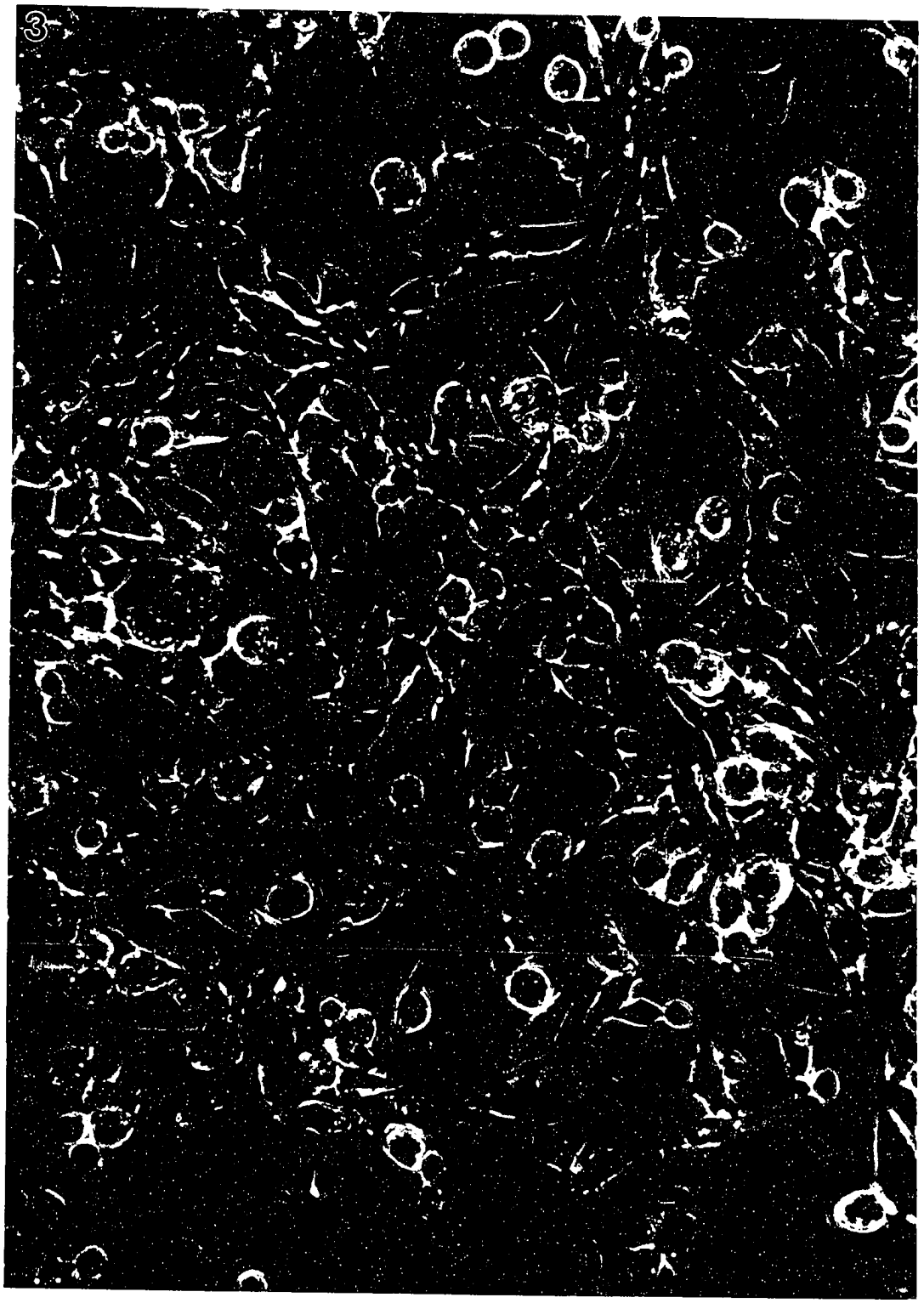

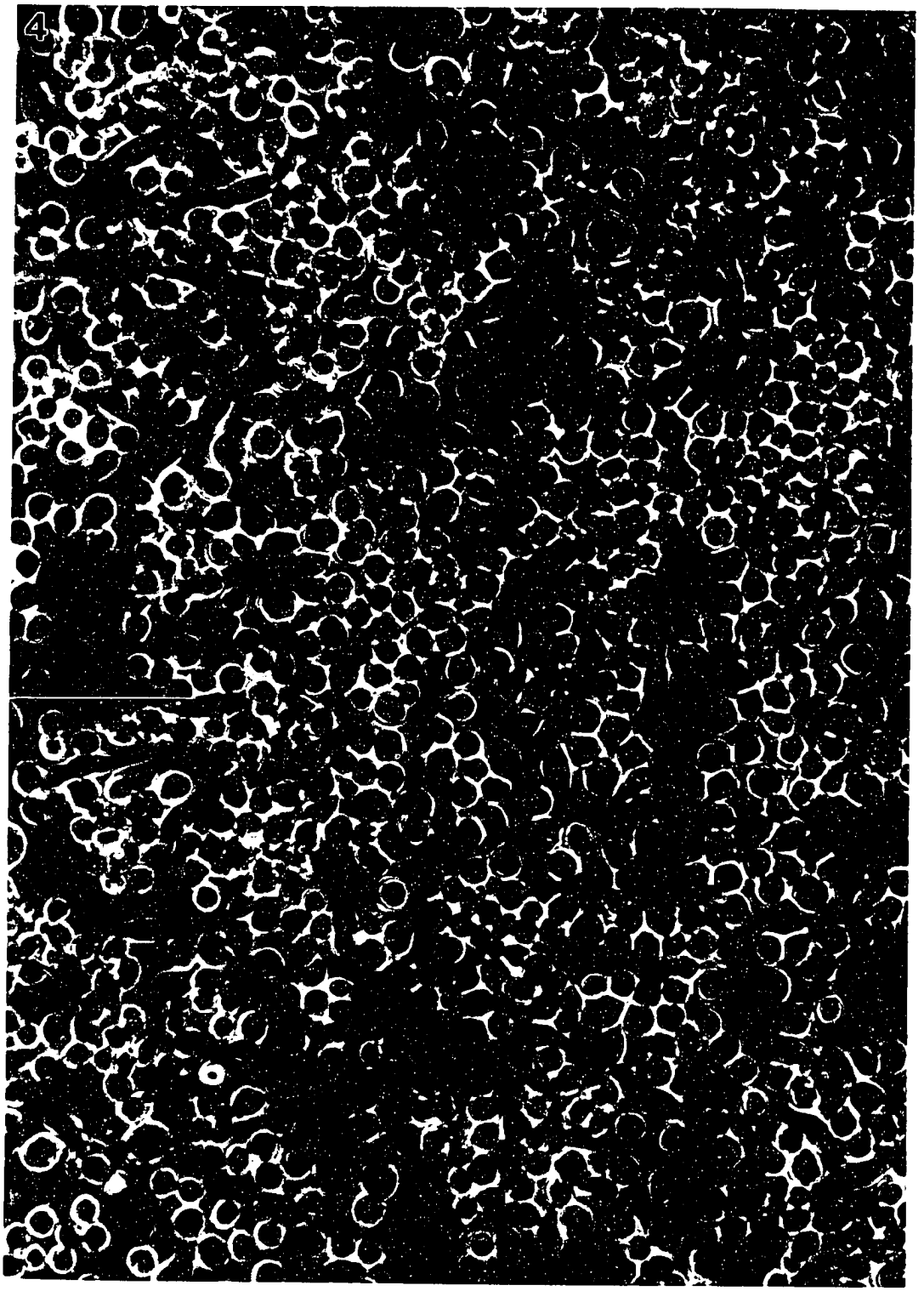

Mouse 3T3 embryonic cells typically grew as flattened spindle-shaped cells in monolayer cell cultures (Figure 5) exhibiting a "pavement-like" growth pattern and cytoplasmic vacuolization. Cells contained single round nuclei and granulated cytoplasm.

II. Growth Curves and Population Doubling Time (T_D):

The growth characteristics of mouse Ehrlich ascites tumor cells, mouse liver cells and mouse 3T3 embryonic cells are shown in Figures 6, 7, and 8. The mouse Ehrlich ascites tumor cells were initially seeded from an exponential growth cell culture at 2 X 10^5 cells per 35 mm tissue culture Petri dish (Figure 6). There was no lag phase before the cell number started to increase. After 72 hours, the cells depleted the medium of the nutrients essential for growth and entered a plateau or stationary phase of growth. The mouse Ehrlich ascites tumor cells had a saturation density of 3.2 X 10^6 cells/35 mm petri dish and a T_D value of 18 hours.

The growth curve of mouse liver cells is shown in Figure 7. The mouse liver cells were also seeded from a exponential growth cell culture at an initial cell number of 1.5 X 10^5 cells per 35 mm tissue culture Petri dish. The mouse liver cells had a T_D of 29 hours and exhibited no lag phase. The cells had a saturation density of 9 X 10^5 cells/35 mm petri dish after 90 hours.

Figure 5. Photomicrograph of mouse 3T3 embryonic cells grown in monolayer cell culture. Photograph was taken through an inverted microscope (400X).

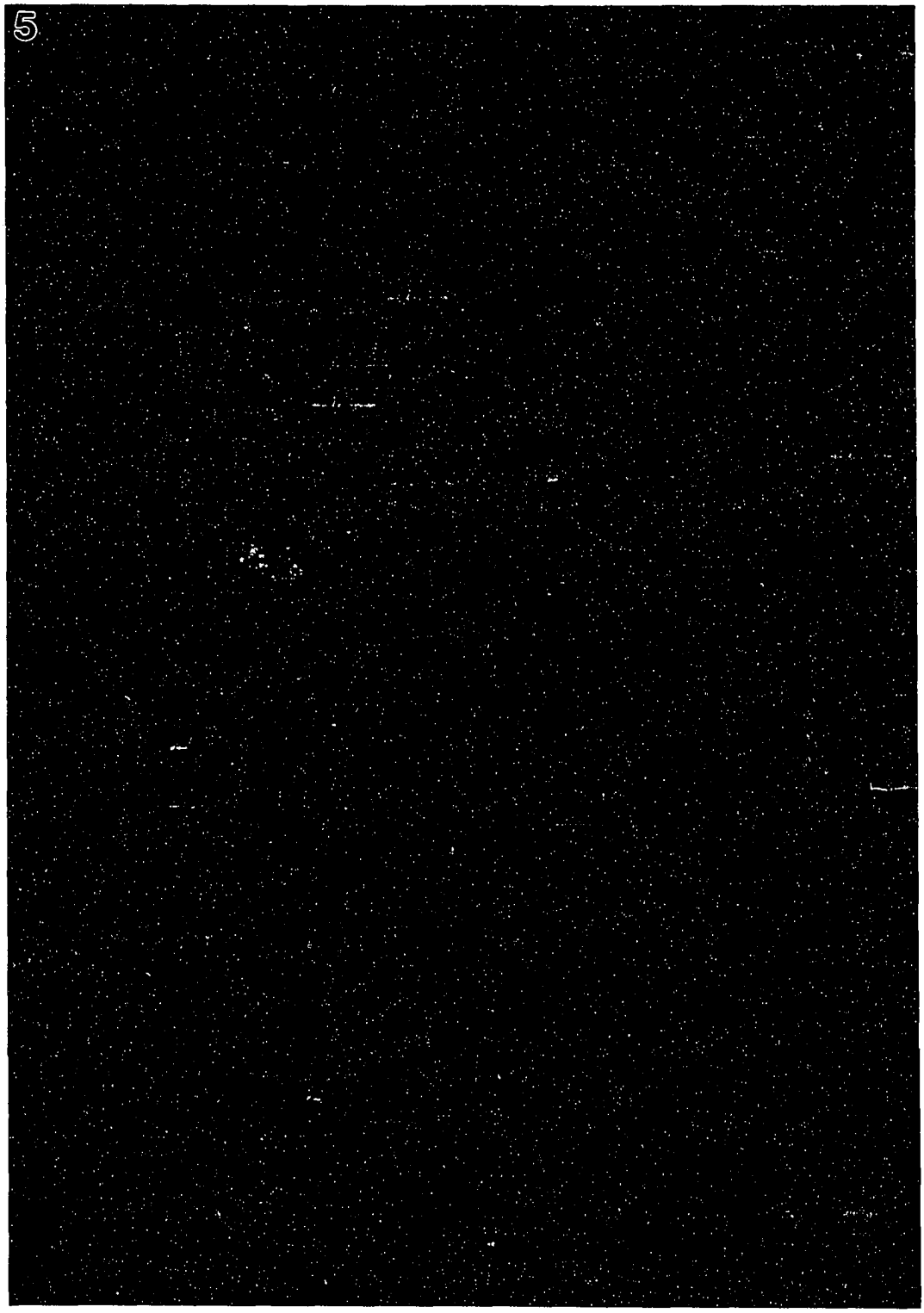

Figure 6. Growth curve of mouse Ehrlich ascites tumor cells. Mouse Ehrlich ascites tumor cells (approximately 200,000 cells) were seeded into 35 mm tissue culture petri dishes containing 5 ml NCTC-135 medium supplemented with 10% fetal bovine serum. The cell numbers were counted twice a day for 4 days, using a hemocytometer. Cell population doubling time (T_D) was calculated from the linear phase of the growth curve. Each data point represents an average of 3 replicate values.

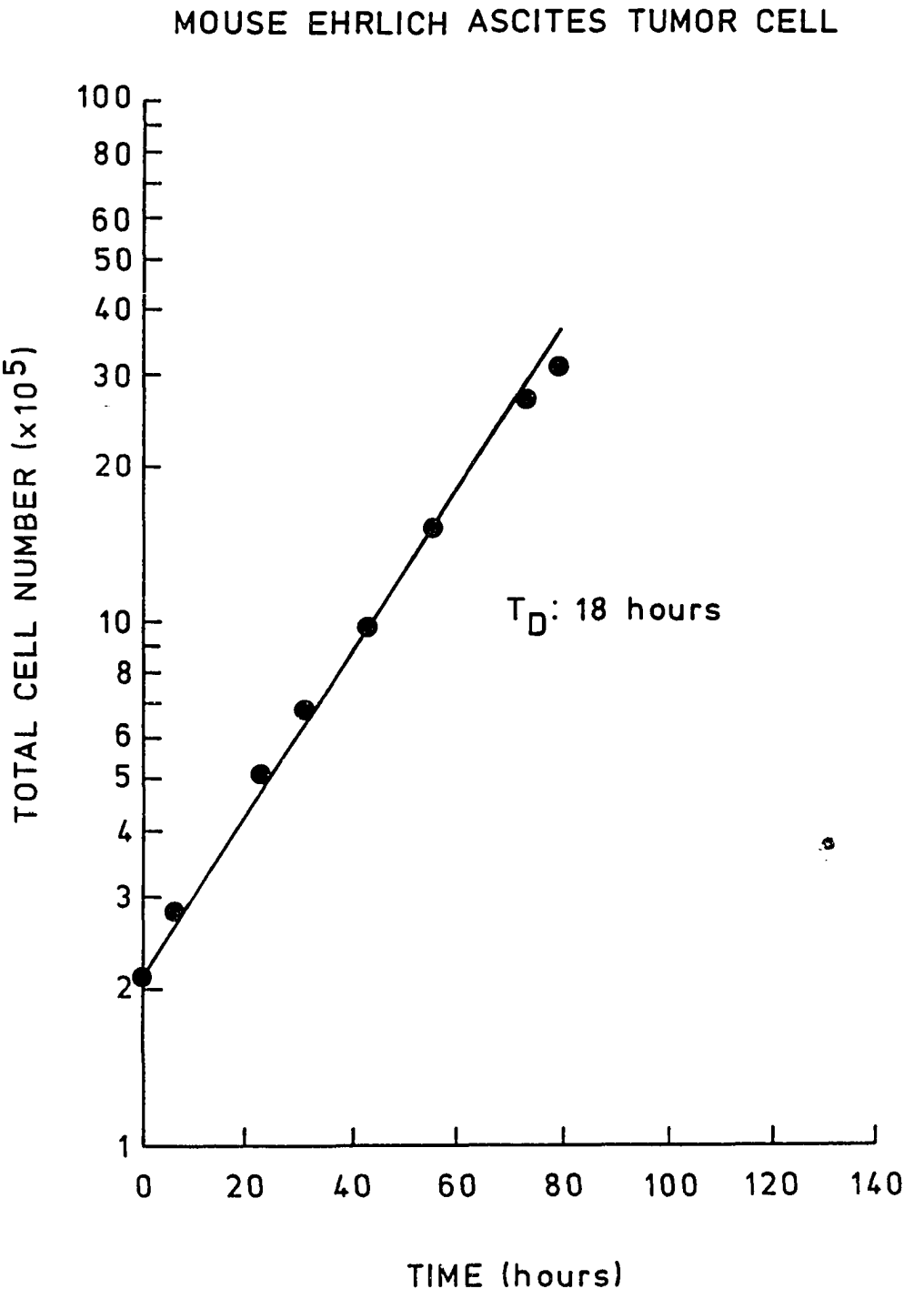

Figure 7. Growth curve of mouse liver cells. Mouse liver cells (approximately 100,000 cells) were seeded into 35 mm tissue culture petri dishes containing 5 ml NCTC-135 medium supplemented with 10% horse serum. The cell numbers were counted twice a day for 6 days, using a hemocytometer. Cell population doubling time (T_D) was calculated from the linear phase of the growth curve. Each data point represents 3 replicate values.

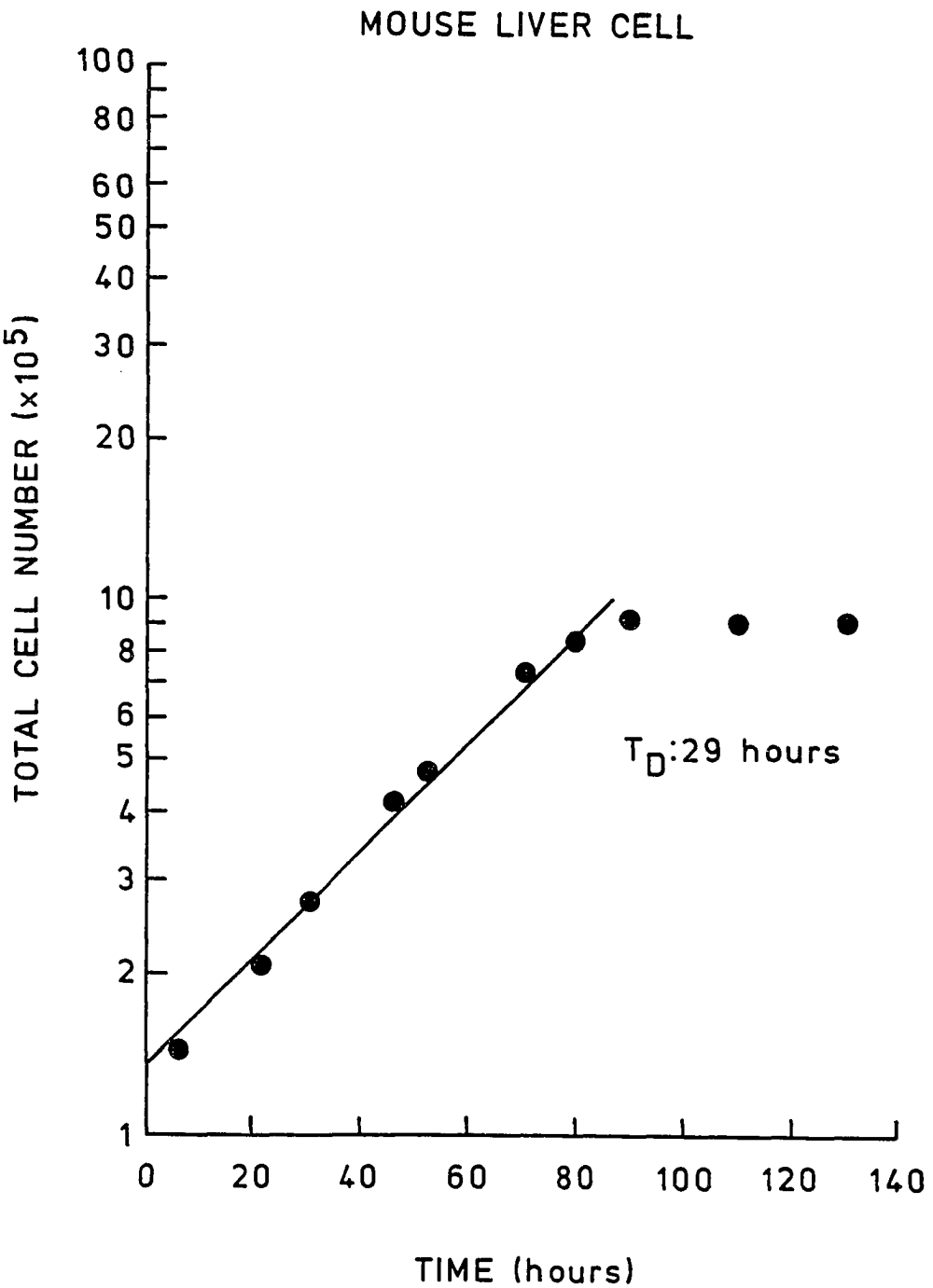

Figure 8 shows the growth curve of mouse 3T3 embryonic cells. The cells were initially seeded at 1 X 10^5 cells per 35 mm tissue culture petri dish from an exponential growth cell culture. The population doubling time (T_D) of mouse 3T3 embryonic cells was 25 hours. There was no lag phase. After 72 hours, the cells entered a plateau phase where a saturation density of 2.7 X 10^5 mouse 3T3 cells/35 mm petri dish was calculated. The results here indicated that there was no apparent correlation between the population doubling time of these three cell lines and their saturation densities and that the doubling times for the cell lines were not dramatically different.

III. Peptidohydrolytic Enzyme Activity Assay:

The objective of this study was to characterize the numbers and kinds of peptidohydrolytic enzymes which were associated with the growth of mouse Ehrlich ascites tumor cells in the abdominal cavity of mice. Tables 1 and 2 summarize the results of intracellular and extracellular peptidohydrolytic enzyme activities from mouse Ehrlich ascites tumor cells. Proteins in ascites fluids and cellular homogenates were separated on the basis of charge using polyacrylamide tube gel electrophoresis. The enzyme L-amino acid oxidase (EC 1.4.3.2) was polymerized within the gel and catalyzed the oxidation of L-amino acids liberated following the hydrolysis of specific peptides by the electrophoretically separated peptidohydrolytic enzymes. The L-amino acid oxidase transfers electrons to phenazine methosulfate which in turn transfers them to the nitroblue tetrazolium

Figure 8. Growth curve of mouse 3T3 embryonic cells. Mouse 3T3 embryonic cells (approximately 100,000 cells) were seeded into 35 mm tissue culture petri dishes containing 5 ml Dulbecco's modified Eagle's medium supplemented with 10% calf serum. The cell numbers were counted twice a day for 3 days, using a hemocytometer. Cell population doubling time (T_D) was calculated from the linear phase of the growth curve. Each data point represents an average of 3 replicate values.

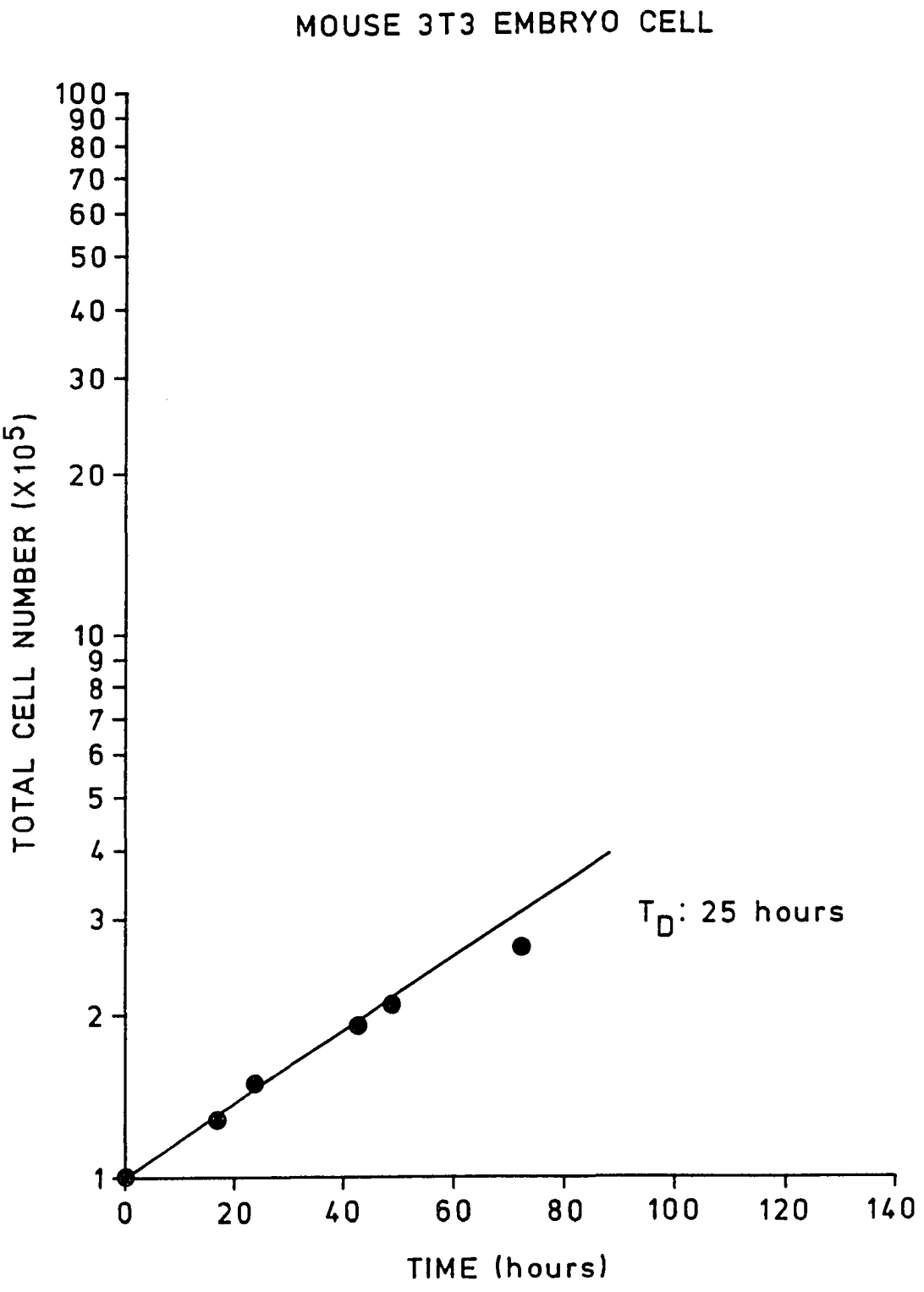

dye. The reduced dye forms an intense blue precipitate, formazan, at the site of peptidohydrolase activity (Figures 9 and 10). Using the thirty seven peptides listed in Table 1 it was possible to distinguish six electrophoretically distinct peptidase activities present in the intracellular extract of mouse Ehrlich ascites tumor cells. In addition, the substrate specificities of these separate activities have been partially characterized according to their abilities to hydrolyze substrate peptides. The peptidohydrolytic activities described in Table 1 are referred to as peptidases A, B, C, D, E and F. Their relative activities with different substrates and R_m values are indicated in Table 1. Certain peptides, for example L-leucyl-L-histidine and glycyl-L-leucyl-L-tyrosine, appeared to be readily hydrolyzed by several of these peptidases, such that when they were used as substrates a complex pattern of stained activity bands was seen (Figure 9). With other peptide substrates, simpler patterns were observed because they are hydrolyzed by only one of the peptidases present, i.e. activity against L-alanyl-L-tyrosine and glycyl-beta-alanine appeared to be restricted to peptidase D and activity against L-leucyl-L-alanine, L-leucyl-glycine and L-histidyl-L-leucine was restricted to peptidase C.

Peptidase A, which has a R_m value range from 0.26 to 0.28, hydrolyzed 3 dipeptides (L-leucyl-L-histidine, L-leucyl-L-tyrosine, L-methionyl-L-histidine). It is very active against L-leucyl-L-tyrosine and weaker against L-leucyl-L-histidine and L-methionyl-L-histidine. No hydrolysis of any of the tripeptides by peptidase A has been observed.

Figure 9. Peptidohydrolytic enzyme activities of cell extracts of mouse Ehrlich ascites tumor cells. Proteins (peptidohydrolases) were separated by 7.5 % polyacrylamide tube gel electrophoresis and stained using an in situ activity stain as described in the materials and methods. The bands represent the activities of peptidohydrolytic enzymes.

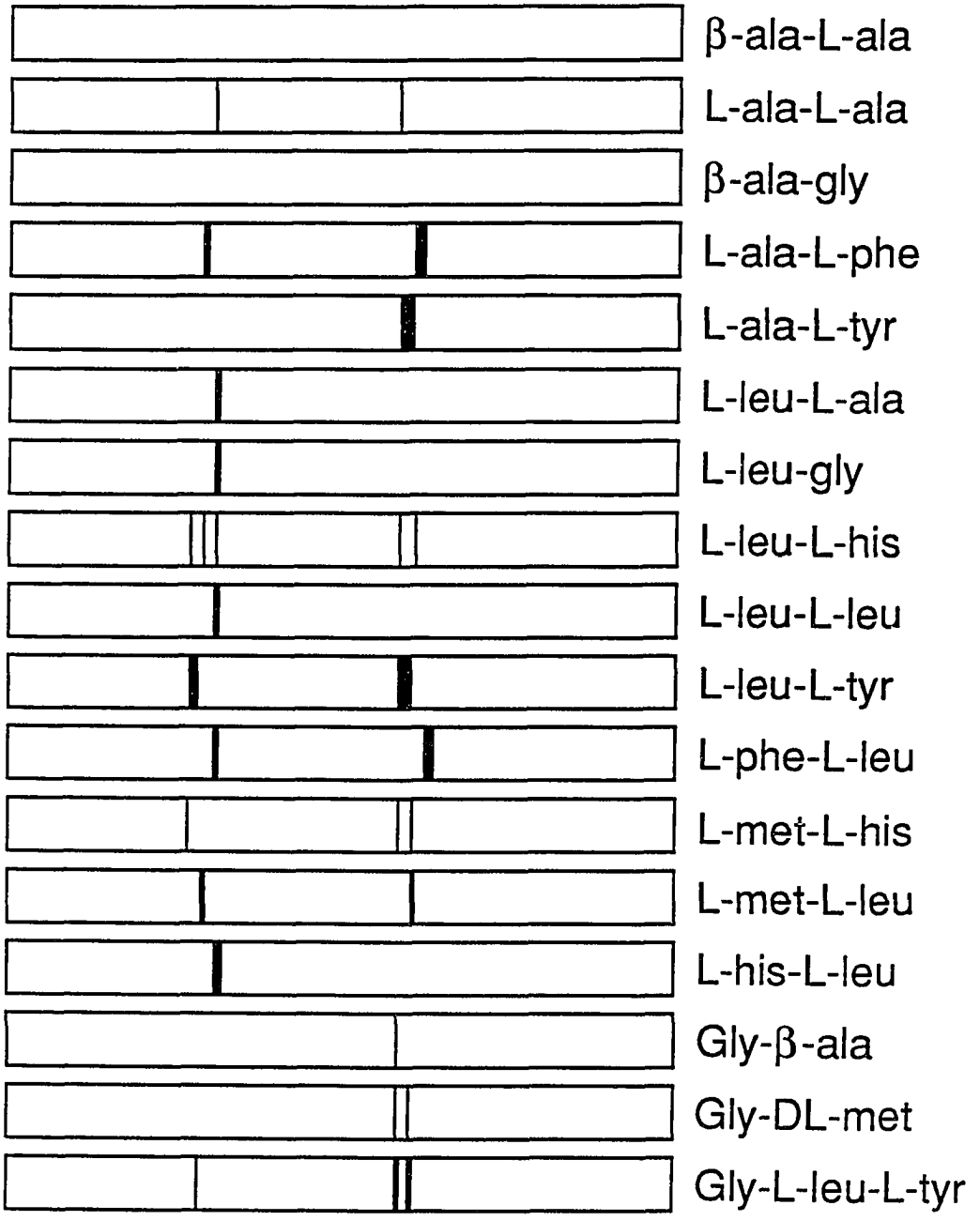

Table 1. Analysis of intracellular peptidohydrolytic enzyme activity using 7.5% polyacrylamide gel electrophoresis with in situ staining at pH 7.0. Hydrolysis of the peptide is indicated by the presence of bands in the gels and shown as -(no hydrolysis), +(very weak hydrolysis), + +(weak hydrolysis), + + +(medium hydrolysis), + + + +(strong hydrolysis).

Peptide	Band					
	A	B	C	D	E	F
Beta-ala-L-ala	-	-	-	-	-	-
L-ala-L-ala	-	-	+	+	-	-
Beta-ala-gly	-	-	-	-	-	-
L-ala-phe	-	++	-	-	++++	-
L-ala-L-tyr	-	-	-	++++	-	-
L-leu-L-ala	-	-	++	-	-	-
L-leu-gly	-	-	++	-	-	-
L-leu-L-his	+	+	+	+	+	-
L-leu-L-leu	-	-	++	-	-	-
L-leu-L-phe	-	-	-	-	-	-
L-leu-L-tyr	+++	-	-	++++	-	-
L-phe-L-leu	-	-	++	-	-	-
L-met-L-his	+	-	-	+	+	-
L-met-L-leu	-	++	-	++	-	-
L-his-L-leu	-	-	+++	-	-	-
Gly-beta-ala	-	-	-	+	-	-
Gly-DL-met	-	-	-	+	+	-
Gly-L-tyr	-	-	-	-	-	-
L-ala-L-ala-L-ala	-	-	-	-	-	-
L-ala-gly-gly	-	-	-	-	-	-
Gly-L-ala-L-leu	-	-	-	-	-	-
Gly-gly-gly	-	-	-	-	-	-
Gly-gly-L-leu	-	-	-	-	-	-
Gly-gly-D-leu	-	-	-	-	-	-
Gly-DL-leu-DL-alpha-ala	-	-	-	-	-	-
Gly-L-leu-L-tyr	-	+	-	++	++	-
Gly-L-phe-L-phe	-	-	-	-	-	-
Gly-sarcosine	-	-	-	-	-	-
L-his-L-gly-gly	-	-	-	-	-	-
L-leu-gly-gly	-	-	-	-	-	-
L-leu-L-leu-L-leu	-	-	-	-	-	-
Tetra-L-ala	-	-	-	-	-	-
Tetra-gly	-	-	-	-	-	-
Gly-gly-L-tyr-arg	-	-	-	-	-	-
Penta-gly	-	-	-	-	-	-
Hexa-gly	-	-	-	-	-	-
Poly-gly	-	-	-	-	-	-

R_m values corresponding to peptides:

A: 0.260- 0.280
B: 0.280- 0.300
C: 0.300- 0.320
D: 0.580- 0.600
E: 0.600- 0.620
F: 0.620- 0.640

Peptidase B, which has a R_m range from 0.28 to 0.30, hydrolyzed three dipeptides (L-alanyl-L-phenylalanine, L-leucyl-L-histidine, L-methionyl-L-leucine) and one tripeptide (glycyl-L-leucyl-L-tyrosine).

Peptidase C, which has a R_m range from 0.30 to 0.32, shows strong activity against a number of the dipeptides listed in Table 1, but not against any of the tripeptides tested. Its substrate specificity, however, was very different from that of peptidase A, except that it also appeared to be primarily a dipeptidase.

Peptidase D, which had a R_m range from 0.58 to 0.60, was very active against L-alanyl-L-tyrosine, L-leucyl-L-tyrosine and the tripeptide glycyl-L-leucyl-L-tyrosine. It showed weaker activity against the dipeptides L-alanyl-L-alanine, L-leucyl-L-histidine, L-methionyl-L-histidine, glycyl-beta-alanine, and glycyl-DL-methione.

Peptidase E, which has a R_m range from 0.60 to 0.62, showed very strong activity towards L-alanyl-L-phenylalanine and also had been detected with L-leucyl-L-histidine, L-methionyl-L-histidine, L-methionyl-L-leucine, glycyl-D-methione and glycyl-L-leucyl-L-tyrosine, but its activity in each case was relatively weak.

Peptidase F had a R_m value range from 0.62 to 0.64, and has so far only been found to show significant activity against L-phenylalanyl-L-leucine.

Therefore, at the substrate concentrations tested, peptidases A, C and F can be defined as dipeptidases and peptidases B, D, E were able to hydrolyze both dipeptides and tripeptides.

Among the eighteen dipeptides tested, only four were resistant to hydrolysis by intracellular peptidohydrolytic enzymes. They are beta-alanyl-L-alanine, beta-alanyl-L-glycine, L-leucyl-L-phenylalanine and glycyl-L-tyrosine. It is suggested therefore that peptides containing an amino terminal beta-amino acid i.e. beta-alanyl-glycine, beta-alanyl-L-alanine, are resistant to hydrolysis by available intracellular peptidases and thus should make good substrates for the study of peptide transport and cancer chemotherapy using peptide-like anticancer drugs. Of all tripeptides tested only glycyl-L-leucyl-L-tyrosine was hydrolyzed by the sum-total intracellular peptidohydrolytic enzymes, the rest of them were shown to be relatively resistant to hydrolysis under the assay conditions employed.

Analysis of extracellular peptidohydrolytic enzyme activity (Figure 10 and Table 2) revealed a total of three electrophoretically distinct peptidase activities. Peptidase 'A', which had a R_m value range from 0.13 to 0.135 hydrolyzed a number of dipeptides (Table 2). The peptidase activity varied somewhat from substrate to substrate in that it was very active against L-leucyl-L-tyrosine, but less

Figure 10. Peptidohydrolytic enzyme activities in ascites fluid of mouse Ehrlich ascites tumor cell bearing mice. Proteins (peptidohydrolases) were separated by 7.5 % polyacrylamide tube gel electrophoresis and stained using an in situ activity stain as described in the materials and methods. The bands represent the activities of peptidohyrolytic enzymes.

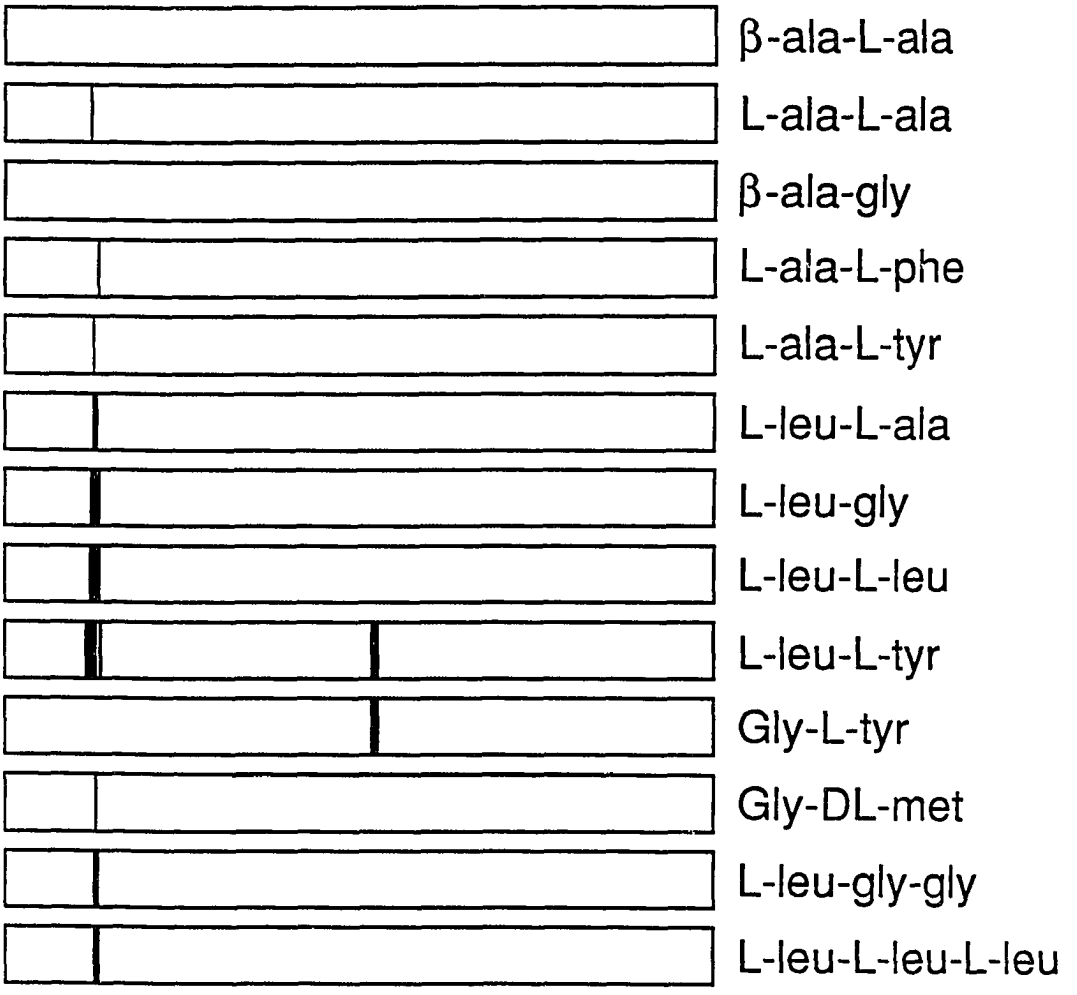

Table 2. Analysis of extracellular peptidohydrolytic enzyme activity using 7.5% polyacrylamide gel electrophoresis with in situ staining at pH 7.0. Hydrolysis of the peptide is indicated by the presence of bands in the gels and shown as -(no hydrolysis), +(very weak hydrolysis), + +(weak hydrolysis), + + +(medium hydrolysis), + + + +(strong hydrolysis), + + + + +(very strong hydrolysis).

Peptide	Band		
	A'	B'	C'
Beta-ala-L-ala	-	-	-
L-ala-L-ala	+	-	-
Beta-ala-gly	-	-	-
L-ala-L-phe	-	+	-
L-ala-L-tyr	+	-	-
L-leu-L-ala	+ +	-	-
L-leu-gly	+ +	-	-
L-leu-L-leu	+ + +	-	-
L-leu-L-tyr	+ + + + +	+	+ +
Gly-L-tyr	-	-	+ +
Gly-DL-met	+	-	-
Tri-L-ala	-	-	-
L-ala-gly-gly	-	-	-
Gly-L-ala-L-leu	-	-	-
Tri-gly	-	-	-
Gly-gly-L-leu	-	-	-
Gly-gly-D-leu	-	-	-
Gly-DL-leu-alpha-ala	-	-	-
Gly-L-phe-L-phe	-	-	-
Gly-sarcosine	-	-	-
L-his-gly-gly	-	-	-
L-leu-gly-gly	+ +	-	-
L-leu-L-leu-L-leu	+ +	-	-
Tetra-L-ala	-	-	-
Tetra-gly	-	-	-
Gly-gly-L-tyr-L-arg	-	-	-
Penta-gly	-	-	-
Hexa-gly	-	-	-
Poly-gly	-	-	-

R_m values corresponding to peptides:

A': 0.130- 0.135
B': 0.140- 0.145
C': 0.520- 0.550

active towards the tripeptides, L-leucyl-glycyl-glycine and L-leucyl-L-leucyl-L-leucine (Table 2). Peptidase B', which had a R_m range from 0.140 to 0.145, showed weak activity against L-alanyl-L-phenylalanine and L-alanyl-L-tyrosine. No hydrolysis of any of the tripeptides was observed. Peptidase C', which had a R_m value range from 0.520 to 0.550, also hydrolyzed two dipeptides, L-alanyl-L-tyrosine and glycyl-L-tyrosine, and none of the tripeptides. Both peptidase B' and C' appear to be primarily dipeptidases.

Among the eleven dipeptides tested, only beta-alanyl-L-alanine and beta-alanyl-glycine were resistant to hydrolysis by extracellular peptidohydrolytic enzymes. These results support the suggestion that peptides containing an amino terminal beta-amino acid are good candidates for use in the design of anticancer drugs and of those peptides larger than a dipeptide, only L-leucyl-glycyl-glycine and L-leucyl-L-leucyl-L-leucine were hydrolyzed under conditions of this assay by the extracellular peptidohydrolytic enzymes.

IV. Synthesis and Purification of Beta-alanyl-melphalan (BAM):

The synthesis of the dipeptide utilized in this study involved the condensation of N-tert-butyloxycarbonyl-beta-alanine (BOC-beta-alanine) with the bifunctional alkylating agent melphalan. The melphalan and BOC-beta-alanine were purchased from Sigma Chemical Company. Analysis of the purity of these two reactants by high-performance liquid chromatography (HPLC) (figures 11 and

Figure 11. High-performance liquid chromatographic (HPLC) analysis of BOC-beta-alanine. Retention time (RT; in minutes) of materials eluting from the C_{18} column and absorbing at 210 nm.

[HPLC ANALYSIS OF BOC—BETA—ALANINE]

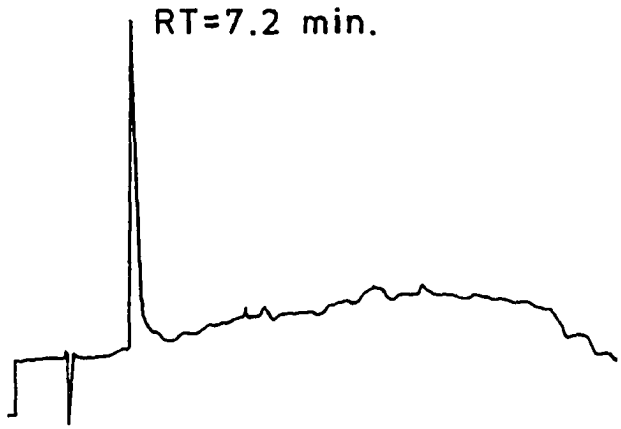

12) revealed that they were essentially pure, as determined by absorbance at 210 nm. The melphalan contained a minor contaminant which eluted early and constituted less than 10% of the 210 nm absorbing material (Figure 12).

Following condensation of the reactants, the dipeptide BOC-beta-alanyl-melphalan was analyzed for purity and completeness of reaction. The reaction was continuously monitored for ninhydrin-positive materials during the course of the reaction. HPLC analysis of the final product revealed the presence of a minor trace of materials absorbing at 210 nm, and a major peak at the position of 21.2 min, at which the BOC-beta-alanyl-melphalan eluted and which comprised over 96% of the available material eluting from the column (Figure 13). As demonstrated in Figure 11, the product was essentially pure, and the major portion of the synthetic product was stored frozen (-20° C) in a desiccator. The derivitized dipeptide was a white powdery material that could be easily weighed and aliquoted. Deblocking the peptide, i.e. conversion of BOC-beta-alanyl-melphalan to beta-alanyl-melphalan (BAM), resulted in the conversion of a dry powdery material into an oily residue which was difficult to weigh. Consequently, only a sufficient quantity of dipeptide was deblocked at any one time to permit testing over a period of 1 to 2 months.

Following deblocking, the TFA salt form of beta-alanyl-melphalan (Figure 14) was converted to the HCl salt form prior to analysis and utilization in toxicity testing. HPLC analysis of the TFA salt form of beta-alanyl-melphalan revealed a

Figure 12. High-performance liquid chromatographic (HPLC) analysis of melphalan. Retention time (RT; in minutes) of materials eluting from the C_{18} column and absorbing at 210 nm.

[HPLC ANALYSIS OF MELPHALAN]

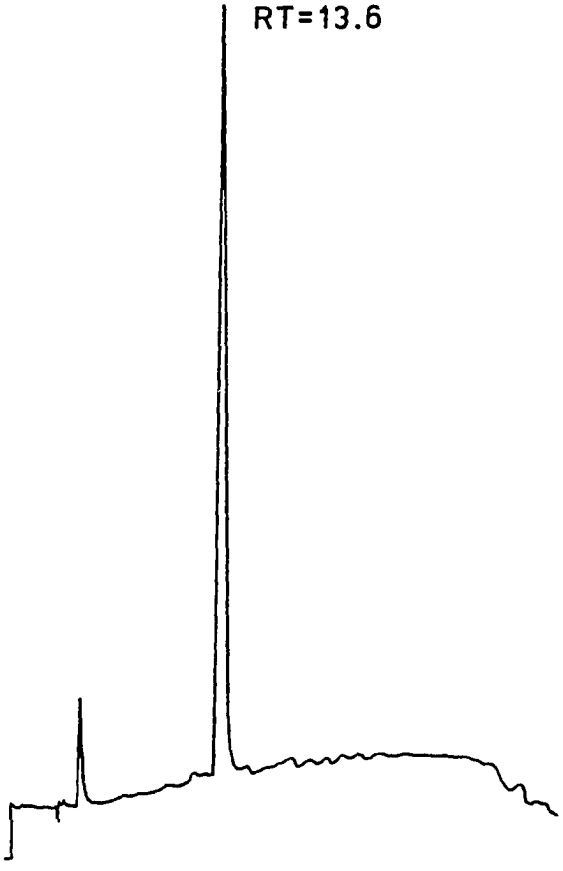

Figure 13. High-performance liquid chromatographic (HPLC) analysis of the immediate product of peptide synthesis, BOC-beta-alanyl-melphalan. Retention time (RT; in minutes) of materials eluting from the C_{18} column and absorbing at 210 nm.

[HPLC ANALYSIS OF BOC—BETA—ALANYL—MELPHALAN]

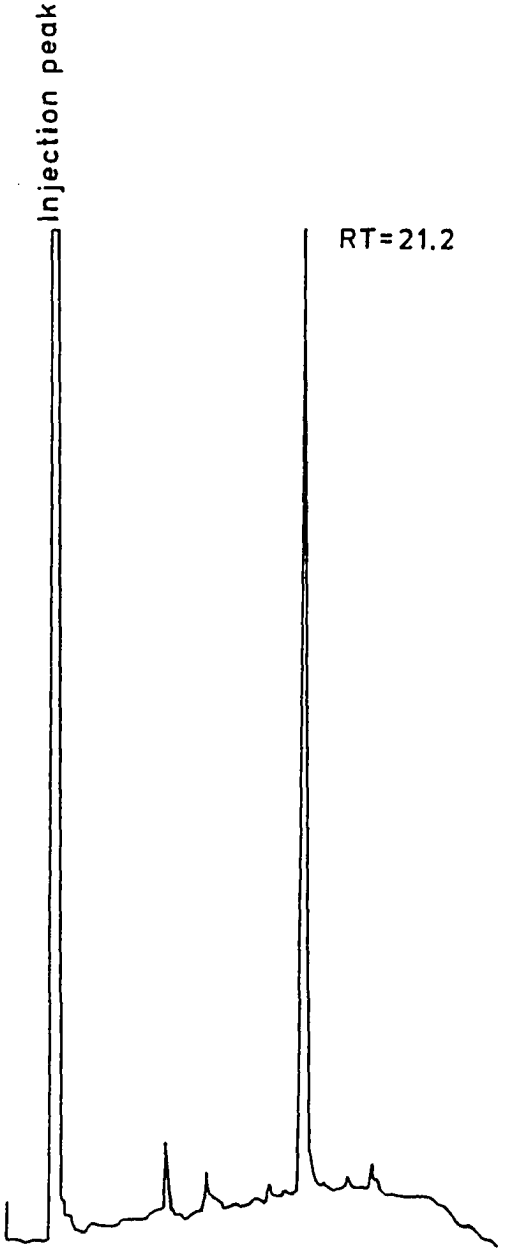

Figure 14. High-performance liquid chromatographic (HPLC) analysis of the TFA salt form of beta-alanyl-melphalan. Retention time (RT; in minutes) of materials eluting from the C_{18} column and absorbing at 210 nm.

[HPLC ANALYSIS OF BETA—ALANYL—MELPHALAN • TFA]

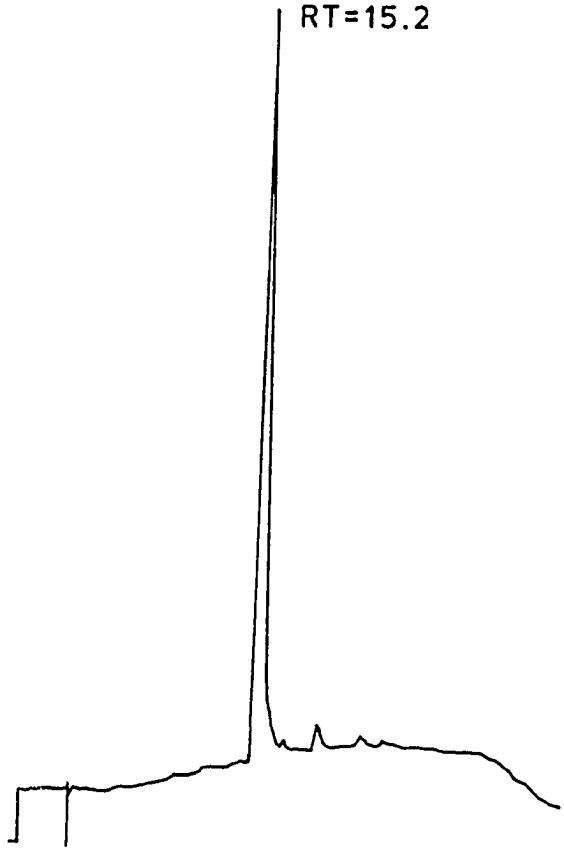

single major peak of 210 nm absorbing eluting at 15.2 min. Analysis of the HCl salt form of beta-alanyl-melphalan by HPLC revealed the presence of at least three 210 nm absorbing compounds comprising less than 14% of the total 210 nm absorbing materials. The absorbance of these "contaminant" peaks in the HCl salt form of the beta-alanyl-melphalan indicates that they are the result of the generation of the HCl salt form of beta-alanyl-melphalan from the TFA salt form of beta-alanyl-melphalan. The major peak of 210 nm absorbing materials (beta-alanyl-melphalan) eluted at 15.2 min and comprised over 85% of the available material eluting from the column (Figure 15). The retention time of beta-alanyl-melphalan HCl was significantly different from the retention times of melphalan (13.6 minutes) and BOC-beta-alanine (7.2 minutes).

V. Chemical Stability of Melphalan and Beta-alanyl-melphalan:

Alkylating agents are typically chemically reactive, i.e. unstable, and are thus inherently difficult to work with. The main product of hydrolysis is the dihydroxy compound, and the intermediate monohydroxy compound also can be found (diagram 1). High-performance liquid chromatography (HPLC) was used to investigate stability of solutions of melphalan under conditions that pertain to analysis of in vitro toxicity and in vivo chemotherapy.

A representative example (melphalan) of the chromatograms produced with HPLC used in this work is given in Figure 16. The chromatogram shows a minor

Figure 15. High-performance liquid chromatographic (HPLC) analysis of the HCl salt form of beta-alanyl-melphalan. Retention time (RT; in minutes) of materials eluting from the C_{18} column and absorbing at 210 nm.

[HPLC ANALYSIS OF BETA—ALANYL—MELPHALAN • HCl]

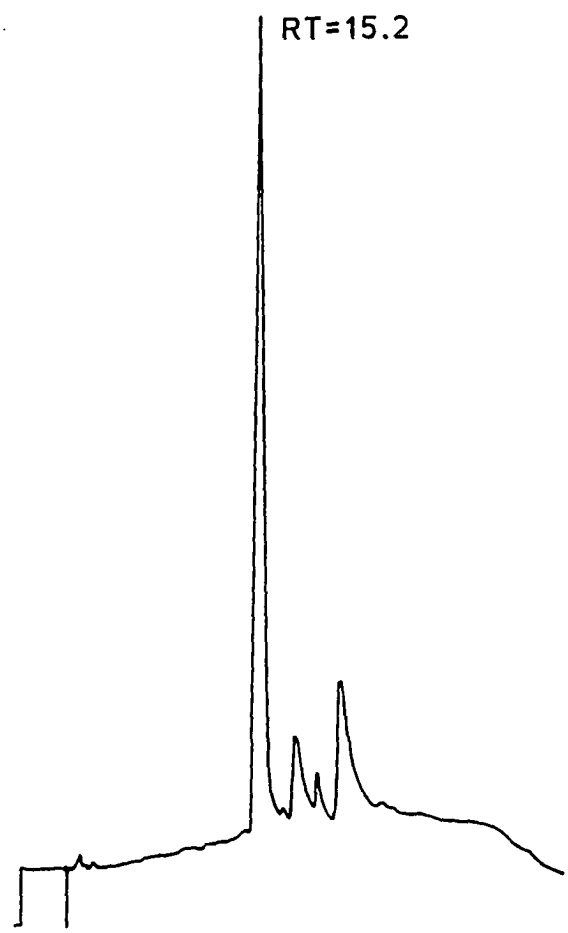

Diagram 1:

Spontaneous degradation of melphalan in aqueous solution.

Melphalan (4-bis-(2-chloroethyl) amino-L-phenylalanine)

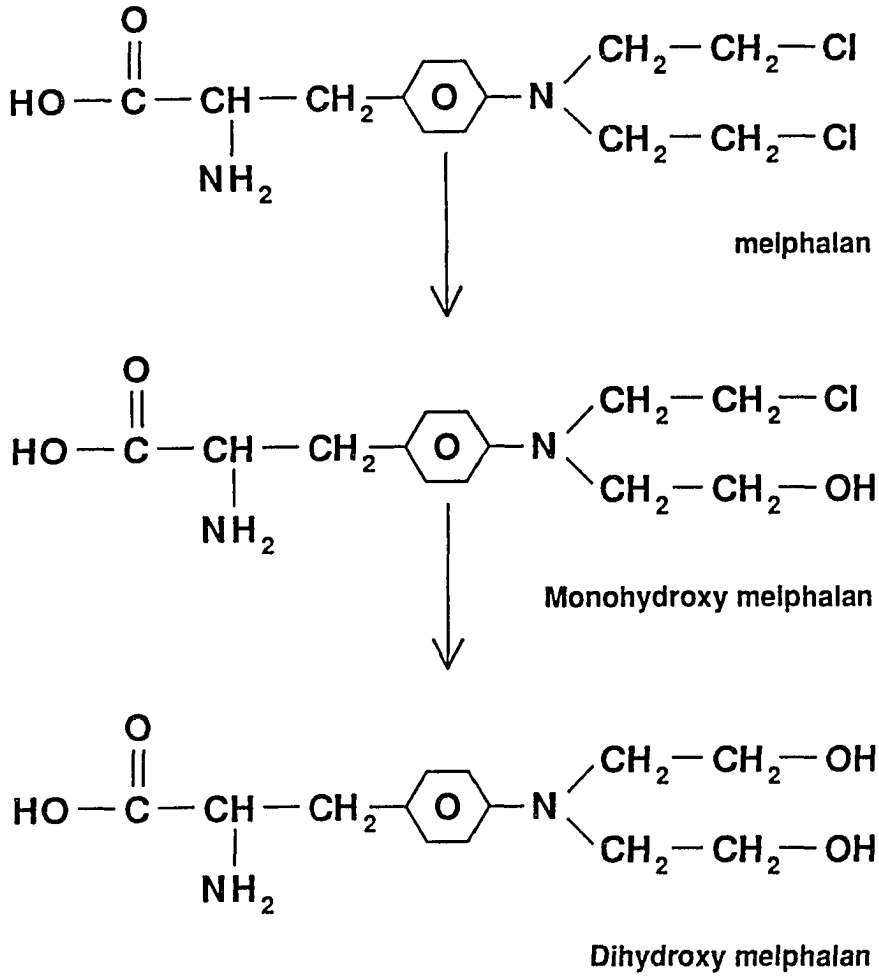

Figure 16. Chromatogram from the high-performance liquid chromatograph (HPLC) showing peaks of freshly-made melphalan (3 mg/ml) dissolved in distilled water. Absorbance monitored at 254 nm. The injection point is indicated by a vertical line. Two products were present, one eluting at 2.25 minutes and the other, at 8.81 minutes. Peak 2 represents melphalan and peak 1 represents the hydrolysis product of melphalan (dihydroxy melphalan). The first peak constitutes 7% of total material which indicates the purity of melphalan is 93%.

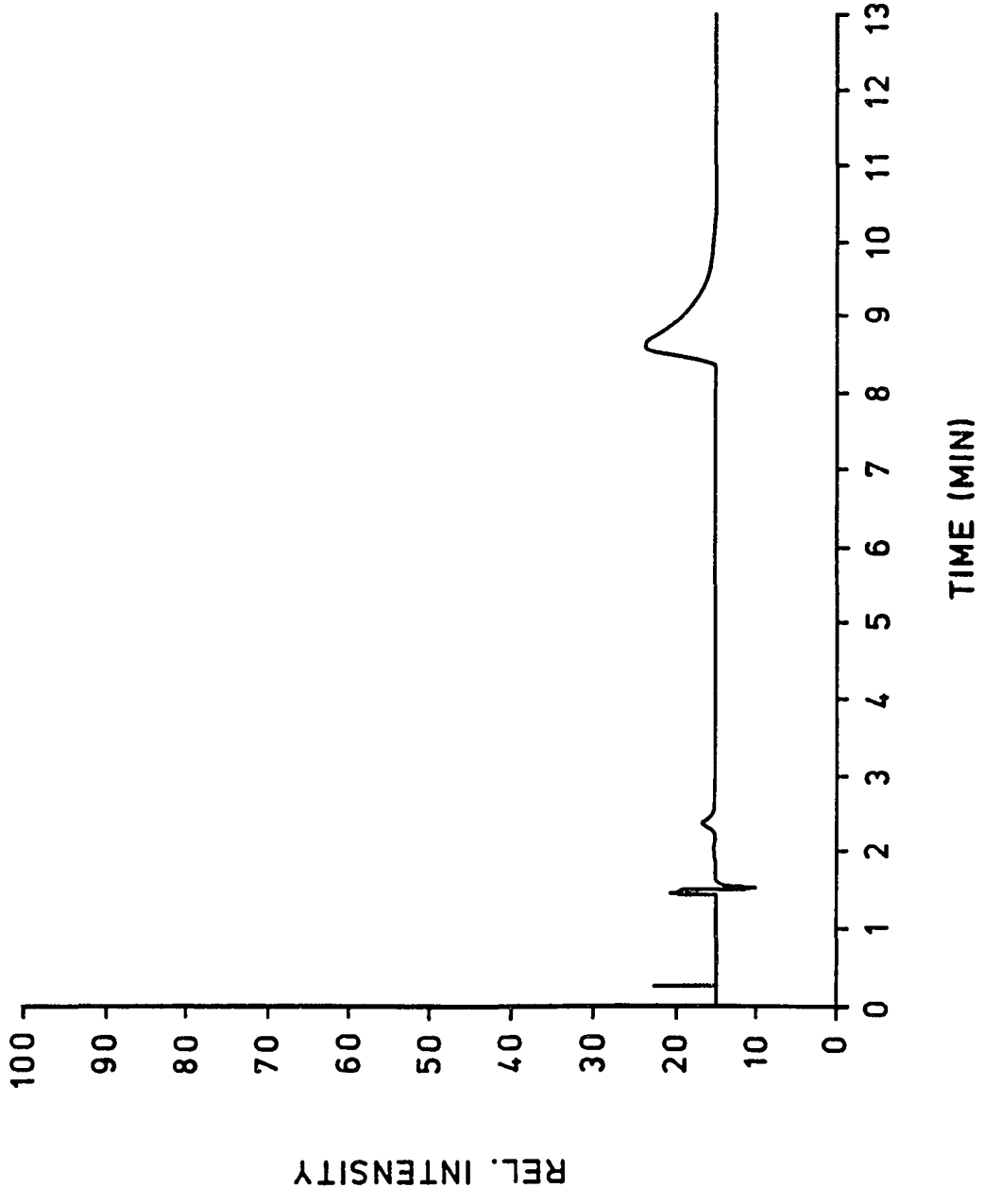

peak (peak 1) at 2.25 minutes and a major peak (peak 2) at 8.81 minutes. The major peak represents melphalan whereas the minor peak represents the breakdown products of melphalan, either monohydroxy melphalan or dihydroxy melphalan. It is unknown whether the monohydroxy or dihydroxy form of melphalan is preferentially formed during chemical decomposition of melphalan. In order to identify peak 1 in the HPLC chromatogram, dihydroxy melphalan was obtained via a complete hydrolysis of melphalan by incubation in glass distilled H_2O at 60° C in a water bath for 2 hours. HPLC analysis of this incubation solution revealed only one major peak with a retention time of 2.17 minutes (Figure 17). The results indicated that the first peak in the chromatographic profile in Figure 16 is dihydroxy melphalan. These results further indicated that this type of analysis is suitable for study of the stability of melphalan, as the peak of the only known degradation product was well separated from the peak of its parent drug melphalan.

The hydrolysis rate of melphalan to dihydroxy melphalan in distilled water at different temperatures was studied. Melphalan (3 mg/ml) was dissolved in distilled water and incubated at 0° C and 37° C. Samples were taken at designated times and analyzed by HPLC. As shown in Table 3, the percentage of peak area of melphalan (peak 2) decreases from 92.45% (9.088 nmole) at zero time to 42.33% (4.161 nmole) after 120 minutes of incubation at 37° C. In contrast, peak 1 (dihydroxy melphalan) exhibited an increase in the percentage of peak area from 7.54% (0.741 nmole) at zero time to 57.67% (5.668 nmole) after

Figure 17. Chromatogram from the high-performance liquid chromatography (HPLC) of the hydrolysis product of melphalan (dihydroxy melphalan). Dihydroxy melphalan was obtained via a complete hydrolysis of melphalan (3 mg/ml) in distilled water at 60° C in a water bath for 2 hours. Only one product was present with a retention time of 2.17 minutes.

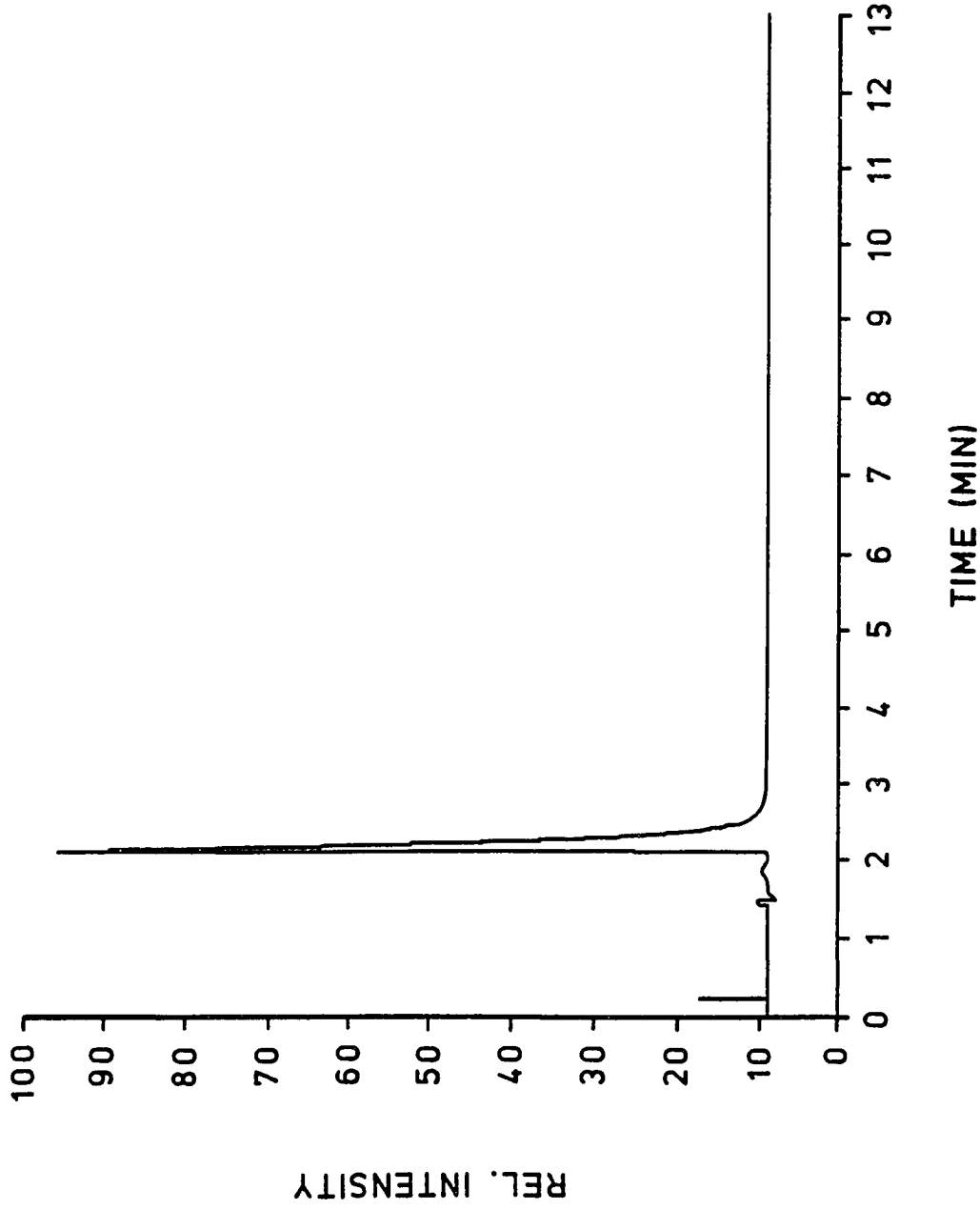

Table 3. High-performance liquid chromatography (HPLC) Analysis of Melphalan in distilled water at 0° C.

Time	Peak #	RT	% of Peak Area	Concentration
0	1	2.35	6 .92	0.680
	2	8.65	93.08	9.150
60	1	2.54	6.36	0.625
	2	8.79	93.64	9.205
120	1	2.19	6.89	0.677
	2	8.21	93.11	9.153

a. Peak number corresponds to appearance of 254 nm absorbance material from C_{18} column.

b. RT= Retention Time in minutes.

c. % of Peak Area is obtained by adding the peak areas of 1 and 2, and then dividing each peak area by the total area.

d. concentration is obtained from a standard curve of melphalan correlating peak area of peak 2 with nmole of melphalan analyzed.

120 minutes incubation at 37° C. These results indicated that 45% of the melphalan had broken down to dihydroxy melphalan after 120 minutes incubation at 37° C. Table 4 presents data from the HPLC analysis of melphalan in distilled water at 0° C. The results revealed that the percentage of the peak area of peak 2 (melphalan) decreased from 93.08% (9.150 nmole) at zero time and to 93.11% (9.153 nmole) after 120 minutes incubation at 0° C. The percentage of peak 1 (dihydroxy melphalan) decreased from 6.92% (0.680 nmole) at zero time to 6.89% (0.677 nmole) after 120 minutes incubation at 0° C. The results indicated that melphalan did not break down over the 120 minutes of incubation at 0° C. The hydrolysis of melphalan in distilled water as a function of incubation time at 0° C and 37° C is shown graphically in Figures 18 and 19, respectively. When melphalan solution was incubated on ice, the results revealed that there was no significant change in peak area of either peak 1 or 2 over an incubation interval of 120 minutes (Figure 18). The degradation rate of melphalan at 37° C (Figure 19) is much faster than at 0° C. These results indicated that melphalan was degraded to hydroxy melphalan as a linear function of time. A direct comparison of hydrolysis of melphalan in distilled water at 0° C and 37° C is shown in Figure 20. A rapid degradation is shown with a rate constant of 0.433 nmole of melphalan degradation per minute at 37° C. A very slow degradation rate was observed with a rate constant of 0.00025 nmole of melphalan degradation per minute at 0° C. An Analysis of Covariance (ANCOVA), examining the significance of the difference of slope between 37° C and 0° C, was statistically significant ($p < 0.005$). This shows that the breakdown process of melphalan was

Table 4. High-performance liquid chromatography (HPLC) Analysis of Melphalan in distilled water at 37° C.

Time	Peak #	RT	% of Peak Area	Concentration
0	1	2.49	7.54	0.741
	2	9.01	92.45	9.088
30	1	2.32	13.73	1.350
	2	8.55	86.27	8.480
60	1	2.39	29.82	2.931
	2	8.44	70.18	6.899
120	1	2.23	57.67	5.668
	2	8.19	42.33	4.161

a. Peak number corresponds to appearance of 254 nm absorbance material from C_{18} column.

b. RT= Retention Time in minutes.

c. % of Peak Area is obtained by adding the peak areas of 1 and 2, and then dividing each peak area by the total area.

d. concentration is obtained from a standard curve of melphalan correlating peak area of peak 2 with nmole of melphalan analyzed.

Figure 18. Degradation of melphalan (3 mg/ml) in distilled water at 0° C. Samples were taken at designated times and analyzed by high-performance liquid chromatography (HPLC). Peak 1 represents the hydrolysis product of melphalan whereas peak 2 represents melphalan. Peak areas integrated using the Isco ChemResearch computer program were converted to the concentrations of melphalan (in nmole) using a standard curve of melphalan concentrations versus peak areas.

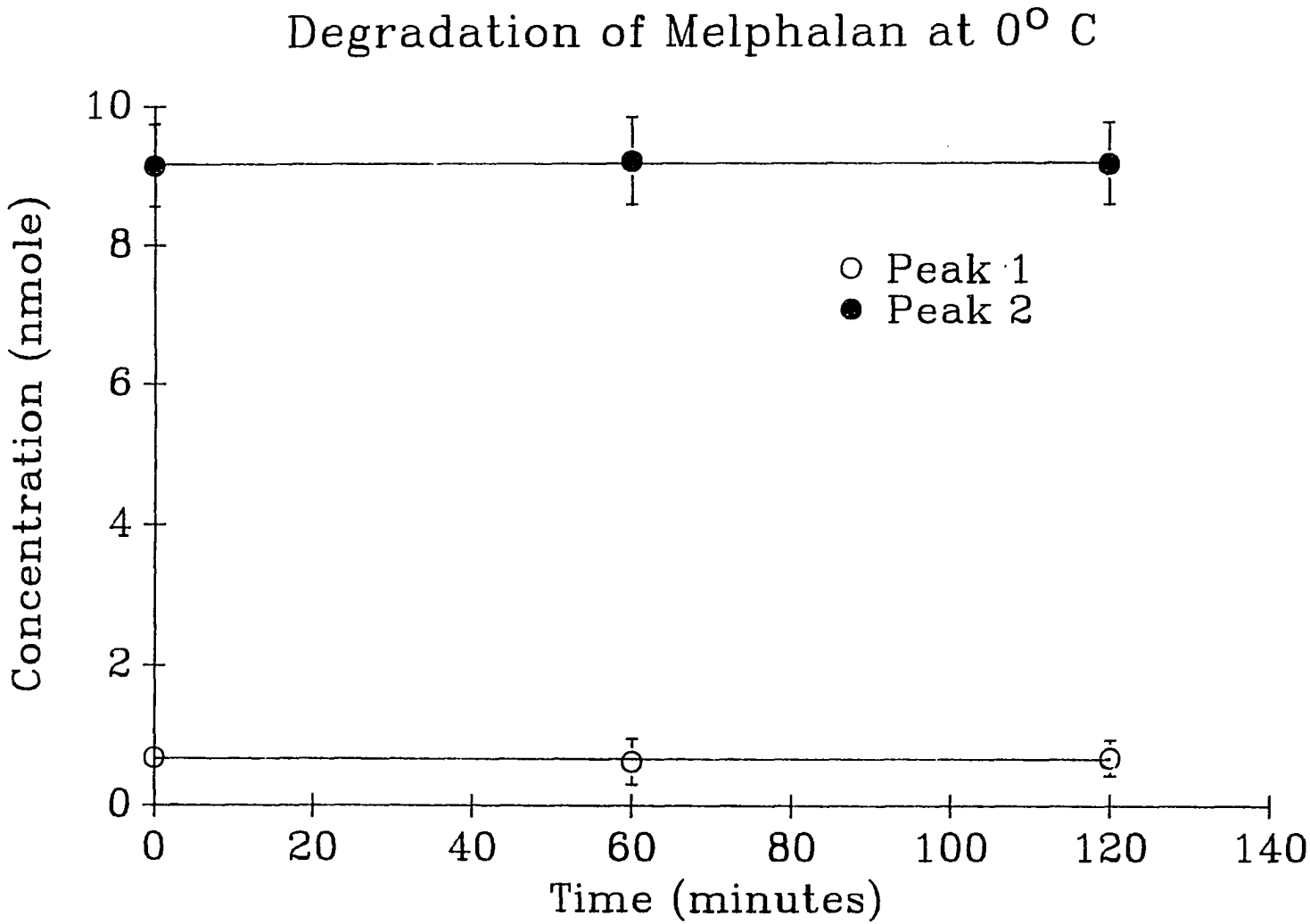

Figure 19. Degradation of melphalan (3 mg/ml) in distilled water at 37° C. Samples were taken at designated times and analyzed by high-performance liquid chromatography (HPLC). Peak 1 represents the hydrolysis product of melphalan whereas peak 2 represents melphalan. Peak areas integrated using the Isco ChemResearch computer program and then converted to the concentration of melphalan (in nmole) using a standard curve of melphalan concentrations versus peak areas.

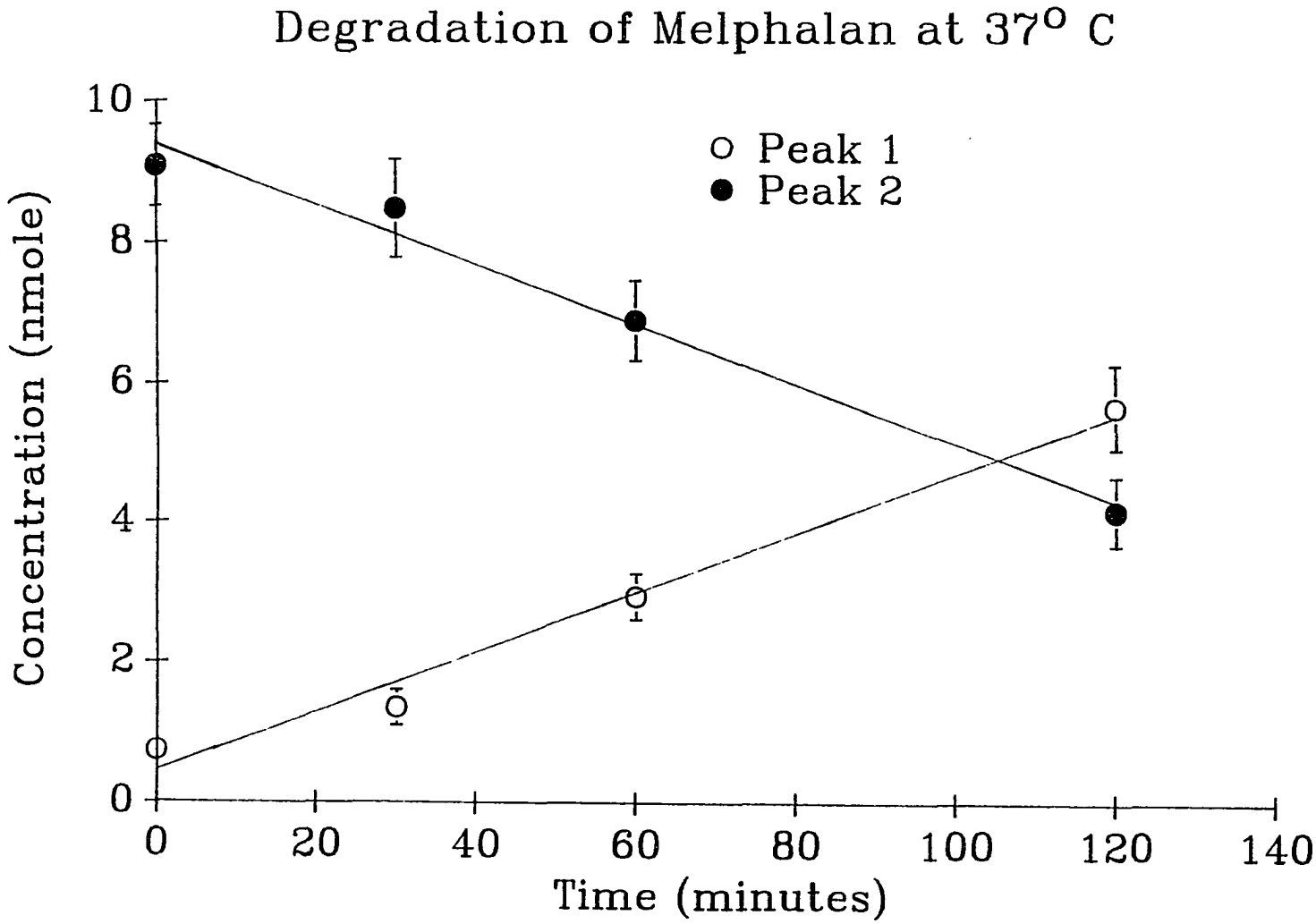

Figure 20. Comparison of degradation of melphalan (3 mg/ml) in distilled water at 0° C and 37° C. Samples were taken at designated times and analyzed by high-performance liquid chromatography (HPLC). Peak areas integrated using the Isco ChemResearch computer program were converted to the concentration of melphalan (in nmole) using a standard curve of melphalan concentration versus peak area.

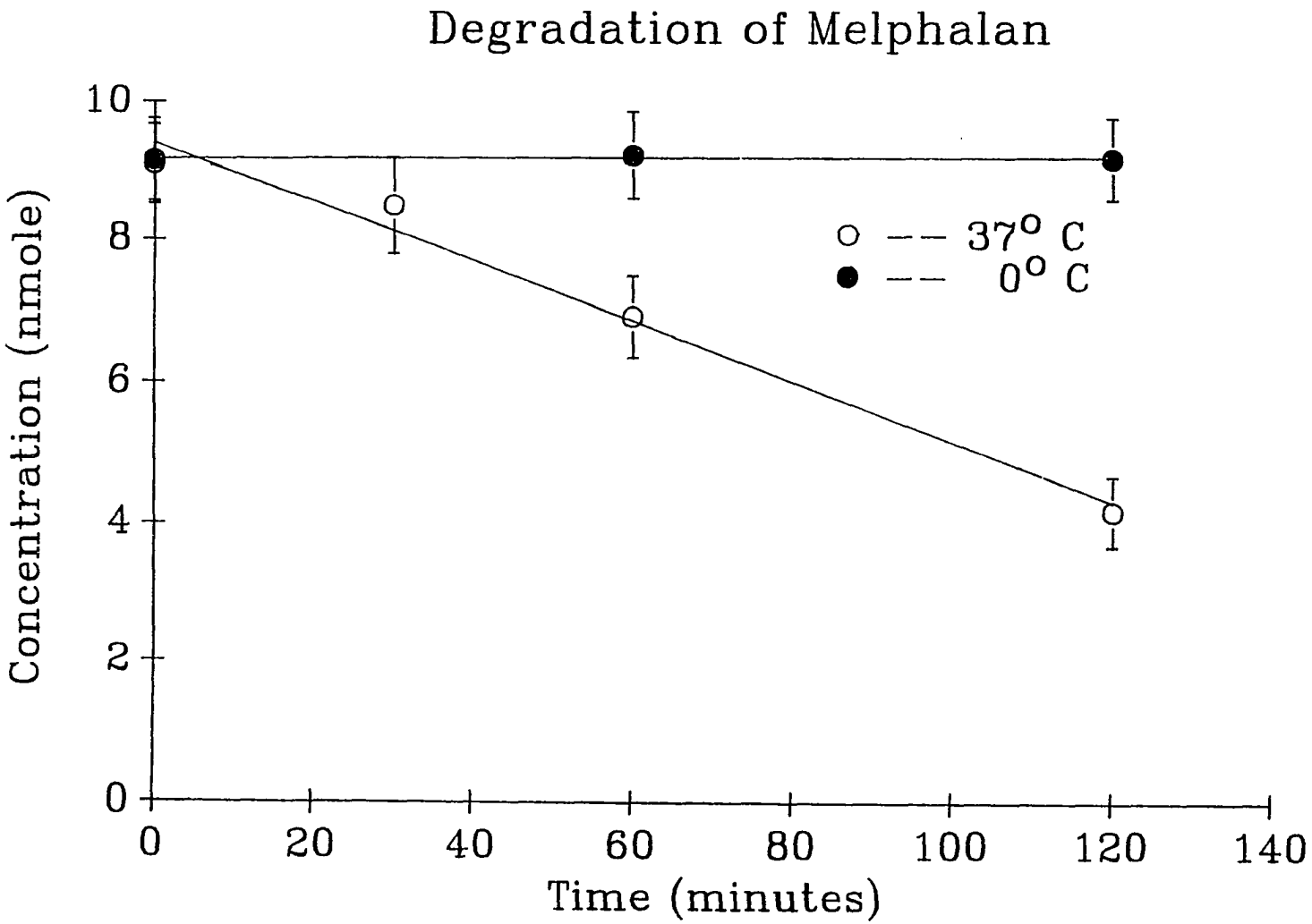

slower at the lower temperature.

The stability of melphalan was also studied under a variety of aqueous conditions. Melphalan was added to various concentrations of bovine serum albumin and incubated at 37° C. The hydrolysis of melphalan in water solutions of bovine serum albumin at 37° C as a function of incubation time is shown in Figure 21. Hydrolysis rate constants of melphalan in BSA solution are 0.313 nmole per minute (10% BSA) and 0.227 nmole per minute (30% BSA). The results revealed that the hydrolysis rate of melphalan was retarded approximately 25% and 48% by 10% and 30% BSA, respectively. ANCOVA analysis showed that there was no significant difference between melphalan degradation in 0% BSA and 10% BSA, but there was a significant difference between melphalan degradation in 0% BSA and 30% BSA ($p < 0.005$). When melphalan degradation rates in 10% BSA and 30% BSA were compared, significant differences were also found ($p < 0.005$). The results indicated that inclusion of BSA, and perhaps other proteins, may stabilize melphalan, especially at higher concentrations of BSA.

Having determined the stability of melphalan before it was put into an in vitro assay, experiments were performed to determine its stability under typical in vitro assay conditions. Melphalan was added to NCTC-135 cell culture medium supplemented with 10% fetal bovine serum (FBS) and incubated at 37° C. The degradation of melphalan in FBS supplemented NCTC-135 medium at 37° C as a

Figure 21. Comparison of degradation rates of melphalan (3 mg/ml) in varied concentrations (0%, 10%, 30%, w/v) of bovine serum albumin (BSA). Samples were taken at designated times and analyzed by high-performance liquid chromatography (HPLC). Peak areas integrated using the Isco ChemResearch computer program were converted to the concentration of melphalan (in nmole) using a standard curve of melphalan concentration versus peak area.

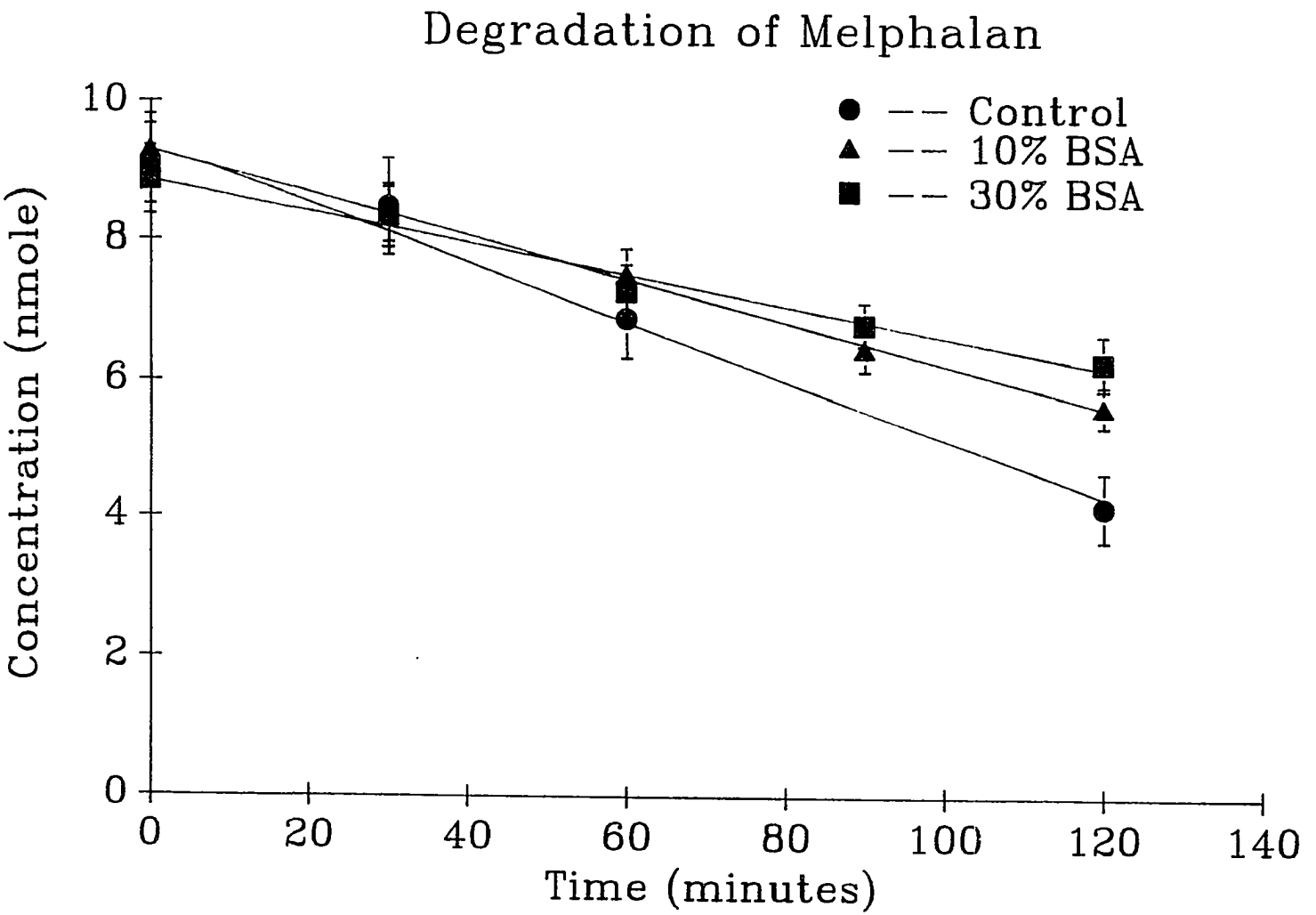

Figure 22. Degradation of melphalan (3 mg/ml) in NCTC-135 medium supplemented with 10% fetal bovine serum at 37°C. Samples were taken at designated times and analyzed by high-performance liquid chromatography (HPLC). Peak areas integrated using the Isco ChemResearch computer program were converted to the concentrations of melphalan using a standard curve of melphalan concentration versus peak area. Peak 1 represents the hydrolysis product of melphalan and peak 2 represents melphalan.

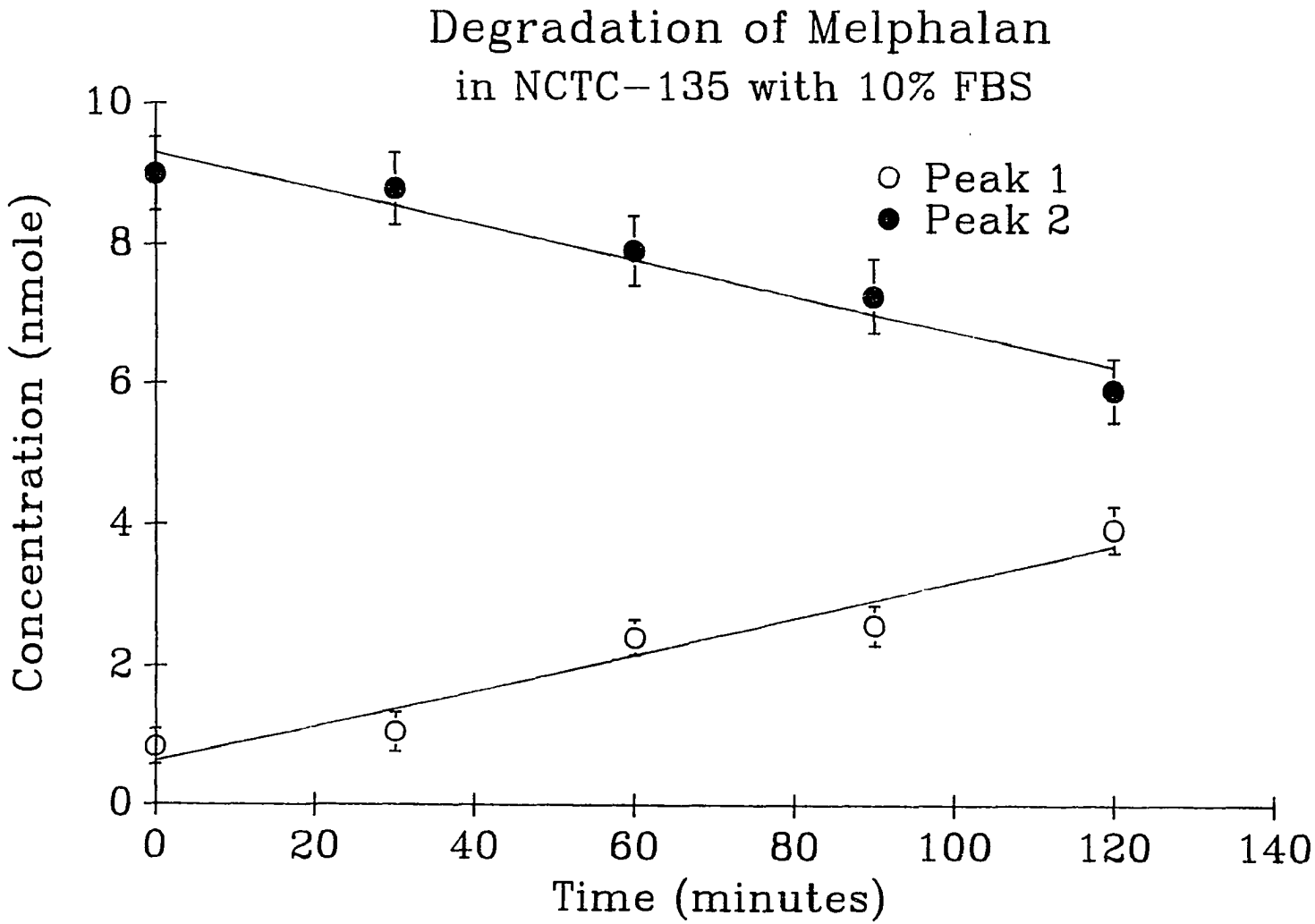

function of incubation time is shown in Figure 22. The hydrolysis rate of melphalan in FBS supplemented NCTC-135 medium is 0.262 nmole per minute. ANCOVA analysis revealed there is no significant difference between melphalan degradation in FBS supplemented NCTC-135 medium and distilled water, or 10% BSA, or 30% BSA. However, the results still indicated that FBS supplemented NCTC-135 medium slowed down the hydrolysis process by 37% when compare to the rate of hydrolysis in distilled water.

No significant change in melphalan concentration was seen when 3 mg/ml melphalan was stored at 0° C for 3 weeks (9.25 nmole to 8.20 nmole). However, from the results in Table 5 a half-life of 105.21 minutes was calculated for melphalan incubated at 37° C. The calculated half-life of melphalan was 176.72 minutes and 142.64 minutes when melphalan was incubated at 37° C in aqueous solutions of 30% and 10% BSA (w:v) respectively. A half-life of 166.82 minutes was calculated for melphalan incubation in NCTC-135 medium supplemented with 10% FBS. There is essentially no difference in decomposition of melphalan in 30% BSA, 10% BSA and supplemented NCTC-135 medium, however, the results showed that there was a significant difference between distilled water and 30% BSA at 37° C ($p < 0.005$). There was also a significant difference between 10% BSA and 30% BSA at 37°C ($p < 0.005$). Based on the available results to may be suggested that melphalan can be stored at 0° C for a period of 3 weeks without significant decomposition.

Table 5. Stability of melphalan in various solutions as analyzed by high-performance liquid chromatography (HPLC).

Condition	Half-life (minute)
Distilled water, 0° C	Below Detection Limit
Distilled water, 37° C	105.21
Bovine serum albumin (10%), 37° C	142.64
Bovine serum albumin (30%), 37° C	176.72
NCTC-135 medium with 10% fetal bovine serum, 37° C	166.82

Studies on the stability of beta-alanyl-melphalan has been restricted, due to a limited supply of beta-alanyl-melphalan. A typical HPLC chromatograph of beta-alanyl-melphalan is shown in Figure 23. One major peak (peak 2) was seen at about 13.3 minutes and one minor peak (peak 1) was seen at about 7.4 minutes. According to the study of melphalan hydrolysis, the major peak presumably represents beta-alanyl-melphalan and the minor peak represents hydrolysis product, i.e. beta-alanyl-dihydroxy-melphalan.

Freshly prepared beta-alanyl-melphalan (4.13 mg/ml) was dissolved in distilled water and incubated at 37° C in a water bath. As shown in table 6, the percentage of peak area of beta-alanyl-melphalan decreased from 93.35% (6.254 nmole) at zero time to 84.92% (5.690 nmole) after 120 minutes incubation at 37° C. The percentage of peak area of peak 1 (dihydroxy form of beta-alanyl-melphalan) increased from 6.65% (0.446 nmole) at zero time to 15.08% (1.010 nmole) after 120 minutes incubation. The hydrolysis of beta-alanyl-melphalan in distilled water at 37° C as a function of time is shown in Figure 24. A degradation rate of 0.0705 nmole per minute was calculated, which is much slower than the calculated hydrolysis rate of melphalan at 37° C (0.433 nmole per minute). The calculated half-life of beta-alanyl-melphalan in distilled water at 37° C was 607.71 minutes, which was about 5.6 times longer than the half-life of melphalan incubated in distilled water at 37° C.

Figure 23. Typical high-performance liquid chromatography (HPLC) tracing showing peaks of freshly-made beta-alanyl-melphalan (4.13 mg/ml) dissolved in distilled water. Absorbance was monitored at 254 nm. The injection point is indicated by a vertical line. One minor peak eluted at 7.4 minutes and one major peak eluted at 13.3 minutes. Peak 1 presumably represents the hydrolysis product of beta-alanyl-melphalan (beta-alanyl-dihydroxy-melphalan) and peak 2 represents beta-alanyl-melphalan.

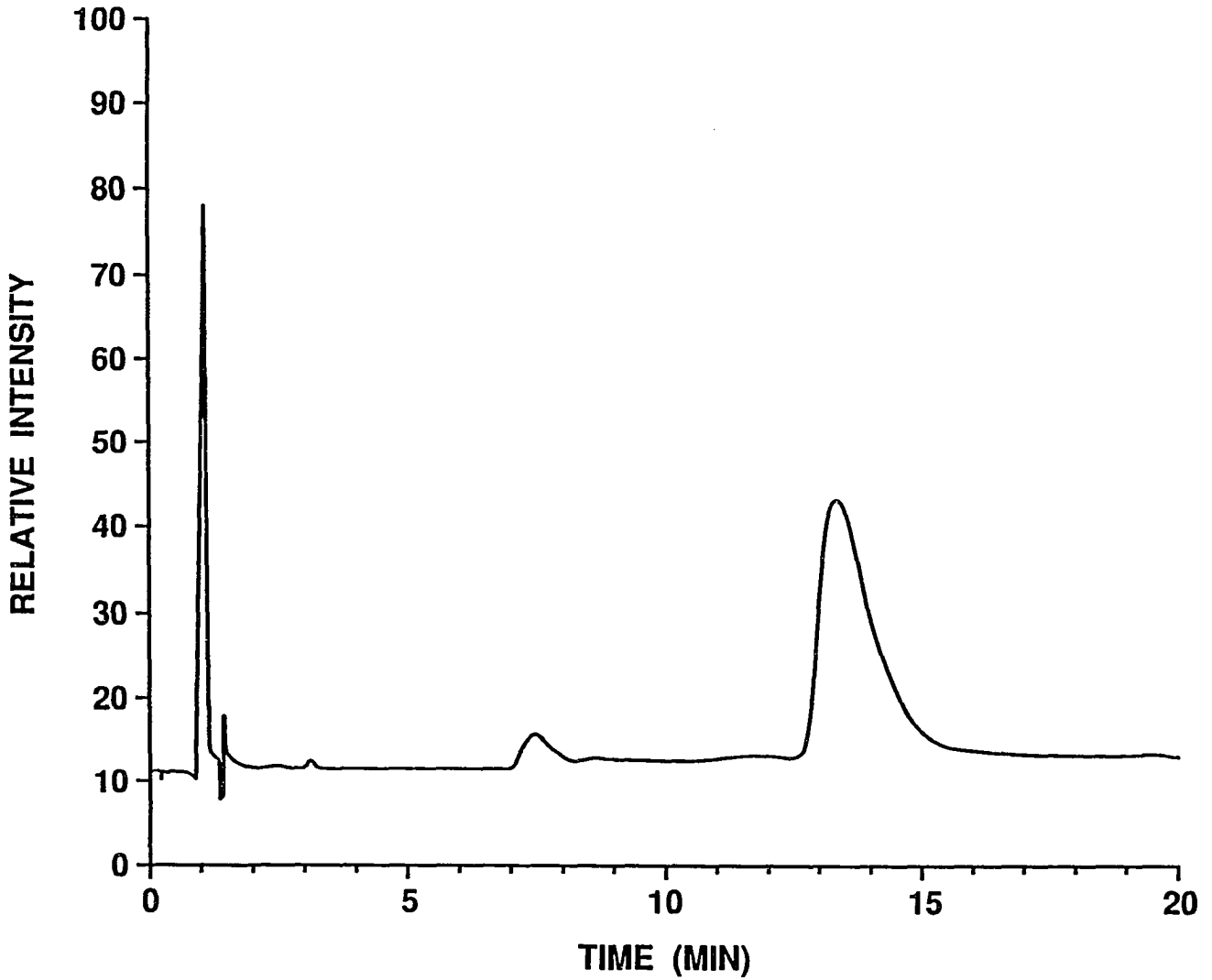

Table 6. High-performance liquid chromatography (HPLC) analysis of beta-alanyl-melphalan incubated in distilled water at 37° C for the indicated time intervals.

Time	Peak #	RT	% of Peak Area	Concentration
0	1	6.8	6.65	0.446
	2	12.8	93.35	6.254
30	1	7.2	9.96	0.667
	2	13.2	90.04	6.033
60	1	7.9	10.90	0.730
	2	13.8	89.10	5.970
90	1	7.6	14.26	0.955
	2	13.5	85.74	5.745
120	1	7.8	15.08	1.010
	2	13.9	84.92	5.690

a. Peak number corresponds to appearance of 254 nm absorbance material from C_{18} colum.

b. RT= Retention Time in minutes.

c. % of Peak Area is obtained by adding the peak areas of 1 and 2, and then dividing each peak area by the total area.

d. Concentration is obtained from a standard curve of beta-alanyl-melphalan where peak area was correlated with nmole of peptide analyzed.

Figure 24. Degradation of beta-alanyl-melphalan (4.13 mg/ml) in distilled water at 37°C. Samples were taken at designated times and analyzed by high-performance liquid chromatography (HPLC). Peak 1 represents the hydrolysis product of beta-alanyl-melphalan whereas peak 2 represents beta-alanyl-melphalan. Peak areas were integrated using the Isco ChemResearch computer program were converted to concentrations of beta-alanyl-melphalan using a standard curve of beta-alanyl-melphalan concentration versus peak area.

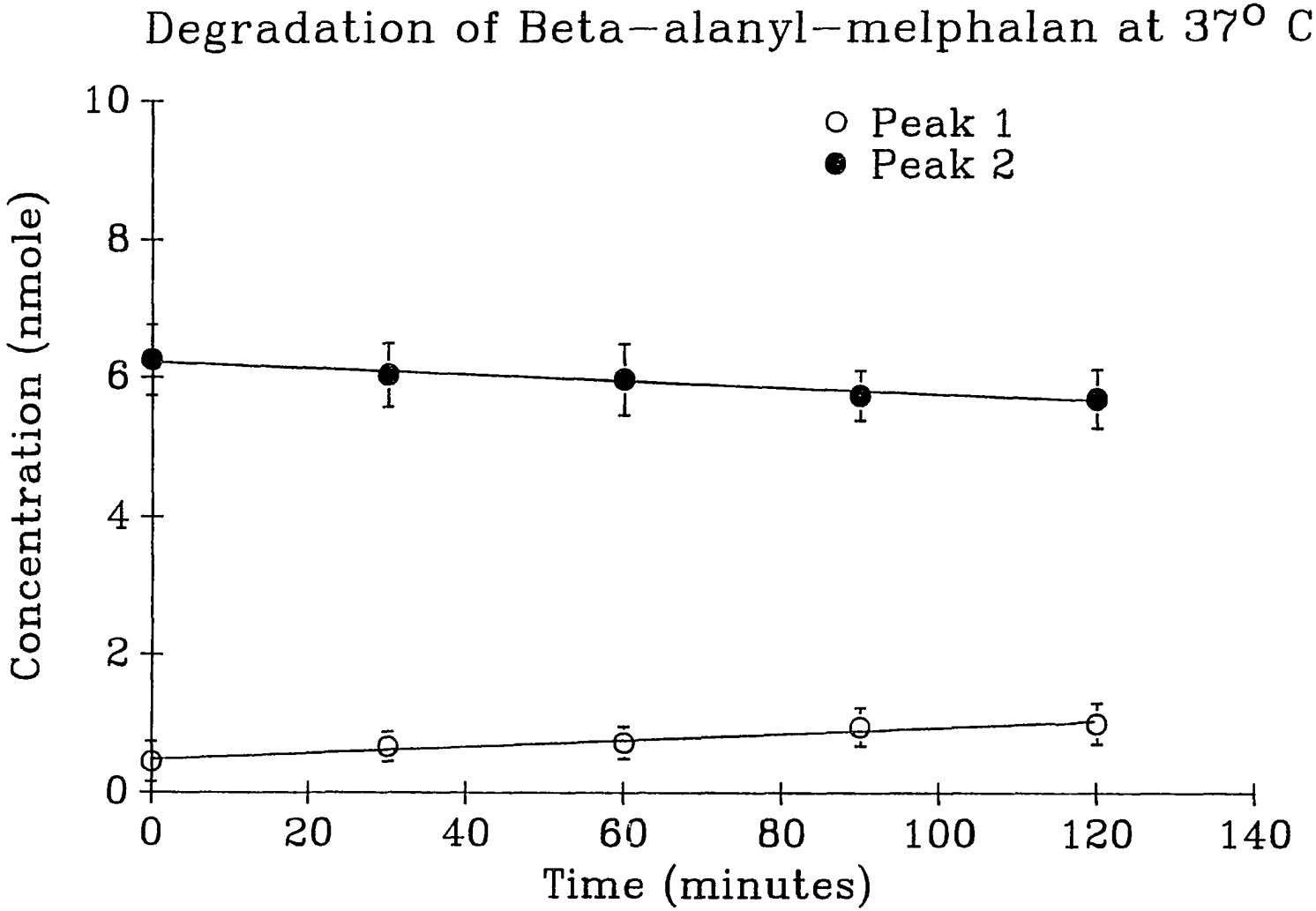

When beta-alanyl-melphalan was stored at 0° C for three weeks only 6.5% degradation was observed, i.e. from 6.33 nmole to 5.92 nmole. These limited results indicated that the dipeptide beta-alanyl-melphalan was more stable than melphalan in distilled water.

VI. Reactivity of Melphalan and Beta-alanyl-melphalan Toward Peptidohydrolytic enzymes:

Although the reported mechanism of melphalan toxicity toward cells involves its reactivity toward guanine residues in DNA (Hansson, et al., 1987), the bifunctional alkylating group at the para-position on the aromatic side group of phenylalanine could also be reactive toward proteins, i.e. through primary amine reactivity. In order to test this possibility, we assayed the ability of melphalan to react with and inhibit peptidohydrolytic enzymes.

Rather than attempting to test a large number of peptidohydrolytic enzymes, a typical peptidohydrolytic enzyme, L-leucine aminopeptidase, was chosen for analysis. L-leucine aminopeptidase digests L-leucine-p-nitroanilide into L-leucine and p-nitroaniline, the later of which is a yellow compound that can be detected by use of a spectrophotometer set at 405 nm. Enzyme activity assays were performed by incubation of dialyzed intracellular extract or dialyzed ascites fluid with L-leucine-p-nitroanilide in the presence and absence of melphalan. Intracellular extract represents the component which is inside the mouse Ehrlich

ascites tumor cells and ascites fluid represents the extracellular component which is secreted from Ehrlich ascites tumor cells and the mouse.

The kinetic properties of L-leucine aminopeptidase associated with the intracellular extract of mouse Ehrlich ascites tumor cells and ascites fluid from mouse Ehrlich ascites tumor cell bearing mice were evaluated at several concentrations of substrate (L-leucine-p-nitroaniline). L-leucine aminopeptidase activity in intracellular extracts from mouse Ehrlich ascites tumor cells exhibited typical Michaelis-Menten saturation kinetics (Figure 25). This L-leucine aminopeptidase activity was inhibited by 10 mg melphalan (Figure 25). A Lineweaver-Burk plot for inhibition of intracellular extract of mouse Ehrlich ascites tumor cells is shown in Figure 26. The effect of melphalan was not overcome by increasing the concentration of substrate (l-leucine-p-nitroanilide) and thus a decrease in apparent V_{max}, was observed, without a change in the apparent K_m (Table 7) for intracellular extract in the presence of melphalan (0.16 nM). The apparent K_m values, from the double-reciprocal plot, were calculated to be 0.92 mM for intracellular extract and intracellular extract in the presence of melphalan (Table 7). The maximum hydrolytic activities (V_{max}) were 4.18 and 3.23 umole/minute/mg protein for intracellular extract and intracellular extract in the presence of melphalan, respectively (Table 7). These results indicate that melphalan acts as a noncompetitive inhibitor of L-leucine aminopeptidase activity present in the intracellular extract of mouse Ehrlich ascites tumor cells. Therefore, melphalan may bind to either free L-leucine aminopeptidase or the L-

Figure 25. L-leucine aminopeptidase activity associated with intracellular extract of mouse Ehrlich ascites tumor cells in the presence and absence of melphalan (0.16 mM). Data are presented as reaction velocity versus substrate (l-leucine-p-nitroanilide) concentration.

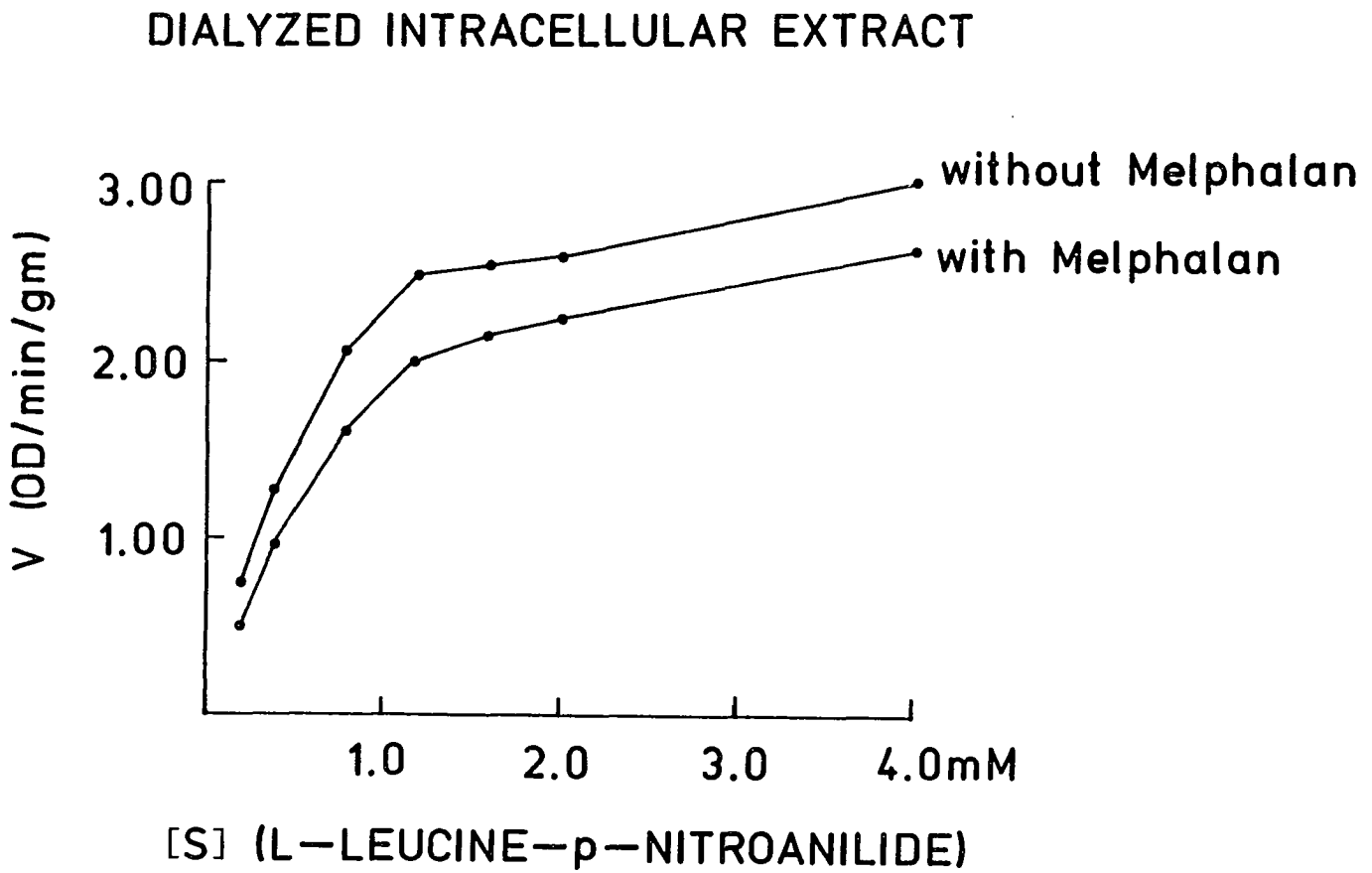

Figure 26. A double-reciprocal plot (Lineweaver-Burk plot) of L-leucine aminopeptidase activity associated with intracellular extract of mouse Ehrlich ascites tumor cells in the presence and absence of melphalan (0.16 mM).

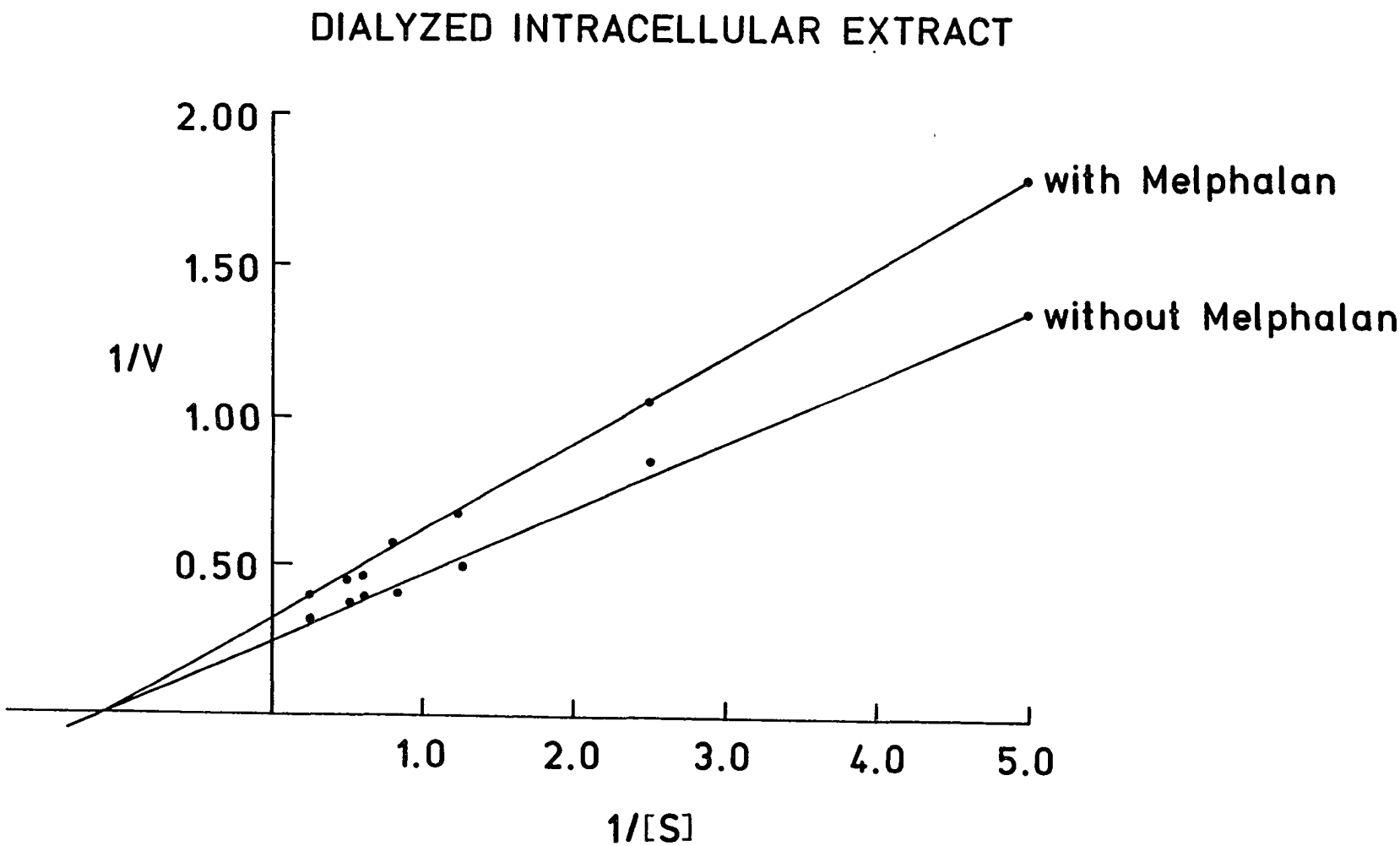

Table 7. Kinetic constants for L-leucine aminopeptidase activity in the presence and absence of melphalan.

	K_m	V_{max}
Dialyzed ascites fluid	2.08	0.63
Dialyzed ascites fluid with melphalan (5 mg)	1.67	0.42
Dialyzed intracellular extract	0.92	4.18
Dialyzed intracellular extract with melphalan (5 mg)	0.92	3.23

Measured as hydrolysis of L-leucine-p-nitroanilide.

K_m as mM.

V_{max} as umole/minute/mg protein.

leucine aminopeptidase/L-leucine-p-nitroanilide complex (enzyme/substrate complex) or by this, or a similar mechanism, to reduce enzyme activity.

Results from the analysis of L-leucine aminopeptidase activity in dialyzed ascites fluid are shown in Figure 27. These results clearly demonstrate that the ascites fluid also had the ability to catalyze the hydrolysis of L-leucine-p-nitroanilide and that the enzyme activity was inhibited by melphalan. A Lineweaver-Burk plot for melphalan inhibition of L-leucine aminopeptidase activity in ascites fluid is shown in Figure 28. The kinetic constants of L-leucine aminopeptidase activity in ascites fluid were calculated from the double reciprocal plot (Figure 28) and the apparent K_m values were 2.08 mM and 1.67 mM for dialyzed ascites fluid and dialyzed ascites fluid in the presence of melphalan, respectively (Table 7). The maximum hydrolytic activity (V_{max}) for dialyzed ascites fluid and dialyzed ascites fluid plus melphalan were 0.63 and 0.42 umole/minute/mg protein, respectively (Table 7). These results indicate that melphalan inhibited the L-leucine aminopeptidase activity in ascites fluid in an uncompetitive manner. The kinetics of uncompetitive inhibition are characterized by changes in both apparent V_{max} and K_m values in presence of inhibitor. Therefore, melphalan may bind to the enzyme/substrate complex or analogous to inhibit enzyme activity.

Results describing the inhibition of L-leucine aminopeptidase activity by beta-alanyl-melphalan was presented in Figure 29. Due to the limited supply of beta-

Figure 27. L-leucine aminopeptidase activity associated with ascites fluid from mouse Ehrlich ascites tumor cell bearing mice in the presence and absence of melphalan (0.16 mM). Data are presented as reaction velocity versus substrate (L-leucine-p-nitroanilide) concentration.

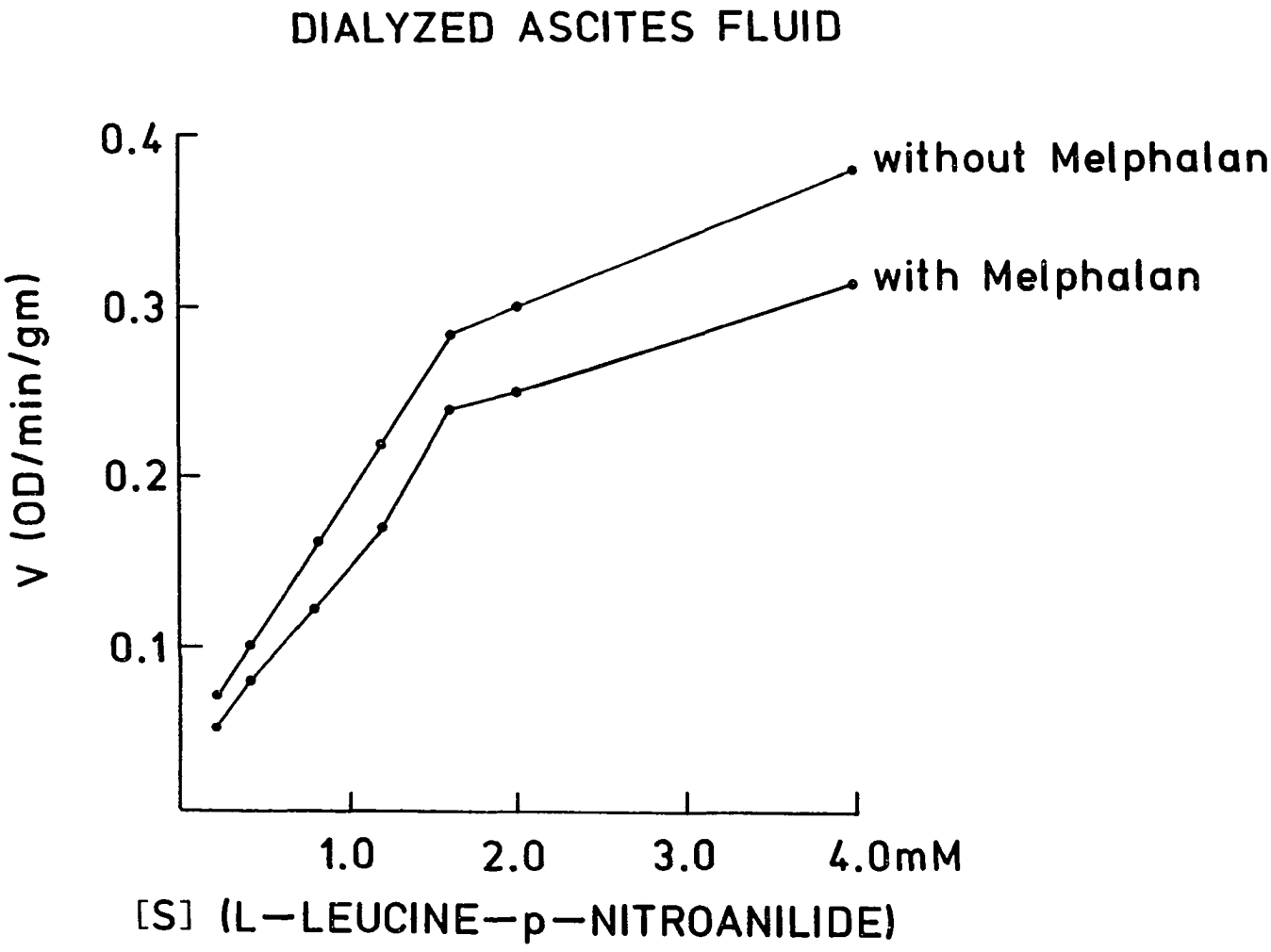

Figure 28. A double-reciprocal plot (Lineweaver-Burk plot) of L-leucine aminopeptidase activity associated with ascites fluid from mouse Ehrlich ascites tumor cell bearing mice in the presence and absence of melphalan (0.16 mM).

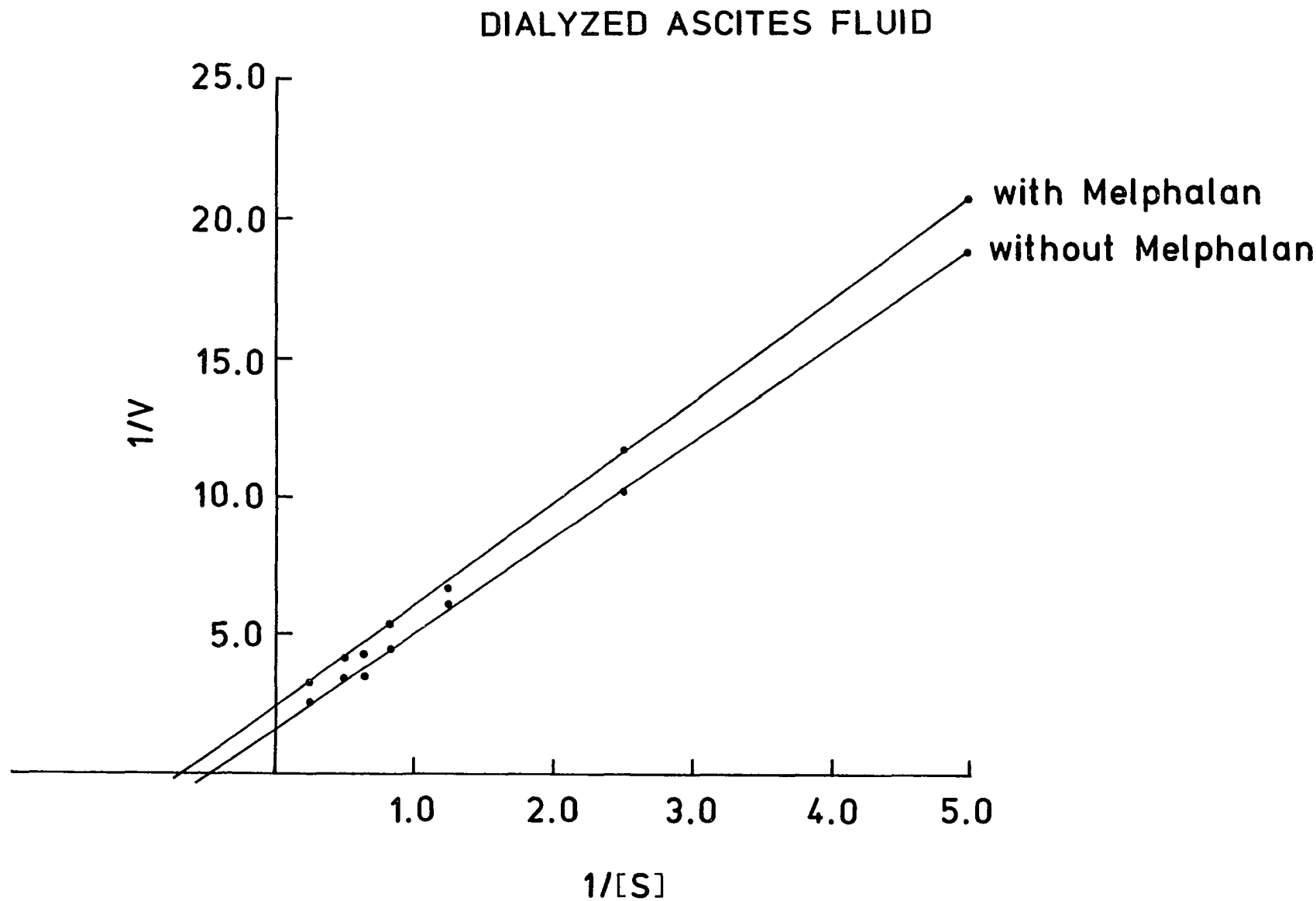

Figure 29. L-leucine aminopeptidase activity associated with intracellular extract of Ehrlich ascites tumor cells at the substrate concentration of 2 mM in the presence and absence of beta-alanyl-melphalan (0.68 mM). Data are presented as a plot of absorbance versus time.

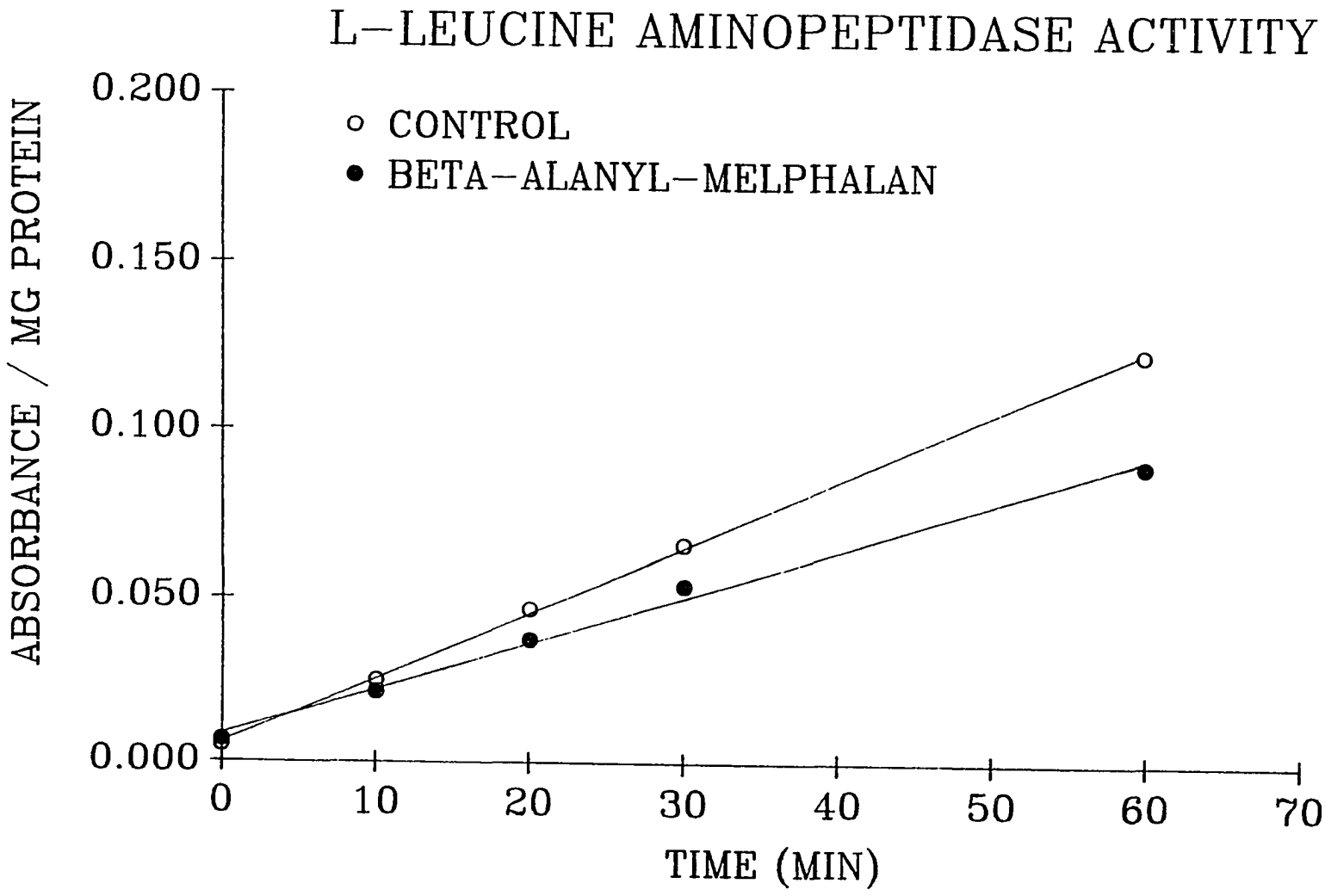

alanyl-melphalan, the kinetic properties of L-leucine aminopeptidase were studied only in intracellular extracts with a substrate concentration of 2 mM in the absence and presence of beta-alanyl-melphalan (0.68 mM). Beta-alanyl-melphalan inhibited L-leucine aminopeptidase activity in the intracellular extracts of mouse Ehrlich ascites tumor cells. Although this study was not completed, the preliminary results indicate that beta-alanyl-melphalan might inhibit L-leucine aminopeptidase activity via mechanisms similar to those of melphalan.

VII. <u>In Vitro</u> Toxicity Testing of Melphalan and Beta-alanyl-melphalan:

The objective of the toxicity-testing was to assess the ability of melphalan and beta-alanyl-melphalan to decrease the metabolic viability of the mouse Ehrlich ascites tumor cells, mouse liver cells, and mouse 3T3 embryonic cells. Mouse liver cells and mouse 3T3 embryonic cells were used as control non-neoplastic cell lines. An effort was made to test each cell line during the exponential growth phase. Exponential growth cultures were exposed, for 24 hours, to the test drug at the concentrations indicated (0.001 mM to 0.1 mM). Cell viability was subsequently assessed by trypan blue exclusion. Trypan blue is a vital dye which can penetrate through the cell membrane of metabolically dead cells giving them a blue appearance under light microscopic examination. The living cells are able to exclude the dye and maintain a clear appearance. The percentage of dead cells is obtained by dividing the number of dead cells (blue cells) by the number of total cells (blue cells plus clear cells) and multiplying by 100. This

value was then converted to $\log_{10}$ value ($\log_{10}$% dead cells).

Toxicity of beta-alanine, 1-aminoethyl phosphonic acid, beta-alanyl-aminoethyl phosphonic acid and beta-alanyl-L-alanine against mouse Ehrlich ascites tumor cells: Table 8 presents the results describing the effects of beta-alanine, 1-aminoethyl phosphonic acid (1-AEPA), beta-alanyl-aminoethyl phosphonic acid (beta-alanyl-AEPA), beta-alanyl-L-alanine, melphalan and beta-alanyl-melphalan treatment (in vitro) on the metabolic cell death of mouse Ehrlich ascites tumor cells. Beta-alanine at concentrations of 0.1 mM and 1.0 mM resulted in cell death approximating 24.13% and 23.63%, respectively. Neither concentration of beta-alanine provides for cell death which was significantly different from control nontreated cells ($p > 0.05$, ANOVA). 1-AEPA also showed no significant increase in cell death at concentrations of 0.1 mM and 1.0 mM, i.e. cell death of 20.48% and 21.51%, respectively ($p > 0.05$, ANOVA). Beta-alanyl-AEPA, which is a dipeptide form of AEPA, in concentrations of 0.1 mM and 0.01 mM resulted in cell death of 27.06% and 33.78%, respectively. Cell death due to beta-alanyl-AEPA treatments were not significantly different from the control nontreated cells ($p > 0.05$, ANOVA) at both concentrations tested. Beta-alanyl-L-alanine at a concentration of 1.0 mM was not significantly toxic when ($p > 0.05$, ANOVA) the percentage of cell death (22.9%) was compared to the control nontreated cells (22.78%).

Table 8. The effects of beta-alanine, 1-aminoethyl phosphonic acid (1- AEPA), beta-alanyl-aminoethyl phosphonic acid (beta-alanyl-AEPA), beta-alanyl-alanine, melphalan and beta-alanyl-melphalan treatment in vitro on the metabolic cell death of mouse Ehrlich ascites tumor cells.

Treatment[a]	Dosage (mM)	% dead cells
control	0	22.78 ± 1.56
beta-alanine	0.1	24.13 ± 0.84[e]
beta-alanine	1.0	23.63 ± 7.75[e]
1-AEPA	0.1	20.48 ± 4.83[e]
1-AEPA	1.0	21.51 ± 0.89[e]
beta-alanyl-AEPA	0.1	27.06 ± 8.73[e]
beta-alanyl-AEPA	1.0	33.78 ± 6.13[e]
beta-alanyl-L-alanine	1.0	22.90 ± 4.18[e]
melphalan	0.001	33.11 ± 1.36[d]
melphalan	0.01	54.95 ± 1.98[d]
melphalan	0.1	89.43 ± 1.57[d]
beta-alanyl-melphalan	0.001	31.57 ± 1.47[d]
beta-alanyl-melphalan	0.01	37.94 ± 2.99[d]
beta-alanyl-melphalan	0.1	81.38 ± 1.27[d]

a. Treatment as 24 hours incubation starting 48 hours after tumor cell inoculation (1 million cells per T-25 flask).

b. Metabolic cell death was assessed by trypan blue exclusion and is expressed as percent dead cells.

c. Mean ± SD of 9 flasks from 3 separate experiments.

d. Significantly different from control; $p<0.001$ by ANOVA.

e. Not significantly different from control; $p>0.05$ by ANOVA.

Toxicity of melphalan and beta-alanyl-melphalan against mouse Ehrlich ascites tumor cells: Melphalan at concentrations of 0.001 mM, 0.01 mM, and 0.1 mM caused a significant increase in cell death, i.e. 33.11%, 54.95% and 89.43%, respectively when compared to the control nontreated cells ($p<0.001$ for all concentrations, ANOVA). Figure 30 represents a visual presentation of these results showing $\log_{10}$% dead cells versus melphalan concentration. As the concentration of melphalan is reduced, the toxicity diminishes in a nonlinear manner until at 0.001 mM, cell viability approaches that of nontreated tumor cells.

Beta-alanyl-melphalan treatment resulted in cell death values of 31.57%, 37.94% and 81.38% at concentrations of 0.001 mM, 0.01 mM and 0.1 mM, respectively. These values were significantly different from the control nontreated cells ($p < 0.01$ for 0.001 mM and 0.01 mM, $p < 0.001$ for 0.1 mM, ANOVA). Toxicity of beta-alanyl-melphalan to the mouse Ehrlich ascites tumor cells over the concentration range of 0.001 mM to 0.1 mM (Figure 31) revealed a positive linear correlation of $\log_{10}$% cell death with concentrations of beta-alanyl-melphalan. The activity of beta-alanyl-melphalan against mouse Ehrlich ascites tumor cells was not significantly different from that of melphalan at a concentration of 0.001 mM ($p < 0.01$, ANOVA). Melphalan was more effective than beta-alanyl-melphalan, at 0.01 mM ($p < 0.01$, ANOVA) and 0.1 mM ($p < 0.01$, ANOVA), against mouse Ehrlich ascites tumor cells.

Figure 30. Toxicity assay in vitro of melphalan toward mouse Ehrlich ascites tumor cells. Cells in exponential growth (2 days old) were incubated for 24 hours with melphalan at the concentrations indicated. Metabolic viability was assayed by trypan blue exclusion. The number of cells stained blue was divided by the total number of cells counted and multiplied by 100 to get percent dead cells (%). This value was then converted to $\log_{10}$ ($\log_{10}$%).

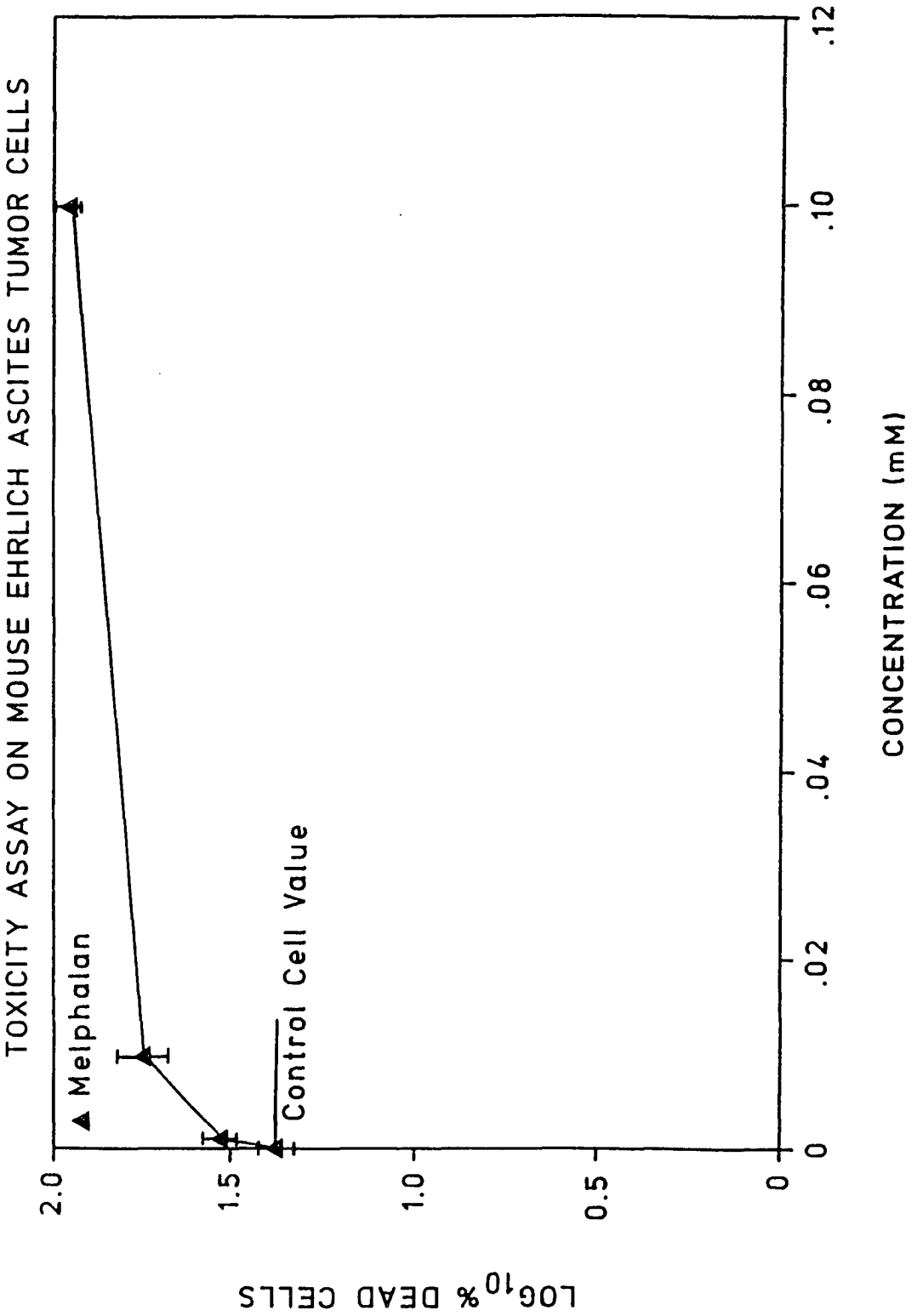

Figure 31. Toxicity assay in vitro of beta-alanyl-melphalan toward mouse Ehrlich ascites tumor cells. Cells in exponential growth (2 days old) were incubated for 24 hours with beta-alanyl-melphalan at the concentrations indicated. Metabolic viability was assayed by trypan blue exclusion. The number of cells stained blue was divided by the total number of cells counted and multiplied by 100 to get percent dead cells (%). This value was then converted to $\log_{10}$ ($\log_{10}$%).

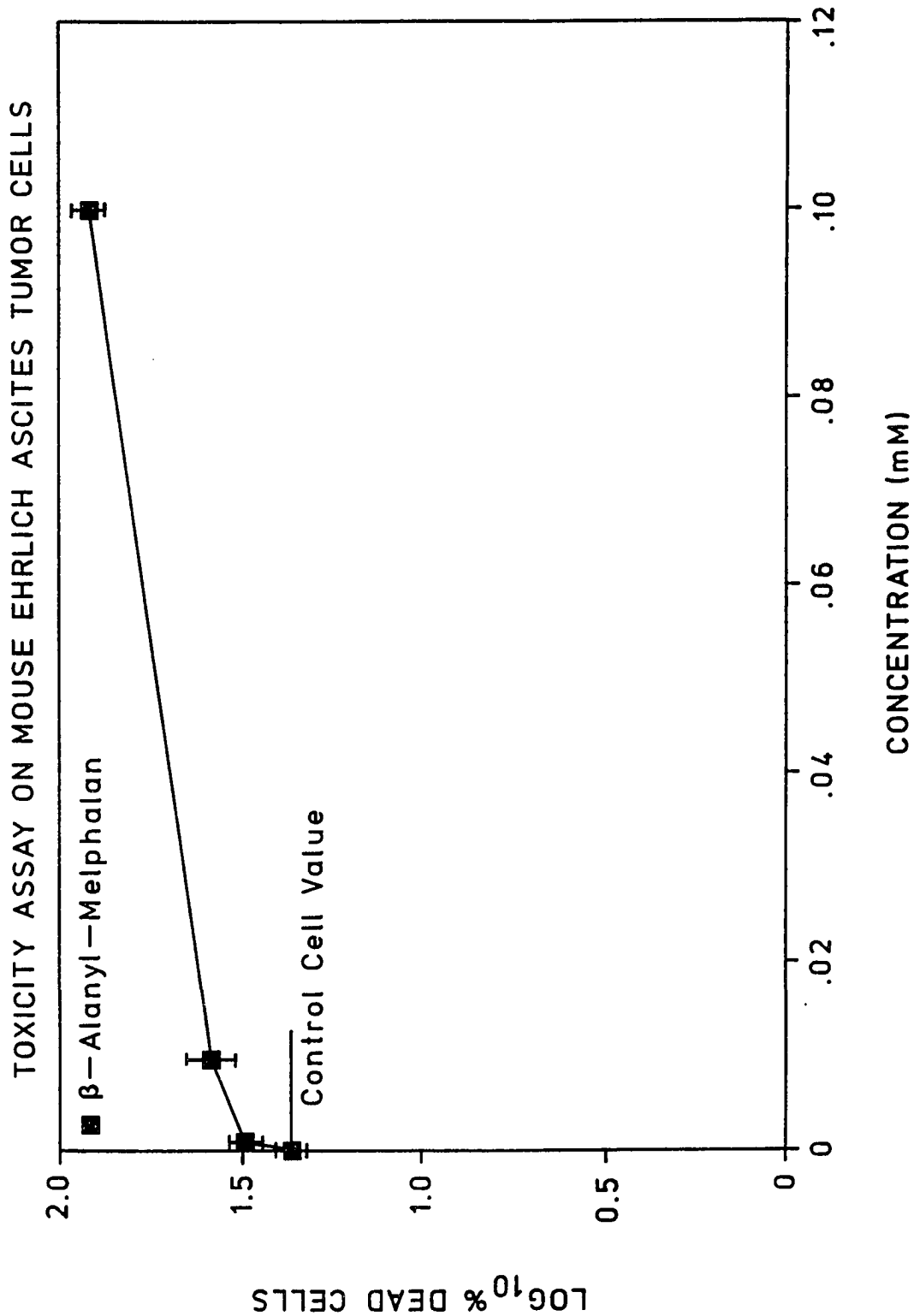

Toxicity of melphalan and beta-alanyl-melphalan against mouse liver cells:

Toxicity studies of melphalan using the mouse liver cells revealed an increase in percent of cell death of 14.36%, 14.88% and 34.88% at melphalan concentrations of 0.001 mM, 0.01 mM and 0.1 mM, respectively (Table 9). These values are significantly different from the percent of cell death value of the control nontreated mouse liver cells ($p < 0.05$ for 0.001 mM and 0.01 mM, $p < 0.001$ for 0.1 mM, ANOVA). The data plot of $\log_{10}$% cell death versus melphalan concentration revealed a positive linear correlation of toxicity with melphalan concentration (Figure 32).

Analysis of toxicity of beta-alanyl-melphalan towards the mouse liver cells revealed a slight increase in the percent of cell death, i.e. 7.79%, 7.97% and 8.76%, at concentrations of 0.001 mM, 0.01 mM and 0.1 mM, respectively (Table 9). These values are not significantly different from the percent of cell death value of the control nontreated liver cells ($p > 0.1$ for all concentrations, ANOVA). A positive linear correlation was observed for $\log_{10}$% cell death versus beta-alanyl-melphalan concentrations in treatments of mouse liver cells (Figure 33). The cytotoxicity of beta-alanyl-melphalan against mouse liver cells was significantly less than that of melphalan at all concentrations used ($p < 0.05$ for 0.001 mM and 0.01 mM, $p < 0.001$ for 0.1 mM, ANOVA). It is emphasized that none of these values were significantly different from each other or control nontreated cells.

Table 9. The effects of melphalan and beta-alanyl-melphalan treatment (in vitro) on the metabolic cell death of mouse liver cells.

	Melphalan		Beta-alanyl-melphalan	
Conc.	Log_{10} %	%	Log_{10} %	%
Control	0.77 ± 0.20	6.40 ± 2.73	0.77 ± 0.20	6.40 ± 2.73
0.001 mM	1.15 ± 0.06	14.36 ± 1.93[b]	0.88 ± 0.09	7.79 ± 1.69[c]
0.01 mM	1.17 ± 0.06	14.88 ± 2.23[b]	0.89 ± 0.12	7.97 ± 2.15[c]
0.1 mM	1.52 ± 0.17	34.88 ± 2.54[b]	0.94 ± 0.09	8.76 ± 1.85[c]

Treatments of 24 hours incubation of monolayer cell cultures starting 48 hours after mouse liver cell inoculation (1 million cells per T-25 flask). Metabolic cell death was assessed by trypan blue exclusion and is expressed as percent dead cells and log_{10}% dead cells.

a. Mean ± SD of 9 flasks from three separate experiments.

b. Significantly different from control; $p<0.001$ by ANOVA.

c. Not significantly different from control; $p>0.05$ by ANOVA.

Figure 32. Toxicity assay in vitro of melphalan toward mouse liver cells. Cells in exponential growth (2 days old) were incubated for 24 hours with melphalan at the concentrations indicated. Metabolic viability was assayed by trypan blue exclusion. The number of cells stained blue was divided by the total number of cells counted and multiplied by 100 to get percent dead cells (%). This value was then converted to $\log_{10}$ ($\log_{10}$%).

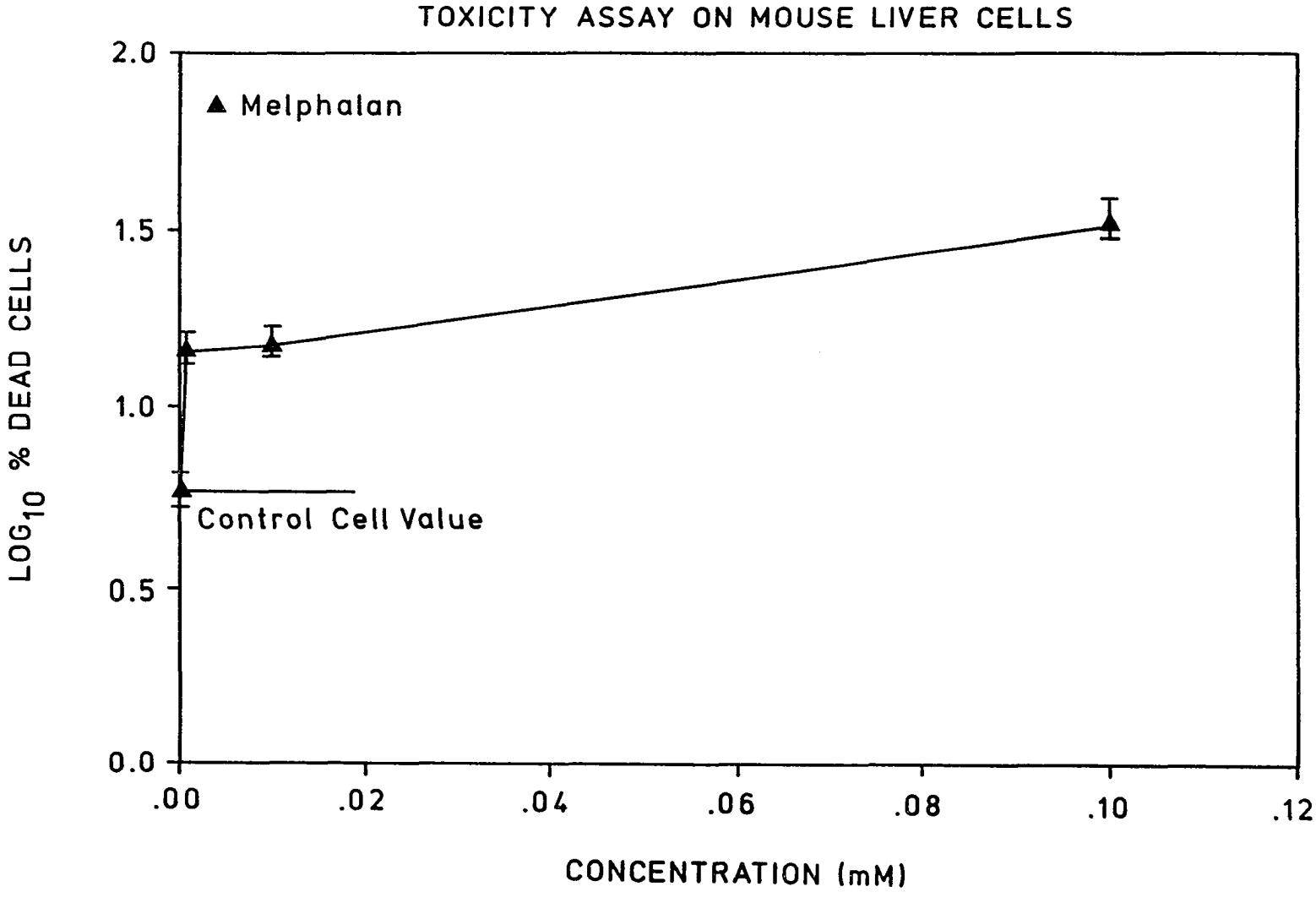

Figure 33. Toxicity assay in vitro of beta-alanyl-melphalan toward mouse liver cells. Cells in exponential growth (2 days old) were incubated for 24 hours with beta-alanyl-melphalan at the concentrations indicated. Metabolic viability was assayed by trypan blue exclusion. The number of cells stained blue was divided by the total number of cells counted and multiplied by 100 to get percent dead cells (%). This value was then converted to $\log_{10}$ ($\log_{10}$%).

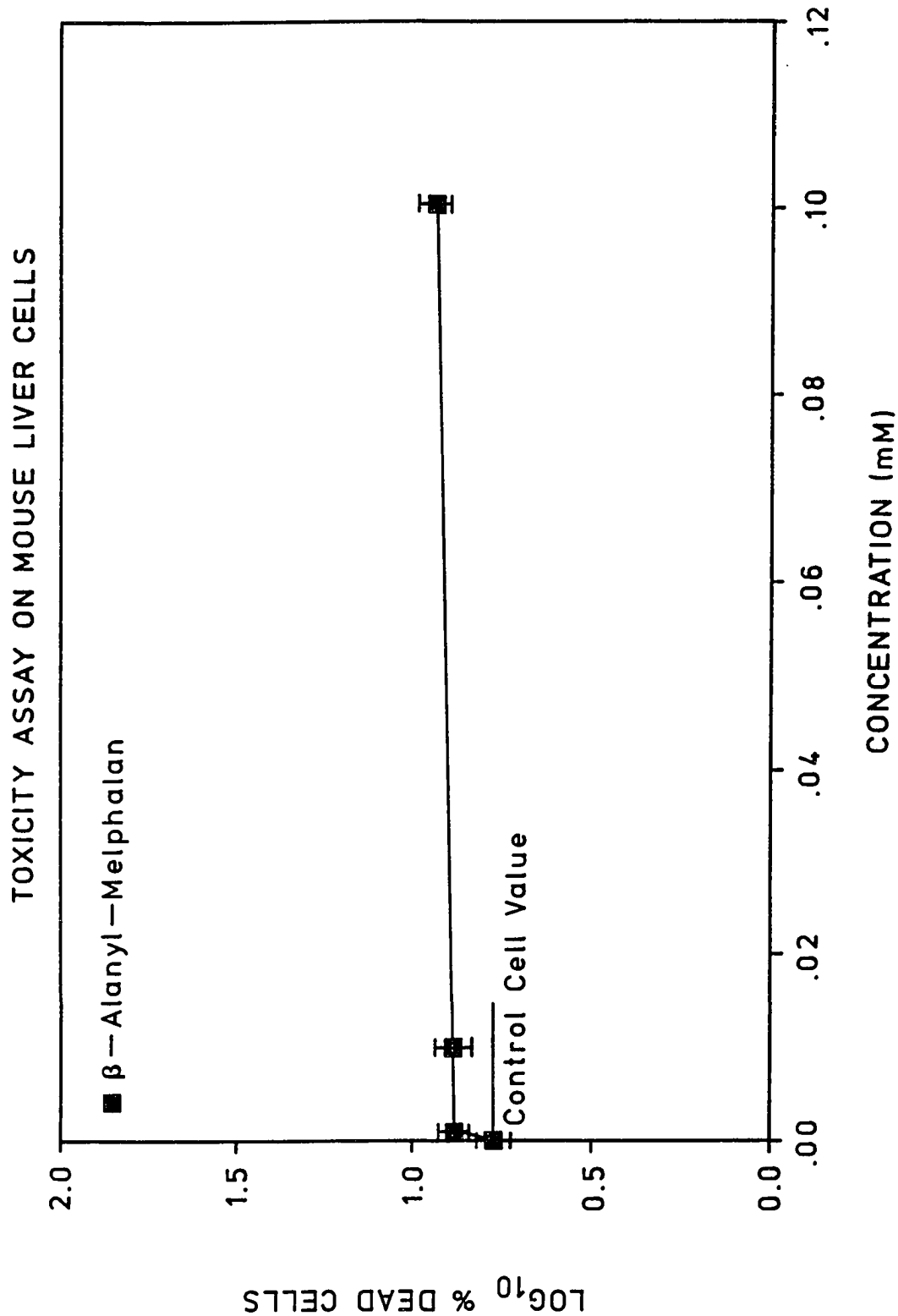

Toxicity of melphalan and beta-alanyl-melphalan against mouse 3T3 embryonic cells: Analysis of toxicity of melphalan towards the 3T3 mouse embryonic cells over the same concentration range utilized against the tumor and liver cells revealed an increase in the percent of cell death of 19.05%, 20.42% and 47.86% at melphalan concentrations of 0.001 mM, 0.01 mM and 0.1 mM, respectively (Table 10). The cytotoxicity of melphalan at concentrations of 0.001 mM and 0.01 mM was not significantly different from the control ($p > 0.5$ for 0.001 mM and $p > 0.1$ for 0.01 mM, ANOVA), and only the concentration of 0.1 mM was significantly different from the control ($p < 0.001$, ANOVA). Unlike the melphalan toxicity study in tumor cells, the data plot of $\log_{10}$% cell death versus melphalan concentration for the 3T3 cells revealed a positive linear correlation of cell death with melphalan concentrations between 0.1 and 0.001 mM (Figure 34).

Equivalent testing of beta-alanyl-melphalan for toxicity to mouse 3T3 embryonic cells (Table 10) revealed that over the concentration range 0.001 mM to 0.1 mM, beta-alanyl-melphalan was dramatically more toxic to the mouse 3T3 embryonic cells than to the tumor cells or liver cells. Beta-alanyl-melphalan treatments yielded cell death values of 25.85%, 31.62% and 67.61% at concentrations of 0.001 mM, 0.01 mM and 0.1 mM, respectively. These values were significantly different from the control nontreated cell values ($p < 0.001$ for all concentrations used, ANOVA). Beta-alanyl-melphalan-treated cells exhibited a positive linear correlation of $\log_{10}$% cell death with increasing concentrations (Figure 35).

Table 10. The effects of melphalan and beta-alanyl-melphalan treatment (in vitro) on the metabolic cell death of mouse 3T3 embryonic cells.

	Melphalan		Beta-alanyl-melphalan	
Conc.	Log_{10} %	%	Log_{10} %	%
Control	1.26 ± 0.18	18.20 ± 1.53	0.89 ± 0.13	7.76 ± 1.34
0.001 mM	1.28 ± 0.24	19.05 ± 1.75[c]	1.41 ± 0.19	25.85 ± 1.55[b]
0.01 mM	1.31 ± 0.23	20.42 ± 1.68[c]	1.50 ± 0.20	31.62 ± 1.59[b]
0.1 mM	1.68 ± 0.23	47.86 ± 1.71[b]	1.83 ± 0.13	67.61 ± 1.36[b]

Treatments of 24 hours incubation of monolayer cell cultures starting 48 hours after mouse 3T3 embryonic cell inoculation (1 million cells per T-25 flask). Metabolic cell death was assessed by trypan blue exclusion and is expressed as percent dead cells and log_{10}% dead cells.

a. Mean ± SD of 9 flasks from three separate experiments.

b. Significantly different from control; $p<0.001$ by ANOVA.

c. Not significantly different from control; $p>0.05$ by ANOVA.

Figure 34. Toxicity assay in vitro of melphalan toward mouse 3T3 embryonic cells. Cells in exponential growth (2 days old) were incubated for 24 hours with melphalan at the concentrations indicated. Metabolic viability was assayed by trypan blue exclusion. The number of cells stained blue was divided by the total number of cells counted and multiplied by 100 to get percent dead cells (%). This value was then converted to $\log_{10}$ ($\log_{10}$%).

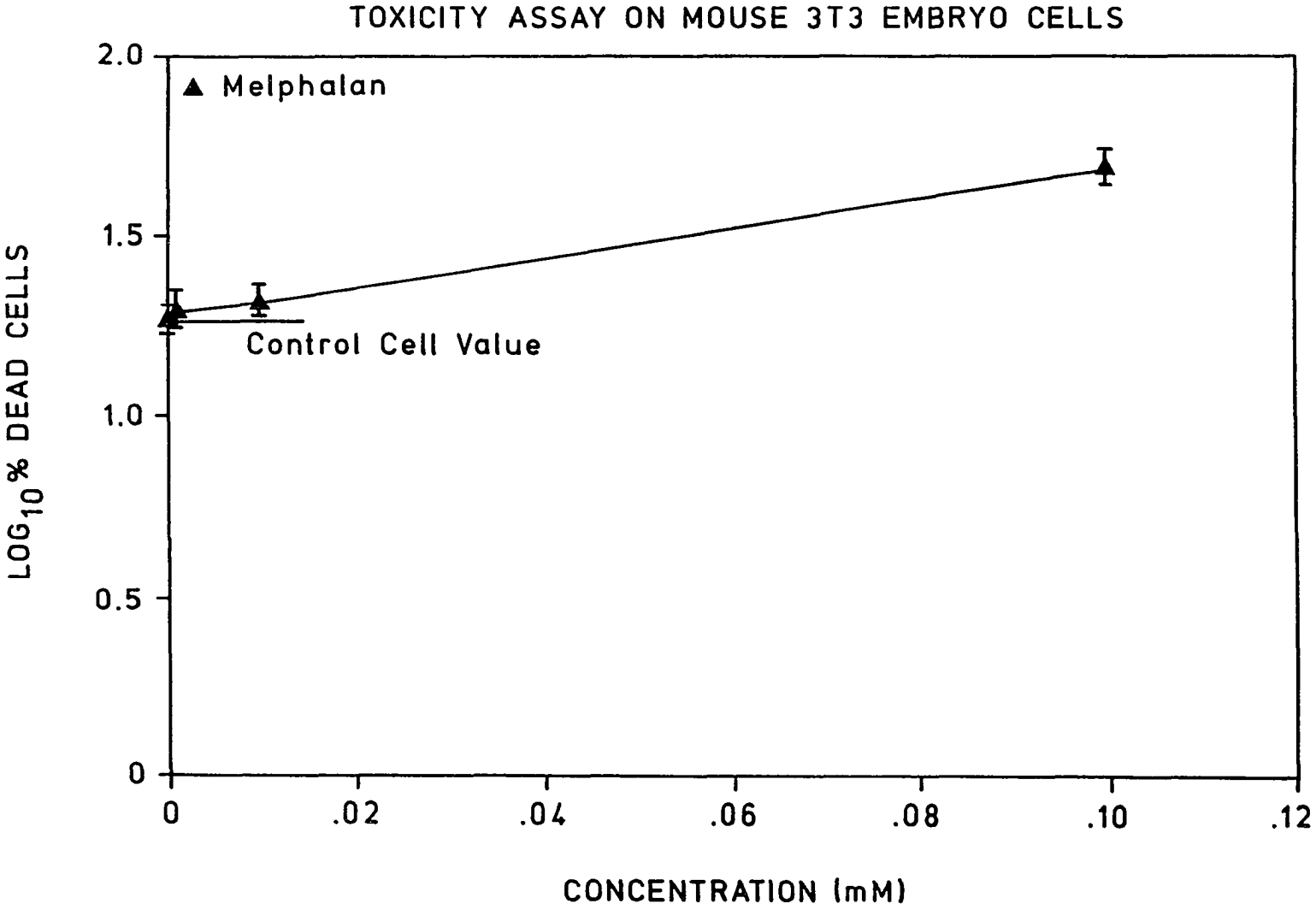

Figure 35. Toxicity assay in vitro of beta-alanyl-melphalan toward mouse 3T3 embryonic cells. Cells in exponential growth (2 days old) were incubated for 24 hours with melphalan at the concentrations indicated. Metabolic viability was assayed by trypan blue exclusion. The number of cells stained blue was divided by the total number of cells counted and multiplied by 100 to get percent dead cells (%). This value was then converted to $\log_{10}$ ($\log_{10}$%).

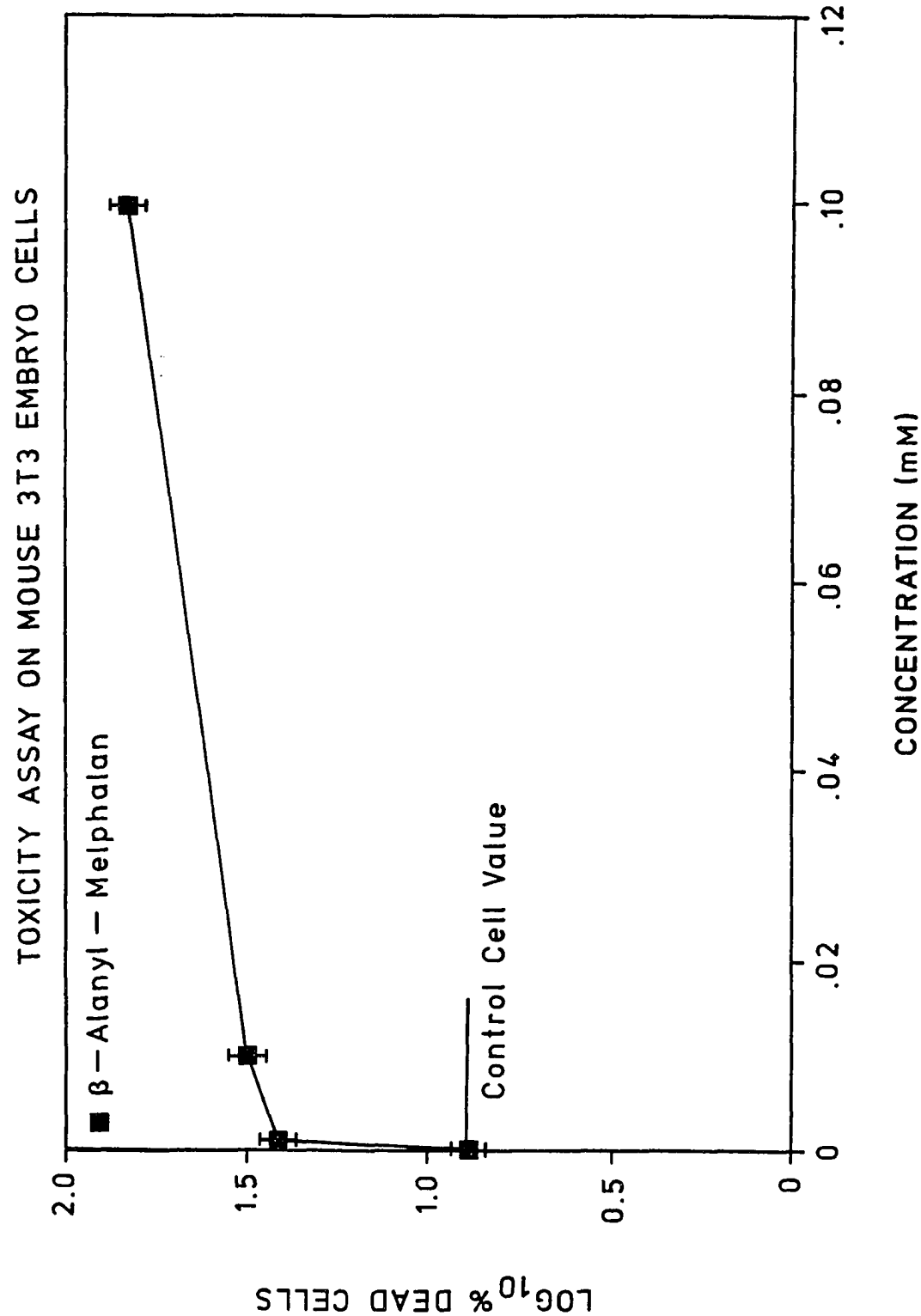

The final results of toxicity testing of melphalan revealed that melphalan was toxic to mouse liver cells and mouse Ehrlich ascites tumor cells at all concentrations tested and is only toxic to mouse 3T3 embryonic cells at a concentration of 0.1 mM. Figure 36 illustrates a comparison of the effects of melphalan (0.1 mM) and beta-alanyl-melphalan (0.1 mM) on the three different cell lines. The results revealed that melphalan is more toxic to the mouse liver cells, i.e. increasing the percent of cell death from 7.76% for control liver cells to 42.29% cell death for melphalan-treated liver cells. Cell death was 7.76% for control mouse Ehrlich ascites tumor cells compared to 30.50% cell death for melphalan-treated mouse Ehrlich ascites tumor cells. In mouse 3T3 embryonic cells, melphalan treatment only increased the percent of cell death from 7.76% for the control mouse 3T3 embryonic cells to 20.40% of cell death of melphalan-treated mouse 3T3 embryonic cells (Figure 36).

The results further indicated that beta-alanyl-melphalan is toxic to mouse Ehrlich ascites tumor cells and mouse 3T3 embryonic cells at all concentrations tested and is not toxic to the mouse liver cells at any concentration tested. Beta-alanyl-melphalan at a concentration of 0.1 mM caused 27.70% cell death in mouse Ehrlich ascites tumor cells. Beta-alanyl-melphalan treatment at a concentration of 0.1 mM only increased the percent of cell death from 7.76% for the control mouse liver cells to 10.63% for the beta-alanyl-melphalan treated mouse liver cells. In mouse 3T3 embryonic cells, beta-alanyl-melphalan treatment

Figure 36. The effects of 0.1 mM melphalan and 0.1 mM beta-alanyl-melphalan in vitro on metabolic viability of mouse Ehrlich ascites tumor cells (Ehrlich), mouse liver cells (Liver) and mouse 3T3 embryonic cells (3T3). Metabolic viability was assayed by trypan blue exclusion. The percent of dead cells represents the number of cells stained blue divided by the total number of cells counted and multiplied by 100. In order to compare the results, data were normalized by the percent of dead cells in the control group (7.76%).

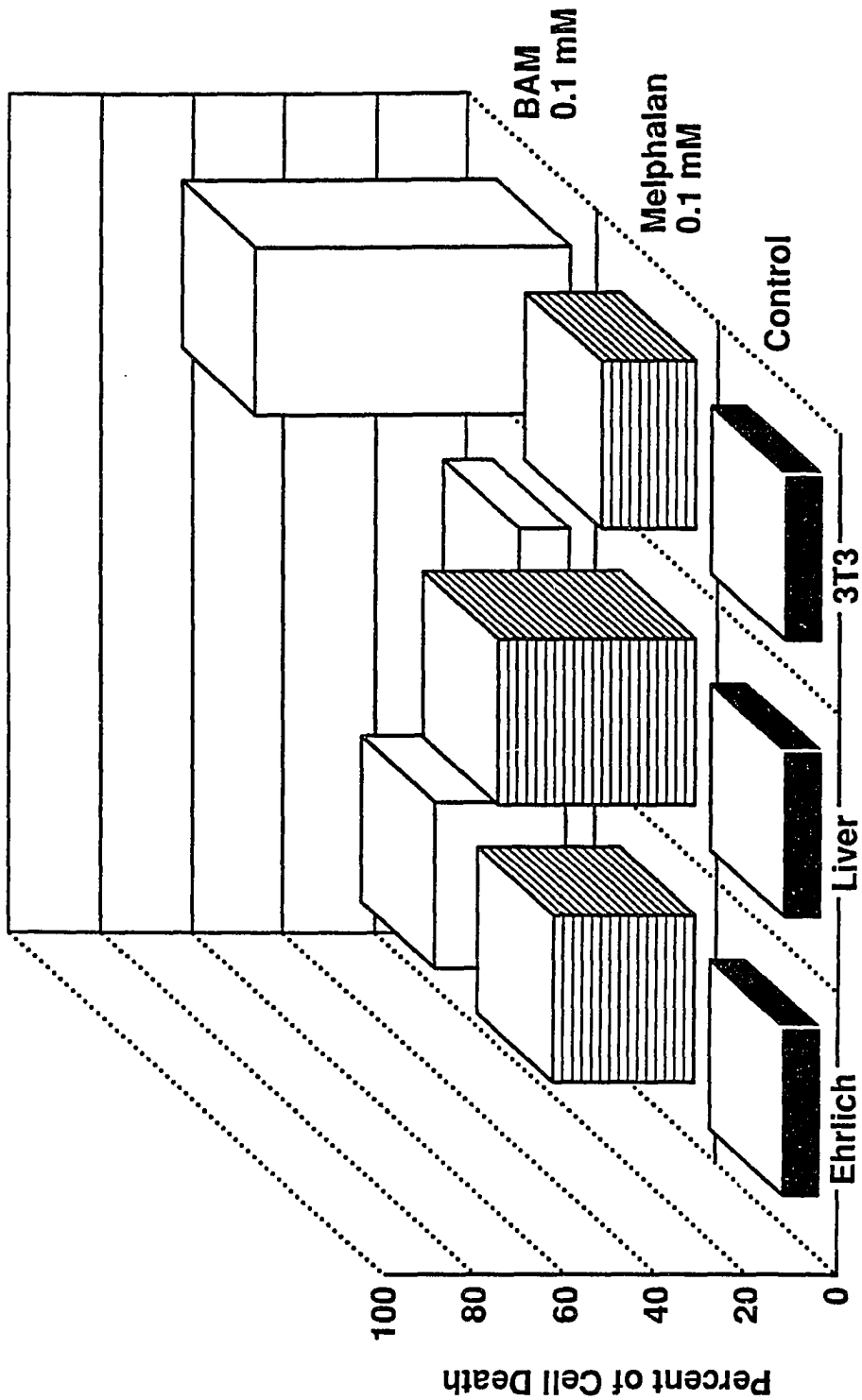

dramatically increased the percent of cell death from 7.76% for the control mouse 3T3 embryonic cells to a 67.61% cell death for the beta-alanyl-melphalan treated mouse 3T3 embryonic cells (Figure 36).

In summary, melphalan at a concentration of 0.1 mM is more toxic to mouse liver cells than mouse Ehrlich ascites tumor cells and mouse 3T3 embryonic cells while beta-alanyl-melphalan at a concentration of 0.1 mM is more toxic to mouse 3T3 embryonic cells than mouse Ehrlich ascites tumor cells and is not toxic to mouse liver cells.

VIII. In Vitro Cell Survival Testing of Melphalan and Beta-alanyl-melphalan:

The objective of the cell survival study was to assess the ability of melphalan and beta-alanyl-melphalan to affect the proliferation activity of the mouse Ehrlich ascites tumor cells, mouse liver cells and mouse 3T3 embryonic cells. Sensitivity to a 2-hour treatment with melphalan and beta-alanyl-melphalan was compared among the three cell lines by assessing in vitro growth after treatment (see materials and methods).

Figure 37 illustrates the results of a 2-hour incubation with 0.1 mM melphalan and 0.1 mM beta-alanyl-melphalan on the subsequent growth of mouse Ehrlich ascites tumor cells. The control group of mouse Ehrlich ascites tumor cells exhibited a steady increase in cell number with time with a proliferation rate

Figure 37. The effect of 2 hours exposure to melphalan (0.1 mM) and beta-alanyl-melphalan (0.1 mM) on the growth of mouse Ehrlich ascites tumor cells. Cells in exponential growth were incubated for 2 hours with 0.1 mM melphalan and 0.1 mM beta-alanyl-melphalan then inoculated to new cell culture flasks. Total cell number was counted at timed intervals. Data were plotted on semi-log paper.

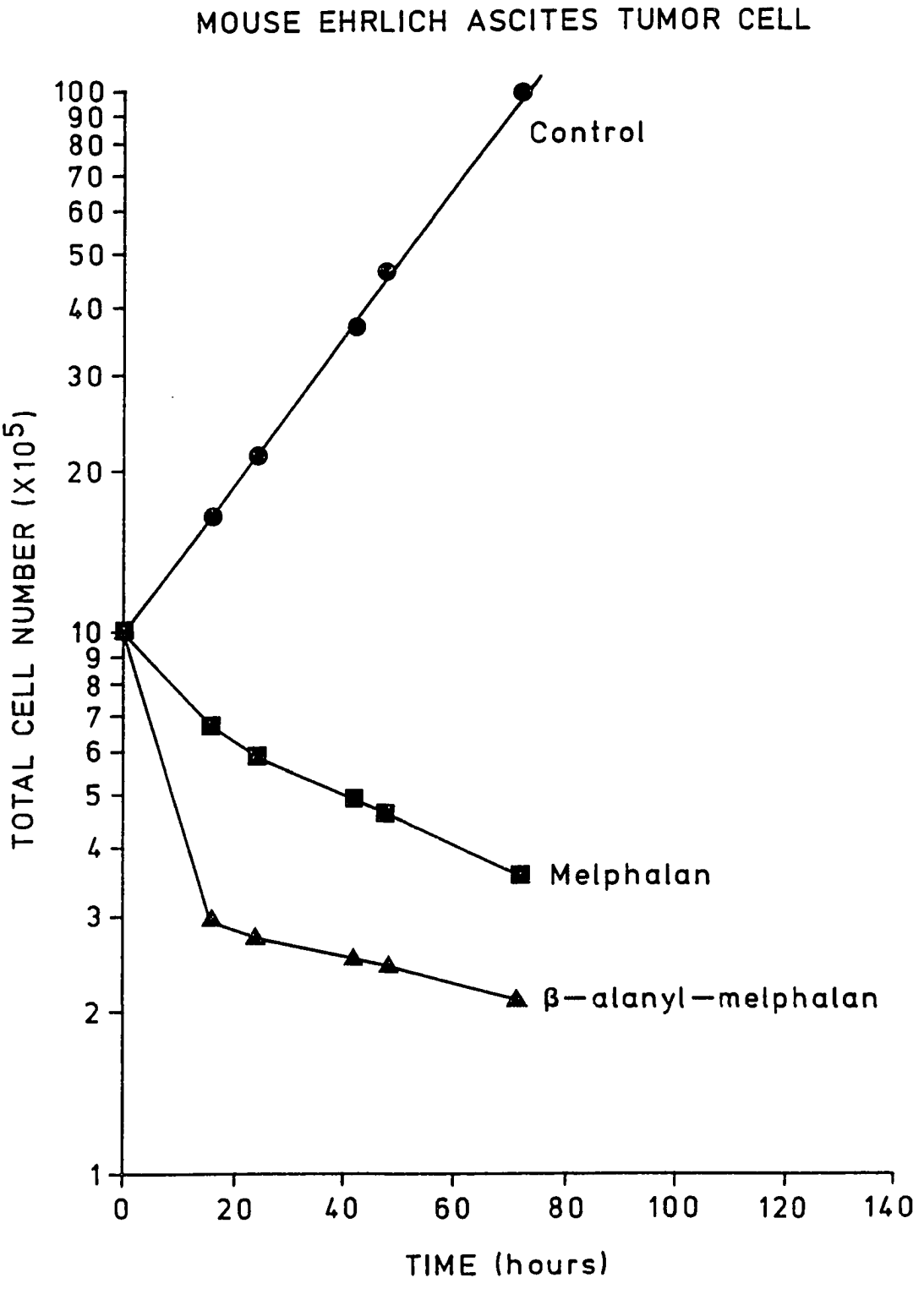

of 40,000 cells per hour.

Treatment of mouse Ehrlich ascites tumor cells with 0.1 mM melphalan resulted in a nearly linear reduction in cell number with time indicating that a 2-hour treatment resulted in a time-dependent cell death. Within the first 16 hours post treatment, the number of mouse Ehrlich ascites tumor cells declined by 33.5% and then 65% at 72 hours post treatment for a cell reduction rate of 20,000 cells per hour.

Treatment of mouse Ehrlich ascites tumor cells with 0.1 mM beta-alanyl-melphalan resulted in a dramatic decline in cell numbers to approximately 71% of the initial cell number in the first 16 hours. Sixteen hours after treatment, the decline in cell number became linear exhibiting a cell reduction rate of 1,550 cells per hour and reaching a final cell reduction of 79% of the initial number after 72 hours.

These results indicate that both agents not only affected cell proliferation, restricting the ability of cells to resume replication, but also resulted in cell death and lysis. The results also reveal that beta-alanyl-melphalan was significantly more effective than melphalan in killing and inhibiting subsequent mouse Ehrlich ascites tumor cell proliferation ($p < 0.001$, ANCOVA).

Figure 38 presents the results of a 2-hour incubation with 0.1 mM melphalan and 0.1 mM beta-alanyl-melphalan on the growth of mouse liver cells. The control group of nontreated mouse liver cells showed a slower growth rate (60,000 cells per hour) when compared to the control group of mouse Ehrlich ascites tumor cells.

Treatment of mouse liver cells with 0.1 mM melphalan resulted in an initial slight increase in cell number with time (3,000 cells per hour) for the first 48 hours post treatment. After 48 hours post treatment, cell numbers increased at a faster rate of 20,000 cells per hour. This rate was however only about 33 % of the proliferation rate of nontreated mouse liver cells.

Treatment of mouse liver cells for 2 hours with 0.1 mM beta-alanyl-melphalan resulted in a growth rate of 50,000 cells per hour. This growth rate was about 80% of the growth rate of the control nontreated mouse liver cells indicating that mouse liver cells are relatively insensitive to treatment with beta-alanyl-melphalan. These results reveal that melphalan dramatically affected mouse liver cell proliferation immediately after treatment but that cell replication resumed at a less reduced rate approximately 48 hours post-treatment. Beta-alanyl-melphalan only slightly restricted the growth rate of mouse liver cells and this reduction was not significant. These results also reveal that mouse liver cells respond to both agents differently than mouse Ehrlich ascites tumor cells indicating that mouse liver cells are insensitive to beta-alanyl-melphalan and were

Figure 38. The effect of 2 hours exposure to melphalan (0.1 mM) and beta-alanyl-melphalan (0.1 mM) on the growth of mouse liver cells. Cells in exponential growth were incubated for 2 hours with 0.1 mM melphalan and 0.1 mM beta-alanyl-melphalan then inoculated to new cell culture flasks. Total cell number was counted at timed intervals. Data were plotted on semi-log paper.

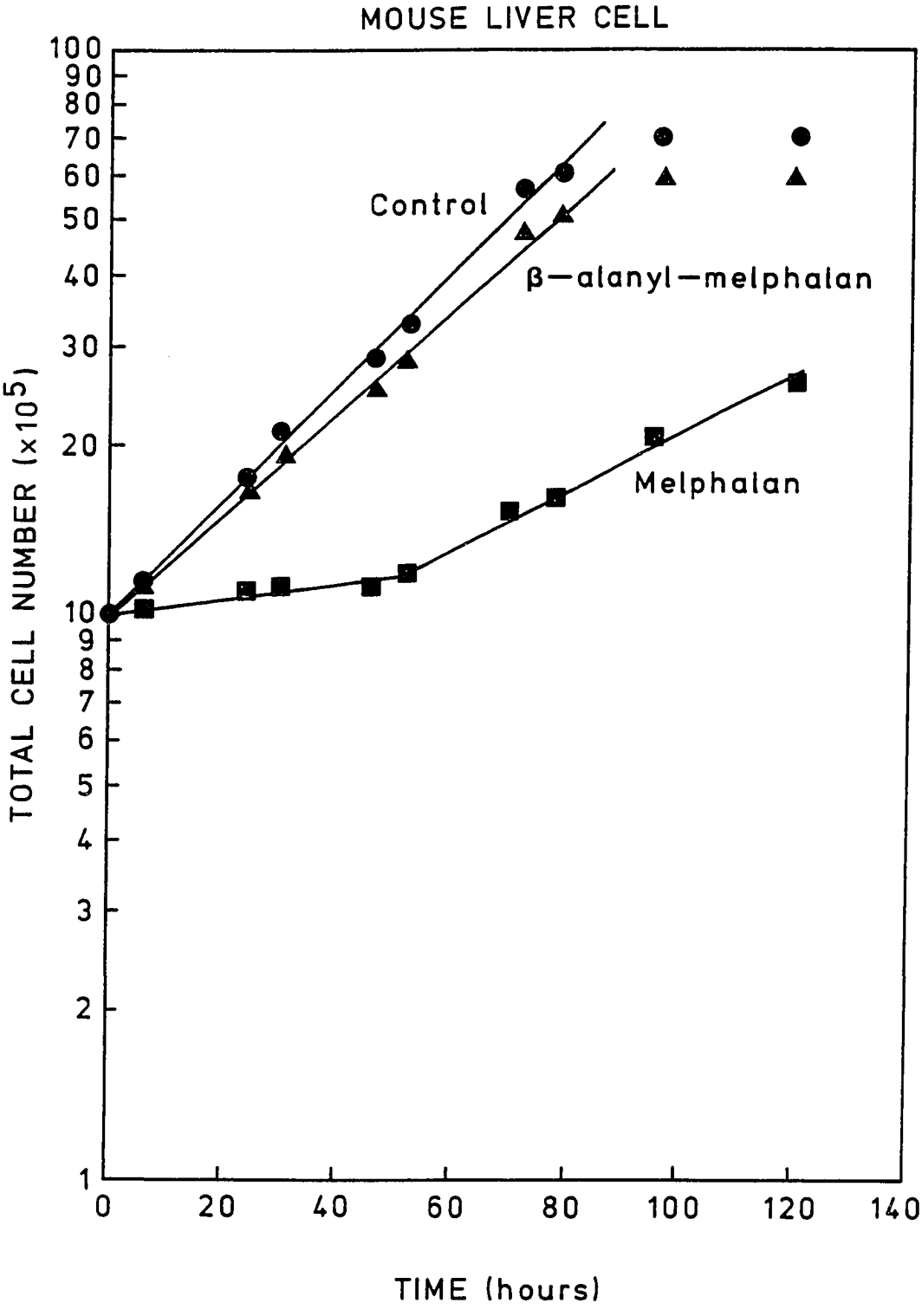

only delayed in cellular proliferation by melphalan.

Figure 39 illustrates the results of a 2-hour incubation with 0.1 mM melphalan and 0.1 mM beta-alanyl-melphalan on the growth of mouse 3T3 embryonic cells. The control group of mouse 3T3 embryonic cells exhibited a growth rate of 23,000 cells per hour.

Results of these experiments reveal that beta-alanyl-melphalan is more toxic than melphalan to mouse 3T3 embryonic cells. Treatment of mouse 3T3 embryonic cells with 0.1 mM melphalan resulted in a dramatic decline in cell number, i.e. approximately 62.3% of the initial cell number within 42 hours after treatment for a cell reduction rate of 17,000 cells per hour. Forty-two hours after treatment, the cell number began to increase at a rate of 6,000 cells per hour. This rate represents a growth potential equivalent to 26% of the control growth rate of nontreated mouse 3T3 embryonic cells. Treatment of mouse 3T3 embryonic cells with 0.1 mM beta-alanyl-melphalan resulted in an equally dramatic decline in cell number, i.e. approximately 63.1% of the initial cell number within 16 hours after treatment for a cell reduction rate of 40,000 cells per hour. Sixteen hours after treatment, cell numbers increased at a rate of 1,750 cells per hour over 32 hours eventually assuming a rate of 10,000 cells per hour. This latter proliferation rate approximated 40% of the cell proliferation rate of nontreated mouse 3T3 embryonic cells.

Figure 39. The effect of 2 hours exposure to melphalan (0.1 mM) and beta-alanyl-melphalan (0.1 mM) on the growth of mouse 3T3 embryonic cells. Cells in exponential growth were incubated for 2 hours with 0.1 mM melphalan and 0.1 mM beta-alanyl-melphalan then inoculated to new cell culture flasks. Total cell number was counted at timed intervals. Data were plotted on semi-log paper.

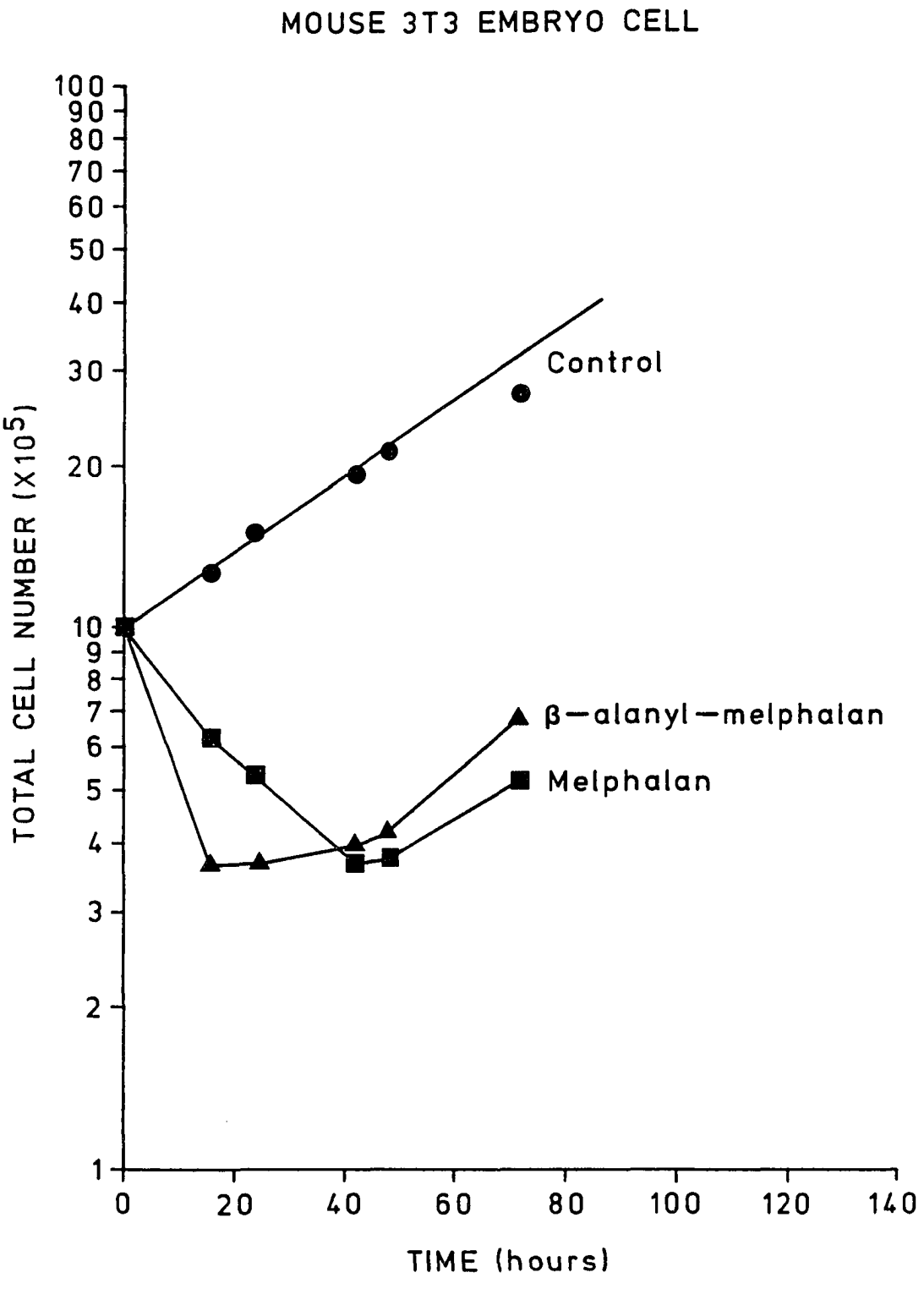

IX. Morphological Studies:

Effect of melphalan and beta-alanyl-melphalan on the morphology of mouse Ehrlich ascites tumor cells using scanning electron microscopy: The SEM micrographs demonstrate the classic characteristics of transformed cells (mouse Ehrlich ascites tumor cells) in Figures 40a and 40b. The cell population was composed predominantly of spherical cells but bipolar cells were also observed. The cell diameter varied from 10 uM to 30 uM and the surfaces of the cells contained short microvilli. Filopodia attached the cell to the substrate and small ruffles could be seen on the top surface and marginal regions of the cells. Blebs could be found on some cell surfaces associated with other cytopodia, (i.e. microvilli, filopodia), whereas other cells demonstrated only blebs -- giving them a "bubbly" appearance.

The SEM micrographs of mouse Ehrlich ascites tumor cells treated with 0.1 mM melphalan for 24 hours are shown in Figures 41a, 41b and 41c. Cell densities were decreased when compared to the mouse Ehrlich ascites tumor cell controls (Figure 40a), and a greater variation in cell size and shape of treated cells was observed. Damaged cells appeared flattened and had lost significant portions of plasma membrane leaving behind a sponge-like mass.

Mouse Ehrlich ascites tumor cells treated with 0.1 mM beta-alanyl-melphalan for 24 hours (Figures 42a, 42b and 42c) demonstrated a dramatic reduction of

Figures 40 (a-b). Scanning electron micrograph of monolayer cell culture of mouse Ehrlich ascites tumor cells which were treated with Dulbecco's phosphate buffered saline. Cells are covered by microvilli (M), and blebs (B). Filopodia (F) are seen attaching to the substrate. Small ruffles (R) are seen on the facing surface. (a. 263X, b. 1,774X).

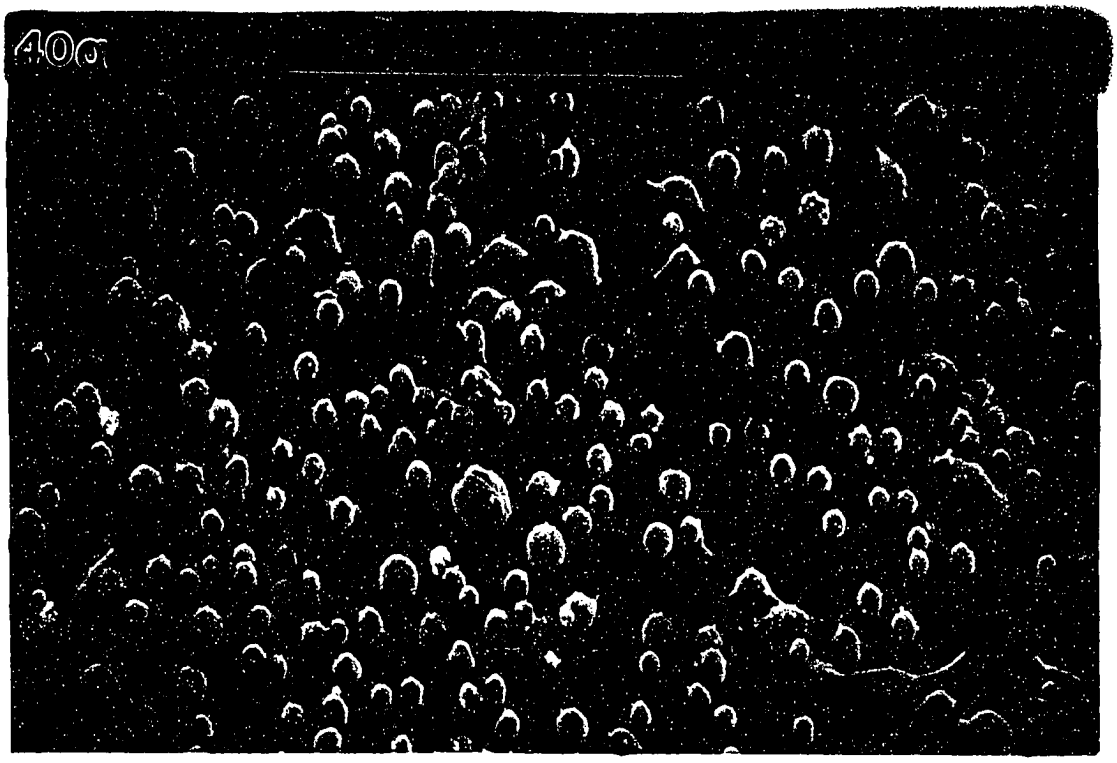

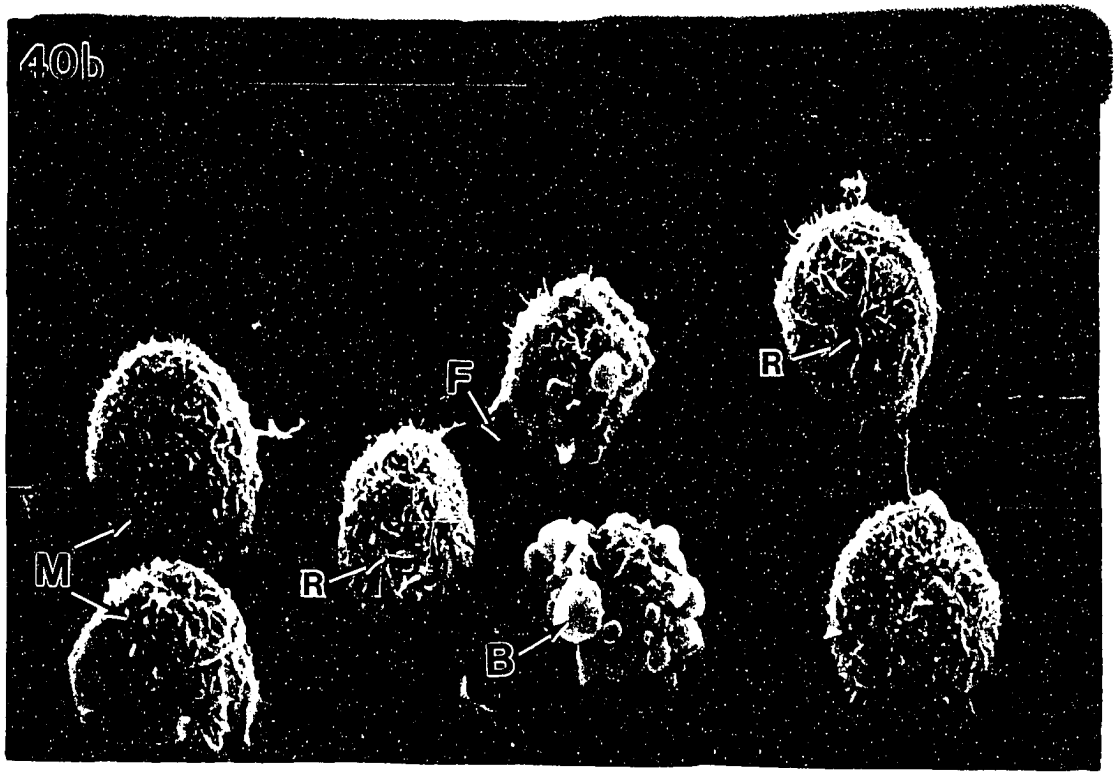

Figures 41 (a-c). Scanning electron micrograph of a monolayer cell culture of mouse Ehrlich ascites tumor cells which were treated with 0.1 mM melphalan for 24 hours. Damaged cells (*) are clearly illustrated. Absence of cell membrane is well demonstrated (Figure 41c). (a. 109X, b. 938X, c. 1,368X).

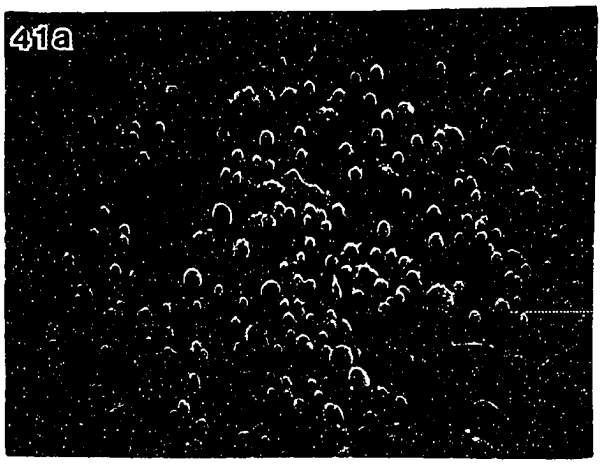

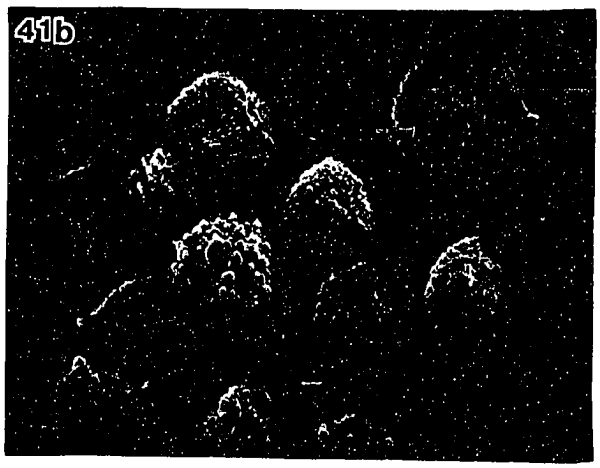

Figures 42 (a-c). Scanning electron micrograph of a monolayer cell culture of mouse Ehrlich ascites tumor cells which were treated with 0.1 mM beta-alanyl-melphalan for 24 hours. (a. 148X, b. 1,323X, c. 906X).

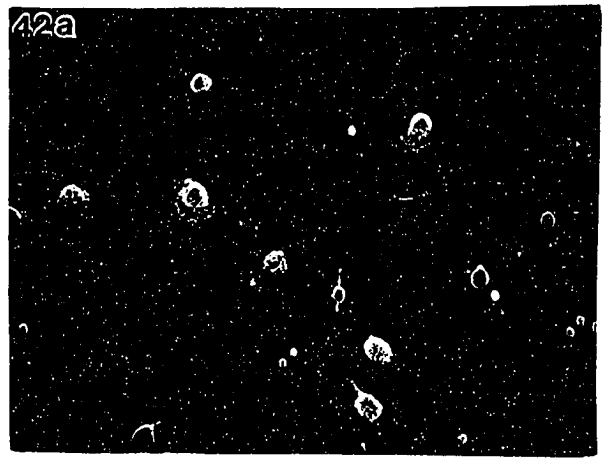

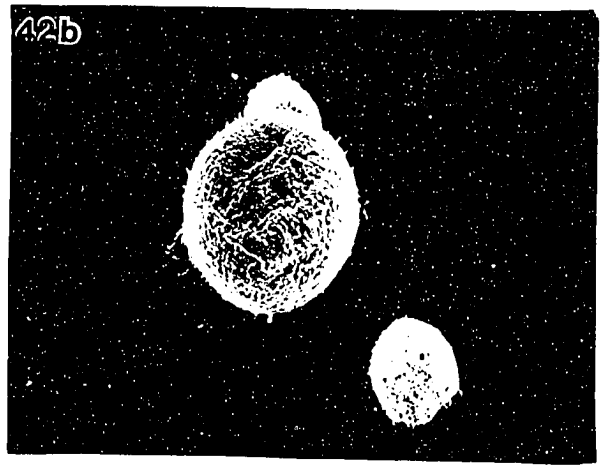

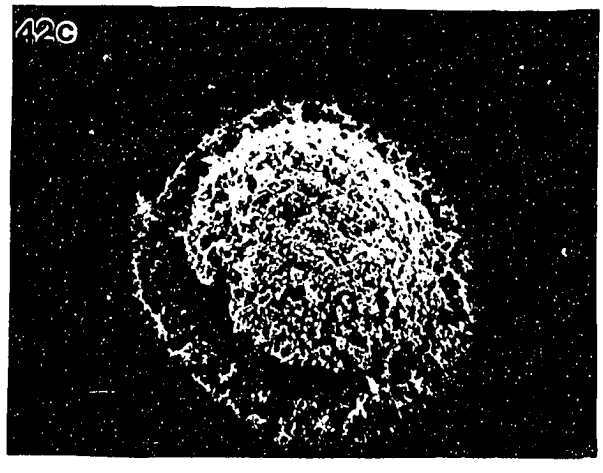

cell density and a reduction or absence of the cytopodia found with nontreated cells. Damaged cells were more common. The appearance of these cells was exhibiting an appearance similar to that of the melphalan-treated cells.

Effect of melphalan and beta-alanyl-melphalan on morphology of mouse liver cells using scanning electron microscopy: The SEM micrographs of control mouse liver cells revealed a dense monolayer of well attached cells (Figures 43a and 43b). Many round and spindle shaped cells and multiple cell clusters were also observed. Surface features included those cytopodia typically found in normal liver cells, i.e. microvilli, pseudopodia and filopodia.

Mouse liver cell cultures treated 24 hours with 0.1 mM melphalan (Figures 44a and 44b) exhibited a marked decrease in cell density. Bipolar and multipolar cells demonstrated a flattened appearance and shrinkage at the marginal regions where they anchored to the culture dish. Round cells demonstrated an irregular shape and cell surfaces that retained the microvilli and filopodia characteristic of nontreated cells.

Mouse liver cells treated with 0.1 mM beta-alanyl-melphalan for 24 hours (Figures 45a and 45b) demonstrated the typical dense monolayer of well attached cells found in the control nontreated mouse liver cells. There was no significant reduction in cell density and bipolar, multipolar and round cells maintained their shape better than melphalan-treated cells. The typical cell was also less flattened

Figures 43 (a-b). Scanning electron micrograph of a monolayer cell culture of mouse liver cells which were treated with Dulbecco's phosphate buffered saline. These control mouse liver cells demonstrate microvilli (M), filopodia (F), and pseudopodia (P). (a. 269X, b. 1,843X).

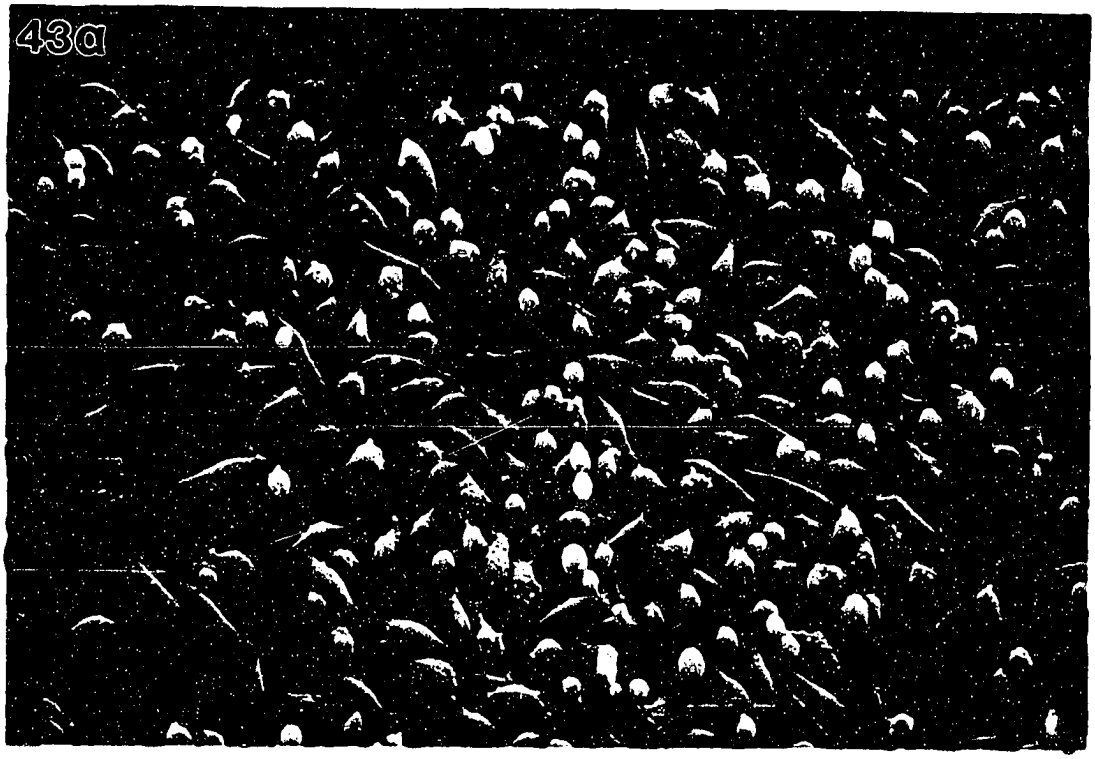

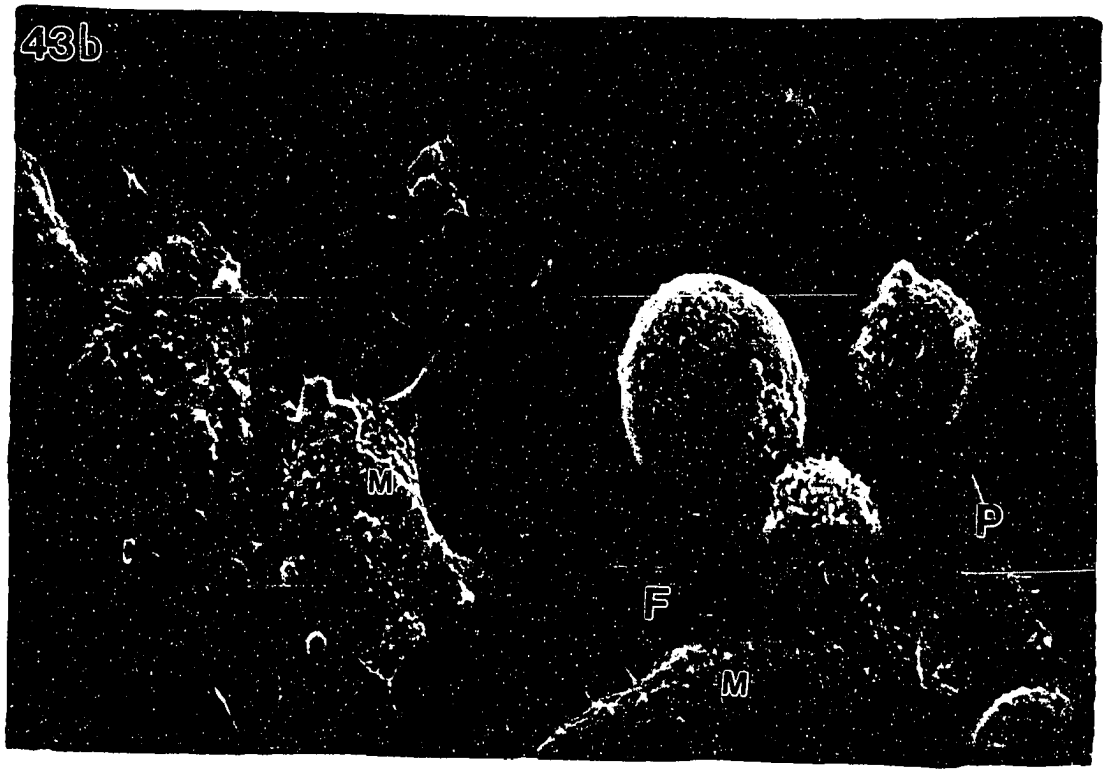

Figures 44 (a-b). Scanning electron micrograph of a monolayer cell culture of mouse liver cells which were treated with 0.1 mM melphalan for 24 hours (a. 280X, b. 1,768X).

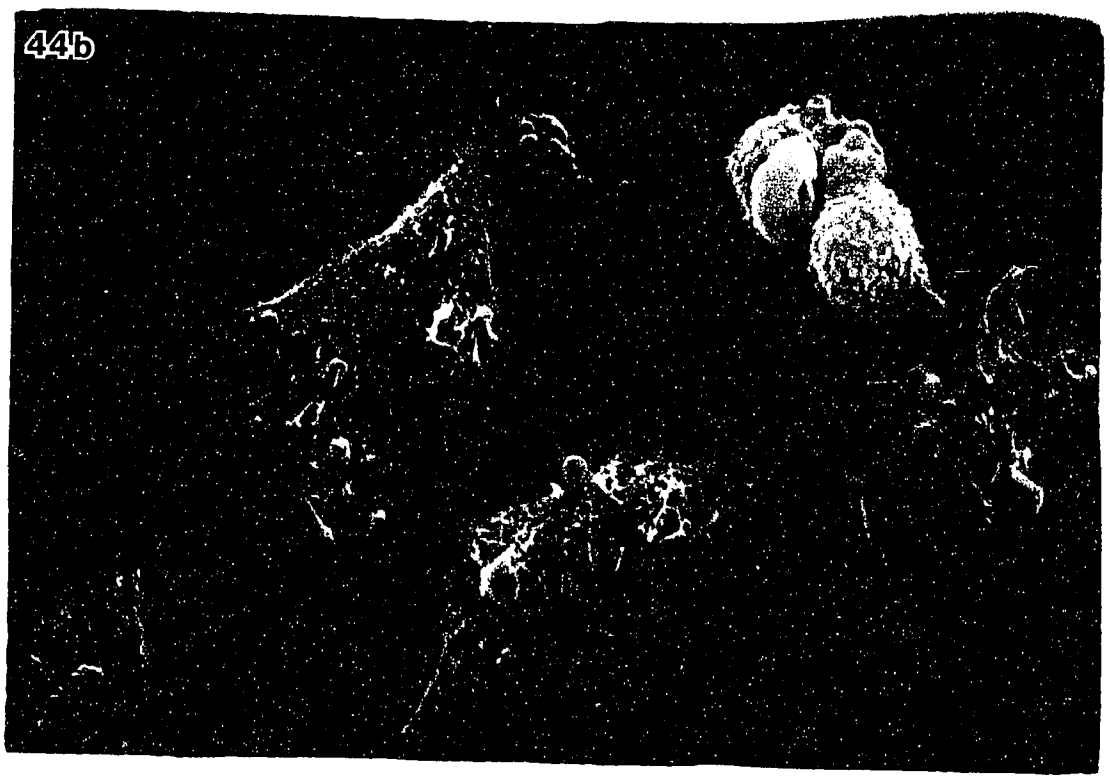

Figures 45 (a-b). Scanning electron micrograph of a monolayer cell culture of mouse liver cells which were treated with 0.1 mM beta-alanyl-melphalan for 24 hours (a. 268X, b. 2,670X) .

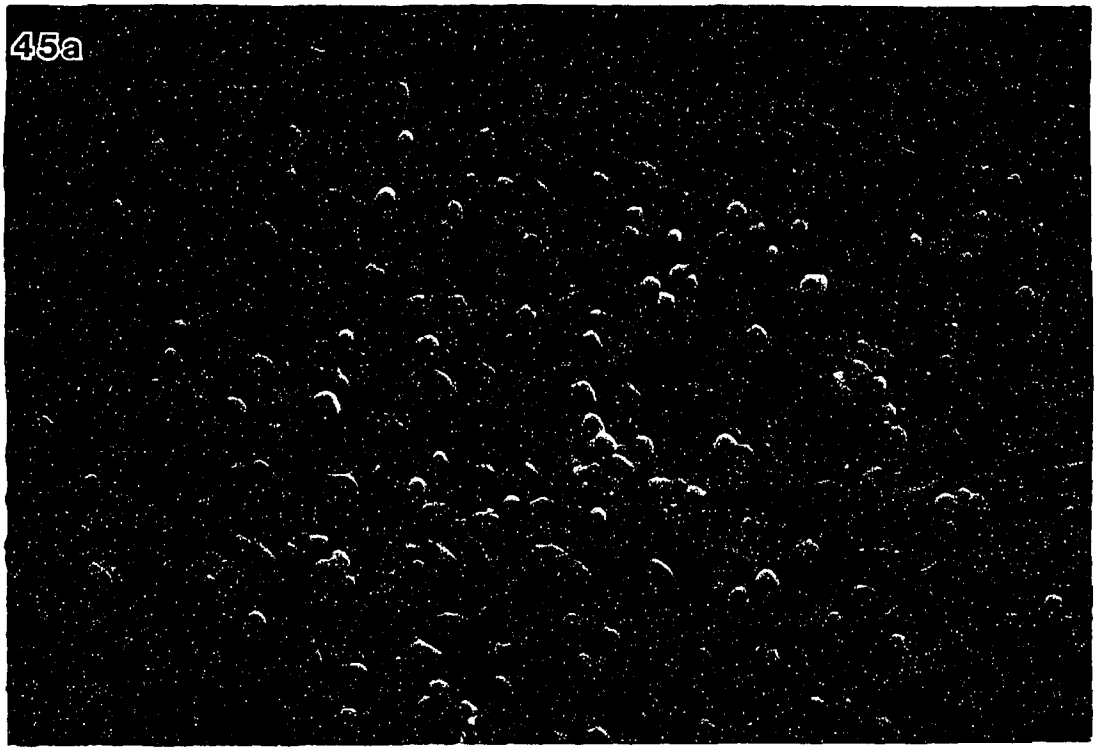

but did exhibit some shrinkage at the marginal attachment areas. Surface cytopodia were common.

Effect of melphalan and beta-alanyl-melphalan on morphology of mouse Ehrlich ascites tumor cells using light microscopy: A light microscope photograph of mouse Ehrlich ascites tumor cells is presented in Figure 46. Polymorphonucleated cells were clearly visible. Cell surfaces were irregular and cytoplasm was filled with vacuoles. In some cells, large vacuoles, were observed, which appeared to displace the nucleus peripherally.

Mouse Ehrlich ascites tumor cells which were treated with 0.1 mM melphalan for 24 hours (Figure 47) exhibited less vacuolated and more dense granular inclusions in the cytoplasm than the control nontreated mouse Ehrlich ascites tumor cells (Figure 46). Large vacuolated cells demonstrated a collapsed morphology and cell debris was observed.

In Figure 48, beta-alanyl-melphalan treated mouse Ehrlich ascites tumor cells exhibited a greatly increased amount of cell debris when compared with the control nontreated mouse Ehrlich ascites tumor cells. Cells were also less vacuolated than control nontreated mouse Ehrlich ascites tumor cells.

Effect of melphalan and beta-alanyl-melphalan on morphology of mouse liver cells using light microscopy: The light microscope photograph of mouse liver

Figure 46. Light microscope photograph of mouse Ehrlich ascites tumor cells which were treated with Dulbecco's phosphate buffered saline (400X).

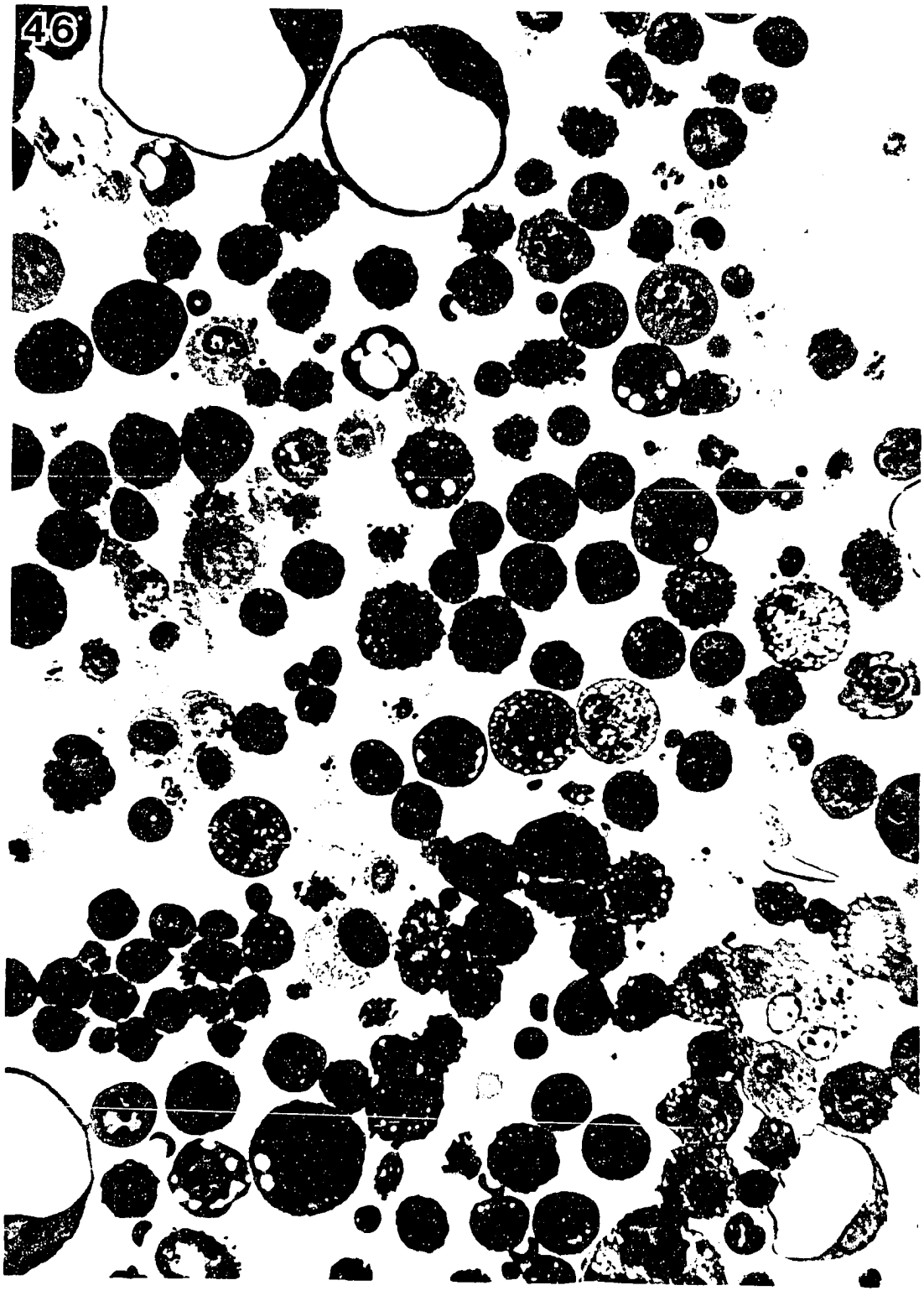

Figure 47. Light microscope photograph of mouse Ehrlich ascites tumor cells which were treated with 0.1 mM melphalan for 24 hours (400X).

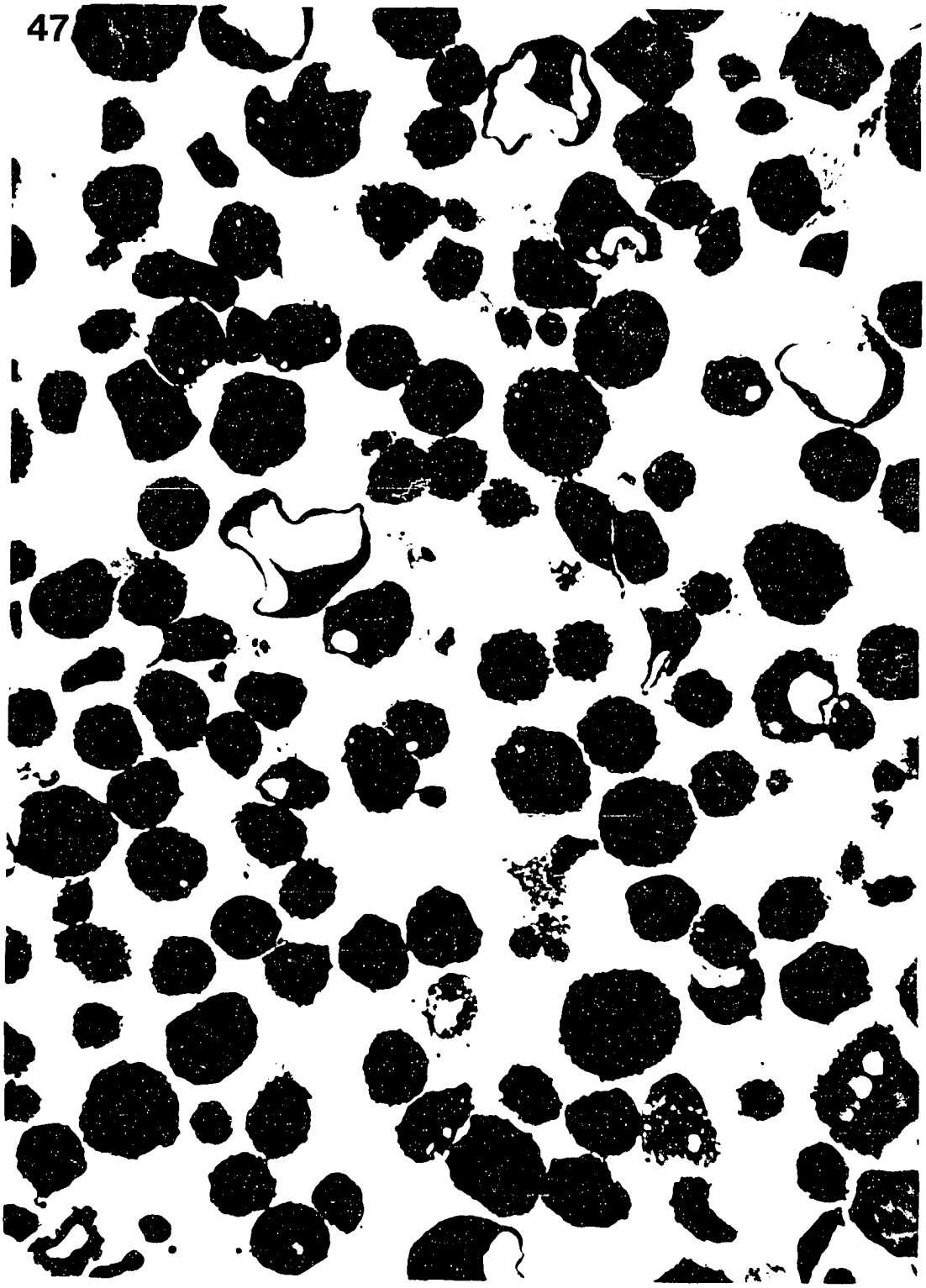

Figure 48. Light microscope photograph of mouse Ehrlich ascites tumor cells which were treated with 0.1 mM beta-alanyl-melphalan for 24 hours (400X).

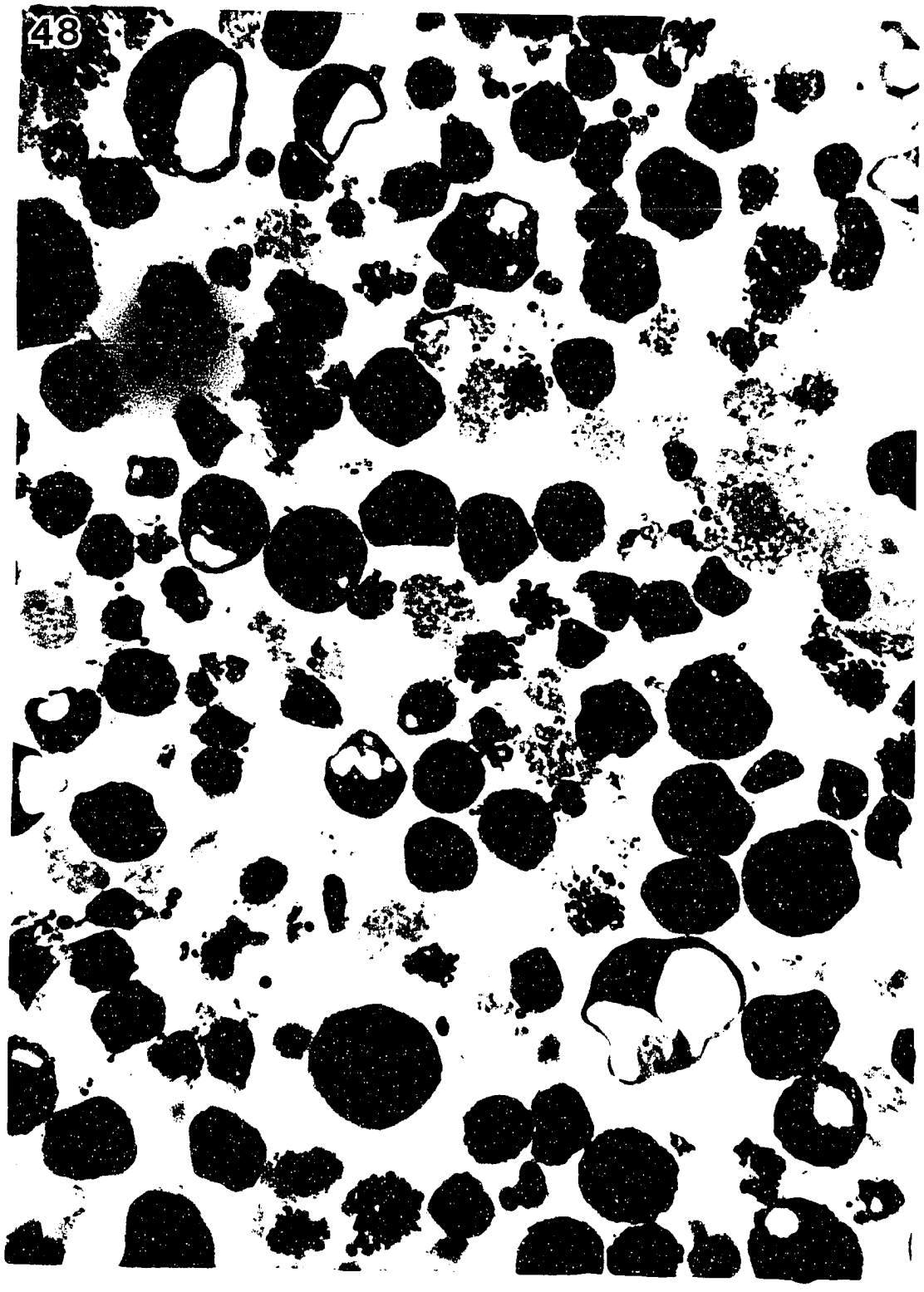

cells is shown is Figure 49. Irregular cell surfaces were seen and represented typical surface morphology i.e. microvilli. Cells demonstrated highly vacuolated cytoplasm and typical nuclei were observed.

Mouse liver cells treated with 0.1 mM melphalan for 24 hours (Figure 50) exhibited a gross vacuolation of the cytoplasm. Much cell debris was observed which indicating the cells were extensively disrupted by the treatment. Cells contained marked numbers of dense granular bodies and smoother surfaces than the control nontreated mouse liver cells.

In Figure 51, 0.1 mM beta-alanyl-melphalan-treated mouse liver cells revealed an appearance similar to that found in the control nontreated mouse liver cells. Cells contained small vacuoles and a single nucleus.

Effect of melphalan and beta-alanyl-melphalan on morphology of mouse Ehrlich ascites tumor cells using transmission electron microscopy: Figures 52a, 52b, 52c shows the ultrastructure of a representative intact mouse Ehrlich ascites tumor cell in which the cytoplasmic organelles appeared typical for a neoplastic cell. The cell displayed a large nucleus containing a characteristically prominent nucleolus with a tightly woven nucleonema (Figure 52a). There was a moderate degree of chromatin condensation with clumping of the heterochromatin in the vicinity of the nucleolus (Figure 52b). Perichromatin granules were also seen at the periphery of the nucleus (Figures 52a, 52b, 52c). A nuclear invagination and

Figure 49. Light microscope photograph of mouse liver cells which were treated with Dulbecco's phosphate buffered saline (400X).

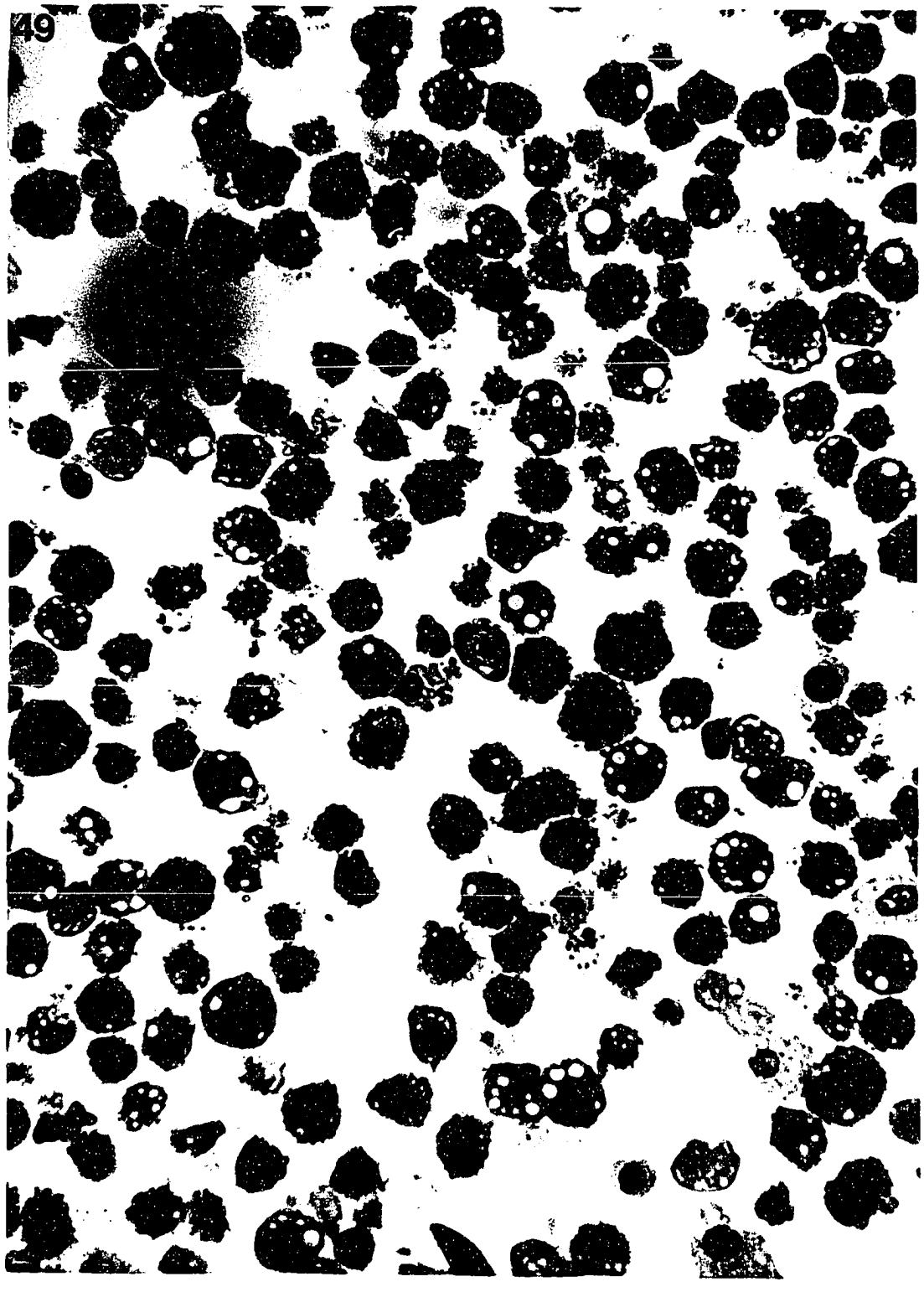

Figure 50. Light microscope photograph of mouse liver cells which were treated with 0.1 mM melphalan for 24 hours (400X).

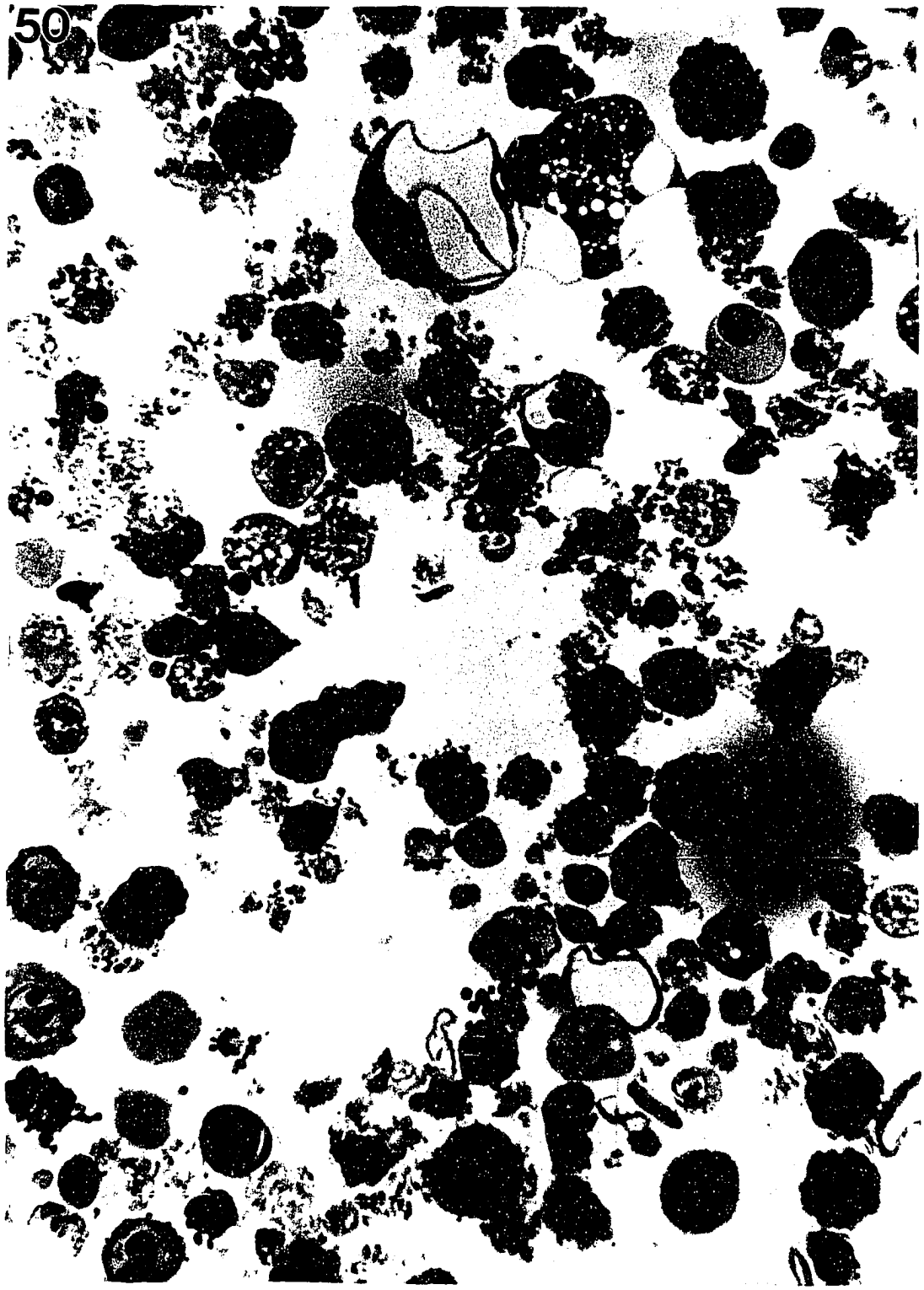

Figure 51. Light microscope photograph of mouse liver cells which were treated with 0.1 mM beta-alanyl-melphalan for 24 hours (400X).

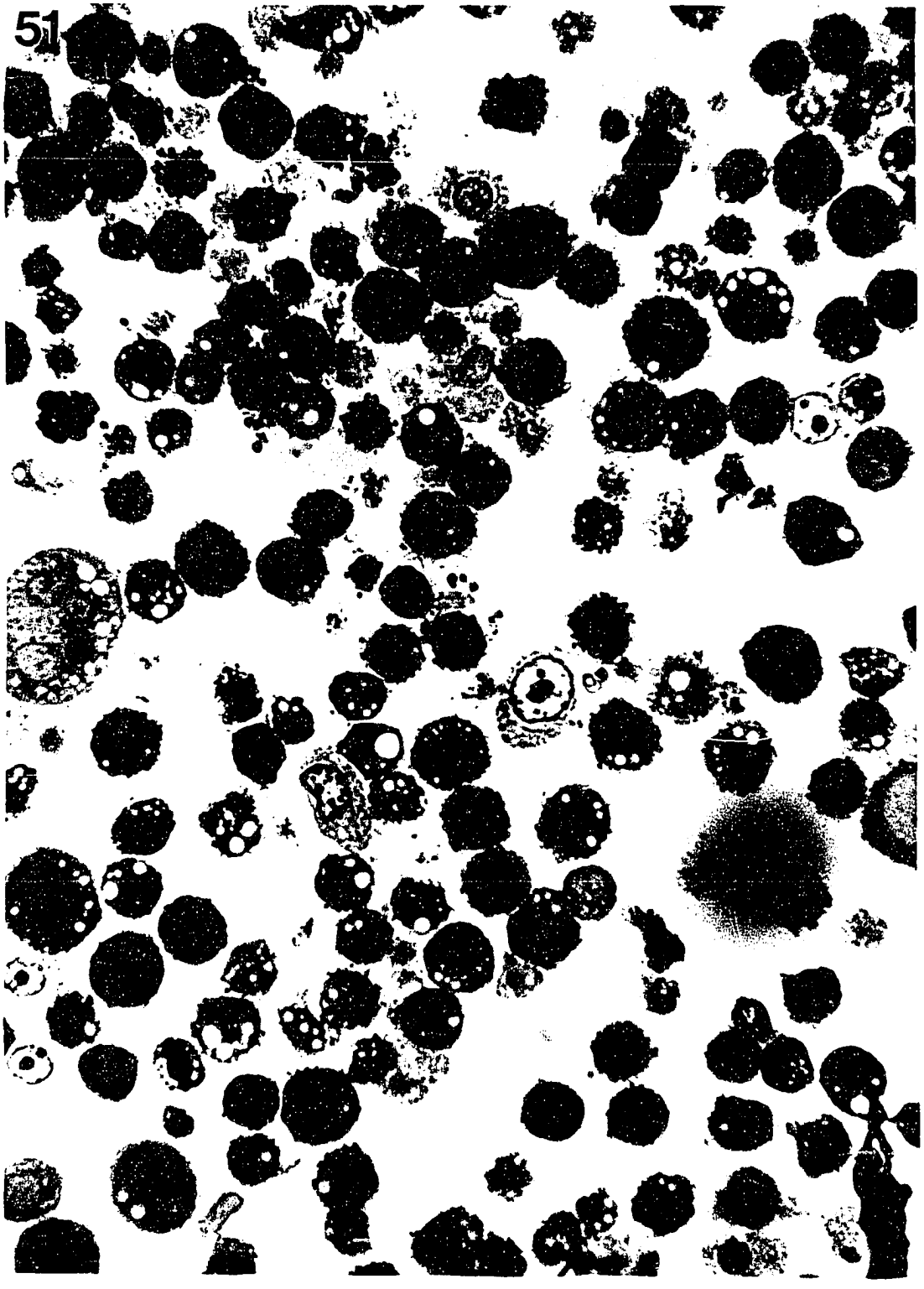

Figures 52 (a-c). Transmission electron microscope photograph of mouse Ehrlich ascites tumor cells which were treated with Dulbecco's phosphate buffered saline. Mitochondria (m), rough endoplasmic reticulum (RER) and Golgi apparatus (G) are shown in these micrographs as well as lipid droplets (L), lysosomes (LY), microvilli (M), and blebs (B). A nucleonema (NL), and perichromatin (PC) are seen in each nucleus. Note nucleus invagination (*) in Figure 52b and multinucleation in Figure 52c. (a. 18,500X, b. 12,800X, c. 17,500X).

52a

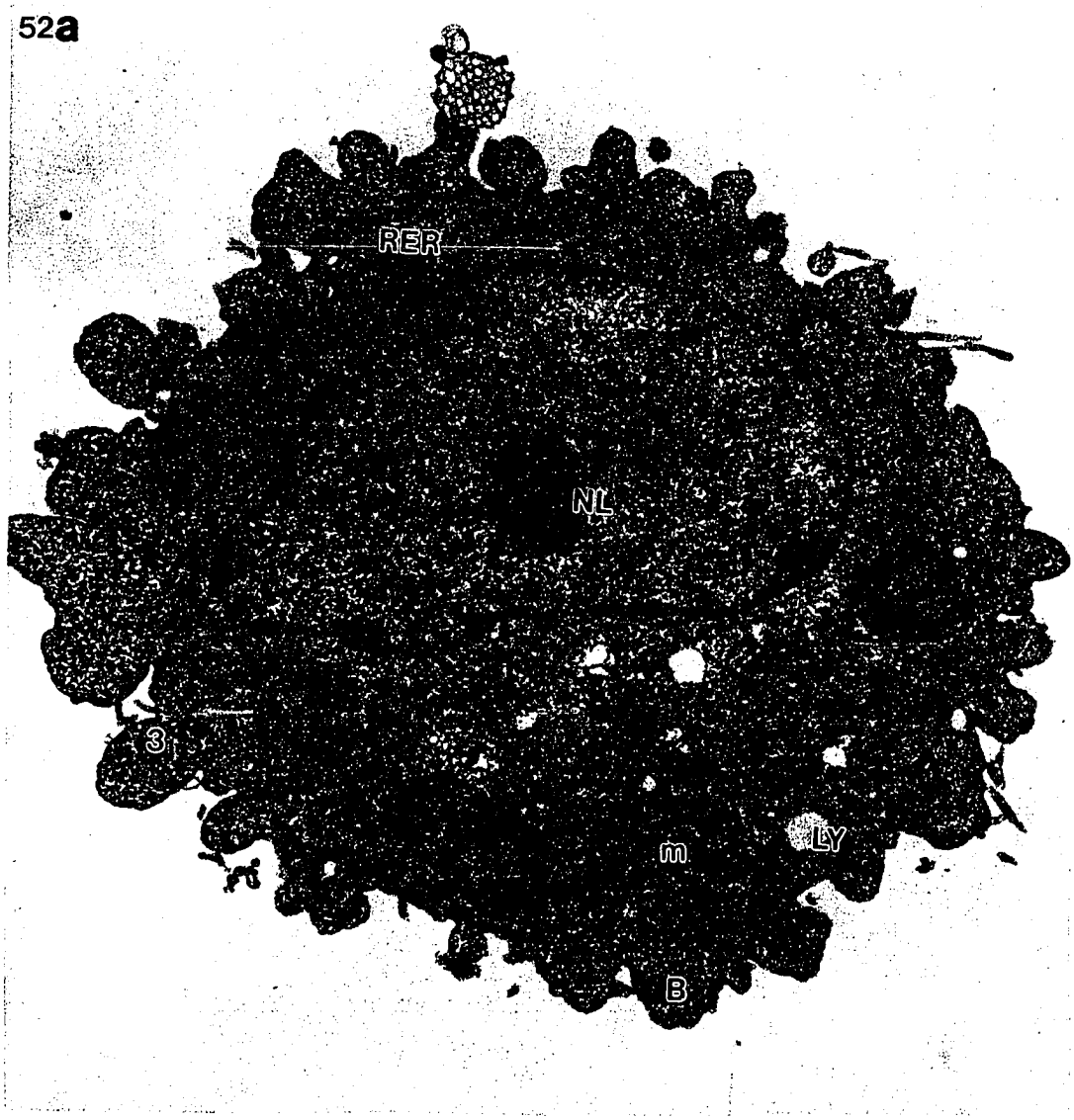

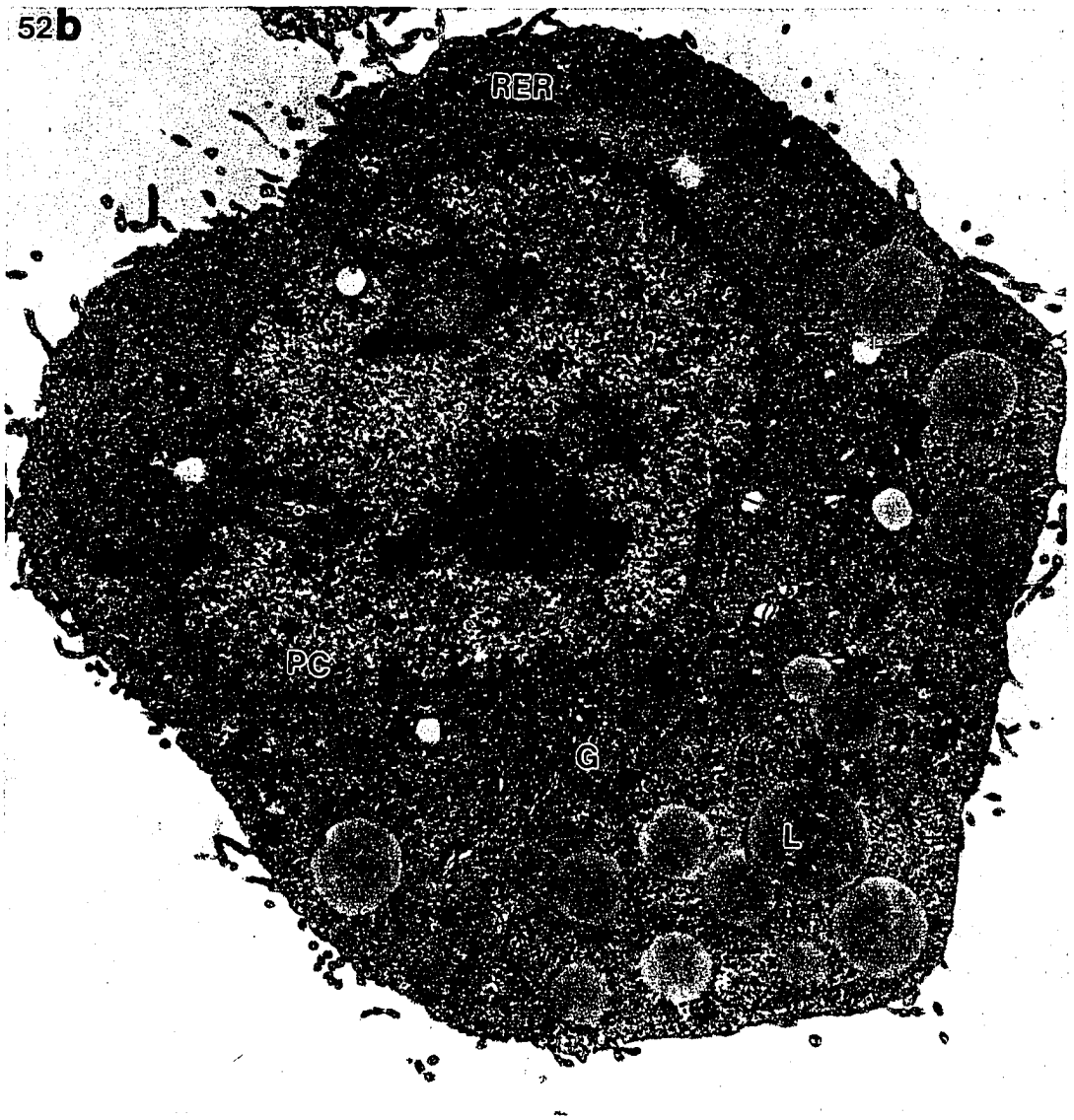

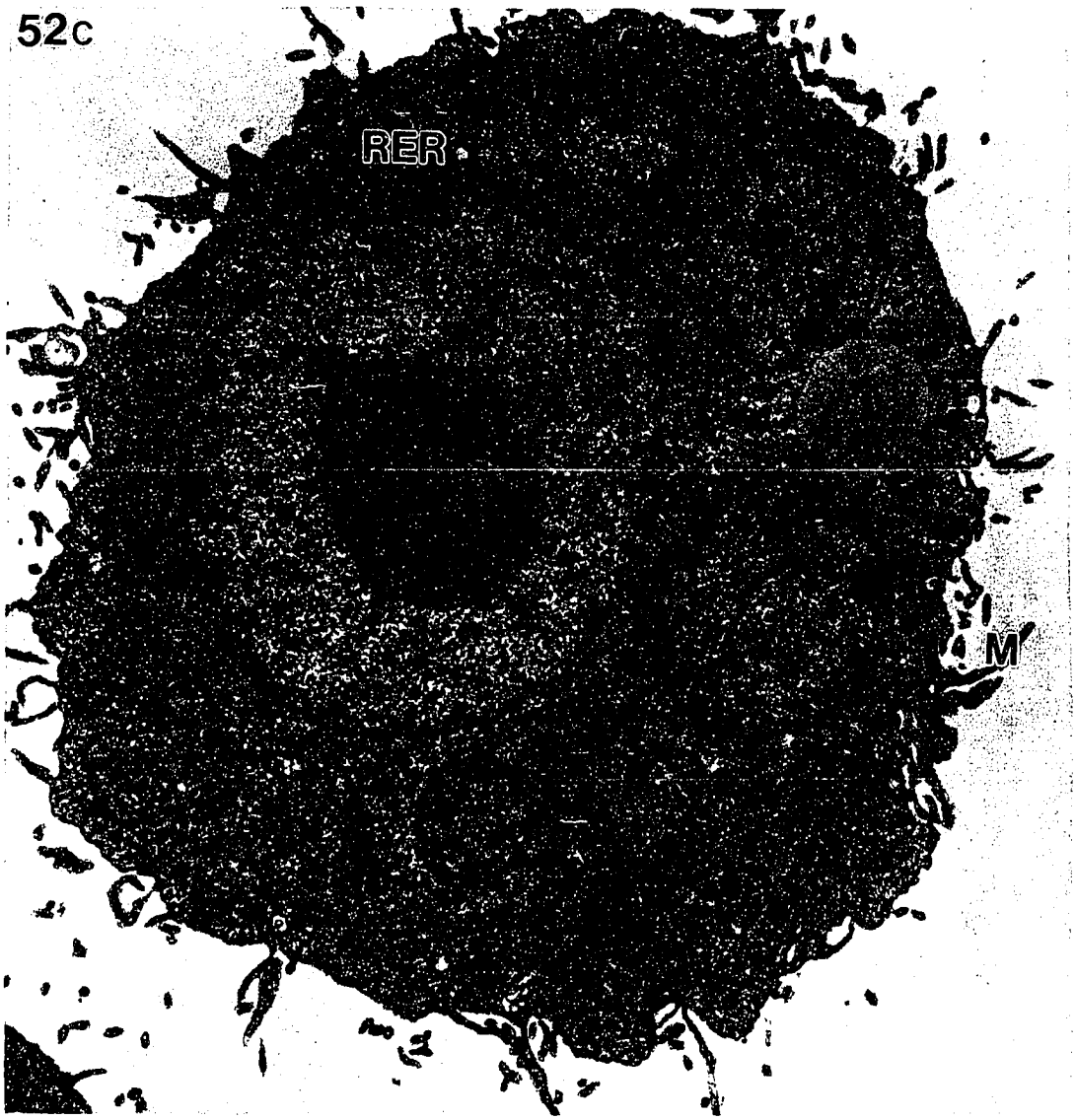

nuclear inclusions were also observed (figure 52b). A relatively common finding in neoplastic cells is the presence of shallow or deep infoldings of the nuclear envelope. Cleaved nuclei having one or two deep invaginations are prominent in mouse Ehrlich ascites tumor cells. Large nuclear inclusions consisting of cytoplasm delineated by the nuclear envelope (Figure 52b) and normal-looking mitochondria, i.e. rod-shaped or oval-shaped, with thin cristae, are seen in the cytoplasm. Some tubular rough endoplasmic reticulum was observed and numerous free ribosomes and cluster ribosomes were abundant in the cytoplasm. Lipid droplets and Golgi apparatus were also visible (Figure 52b). Few lysosomes were visible in the cytoplasm and the cell surface showed microvilli (Figures 52b, 52c) or blebs (Figure 52c) in some cells.

Figures 53a and 53b show typical mouse Ehrlich ascites tumor cells incubated with 0.1 mM melphalan for 24 hours. Morphologically damaged and non-damaged cells were seen. The majority of cells exhibited an irregularity in shape. Morphological non-damaged cells showed an appearance similar to the control nontreated mouse Ehrlich ascites tumor cells, i.e. cell membrane with microvilli or blebs, large nuclei with nucleoli, nuclear invaginations, nuclear inclusions, rough endoplasmic reticulum, ribosomes, lipid droplets, Golgi apparatus, and lysosomes. Mitochondria appeared swollen and an increased heterochromatization was also seen indicating a reduction in active genetic information. Damaged cells were severely disrupted. The number of lysosomes and large vacuoles was increased. In the cell shown, the cell membrane was

Figures 53 (a-b). Transmission electron microscope photograph of mouse Ehrlich ascites tumor cells which were treated with 0.1 mM melphalan for 24 hours. Large vacuoles (V) and cell debris (CD) are seen in addition to the typical characteristics of mouse Ehrlich ascites tumor cells. (a. 4,940X, b. 7,457X).

53a

destroyed and cytoplasm expelled (Figure 53b).

Figures 54a and 54b show the ultrastructure of mouse Ehrlich ascites tumor cells treated with 0.1 mM beta-alanyl-melphalan for 24 hours. The majority of cells examined showed great amounts of cell debris. Mitochondria appeared swollen and an increasing number of lysosomes could be seen. Aggregations of heterochromatin appeared to have migrated to the peripheral area of the nucleus.

Effect of melphalan and beta-alanyl-melphalan on morphology of mouse liver cells using transmission electron microscopy: As observed with transmission electron microscopy, monolayer cultures of mouse liver cells possessed the well-defined features characteristic of mouse liver cells. Cytoplasm contained a single nucleus, and many mitochondria. A variable number of small electron-lucent vesicles were located in the Golgi region. Some lysosomes, a well-developed endoplasmic reticulum, and an abundance of Golgi apparatus were seen in the cytoplasm (Figures 55a and 55b).

Figures 56a, 56b and 56c show the ultrastructure of mouse liver cells treated with 0.1 mM melphalan for 24 hours. Morphologically damaged and non-damaged cells were seen. Some cells showed extremely decreased cytoplasmic volume and the nucleus occupied approximately 90% of visible cytoplasmic space and appeared to push organelles to one end (Figure 56a). The perinuclear space was dilated (Figures 56a and 56b). Morphologically damaged cells showed

Figures 54 (a-b). Transmission electron microscope photograph of mouse Ehrlich ascites tumor cells which were treated with 0.1 mM beta-alanyl-melphalan for 24 hours. Mitochondria (m), Lysosomes (LY), Cell debris (CD), Nuclear inclusions (NI), Lipid droplets (L). (a. 14,000X, b. 16,278X).

54a

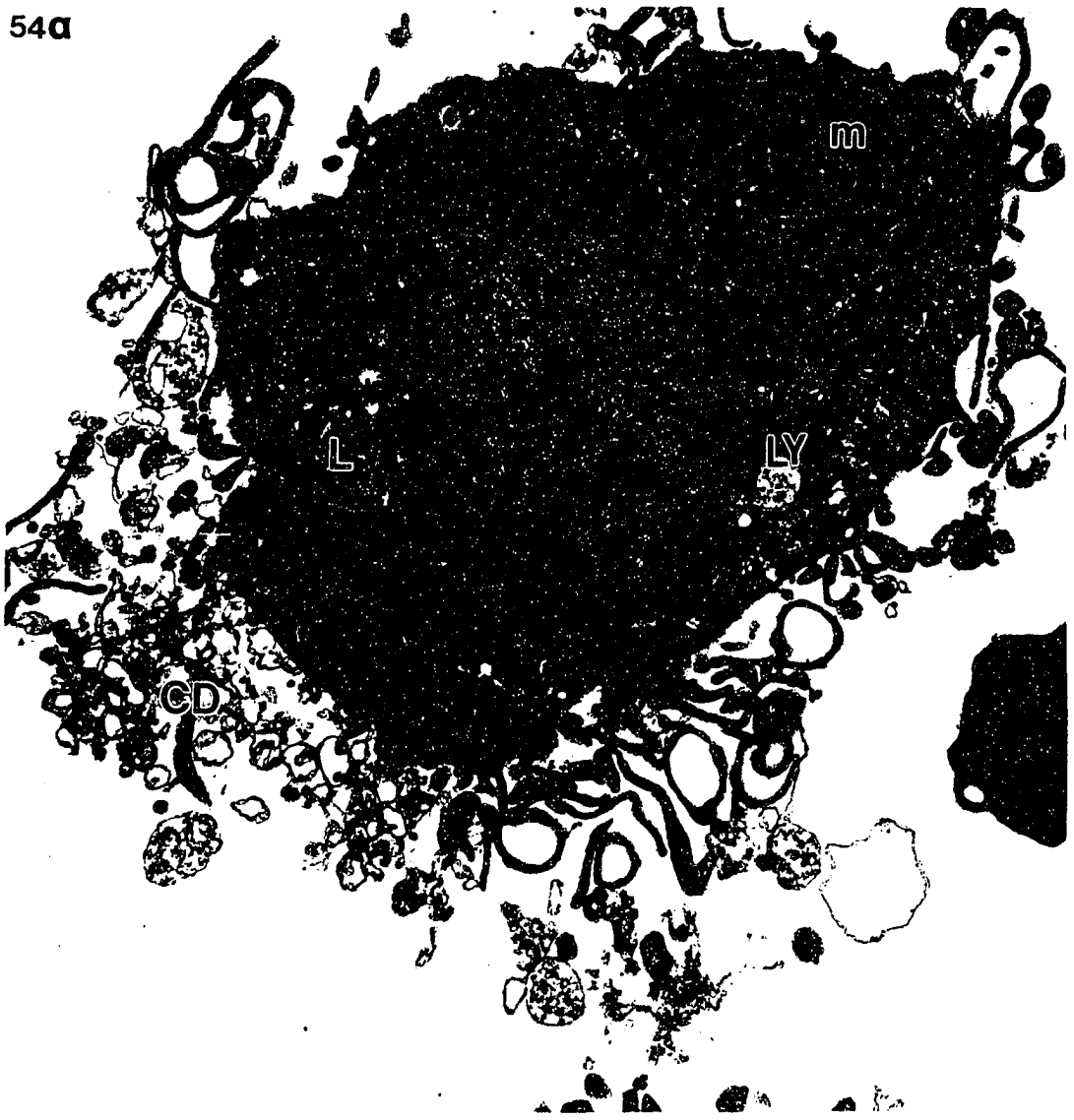

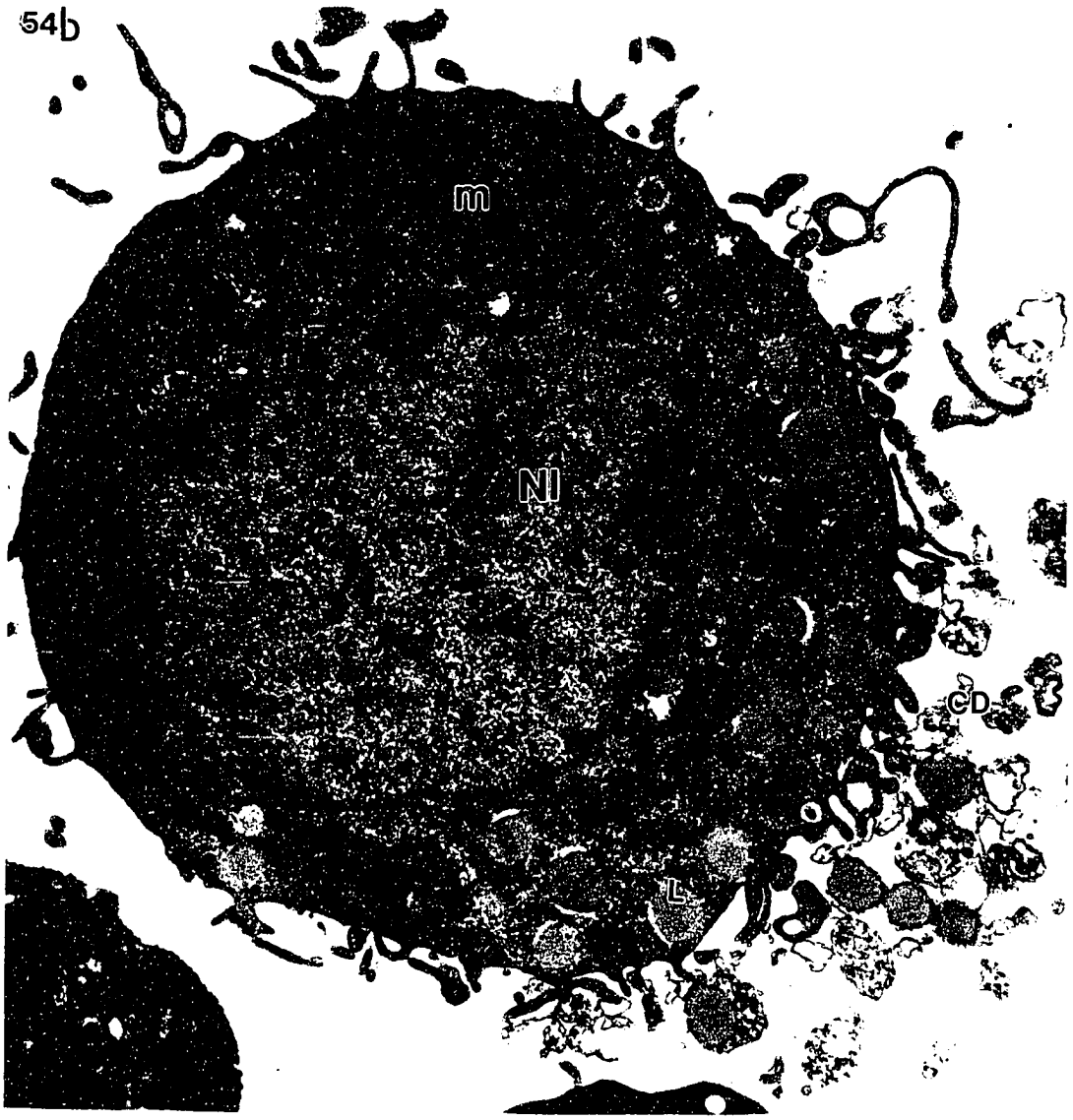

Figures 55 (a-b). Transmission electron microscope photograph of mouse liver cells which were treated with Dulbecco's phosphate buffered saline. Mitochondria (m), Golgi apparatus (G), Endoplasmic reticulum (ER). (a. 9,921X, b. 11,520X).

Figures 56 (a-c). Transmission electron microscope photograph of mouse liver cells which were treated with 0.1 mM melphalan for 24 hours. Nuclear inclusions (NI), Dilated nuclear membrane (arrows), Cell debris (CD), Osmiophilic lipid droplets (LD). (a. 24,150X, b. 8,400X, c. 20,800X).

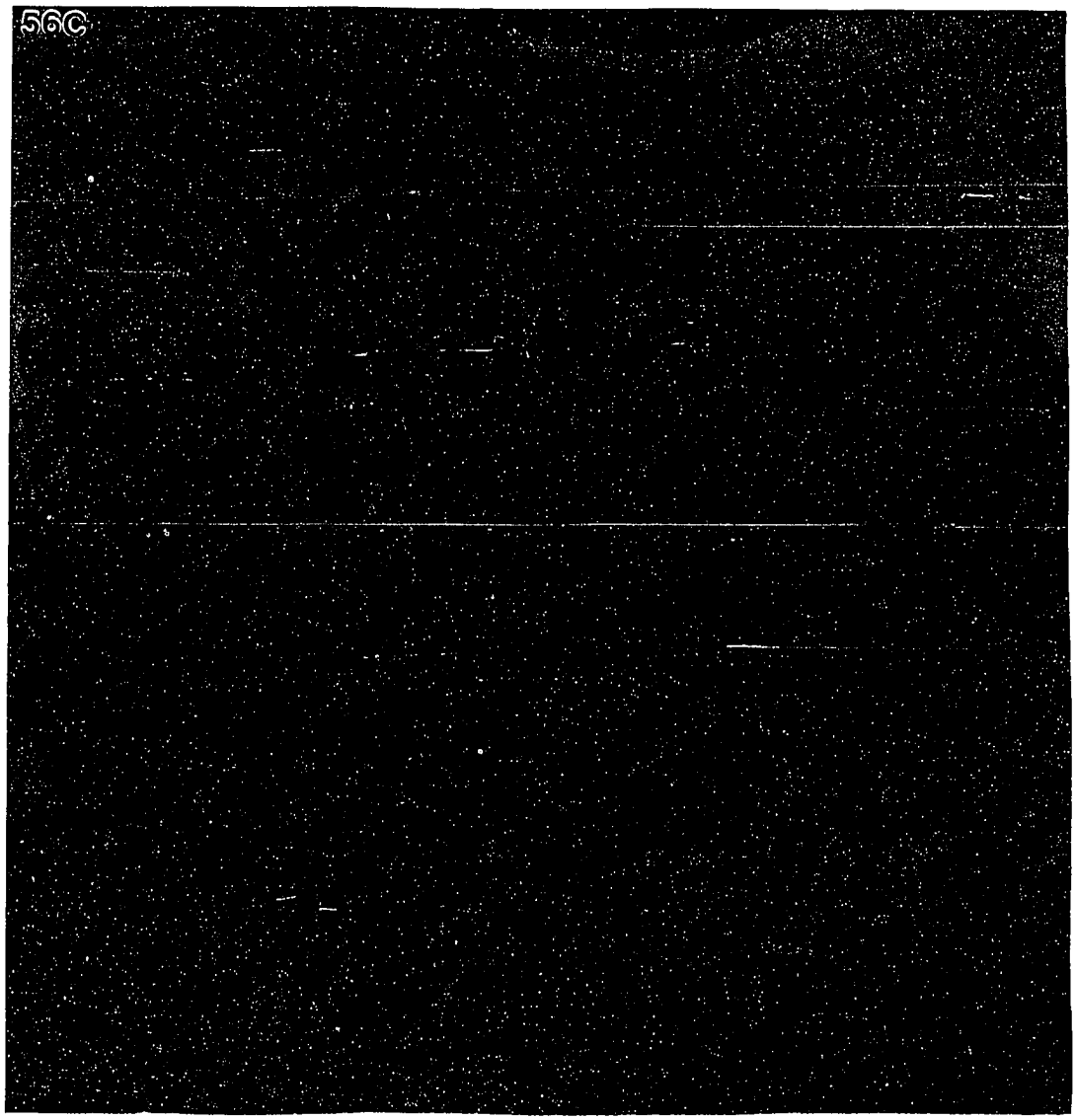

membrane disruption and the cytoplasm being extruded. The number of lysosomes was dramatically increased and dark granules were observed (Figure 56b). Some cells showed severe damage (Figure 56c). Cell membranes, nuclear membranes as well as most of the organelles were totally destroyed. Only some lysosomes and nuclear material could be recognized (Figure 56c). These results indicated that melphalan is extremely toxic to the mouse liver cells.

Figures 57a and 57b show the ultrastructure of mouse liver cells treated with 0.1 mM beta-alanyl-melphalan for 24 hours. Treated cells appeared similar to the control nontreated mouse liver cells. Cytoplasm contained numerous organelles, i.e. mitochondria, rough endoplasmic reticulum, free ribosomes, Golgi apparatus and lipid droplets (Figures 57a and 57b). Nuclear membranes and cell membranes appeared intact. Cell surfaces demonstrated microvilli. These results indicated that beta-alanyl-melphalan is not toxic to the mouse liver cells.

X. In Vivo Chemotherapy Assays:

Traditional chemotherapy assays were performed in an effort to assess the ability of melphalan and beta-alanyl-melphalan to inhibit the growth of tumor cells in vivo. Both compounds had been demonstrated to be toxic to the tumor cells in the in vitro assays, and since melphalan had already been demonstrated to be toxic to the mouse when utilized at concentrations greater than 15 mg/kg (De Barieri, 1983), we chose to test melphalan at a maximum concentration of 10

Figures 57 (a-b). Transmission electron microscope photograph of mouse liver cells which were treated with 0.1 mM beta-alanyl-melphalan for 24 hours. Mitochondria (m), Golgi apparatus (G), rough endoplasmic reticulum (RER), Microvilli (M). (a. 13,736X, b. 22,400X).

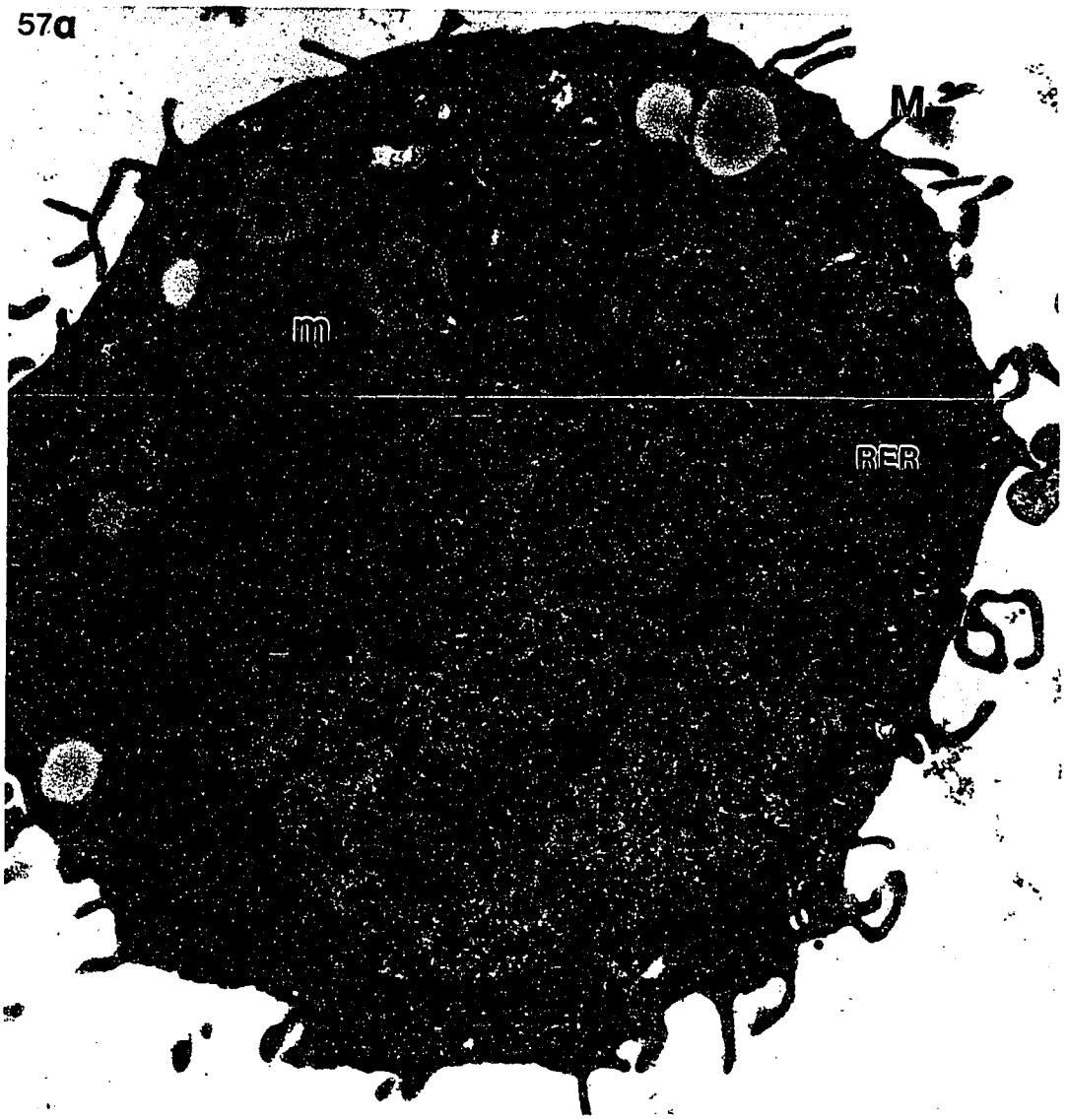

mg/kg.

One million tumor cells were injected intraperitoneally (i.p.) and followed 24 hours later by the drug treatment (also injected i.p.). The body weight, food and water consumption were monitored daily in each group as well as the survival time for each mouse.

Figure 58 shows the average body weight of mice receiving approximately 1 million tumor cells at day 0 followed by drug treatment on day 1. The average body weight of the control group of mice (i.e. no drug treatment) increased significantly 9 days after tumor injection to an average body weight of 50 gms. For the melphalan treatment group, body weight remained steady over the 30-day study period (averaging 32.72 gm). These results indicate that melphalan significantly inhibited tumor cell proliferation (ANCOVA, $p < 0.001$). The average body weight of the beta-alanyl-melphalan (40 mg/kg) treatment group remained constant for the first 21 to 22 days, significantly increasing over initial body weight only in the last 8 days of the experiment. During the 30-day study period, beta-alanyl-melphalan treated mice increased their body weights approximately 20% over the original body weight. Statistical analysis of these data revealed that the increased body weights of beta-alanyl-melphalan treated mice were significantly lower than the control nontreated mice ($p < 0.001$, ANCOVA). The results indicated that melphalan and beta-alanyl-melphalan significantly decreased tumor cell proliferation and ascites fluid production.

Figure 58. The effects of anticancer drug treatment on the body weight of adult CF-1 albino mice with tumor cell injection. The mice (6) in each group were injected with approximately 1 million tumor cells in Dulbecco's phosphate buffered saline on day 0 followed by Dulbecco's phosphate buffered saline without (○-○) or with 10 mg/kg melphalan (•--•), or 40 mg/kg beta-alanyl-melphalan (▲-▲) on day 1. Body weight was recorded daily and average body weight was calculated as Mean ± SD in gm and plotted as a function of time. By day 20, all mice in the DPBS treatment group had died.

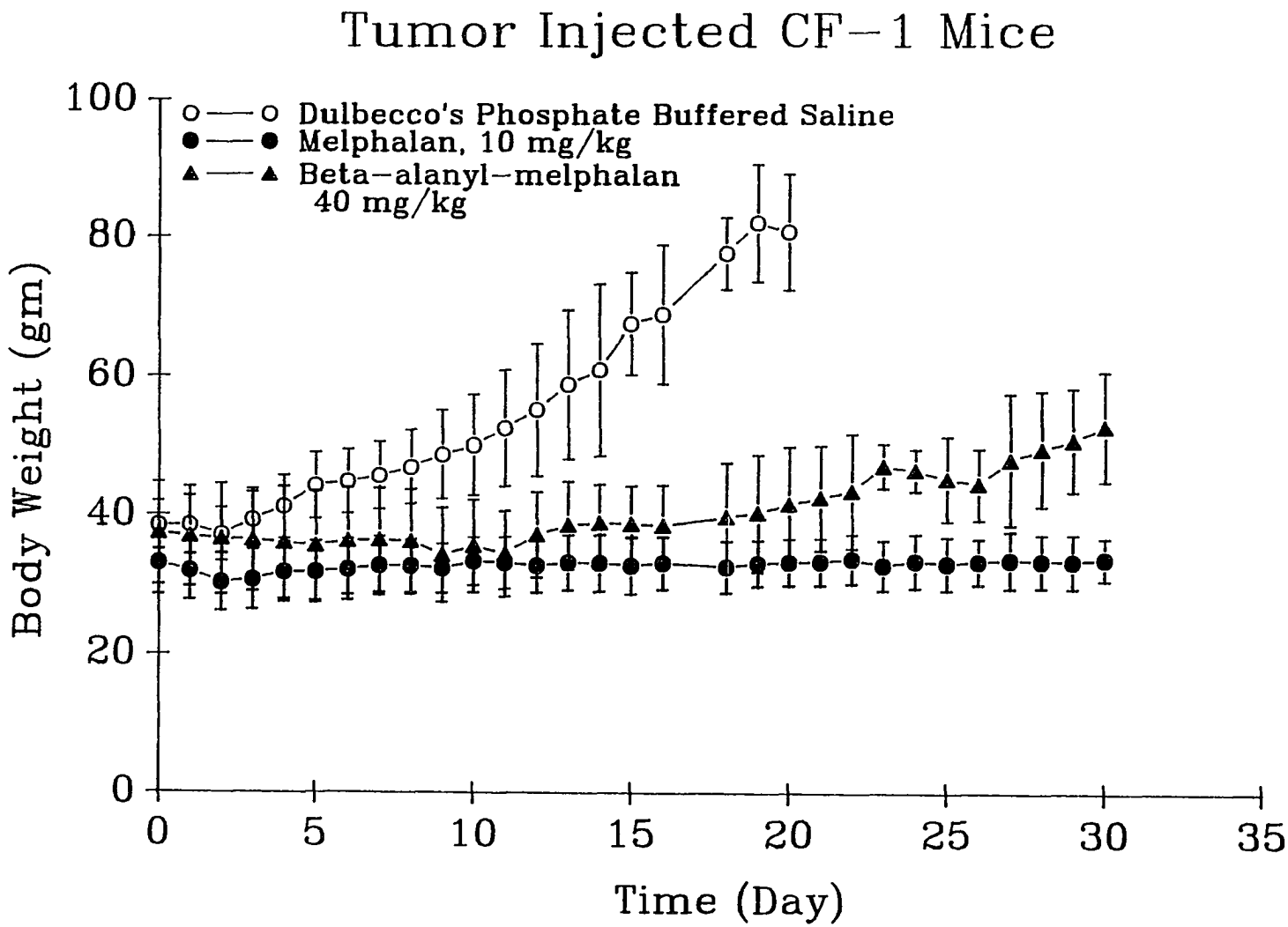

To examine the effect of both agents on body weight of noncancerous mice, CF-1 mice received an injection of Dulbecco's phosphate buffered saline (DPBS) at day 0 followed by DPBS as control, 10 mg/kg melphalan in DPBS, or 40 mg/kg beta-alanyl-melphalan in DPBS at day 1. Average body weights of 31.59 gm, 37.59 gm, and 32.79 gm were found for control, melphalan, and beta-alanyl-melphalan injected mice over the 30 day study period respectively. Figure 59 shows that the body weight of animals treated with 10 mg/kg melphalan and 40 mg/kg of beta-alanyl-melphalan were not significantly different from those of control mice. No deaths occurred in mice given 10 mg/kg and 40 mg/kg beta-alanyl-melphalan.

To assess the effects of both drugs in daily food and water intake on noncancerous mice and tumor-bearing mice, both groups of mice received DPBS, melphalan (10 mg/kg) and beta-alanyl-melphalan (40 mg/kg) injection 1 day after tumor injection (DPBS injection for noncancerous mice).

The results of the study of daily food and water intake during the 22-day study are shown in Figures 60, 61, 62, 63. Figure 60 reveals the average daily water consumption of CF-1 mice receiving tumor cells on day 0 and DPBS, 10 mg/kg melphalan or 40 mg/kg beta-alanyl-melphalan on day 1. The DPBS injected group, i.e. no drug treatment, demonstrated a reduction of daily water consumption, ie. 8.2 ml to 2.4 ml over the 22 days. Melphalan treated mice

Figure 59. The effects of anticancer drug treatment on the body weight of adult CF-1 albino mice with no tumor injection. The mice (6) of each group were injected with Dulbecco's phosphate buffered saline on day 0 followed by Dulbecco's phosphate buffered saline without (○-○), or with 10 mg/kg melphalan (•--•), or 40 mg/kg beta-alanyl-melphalan (▲-▲) on day 1. Body weight was recorded daily and average body weight was calculated as Mean ± SD in gm and plotted as a function of time.

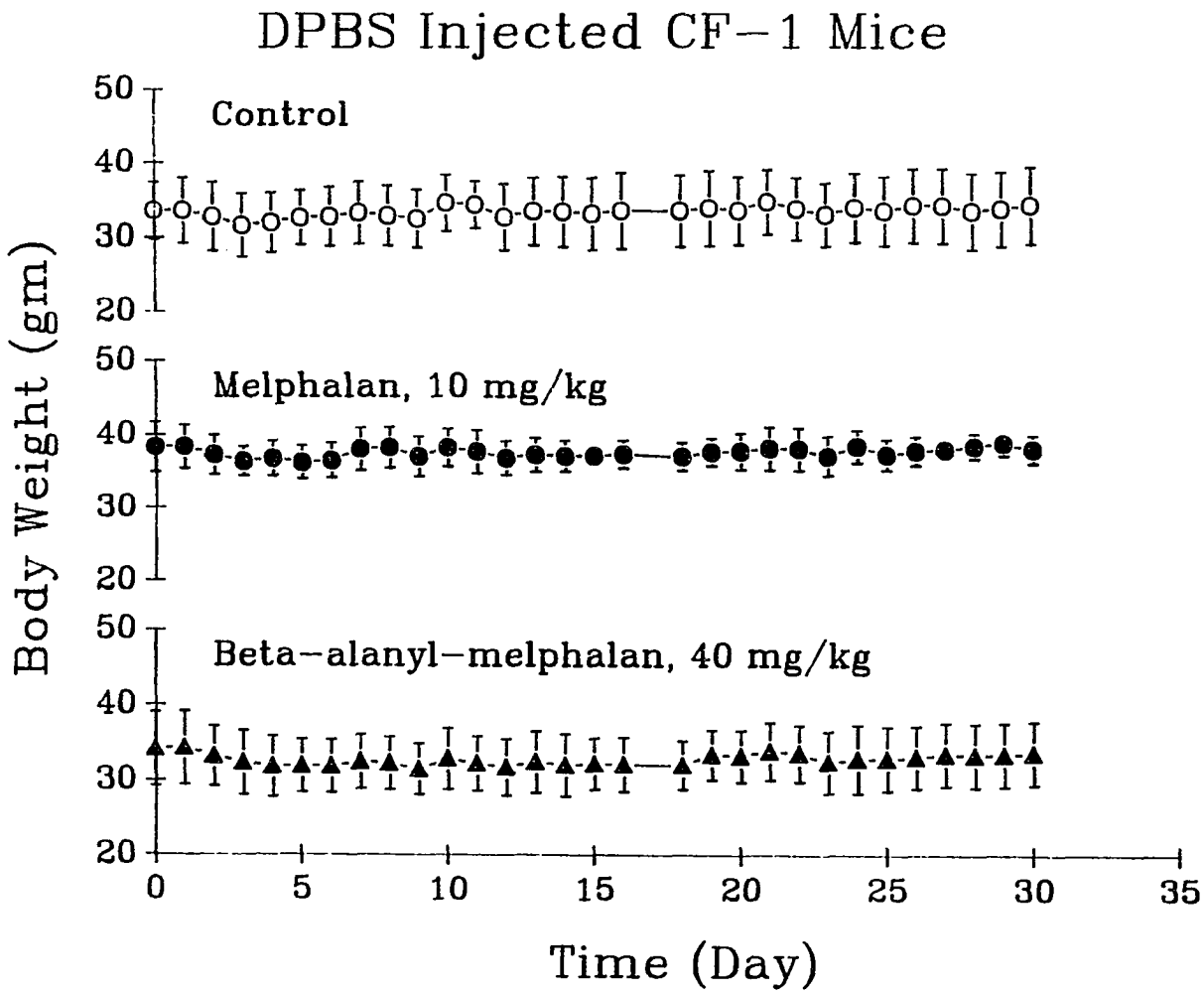

Figure 60. The effects of anticancer drugs on water consumption of tumor-bearing mice. Daily ad libatum water consumption during a 22-day study for tumor-bearing mice which received a 1 million tumor cell injection on day 0 and followed by dulbecco's phosphate buffered saline (O-O), 10 mg/kg melphalan (•--•), 40 mg/kg beta-alanyl-melphalan (▲-▲) injection on day 1. Water consumption was recorded daily and average water consumption was calculated as Mean ± SD in ml and plotted as a function of time.

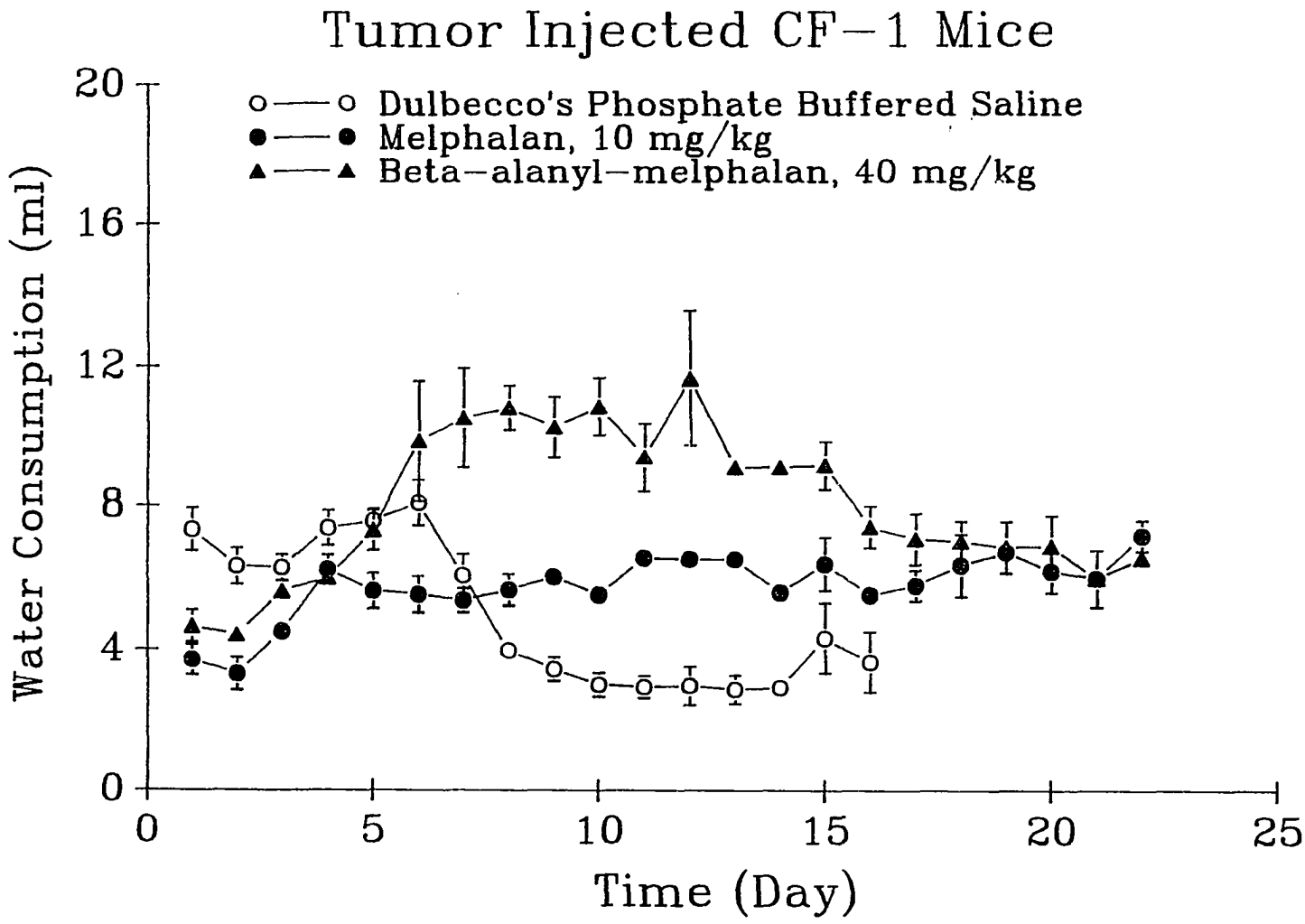

exhibited a steady water intake with an average of 5.65 ml/day. Beta-alanyl-melphalan treated mice exhibited fluctuations in water consumption, increasing over the first 6 days followed by a plateau for the next 6 days then declining over the next 10 days to a value similar to that of the melphalan treated group (2.4 ml).

Figure 61 reveals that CF-1 mice were injected with Dulbecco's phosphate buffered saline (DPBS) and received DPBS, 10 mg/kg melphalan, and 40 mg/kg beta-alanyl-melphalan. Averaged water intake of 5.46 ± 0.81, 5.59 ± 1.27, 7.27 ± 1.24 ml over the 22 days of study were observed. Only the beta-alanyl-melphalan group demonstrated a trend of increase in average daily water consumption when compared to the control group ($p > 0.01$, ANCOVA).

Measurements of average daily food consumption in the cancerous groups, i.e. injected with 1 million ascites tumor cells on day 0, receiving DPBS therapy on day 1, revealed a dramatic decline after 5 days (Figure 62). The melphalan treated group of tumor-bearing mice showed a slight increase in food consumption but this increase was not significant with increasing time providing an average value of 4.51 ± 1.31 gm/day/mouse (Figure 62). The beta-alanyl-melphalan treated group of tumor-bearing mice demonstrated a steady food consumption with an average of 3.38 ± 0.66 gm/day/mouse (Figure 62). The average daily food consumption by the DPBS treated group of tumor-bearing mice was significantly different (reduced) from the other treatment groups after

Figure 61. The effects of anticancer drugs on water consumption in noncancerous mice. Daily ad libatum water intake during a 22-day study of Dulbecco's phosphate buffered saline injected CF-1 mice (noncancerous mice) which received Dulbecco's phosphate buffered saline on day 0 and followed by Dulbecco's phosphate buffered saline (○-○), 10 mg/kg melphalan (•--•), or 40 mg/kg beta-alanyl-melphalan (▲-▲) 24 hours later. Water consumption was recorded daily and average water consumption (in ml) was calculated as Mean ± SD and plotted as a function of time.

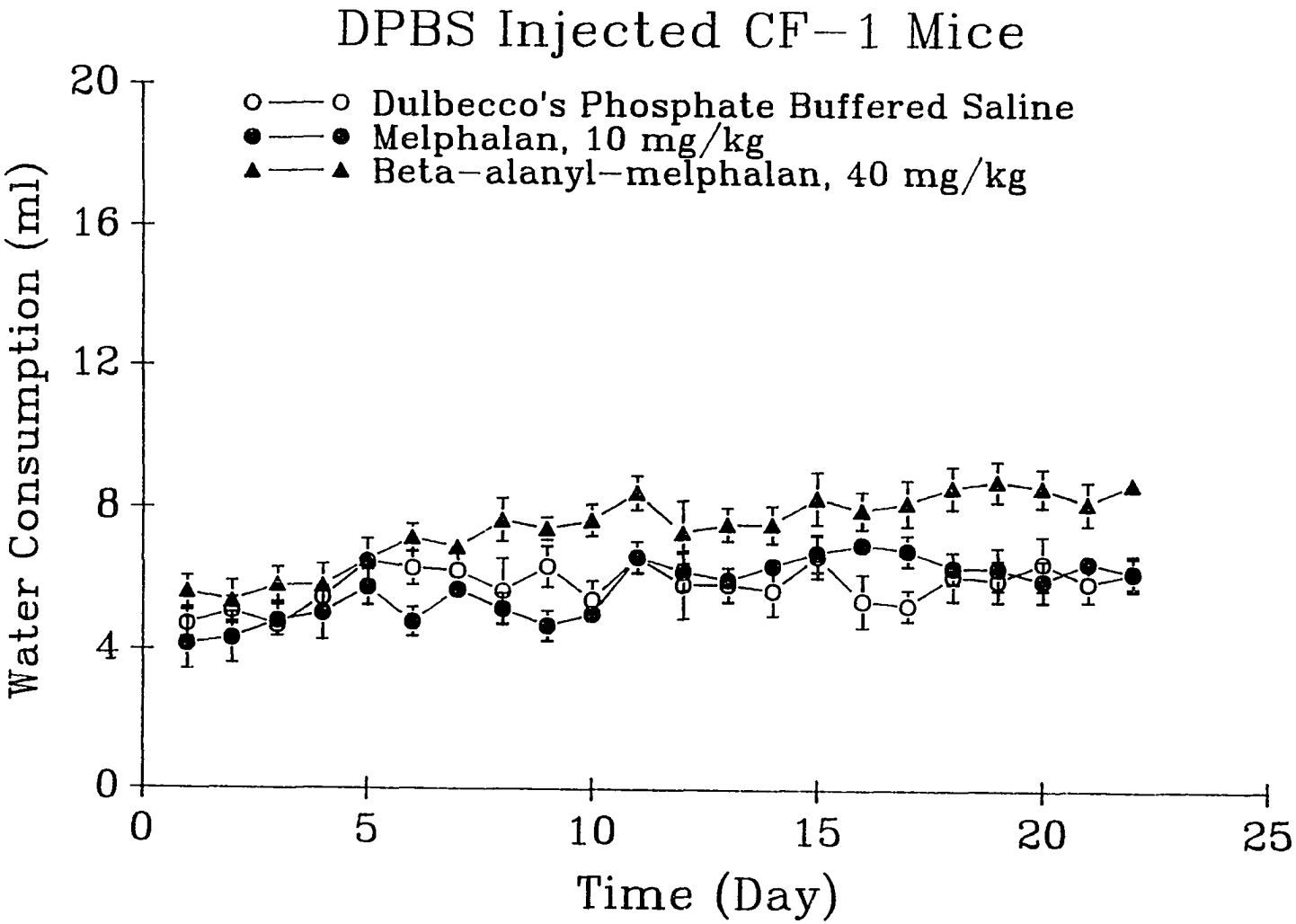

Figure 62. The effects of anticancer drugs on food consumption in tumor-bearing mice. Daily ad libatum food consumption during a 22-day study for tumor-bearing mice which received 1 million tumor cells on day 0 and followed by Dulbecco's phosphate buffered saline (○-○), 10 mg/kg melphalan (•--•), or 40 mg/kg beta-alanyl-melphalan (▲-▲) on day 1. Food consumption was recorded daily and average food consumption (in grams) was calculated as Mean ± SD and plotted as a function of time.

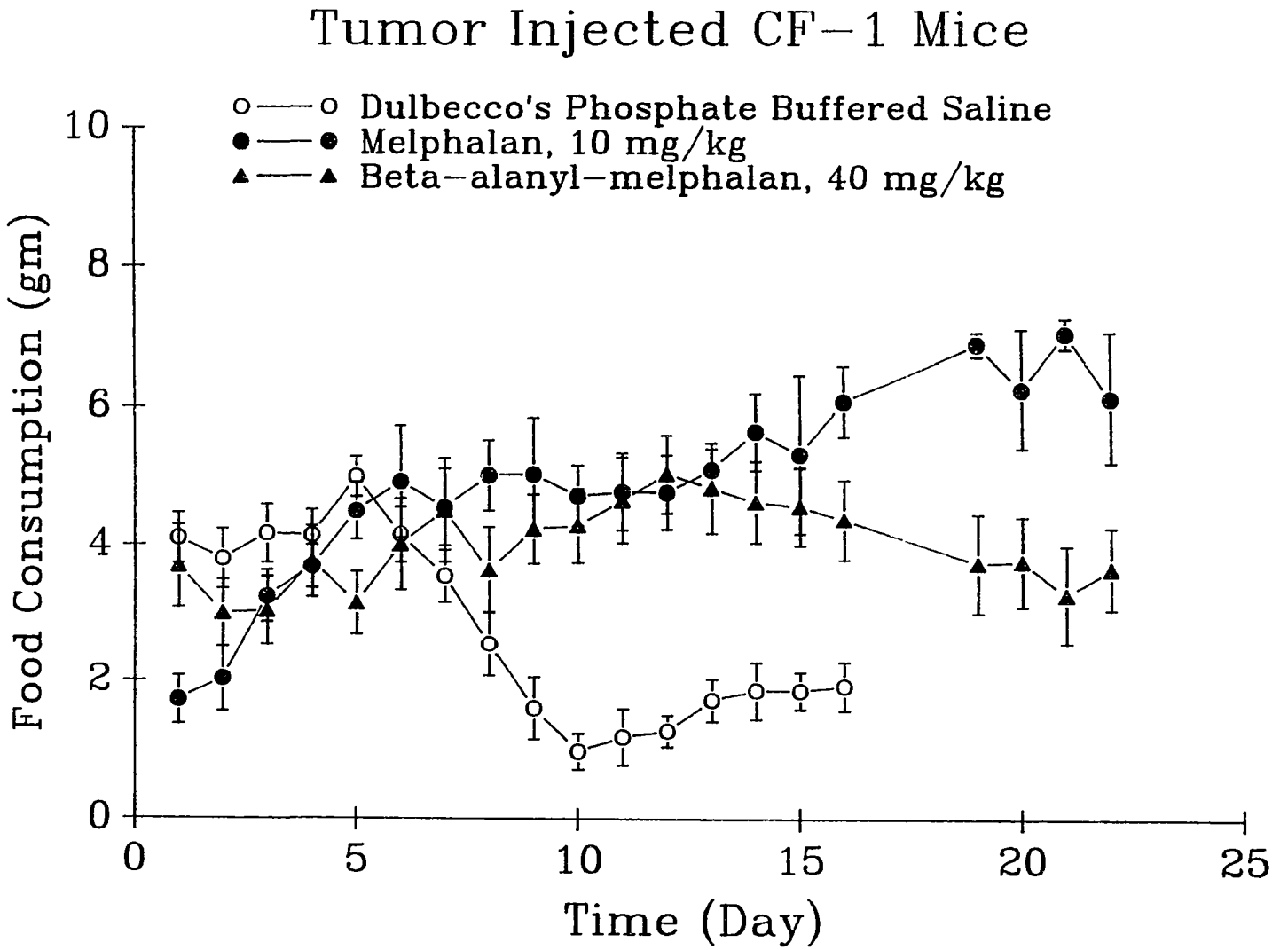

day 9 ($p < 0.001$, ANOVA).

Measurements of average daily food consumption in the noncancerous groups, i.e. injected with DPBS on day 0 followed by drug treatment on day 1 (Figure 63), revealed no significant differences between the DPBS treatment (3.60 ± 0.54 gm/day/mouse), melphalan treatment (4.63 ± 1.13 gm/day/mouse) and beta-alanyl-melphalan treatment (4.21 ± 1.15 gm/day/mouse) ($p > 0.1$, ANOVA).

The average survival times of the mice were recorded in all treatment groups and the average T/C ratio were calculated for each treatment group. The results presented in Table 11 represent 2 separate chemotherapeutic assays performed over 2 consecutive months with each test group containing five or more animals.

An average survival time of 13.4, 14.5, 18.0 days and an average T/C ratio of 103.6, 99.4, 108.1% were found for mice treated with concentrations of beta-alanine of 10, 20 and 50 mg/kg body weight, respectively. As expected, this amino acid did not significantly extend the survival time of cancerous mice (ANOVA, $p > 0.1$).

Treatments of 10 mg/kg, 25 mg/kg, and 50 mg/kg 1-aminoethyl phosphonic acid (1-AEPA) in tumor bearing mice resulted in mean survival times of 14.0, 12.8, 18.2 days, respectively and the corresponding percentage of T/C ratio was 106.6, 84.5 and 110.9% (Table 11). No dose-dependency was found and 1-AEPA

Figure 63. The effects of anticancer drugs on food consumption in noncancerous mice. Daily ad libatum food consumption during a 22-day study for dulbecco's phosphate buffered saline injected mice which received Dulbecco's phosphate buffered saline on day 0 and followed by Dulbecco's phosphate buffered saline (○-○), 10 mg/kg melphalan (•--•), or 40 mg/kg beta-alanyl-melphalan (▲-▲) injection on day 1. Food consumption was recorded daily and average food consumption (in grams) was calculated as Mean ± SD and plotted as a function of time.

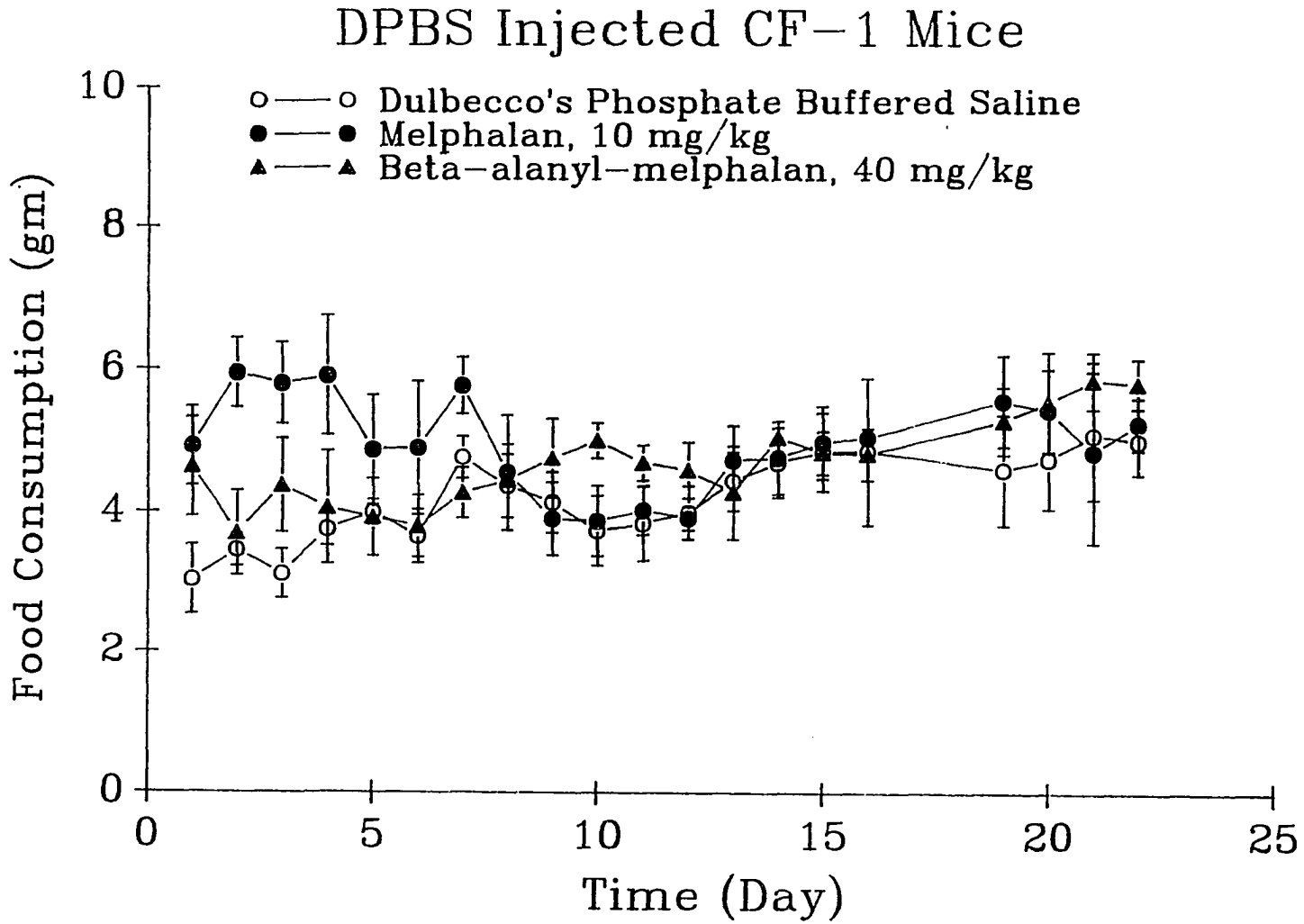

Table 11. Calculated T/C ratio from chemotherapy assays.

Treatment	Dosage (mg/kg)	Survival Time (day)	T/C ratio
control	0	14.5 ± 3.1	100.0
beta-alanine	10	13.4 ± 0.9	103.6 ± 2.8
beta-alanine	25	14.5 ± 3.7	99.4 ± 16.8
beta-alanine	50	18.0 ± 1.6	108.1 ± 8.9
1-AEPA	10	14.0 ± 1.6	106.6 ± 13.0
1-AEPA	25	12.8 ± 3.5	84.5 ± 7.6
1-AEPA	50	18.2 ± 1.7	110.9 ± 8.3
beta-alanyl-AEPA	10	15.0 ± 2.3	114.8 ± 19.2
beta-alanyl-AEPA	25	13.9 ± 1.2	94.6 ± 9.9
beta-alanyl-AEPA	50	15.3 ± 2.9	86.9 ± 9.2
beta-alanyl-L-alanine	25	14.2 ± 3.2	89.8 ± 6.1
melphalan	5*	26.7 ± 4.4	179.9 ± 6.2[b]
melphalan	10*	28.5 ± 2.6	193.9 ± 8.0[b]
beta-alanyl-melphalan	5	18.0 ± 2.0	125.8 ± 6.8[b]
beta-alanyl-melphalan	10	17.5 ± 1.6	125.5 ± 8.6[b]
beta-alanyl-melphalan	20*	21.6 ± 5.3	144.0 ± 21.0[b]
beta-alanyl-melphalan	30*	23.3 ± 4.8	139.6 ± 12.1[b]
beta-alanyl-melphalan	40*	22.5 ± 5.7	152.2 ± 16.2[b]

Mice were injected i.p. with one million cells and after 24 hours, injected i.p. with the drug indicated. Controls received equal volumes of buffer (Dulbecco's phosphate buffered saline). The time the mouse died was recorded as survival day. The survival day of the treatment group divided by the survival day of the control group times 100 gave the T/C ratio. A T/C ratio larger than 120 can be considered to indicate a potent anticancer drug.

AEPA: aminoethyl phosphonic acid.

* Some mice were still alive after 30 days and were declared "dead" for purposes of calculation of the T/C ratio.

a. Each treatment contained at least 5 mice per assay and each treatment was repeated 2-5 times and is expressed as Mean ± SD.

b. Significantly different from control; $p<0.001$ by ANOVA.

did not demonstrate activity against tumors.

Beta-alanyl-AEPA treatments (5 mg/kg, 25 mg/kg, and 50 mg/kg) resulted in mean survival times of 15.0, 13.9, 15.3 days and T/C ratios of 114.8, 94.6 and 86.9%, respectively. This dipeptide form of aminoethyl phosphonic acid demonstrated a negative correlation of concentration and survival time, i.e. the higher the concentration of beta-alanyl-AEPA, the lower T/C ratio was observed. The dipeptide beta-alanyl-alanine also did not significantly extend the survival time of cancerous mice (ANOVA, $p > 0.1$).

Equivalent treatment of cancerous mice with melphalan at 5 mg/kg (the lowest concentration tested) yielded an average survival time of 26.7 days and an average T/C ratio of 179.9% ± 6.2. Treatment with 10 mg melphalan/kg gave an average survival time of 28.5 days and an average T/C ratio of 193.9% ± 8.0. Values for T/C ratio larger than 120% indicate considerable anticancer activity. The survival time of the cancerous mice was significantly prolonged. As indicated in Table 11, the T/C ratios for melphalan treated mice were arbitrarily low, since cancerous mice treated with melphalan routinely survived beyond the 30-day "cut-off" time for termination of the assay. Mice surviving beyond 30 days were arbitrarily declared "dead" at day 30 in order that a T/C ratio could be calculated. Treatment of cancerous mice with beta-alanyl-melphalan concentrations of 5 mg/kg, 10 mg/kg, 20 mg/kg, 30 mg/kg, and 40 mg/kg gave average survival times of 18.0, 17.5, 21.6, 23.3, and 22.5 days and average T/C

ratios of 125.8% ± 6.8, 125.5% ± 8.6, 144.0% ± 21.0, 139.6% ± 12.1, and 152.2% ± 16.2, respectively. Although both the survival time and the T/C ratios appear to exhibit a general upward trend, only those values for the 5 mg/kg and 40 mg/kg concentrations of dipeptide are significantly different (ANOVA, $p < 0.001$). It is of interest that the three highest concentrations of dipeptide utilized were greater than the concentration of melphalan shown to be toxic to the mouse. No toxic reactions to the dipeptide were observed at any concentration tested by tumor-bearing mice or by mice having received a sham injection (Dulbecco's phosphate buffered saline followed by drug treatment).

DISCUSSION

The research described here came about as a result of research on the ability of the eukaryotic fungus *Neurospora crassa* to transport and utilize small peptides as sources of nitrogen. The presence of a transport mechanism in this microorganism for small tri- to pentapeptides had been suggested (Wolfinbarger and Marzluf, 1974), and it was demonstrated that *Neurospora crassa* was capable of growing on peptides as a sole source of leucine only so long as they were small enough to be transported by this peptide transport mechanism. In a later study (Wolfinbarger and Costellano, 1983), it was demonstrated that *Neurospora crassa* could grow on all sizes of peptideS provided it was forced to utilize the peptides as a sole source of nitrogen and leucine. Analysis of the culture media for peptidohydrolytic enzymes revealed the interesting observation that growth on the larger (nontransportable) peptides resulted from the production and secretion of extracellular peptidohydrolytic enzymes, and so long as these peptides were too large to be transported by the peptide transport system, the peptides served to "induce" the hydrolytic enzymes. Growth on a transportable peptide precluded induction and secretion of hydrolytic enzymes. In short, the ability of a peptide to act extracellularly in the induction of a physiological response by the

microorganism, i.e., hydrolytic enzyme production, depended on the ability/ inability of the cell to transport it.

As a logical extension to neoplastic cells, it had been reported that Ehrlich ascites tumor cells were capable of transporting small peptides (Christensen and Rafn, 1952). Indeed, only two additional types of cells, those lining the small intestine and the kidney proximal tubules (both noncancerous), have been reported as being capable of small peptide transport (Addison et al., 1973; Ganapathy and Leibach, 1983). Demonstration of a peptide transport mechanism in one type of mammalian cell is indicative of the genetic potential for peptide transport in all cells of that mammal and if it is not expressed it must be repressed by some undefined regulatory mechanism. Derepression of repressed genetic functions in cancer cells is not uncommon, and the assumption that noncancerous cells might routinely be incapable of small peptide transport, whereas transformation to the cancerous state might result in the derepression of this genetic capability, led to this study. Since small peptide hormones are accepted as normal regulators of cell function, and cancerous cells appear to be altered in their responses to peptide hormones, we reasoned that the ability of cancer cells to transport small peptides might preclude the ability of these peptides, present in the extracellular environment, to induce a physiological response -- a response similar to that observed for *Neurospora crassa.*

If this hypothesis is correct, it would mean that some neoplastic cells might be capable of small peptide transport, and thus small peptides would be an efficient means of targeting toxic amino acid analogues to these cells. It has been demonstrated that Ehrlich ascites tumor cells transport small peptides (Christensen and Rafn, 1952), and indicated that the incorporation of toxic amino acid analogues into small peptides might represent a unique approach in the design of a new group of anticancer drugs (Tsay and Wolfinbarger, 1987). The potential of small peptide mimetics as useful drug molecules lies largely in their ability to act in one of three ways, i.e. as a "carrier" with "targeting" functions, as a peptidase inhibitor, or as an antagonist/agonist of a natural peptide hormone or transmitter. The possibility of using peptides as carriers of cytotoxic agents has been extensively researched as a means of synthesizing more selective antitumor agents. Targeting a drug to specific cell types is possible with certain carrier functions, many of which are peptides (Firestone et al., 1982). These carrier molecules rely largely on their ability to release the active drug moiety at or inside the target cells due to the action of selective peptidases. Tumor cells produce many hydrolytic enzymes, some of which are in part selective for certain tumors, i.e. gamma-glutamyltransferase, plasminogen activator, cathepsin B (Weber et al., 1982; Honn et al., 1982) and thus should clearly be capable of releasing active drug moieties. Peptide derivatization of cytotoxic agents usually renders the drug molecule inactive, until it is in the vicinity of the tumor or inside the tumor cells. The carrier is then cleaved away to reveal the toxic compound. In certain cases peptide derivatization would also appear to enhance selective

active drug uptake and accumulation by the tumor cells (Firestone et al., 1982).

As mentioned earlier, neoplastic cells characteristically secrete large amounts of protein into their environment. Among these proteins, peptidohydrolytic enzymes constitute a potential for metastasis and destruction of noncancerous tissue. Komatsu et al. (1987) analyzed HeLa, KB, and K-44 carcinoma cell lines and observed that the dipeptidyl peptidase II activity was 6- to 24-fold higher in carcinoma cell lines than in human fibroblasts. Tsavaris et al. (1988) examined the enzyme activity of cancerous tissue and the adjacent normal epithelium of 40 patients with breast cancer. It was found that the absence of alkaline phosphatase and cytochrome oxidase and the presence of leucine aminopeptidase, beta-glucuronidase and dehydrogenase in the cancerous tissues was related to poor response to chemotherapy and therefore to poor patient survival. On the contrary, the presence of cytochrome oxidase and alkaline phosphatase and the absence of leucine aminopeptidase, beta-glucuronidase and dehydrogenase in cancerous tissues was related to good response of chemotherapy. Kojima et al. (1987) studied the changes of glycylproline dipeptidyl aminopeptidase and gamma-glutamyl transpeptidase activities, and their subcellular distributions, in human hepatic cancer. The activities of glycylproline dipeptidyl aminopeptidase in cancer tissues were significantly higher than these found in healthy livers. The activity of gamma-glutamyl transpeptidase activity was significantly increased not only in cancer tissues but also in liver tissues adjacent to the tumor.

The finding of cellular peptidase activity in these earlier studies, seems to strongly support the results obtained in this study of the peptidohydrolytic enzymes associated with mouse Ehrlich ascites tumor cells. The results presented in this present study of peptidohydrolytic enzymes confirmed the production and secretion of large numbers of peptidohydrolytic enzymes by mouse Ehrlich ascites tumor cells. A high level of peptidase activity was observed both in extracellular and intracellular extracts. Analysis of intracellular peptidohydrolytic enzyme activity demonstrated six major peptidases possessing different R_m values on gel electrophoresis. Of the 37 peptides tested, 18 were dipeptides and 19 were larger than a dipeptide i.e. tripeptides, tetrapeptides, etc. Of the 18 dipeptides, only 4 were resistant to hydrolysis by intracellular peptidohydrolytic enzymes. Peptides containing a beta-alanine at the amino terminal end of the peptide (such as beta-alanyl-glycine, beta-alanyl-alanine) were resistant to the hydrolysis and thus should make good substrates for study of peptide transport and cancer chemotherapy. Of all tripeptides tested only glycyl-L-leucyl-L-tyrosine was hydrolyzed by intracellular peptidohydrolytic enzymes. The remaining oligopeptides were shown to be resistant to hydrolysis.

Analysis of extracellular peptidohydrolytic enzyme activity in mouse Ehrlich ascites tumor cells revealed three major peptidase activities. A total of 29 peptides were tested against these peptidases. Eleven were dipeptides, 12 were tripeptides and 6 were larger than a tripeptide. Among the 11 dipeptides, only beta-alanyl-L-alanine and beta-alanyl-glycine were resistant to hydrolysis by the

extracellular peptidohydrolytic enzymes. These results confirmed that peptides containing beta-alanine at the amino terminal end of a peptide were resistant to hydrolysis, and suggested a design for anticancer drugs.

Results from the study of peptidohydrolytic enzymes associated with mouse Ehrlich ascites tumor cells were different from those of Payne (1973) who studied peptide utilization in *Escherichia coli* - with a specific focus on peptides containing beta-alanyl residues. Studies of the growth of *Escherichia coli* strain M-123 in differently supplemented media, revealed that beta-alanyl-glycyl-glycine was devoid of nutritional value for M-123. It was suggested that the peptide did not enter the organism or that it was resistant to hydrolysis. Electrophoresis of the products of peptidase action on tripeptides containing beta-alanine showed that beta-alanyl-glycyl-glycine was about 50 % hydrolyzed, and glycine, beta-alanine and uncleaved beta-alanyl-glycyl-glycine were detected. Peptidase-treated glycyl-glycyl-beta-alanine yielded glycine, glycyl-beta-alanine and uncleaved glycyl-glycyl-beta-alanine. No free beta-alanine was detected, indicating that *Escherichia coli* is unable to liberate C-terminal beta-alanyl residues, and that the enzymes may have requirements for a C-terminal alpha-carboxyl group. Demonstration of the release of free glycine from both glycyl-glycyl-beta-alanine, and beta-alanyl-glycyl-glycine makes it unlikely that the nutritional failure of beta-alanyl-glycyl-glycine is attributable to lack of peptidase action, and it appears more likely that the peptide was inadequately accumulated by *Escherichia coli.*

Studies in mammalian systems have revealed that peptides containing beta-alanine are not well hydrolyzed by mammalian proteolytic enzymes (Hansson and Smith, 1948). These researchers found that a carboxypeptidase from frozen beef pancreas hydrolyzed carbobenzoxyglycyl-L-phenylalanine about 800 times faster than carbobenzoxy-beta-alanyl-DL-phenylalanine. A partially purified preparation of prolidase from hog intestinal mucosa hydrolyzed glycyl-L-proline about 30 times more rapidly than beta-alanyl-L-proline and enzymes from human uterus hydrolyzed glycyl-L-leucine about 250 times more rapidly than beta-alanyl-L-leucine. Enzyme extracts from human uterus and rat muscle did not hydrolyze beta-alanyl-glycine or beta-alanyl-beta-alanine, and slowly hydrolyzed glycyl-beta-alanine. A fresh extract of rat muscle hydrolyzed triglycine very rapidly and glycyl-beta-alanyl-glycine and diglycyl-beta-alanine, but the hydrolysis of beta-alanyl-glycyl-glycine was slow. This research, in various mammalian systems, is consistent with the results obtained in this study of peptidohyrolytic enzyme activity from mouse Ehrlich ascites tumor cells. Both extracellular and intracellular extracts demonstrated high levels of peptidase activities. Although 5 peptidases were found in intracellular extracts and only 3 peptidases were found in extracellular extracts, none of the enzymes hydrolyzed beta-alanyl-L-alanine or beta-alanyl-glycine.

Information obtained from the peptidohydrolytic enzyme activity study lead to the decision to synthesize dipeptides containing beta-alanine at the amino terminal end and toxic amino acid analogues at the carboxy-terminal end.

Although most of the tripeptides or peptides larger than a tripeptide tested were resistant to hydrolysis, synthesis of dipeptides was chosen, primarily because dipeptides are easier to synthesize. The rational for synthesizing beta-alanyl-melphalan, as a model drug, was that of creating a substance which was simultaneously endowed with cytotoxic activity due to the alkylating group, resistant to hydrolysis, and which might be selectively accumulated by neoplastic cells. It has been suggested that the introduction of melphalan on a molecular carrier, i.e. a dipeptide, in addition to an alkylating effect, would give the drug antimetabolic properties (De Barbieri, 1972 and 1983; Yagi, 1984a and 1984b).

Melphalan has been an important alkylating agent for the treatment of various cancers including multiple myeloma and ovarian and breast carcinoma, since it was first synthesized (Bergel and Stock, 1954). Little information was available for approximately twenty years concerning its pharmacokinetic properties in human or animals, primarily because of its' rapid hydrolytic degradation, a reaction common to alkylating agents (Chirigos, 1964). In the last decade, accurate methods were developed for determining concentrations of melphalan (Sweeney, 1985) and these methods have been used in pharmacokinetic and drug stability studies (Bosanquet, 1985 and 1988). Melphalan has been found to be labile in solution, degrading via a cyclic aziridiny intermediate to monohydroxymelphalan and then to dihydroxymelphalan (Chang, 1978). Melphalan does not undergo active in vivo metabolism (Evans, 1982). The research described here was designed, therefore, to investigate the stability of

solutions of melphalan and beta-alanyl-melphalan under conditions that pertain to the in vitro toxicity assays and in vivo chemotherapy assays. It was anticipated that synthesis of the dipeptide containing a nitrogen mustard (melphalan) might result in a melphalan containing compound with greater specificity to cancer cells and improved stability. The solvent system utilized in this study did not resolve monohydroxy melphalan from dihydroxy melphalan, but this did not affect separation of breakdown products from the parent drug.

Results presented in this study revealed that melphalan , incubated in distilled water at 37° C, had a half-life of 105 minutes, a value which compared favorably with the half-life of melphalan determined by Bosanquet (1985). He reported that melphalan had a half-life of 2.70 hours at 37° C in normal saline. The results of the present study for the stability of melphalan at 0° C further supported the observation of Bosanquet (1985). He reported melphalan had a half-life of 271 hours at 5° C in normal saline and thus that low temperatures increased the stability of melphalan. Both of these studies are at variance with the results of Yang and Drewinko (1983) who found that 50% of drug activity was lost after storing melphalan at 4° C, -20° C, or -70° C for more than 2 weeks.

Results presented in the present study revealed that decomposition (breakdown) of melphalan must be considered as important in in vivo and in vitro assays of drug activity. The decreases in melphalan concentrations due to chemical decomposition were approximately 39%, 29%, and 34% in 10% bovine

serum albumin, 30% bovine serum albumin, and NCTC-135 medium with 10% fetal bovine serum after 2 hours incubation at 37° C. The corresponding hydrolysis rate constants were 0.31 umole/minute, 0.23 umole/minute, and 0.26 umole/minute. This rate of composition would suggest that during long-term incubation, i.e. 24 hours drug treatment studies, the majority of cell damage must occur early in the treatment period. It is interesting to note however that the absence of protein allows hydrolysis to take place more rapidly than in its' presence. The basis of this difference in decomposition has not been elucidated.

Our findings are consistent with the in vitro studies of Chang et al. (1978a; 1978b) who also demonstrated that bovine serum albumin or human plasma proteins retarded the hydrolysis rate of melphalan in vitro. No change in the plasma melphalan concentration was seen when melphalan was stored at -20° C for 3 weeks. However, when the same sample was removed from - 20° C and placed at 4° C for additional weeks, there was a 35% decrease in the plasma melphalan concentration (Chang et al., 1978a). The hydrolysis rate constants of melphalan in bovine serum albumin solutions were 0.46 umole/hour (8% bovine serum albumin), 0.36 umole/hour (13% bovine serum albumin) and 0.24 umole/hour (25% bovine serum albumin) (Chang et al., 1978b). It is suggested therefore, that melphalan is relatively temperature-sensitive in distilled water, losing 54% of its activity in 2 hours at 37° C and is very stable at 0° C. It is more stable in bovine serum albumin solutions and shows slightly increased stability at higher bovine serum albumin concentrations.

Incorporation of melphalan into a peptide could lengthen the half-life of the alkylating component by reducing intramolecular cyclization and subsequent carbonium ion formation of the 2-chloroethyl side chains involved in alkylation. In addition to a change in the stability of melphalan when incorporated into beta-alanyl-melphalan, the linkage of beta-alanine and melphalan could also alter the cellular uptake compared with melphalan. It has been reported that melphalan enters tumor cells via two leucine-preferring carrier transport systems (Goldenberg, et al., 1979), and exogenous amino acids in the transport medium effectively inhibit this carrier-dependent uptake, particularly in L1210 leukemia cells. Covalent attachment of beta-alanine to melphalan, to yield the dipeptide, alters the transport systems used for uptake.

Bifunctional alkylating agents, the first types of drugs to be used in chemotherapy of malignant disease, are still an important group of drugs in clinical cancer chemotherapy (Colvin,1982). Despite extensive clinical experience with these drugs, their mechanisms of action remain inadequately characterized. The cytotoxic effects of these drugs are generally considered to involve reactions with DNA resulting in various types of DNA damage. Besides monofunctional binding of the drug to a single site in the DNA molecule, drug-induced cross-linking between bases in the same DNA strand (DNA intrastrand cross-links), between complementary strands of the DNA molecule (DNA interstrand cross-links), and between DNA and protein (DNA-protein cross-links) occur (Colvin,

1980; Kohn,1979; Hemminki, 1984). Formation of DNA cross-links induced by melphalan have been described in several studies involving human tumor cells (Hansson, et al., 1987; Lewensohn, et al, 1987). A strong correlation has been obtained between the cytotoxicity of melphalan and the DNA interstrand cross links, indicating that the initial induction of DNA interstrand cross-links are important for the cytotoxic effects of bifunctional alkylating agents (i.e. melphalan) (Hansson, 1987). Although the reported mechanism for melphalan toxicity towards cells involves its reactivity towards guanine residues in DNA (Hansson, et al., 1987), the bifunctional alkylating group at the para-position on the aromatic side group of phenylalanine could be reactive towards proteins, i.e. through primary amine reactivity. The ability of melphalan to inhibit peptidohydrolytic enzymes confirmed that DNA cross linkage is not the only mechanism for melphalan toxicity and/or chemotherapeutic activity and future studies will be needed to asses the impact of this drug on tumor nutrition and metastasis.

The synthetic dipeptide beta-alanyl-melphalan is a new bifunctional alkylating agent of the nitrogen mustard group consisting of beta-alanine in the amino-terminal end with a bis-(2-chloroethyl) amino group in the para position of the benzene ring of the phenylalanine residue. Our in vitro toxicity studies demonstrated marked cytotoxic activity of this synthetic dipeptide against mouse Ehrlich ascites tumor cells, whereas no cytotoxic activity of beta-alanyl-melphalan was found towards mouse liver cells. Degrees of cytotoxicity induced by exposure

to beta-alanyl-melphalan varied with concentrations. Among the cell lines studied, mouse 3T3 embryonic cells were the most sensitive to beta-alanyl-melphalan. The cells least sensitive to beta-alanyl-melphalan were mouse liver cells. Mouse liver cells were the most sensitive to melphalan whereas the least sensitive to melphalan were mouse 3T3 embryonic cells. Therefore, we suggest that the mouse 3T3 embryonic cell line may not represent an appropriate control cell line for this kind of study. We suspect that the mouse 3T3 embryonic cells may be capable of small peptide transport, since they represent a "nondifferentiated" cell line (somewhat analogous to neoplastic cells).

Comparisons of mouse Ehrlich ascites tumor cell survival demonstrated that prolongation of melphalan treatment from 2 hours to 24 hours did significantly increase cellular cytolysis (33.50% versus 89.43%), in contrast, prolongation of beta-alanyl-melphalan treatment from 2 hours to 24 hours did not significantly increase cellular cytolysis (70.50% versus 81.38%). This observation suggested that tumor cells must be exposed to a minimum concentration of melphalan for a longer time in order to be irreversibly damaged. In contrast, tumor cells exposed to a minimum concentration of beta-alanyl-melphalan for only a short period time can be irreversibly damaged.

Comparisons of the cytotoxic effects of beta-alanyl-melphalan in mouse Ehrlich ascites tumor cells with those of the parental molecules, i.e. beta-alanine, and melphalan or other dipeptides beta-alanyl-L-alanine, beta-alanyl-AEPA

(which is a dipeptide with an antibacterial toxin aminoethyl phosphonic acid) revealed that only melphalan and beta-alanyl-melphalan behaved similarly and that the melphalan and beta-alanyl-melphalan both were significantly more cancerocidal than beta-alanine, 1-AEPA, beta-alanyl-AEPA, or beta-alanyl-L-alanine. The cytotoxic activity of beta-alanyl-melphalan was 3- to 3.5-fold greater than the cytotoxicities of equivalent concentrations of beta-alanine, 1-AEPA, beta-alanyl-AEPA and beta-alanyl-L-alanine. This increased cytotoxicity could be accounted for by a variety of mechanisms. It is possible that beta-alanyl-melphalan could exert antimetabolic activity and inhibit protein synthesis as was observed following treatment with the multipeptide complex, peptichemio (De Barieri, 1972).

The 2-hour beta-alanyl-melphalan treatment survival assay demonstrated that tumor cell viability declined significantly with time. This irreversible cytotoxicity of the dipeptide was probably attributable to the bis-(2-chloroethyl) amino component of the molecule which is involved in strongly electrophilic reactions. Alkylation of guanine residues is a primary reaction, and this results in DNA miscoding, excision of altered residues, and possible cross-linking of two nucleic acid chains or nucleic acids to proteins. As a consequence, toxicity is usually expressed at S and G_2 phases of the tumor cell cycle (Furner and Brown, 1980). It appeared that these cytotoxic effects of beta-alanyl-melphalan were not readily repaired by cellular mechanisms, since the viabilities of mouse Ehrlich ascites tumor cells continued to decrease throughout the observation period.

Comparisons of the cytotoxic effects of melphalan and beta-alanyl-melphalan in mouse Ehrlich ascites tumor cells revealed that the cytotoxic activity of melphalan was either similar to or greater than that of beta-alanyl-melphalan at all concentrations used against mouse Ehrlich ascites tumor cells in vitro. These results indicated that at equivalent doses in vivo, melphalan and beta-alanyl-melphalan should have similar antitumor activities. These results also indicated that beta-alanyl-melphalan was not readily hydrolyzed by available extracellular peptidohydrolases followed by transport of free melphalan into cells via amino acid transport systems. If mouse Ehrlich ascites tumor cells or mouse liver cells were able of hydrolyzing beta-alanyl-melphalan extracellularly, we would expect beta-alanyl-melphalan to be as toxic as melphalan to mouse Ehrlich ascites tumor cells and mouse liver cells. Although in general, beta-alanyl-melphalan did not appear to be a more effective agent than melphalan against mouse Ehrlich ascites tumor cells, the covalent linking of melphalan to beta-alanine permitted retention of the antitumor potential of melphalan.

Further comparisons of cytotoxic effects of melphalan and beta-alanyl-melphalan in mouse liver cells revealed that beta-alanyl-melphalan was not toxic to mouse liver cells at any of the concentrations tested whereas melphalan was toxic to mouse liver cells at all concentrations tested. It is suggested that all cell lines tested possess amino acid transport systems which are capable of transporting melphalan, hence similar sensitivities to melphalan. This assumption

is consistent with the research of Goldenberg et al. (1977; 1979), who reported that melphalan transport by L5178Y lymphoblasts was mediated by a carrier mechanism separate from that of other alkylating agents. They also reported that melphalan is actively transported by a mechanism that is mediated by two separate and distinct amino acid transport systems (the sodium dependent ASC-like system and the BCH-sensitive L system) in LPC-1 plasmacytoma (Goldenberg et al., 1979). The dipeptide (beta-alanyl-melphalan) however, was toxic to the mouse Ehrlich ascites tumor cells and nontoxic to the mouse liver cells. Since it has been demonstrated that beta-alanine containing dipeptides were not readily hydrolyzed by the tumor cells, it may be suggested that this differential sensitivity was attributable to different levels of transport.

When cancer cell populations are treated with anticancer agents (whether in vivo or in vitro), large changes may occur in the cell population. Many cells are killed by the treatment, while other cells are not affected at all, either because they are resistant or because of biochemical, cell cycle, or extracellular environmental "sanctuaries". As soon as these environmental conditions are reversed, the cells may express sensitivity again. Other cells, however, are sublethally damaged and, depending upon the accuracy and completeness of the recovery process, it may be assumed that the drug sensitivity of some of these surviving cells could be substantially different from the original population of cells.

Klaassen and Stacy (1982) attempted to characterize chemical-induced reversible and irreversible cell injury with rat hepatocytes, focusing on parameters that measure membrane integrity and metabolic performance. These parameters included intracellular content of glutathione (GSH), calcium ion, potassium ion, ATP, extent of lactate dehydrogenase (LDH) leakage, lipid peroxidation, trypan blue staining, and morphological alterations. The leakage of intracellular enzymes, such as LDH, and the uptake of trypan blue stain occur after cell death and thus suggest irreversible damage (Klaassen and Stacy, 1982). In contrast, alterations in the other parameters occur prior to cell death and indicate more subtle biochemical changes, which may be reversible (Klaassen and Stacy, 1982). Early reversible changes in cellular morphology usually include formation of blebs in the plasma membrane, mild cytoplasmic edema, dilation of the endoplasmic reticulum, slight mitochondria swelling, and marginal aggregation of nuclear chromatin (Jewell et al., 1982; Bridges et al., 1983). Irreversible morphological changes include extensive mitochondria swelling with cristae disruption, gross cytoplasmic swelling with dissolution of organelles, plasma membrane rupture, and nuclear dissolution (Bridges et al., 1983; Trump et al., 1981). Ultrastructural observations in the present study essentially confirmed the antitumor activity of melphalan and beta-alanyl-melphalan demonstrated in the biochemical assays. Results showed that the antitumor effects of melphalan affected the cellular elements causing marked cell damage both in mouse Ehrlich ascites tumor cells and mouse liver cells. In contrast, beta-alanyl-melphalan appeared to affect the cellular elements, with marked cell damage only, in mouse Ehrlich ascites tumor

cells, but not in the mouse liver cells. There were obvious nuclear and cytoplasmic alterations in melphalan and beta-alanyl-melphalan treated mouse Ehrlich ascites tumor cells, i.e. peripheral thickening of chromatin material in nuclei, severe mitochondrial alterations, ribosome accumulation and autolysis phenomena which lead to the destruction of the subcellular structures.

At this point it was considered whether melphalan and beta-alanyl-melphalan were endowed with double cell localizations, at nuclear and cytoplasmic levels, acting with different mechanisms. Alternatively the nuclear alteration, following DNA alkylation, may be considered the only mechanism of all alterations observed both at the nuclear and cytoplasmic level. It must be considered that the electron micrographs showed almost simultaneous lesions in the nucleus and in the cytoplasmic organelles. This observation might support the hypothesis of the double mechanism of action occurring simultaneously at the level of the nucleus (alkylation) and of the cytoplasm (inhibition of protein biosynthesis).

Events that lead to death of an animal, due to chemical exposure, are related to the loss of cellular functions. Although the damage may be expressed as the loss of specific organ function, what happens to cells in that organ to cause cell death is a very important aspect of in vivo toxicity. Thus, for cytotoxic events to be better understood, they need to be examined with both in vivo and in vitro models. Reversible injury can cause acute toxic effects, and such toxicity, whether at the intact animal, organ, or cellular level, is still poorly understood in terms of

how many cells can undergo reversible damage in vivo and allow animal survival after injury. Irreversible events leading to cell death involve a large number of cells prior to loss of organ function.

If one think of cells as being characterized by their ability to isolate themselves from their environment, then one can say that membrane compartmentation protects and enables the cell to maximize its survival. However, one does not know whether loss of membrane compartmentation is the most critical aspect of cell death due to acute toxicity. Portions of the scanning electron microscopic evaluation of melphalan and beta-alanyl-melphalan toxicity indicated an alteration in plasma membrane organization after melphalan treatment, i.e. a loss of membrane compartmentation.

Weight loss in cancer patients is of major concern because it often leads to the development of fatal cachexia (Costa, 1977). The average tumor burden in these patients is reported to be approximately 5% of total body weight (Waterhouse, 1987). In contrast, experimental malignant tumors often grow to approximate 30 to 40% of total body weight (Mider, 1948), and the effects on host weight and spontaneous food intake are not normally detected until the tumor constitutes about 5% of total body weight (Morrison, 1984). Our results confirmed those of both Mider and Morrison and revealed that the average body weight of cancerous mice increased by approximately 16% of original body weight at the seventh day after tumor cell injection and that the increased body weight

affected the water and food consumption, yielding an approximately 24% decrease in water consumption and a 17% decrease in food consumption. Morrison et al. (1984) examined mass loading effect independent of tumor growth using a subcutaneously implantable capsule that could be progressively filled with sterile saline, simulating tumor growth. Compared to the effects of a MCA-induced sarcoma, the implantable inert mass, although increasing the total body weight of the animal, contributed up to 30% of the observed decrease in host actual body weight and up to 20% of the observed decrease of spontaneous food intake at an average inflated capsule weight of 77 g. However, compared to controls during slow capsule inflation the deficit in weight gain was only 11% while depression in food intake was only 15% of that at maximum inflation (Morrison, 1984). The average body weight of noncancerous mice in the present study remained the same (31.59 gm) over the 30 day experiment period whereas the average total body weight of cancerous mice increased by approximately 100% of original body weight. Without the study of Morrison, it might have been assumed that the increased body weight was totally due to the tumor cell growth and ascites fluid production. According to Morrison (1984) however, our assumption might underestimate the tumor mass (subtracting the weight of the original weight of the cancerous mouse from the final weight of a cancerous mouse is not an accurate means of estimating cancer mass), and thus lead to an overestimation of the effects of the increased body weight on depression of the food and water consumption. Kawashima et al. (1988) investigated a carrageenan-induced benign tumor which influenced food intake and decrease

body weight in the rat, as is commonly observed with malignant tumors. Carrageenan-induced benign tumors reached masses of about 40 g, 21 days after injection. During this period, average daily food intake, carcass weight gain, serum albumin and liver weight were significantly lower in the study rats versus the control animals. Results presented in the present study revealed that average body weight increased 58%, 15 days after tumor injection and water consumption and food consumption were significantly decreased (by approximately 40% and 50%, respectively).

Many anticancer agents are characterized by a narrow therapeutic range, reflecting their failure to discriminate effectively between target and normal tissues. Based on the results from the cell culture toxicity assays, it indicated that the reduced toxicity of beta-alanyl-melphalan to the noncancerous cells was the result of reduced cellular accumulation of the bifunctional alkylating agent, melphalan. If this assumption is correct, beta-alanyl-melphalan should retain its' anticancer activity, yet exhibit reduced toxicity to the tumor bearing mice.

In in vivo chemotherapy assays, the antitumor activity of melphalan was either similar to or greater than that of beta-alanyl-melphalan at all concentrations used against mouse Ehrlich ascites tumor cells. Results presented in this study revealed that chemotherapeutic doses of melphalan, at all levels shown not to be lethal to the tumor bearing mice, were very effective in restricting development of the "tumor". Results were consistent with the known

anticancer activities of this drug (melphalan). Beta-alanyl-melphalan did not appear to be a more effective anticancer agent than melphalan, since at equivalent concentrations melphalan constantly demonstrated greater antitumor activities (both in vivo and in vitro). However, beta-alanyl-melphalan was demonstrated to possess significant anticancer activity at doses also shown not to be lethal to the tumor bearing mice. Therefore, beta-alanyl-melphalan appeared to possess similar or slightly less antitumor activity, as compared to melphalan, but was also less toxic towards to the animal. These observations were consistent with the observed reduced chemical reactivity, increased stability, and differential cellular toxicities of beta-alanyl-melphalan. That the phenomenon, was not due simply to the use of dipeptides, was confirmed by the absence of anticancer activity by beta-alanyl-L-leucine and beta-alanyl-aminoethyl phosphonic acid. The latter of which contained the antimetabolite aminoethyl phosphonic acid. We suggest that the reduction in hydrolyzability of beta-alanyl-melphalan explains the lower T/C ratios found for beta-alanyl-melphalan treated mice compared with melphalan treated mice. Our study of the sensitivity of mice to melphalan and beta-alanyl-melphalan have indicated that beta-alanyl-melphalan had a lower toxicity than melphalan. Beta-alanyl-melphalan had no observable toxic effects at concentration of 40 mg/kg in mice whereas, 15 mg/kg of melphalan has been reported as toxic to the animals (De Barieri and Dall'asta, 1983). These observations clearly supported the hypothesis that some neoplastic cells are capable of small peptide transport whereas non-neoplastic liver cells are not capable of transporting small peptides.

In summary, the synthetic dipeptide beta-alanyl-melphalan represents a new bifunctional alkylating agent in the nitrogen mustard group of anticancer drugs. This dipeptide consists of a beta-alanine residue in the L-configuration with a bis-(2-chloroethyl)amino group in the para-position of the benzene ring of the phenylalanine residue. The antitumor activity could be accounted for by a variety of mechanisms, i.e. DNA cross linking and enzyme inactivation. It is possible that beta-alanyl-melphalan could directly affect tumor cell growth as well as metastatic potential of the tumor.

Based on the results presented in this study, the following points appear reasonable:

1.) The inclusion of the amino acid residue beta-alanine in the N-terminal position reduces the susceptibility of the beta-alanyl-melphalan to hydrolysis by peptidohydrolytic enzymes and reduces chemical decomposition of melphalan. Both characteristics may serve to enhance the body half-life of this particular peptide.

2.) Melphalan and beta-alanyl-melphalan chemically react with enzymes, i.e. L-leucine aminopeptidase, and may thus possess cellular toxicity and reduce cancer metastasis by restricting activities of hydrolytic enzymes.

3.) Melphalan is toxic towards both neoplastic and non-neoplastic cells whereas, beta-alanyl-melphalan is toxic only towards neoplastic cells/or undifferentiated cells in culture. Beta-alanyl-melphalan is not toxic towards cultured mouse liver cells and possibly other non-neoplastic cells provided it is not administered orally -- where it may be toxic to the cells lining the small intestine. Toxicity towards the kidney may be possible regardless of the route of administration.

4.) The dipeptide, beta-alanyl-melphalan, exerts a differential toxicity towards the mouse Ehrlich ascites tumor cells, as compared to the mouse liver cells, and indicates a potential for different transport activities for the dipeptide.

5.) Melphalan and beta-alanyl-melphalan demonstrate nuclear and cytoplasmic alterations which lead to the destruction of the mouse Ehrlich ascites tumor cells.

6.) Melphalan is an effective anticancer drug when used in the chemotherapeutic treatment of mouse Ehrlich ascites tumors with a narrow range of safe dosage. Beta-alanyl-melphalan is also an effective anticancer drug and is less toxic than melphalan to the tumor bearing mice.

We conclude that the results of this study were significant in that small peptides containing antimetabolite served to identify a new and exciting approach

to the targeting of anticancer drugs towards neoplastic cells. The research needs to be expanded to include other tumors, solid as well as ascites, human versus animal, and tumors at different sites in the body, i.e. vascularized versus non-vascularized. In short, research utilizing small peptides containing antimetabolites needs to be expended into phase II and clinical trial studies.

REFERENCES

Addison, J. M., D. M. Matthews and D. Burston. Competition Between Carnosine and Other Peptides for Transport by Hamster Jejunum In Vitro. Clin. Sci. Mol. Biol. 46:707-704; 1974.

Adibi, S. A. and M. R. Soleimanpour. Functional Characterization of Dipeptide Transport System in Human Jejunum. J. Clin. Invest. 53:1368-1374; 1974.

Adibi, S. A. Metabolism of Branched-chain Amino Acids in Altered Nutrition. Metabolism 25:1287-1302; 1977.

Alpers, D. H. and B. Seetharam. Pathophysiology of Disease Involving Intestinal Brush-Border Proteins. N. Engl. J. Med. 296:1047-1050; 1977.

Ames, B. N., G. F. Ames, J. D. Young, D. Tsuchiya, and J. Lecocq. Illicit Transport: The Oligopeptide Permease. Proc. Nat. Acad. Sci USA 70:456-458; 1973.

Anson, M. L. The Purification of Cathepsin. J. General Physiol. 23:695-704; 1940.

Bergel, F. and J. Stock. Cyto-active Amino Acid and Peptide Derivatives: Substituted Phenylalanines. J. Chem. Soc. 2409-2416; 1954.

Berteloot, A., A. H. Khan, and K. Ramaswamy. Characteristics of Dipeptide Transport in Normal and Papain-Treated Brush Border Membrane Vesicles from Mouse Intestine. Biochim. Biophys. Acta 686:47-54; 1982.

Berteloot, A., A. H. Khan, and K. Ramaswamy. Characteristics of Dipeptide Transport in Normal and Papain-Treated Brush Border Membrane Vesicles from Mouse Intestine. Biochim. Biophys. Acta 649:179-188; 1981.

Bohem, J. C., W. D. Kingsbury, D. Perry, and C. Gilvarg. The Use of Cysteinyl Peptides to Effect Portage Transport of Sulfhydryl-containing Compounds in *Escherichia Coli*. J. Biol. Chem. 258(24):14850-14855; 1983.

Boisvert, W., K. S. Cheung, S. A. Lerner, and M. Johnston. Mechanisms of Action of Chloroalanyl Antibacterial Peptides. J. Biol. Chem. 261:7871-7878; 1986.

Bond, J. S., and R. J. Beynon. Mammalian Metalloendopeptidases. Int. J. Biochem. 17(5):565-574; 1985.

Bosanquet, A. G. and M. C. Bird. Degradation of Melphalan in Vitro: Rationale for the Use of Continuous Exposure in Chemosensitivity Assays. Cancer Chemother. Pharmacol. 21:211-215; 1988.

Bosanquet, A. G. Stability of Melphalan Solutions During Preparation and Storage. J. Pharmaceutical Sciences 74:348-351; 1985.

Bridges, J. W., D. J. Benford, and S. A. Hubbard. Mechanisms of Toxicity Injury. Ann. N. Y. Acad. Sci. 407:42-63; 1983.

Carone, F. A. and D. R. Peterson. Hydrolysis and Transport of Small Peptides by the Proximal Tubule. Amer. Physiol. Soc. F151-F158; 1980.

Chang, S. Y., D. S. Alberts, D. Farquhar, L. R. Melnick, P. D. Walson, and S. E. Salmon. Hydrolysis and Protein Binding of Melphalan. J. Pharmaceutical Sciences 67(5):682-684; 1978b.

Chang, S. Y., D. S. Alberts, L. R. Melnick, P. D. Walson, and S. E. Salmon. High-pressure Liquid Chromatographic Analysis of Melphalan in Plasma. J. Pharmaceutical Sciences 67(5):679-681; 1978a.

Chirigos, M. A., J. A. R. Mead. Experiments on Determination of Melphalan by Fluorescence. Interaction with Protein and Various Solutions. Anal.

Biochem. 7:259-268; 1964.

Christensen, N. H. and M. L. Rafn. Uptake of Peptides by a Free-cell Neoplasm. Cancer Res. 12:495-497.

Chu, T. G., and M. Orlowski. Soluble Metalloendopeptidase from Rat Brain: Action on Enkephalin-containing Peptides and other Bioactive Peptides. Endocrinology 116(4):1418-1425; 1985.

Colvin, M. The Alkylating Agents. In:Pharmacologic Principles of Cancer Treatment, (B. Chabner, ed.), pp276-308. Philadelphia: W. B. Saunders Co., 1982.

Costa, G. Cachexia, the Metabolic Component of Neoplastic Diseases. Cancer Res. 37:2327-2335; 1977.

Davie, E. W., K. Fujikawa, K. Kurachi, and W. Kisel. The Role of Serine Protease in the Blood Coagulation Cascade. Adv. Enzymol.48:227-318; 1979.

De Barbieri, A. G. Chiappino, R. Di Vittorio, A. Golferini, M. Maugeri, A. P. Mistretta, F. Perrone, G.C. Tassi, O. Temelcou and P. Zapelli. Peptichemio: A Synthesis of Pharmacological, Morphological, Biochemical

and Biomolecular Investigations. Proceedings of the Symposium on Peptichemio Milan 1-46; 1972.

De Barbieri, A., L. Dall'asta, A. Comini, V. Springolo, P. Mosconi, G. Coppi, and G. Bekesi. Synthesis, Acute Toxicity and Chemotherapeutic Anti-Cancer Activates of a New Tripeptidic Mustard. Il Farmaco-Ed. Sc. 4:205-218; 1983.

DiStefano, J.F. Plasma Membrane Proteases and Cancer Invasion: Role of Retroviral Oncogenes. Clin. Res. 33:451A; 1985.

Evans T. L., S. Y. Chang, D. S. Alberts, I. G. Sipes, K. Brendel. In Vitro Degradation of L-phenylalanine Mustard (L-PAM). Cancer Chemother. Pharmacol. 8(2):175-178;1982.

Firestone, R. A., J. M. Pisano, P. J. Bailey, A. Strum, R. J. Bonney, P. Wightman, R. Devlin, C. S. Lin, D. L. Keller, P. C. Tway. Lysosomotropic Agents, Carbobenzoxy Glycylphenylalanyl, A new Protease-sensitive Masking Group for Introduction into cells. J. Med. Chem. 25: 539-544; 1982.

Fisher, A. Mechanisms of the Proteolytic Activity of Malignant Tissue Cells. Nature 157:442; 1946.

Furner, R.L. and R.K. Brown. Phenylalanine Mustard (L-PAM): the First 25 Years. Cancer Treat. Rep. 64:559-573; 1980.

Ganapathy, V. and F. H. Leibach. Role of pH Gradient and Membrane Potential in Dipeptide Transport in Intestinal and Renal Brush-Border Membrane Vesicles from the Rabbit. J. Biol. Chem. 258:14189-14192; 1983.

Ganapathy, V., J. Mendicino, and F.H. Leibach. Evidence for a Dipeptide Transport System in Renal Brush Border Membranes from Rabbit. Biochim. Biophys. Acta 642:381-391; 1981b.

Ganapathy, V., J.F. Mendicino, and F.H. Leibach. Effect of Papain Treatment on Dipeptide Transport into Rabbit Intestinal Brush Border Vesicles. Life Sciences 29:2451-2457; 1981a.

Ganapathy, V., G. Burckhardt, and F.H. Leibach. Characteristics of Glycylsarcosine Transport in Rabbit Intestinal Brush-Border Membrane Vesicles. J. Biol. Chem. 259:8954-8959; 1984.

Ganapathy, V. and F. H. Leibach. Peptide Transport in Rabbit Kidney Studies with L-Carnosine. Biochim. Biophys. Acta 691:362-366; 1982b.

Ganapathy, V., J. Mendicino, D. H. Pashley, and F. H. Leibach. Carrier-Mediated Transport of Glycyl-L-Proline in Renal Brush Border Vesicles. Biochem. Biophys. Res. Commun. 97:1133-1139; 1980.

Ganapathy, V., M.E. Ganapathy, C.N. Nair, V.B. Mahesh, and F.H. Leibach. Evidence for an Organic Cation-Proton Antiport System in Brush-border Membranes Isolated from the Human Term Placenta. J. Biol. Chem. 263:4561-4568; 1988.

Ganapathy, V. and F.H. Leibach. Peptide Transport in Rabbit Kidney Studies with L-Carnosine. Biochim. Biophys. Acta 691:362-366; 1982a.

Goldenberg, G.J., H.B. Land, and D.V. Cormack. Mechanism of Cyclophosphamide Transport by L5178Y Lymphoblasts in vitro. Cancer Res. 34:3274-3282; 1974.

Goldenberg, G.J., H.P. Lam, and A. Begleiter. Active Carrier-mediated Transport of Melphalan by Two Separate Amino Acid Transport Systems in LPC-1 Plasmacytoma Cells in vitro. J. Biol. Chem. 254:1057-1064; 1979.

Goldenberg, G.J., C.L. Vanstone, and I. Bihler. Transport of Nitrogen Mustard on the Transport Carrier for Choline in L5178Y Lymphoblast. Science 172:1148-1149; 1971.

Goldenberg, G.J., C.L. Vanstone, L.G. Isreals, D. Ilse, and I. Bihler. Evidence for a Transport Carrier of Nitrogen Mustard in Nitrogen Mustard-Sensitive and -Resistant L5178Y Lymphoblasts. Cancer Res. 30:2285-2291; 1970.

Goldenberg, G.J., The Role of Drug Transport in Resistance to NItrogen Mustard and Other Alkylating Agents in L5178Y Lymphoblasts. Cancer Res. 35:1687-1692; 1975.

Goldenberg, G., M. Lee, H.P. Lam, and A. Begleiter. Evidence for Carrier-mediated Transport of Melphalan by 5178Y Lymphoblasts in vitro. Cancer Res. 37:755-760; 1977.

Hanson, H. T., and E. L. Smith. The Application of Peptides Containing beta-alanine to the Study of the Specificity of Various Peptidases. J. Biol. Chem. 75:833-848; 1948.

Hansson, J., R. Lewensohn, U. Ringborg, and B. Nilsson. Formation and Removal of DNA Cross-links Induced by Melphalan and Nitrogen Mustard in Relation to Drug-induced Cytotoxicity in Human Melanoma Cells. Cancer Res. 47:2631-2637; 1987.

Hansson, J., M. Edgren, H. Ehrsson, R. Lewensohn, and U. Ringborg. Melphalan-induced DNA Cross-linking in Human Melanoma Cells and Phytohaemagglutinin-stimulated Lymphocytes in Relation to Intracellular Drug Content and Cellular Levels of Glutathione. Anticancer Res. 7:97-104; 1987.

Heimburger, N. Proteinase Inhibitors of Human Plasma: Their Properties and Control Functions. In:Protease and Biological Control, (E. Reich, D.B. Rifkin, and E. Shaw, eds.), Cold Spring Harbor Laboratory: Cold Spring Harbor, New York, 367-386; 1975.

Hemminki, K., and D. B. Ludlum. Covalent Modification of DNA by Antineoplastic Agents. J. Natl. Cancer Res., 37:1021-1028; 1984.

Holmberg, B. On the In Vitro Release of Cutoplasmic Enzymes From Ascites Tumor Cells as Compared with Strain L Cells. Cancer Res. 21:1386-1393; 1961.

Jewell, S. A., G. Bellomo, H. Thor, and S. Orrenius. Bleb Formation in Hepatocytes During Drug Metabolism is Caused by Disturbances in Thiol and Calcium Ion Homeostasis. Science (Washington, D.C.) 217:1257-1259;1982.

Josefesson, L., H. Sjostrom, and O. Noren. Intracellular Hydrolysis of Peptides. In:Peptide Transport and Hydrolysis, New York: Elsevier, pp199-207; 1977.

Kao, R. T., and R. Stern. Collagenases in Human Breast Carcinoma Cell Lines. Cancer Res. 46(3):1349-1354; 1986.

Kawashima, Y., Campos, A. C. L., Meguid, M. M., Kurzer, M., Oler, A., Ability of a Benign Tumor to Decrease Spontaneous Food Intake and Body Weight in Rats. Cancer 63:693-699; 1989.

Keohane, M. E., S. W. Hall, S. R. Vandenberg, S. L. Gonias. Secretion of Alpha-2-macroglobulin, Alpha-2-antiplasmic and Plasminogen Activator Inhibitor-1 by Glioblastoma Multiform in Primary Organ Culture. J. Neurosurgery 73(2):234-241; 1990.

Keren, Z., S. J. LeGrue. Identification of Cell Surface Cathepsin B-like Activity on Murine Melanomas and Fibrosarcomas: Modulation by Butanol Extraction. Cancer Res. 48:1416-1421; 1988.

Kingsbury, W. D., J. C. Boehm, D. Perry, and C. Gilvarg. Portage of Various Compounds into Bacteria by Attachment to Glycine Residues in Peptides. Proc. Natl. Acad. Sci. USA 81:4573-4576; 1984.

Klaassen, C. D., and N. H. Stacy, Use of Isolated Hepatocytes in Toxicity Assessment. In:Toxicology of the Liver (G. Plaa and W.R. Hewitt, eds.), pp147-179. Raven Press, New York, 1982.

Kohn, K. W. DNA as a Target in Cancer Chemotherapy: Measurement of Macromolecular DNA Damage Produced in Mammalian CElls by Anticancer Agents and Carcinogens. In:Methods in Cancer Research (V. T. de Vita, Jr. and H. Busch, eds.), 16:291-345. New York:Academic Press, Inc., 1979.

Kojima, J., Y. Ueno, H. Kasugi, S. Okuda, H. Akedo. Glycylproline Dipeptidyl Aminopeptidase and Gamma-glutamyl Transpeptidase in Human Hepatic Cancer and Embryonal Tissues. Clin. Chem. Acta. 167(3):285-291; 1987.

Komatsu, M., M. Urade, M. Yamaoka, K. Fukasawa, and M. Harada. Alteration in Dipeptidyl Peptidase Activities in Cultured Human Carcinoma Cells. JNCL 78:863-868; 1987.

Larionov, L. F., A. S. Khokhlov, E. N. Shkodinskaia, O. S. Vasina, V. I. Troosheikina, M. A. Novikova. Studies on the Antitumor Activity of p-di-(2-chloroethyl)-amino-phenylalanine (Sarcolysin). Lancet 2:169; 1955.

Lewensohn, R., J. Hansson, U. Ringborg, and H. Ehrsson. Differential DNA Cross-linking and Cytotoxicity in PHA-stimulated Human Lymphocytes Exposed to Melphalan, m-L-sarcolysin and Peptichemio. Eur. J. Cancer Clin. Oncol. 23(6):783-788; 1987.

Liotta, L. A., U. P. Thorgeirsson, and S. Garbisa. Role of Collagenases in Tumor Cell Invasion. Cancer Metastasis Rev. 1:277-288; 1982.

Liotta, L. A., K. Tryggvason, S. Garbisa, I. R. Hart, C. M. Foltz, and S. Shafie. Metastatic Potential Correlates with Enzymatic Degradation of Basement Membrane Collagen. Nature 1980; 284:67-68.

Liotta, L. A., C. N. Rao and W. M. Wewer. Biochemical Interaction of Tumor Cells with the Basement Membrane. Ann. Rev. Biochem. 1986; 55:1037-1057.

Liotta, L. A. Tumor Invasion and Metastasis: Role of the Basement Membrane. Am. J. Pathol. 117:339-348; 1984.

Liotta, L. A., R. H. Goldfarb, R. Brundage, G. P. Siegal, V. Terranova and S. Garbisa. Effect of Plasminogen Activator (Urokinase), Plasmin, and Thrombin on Glycoprotein and Collagenous Components of Basement-Membrane. Cancer Res. 41(11):4629-4636; 1981.

Lowry, O. H., N. J. Rosebrough, A. L. Farr, R. T. Randall. Protein Measurement with the Folin Phenol Reagent. J. Biol. Chem. 193:265-275; 1951.

Maslow, D. E., Collagenase Effects on Cancer Cell Invasiveness and Motility. Invasion. Metastasis. 7(5):297-310; 1987.

Matthews, D. M. Intestinal Absorption of Peptides. Physiological Reviews 55:537-608; 1975.

Matthews, D. M., J. M. Addison and D. Burston. Evidence for Active Transport of the Dipeptide Carnosine (beta-alanyl-L-histidine) by Hamster Jejunum in Vitro. Clin. Sci. Mol. Biol. 46:693-705; 1974.

Mider, G. B., Tesluk, J., Morton, J. J., Effect of Walker Carcinoma 256 on Food Intake, Body Weight and Nitrogen Metabolism of Growing Rats. Acta Univ. Intern. Contra. Cancrum. 6:409-420; 1948.

Morrison S. D., Moley, J. F., Norton, J. A., Contribution of Inert Mass to Experimental Cancer Cachexia in Rats. J. Natl. Cancer Inst. 73:991-998; 1984.

Mort, J. S., M. Leduc and A. D. Recklies. A Latent Thiol Proteinase from Ascites Fluid of Patients with Neoplasia. Biochim. Biophys. Acta. 662:173-180; 1981.

Moscatelli, D., D. B. Rifkin, R. R. Isseroff, and E. A. Jaffe. Plasminogen Activator, Plasmin, and Collagenase Interactions. In:Proteinases and Tumor Invasion, (P. Strauli, A. J.Barrett, and A. Baici, eds.) New York: Raven Press, 143-152; 1980.

Nekeshima, K., H. Kataoka, and M. Koono. Enhanced Migration of Tumor Cells to Collagen Degradation Products and Tumor Cell Collagenolytic Activity. Invasion Metastasis 6:270-286; 1986.

Nyhan W. Effects of Nitrogen Mustards on the Incorporation of Amino Acids into the Proteins of Tissues of Tumor-Bearing Rats. I. Amino Acid Mustards and HN2. J. Pharm. Exp. Ther. 130:268-274; 1960.

Ohlssin, K. Collagenase and Elastase Released During Peritonitis are Complexed by Plasma Proteinase Inhibitors. Surgery 1976; 76:652-657; 1976.

Ottoson, R. and B. Sylven. Changes in the Dipeptidase and Acid Proteinase Activities in the Blood Plasma of Mice Carrying Ascites Tumors. Arch. Biochem. Biophys. 87:41-47; 1960.

Payne, J. W. and G. Bell. A Radioisotope Incorporation Method for Studying the Transport and Utilization of Peptides by *Escherichia coli.* FEMS Letters 1:91-94; 1977.

Payne, J. W. and T, M. Nisbet. Active Transport of Peptides in Bacteria. Biochem. Soc. Trans. 8:683-685; 1980.

Payne, J. W., Peptide Utilization in *Escherichia Coli*: Studies with Peptides Containing beta-alanyl Residues. Biochim. Biophys. Acta, 298:469-478; 1973.

Perry, D. and C. Gilvary. Metabolism of Alanylalanyl-S-[N-(2-thioethyl)] aminopyridine-2,6-dicarboxylic acid] cysteine by Suspensions of *Escherichia Coli.* J. Biol. Chem. 258(24):14856-14860; 1983.

Poole, A. R., K. J. Tiltman, A. D. Recklies and T. A. M. Stoker. Differences in the Secretion of the Proteinase Cathepsin B from the Invading Edge of Mammary Carcinomas and Fibroadenomas. Nature 273:545-547; 1978.

Puca, G. A., E. Nola, V. Sics and F. Bresciani. Estrogen Binding Proteins of Calf Uterus. Molecular and Functional Characterization of the Receptor Transforming Factor: A Ca^{++}-Activated Protease. J. Biol. Chem. 252:1358-

1366 1977.

Quigley, J. D., L. Ossowski, and E. Reich. Plasminogen the Serum Proenzyme Activated by Factors from Cells Transformed by Oncogenic Viruses. J. Biol. Chem. 249:4306-4312; 1974.

Rajendran, V. W., J. A. Barry, J. G. Kleinman, K. Ramaswamy. Proton Gradient-dependent Transport of Glycine in Rabbit Renal Brush-border Membrane Vesicles. J. Biol. Chem. 262(31):14974-14977; 1987.

Recklies, A. D., J. S. Mort and A. R. Poole. Secretion of a Thiol Proteinase from Mouse Mammary Carcinomas and its Characterization. Cancer Res. 42:1026-1032; 1982.

Reville, W. J., D. E. Golle, M. H. Stromer, R. M. Robson and W. R. Dayton. A Ca^{++}-Activated Protease Possibly Involved in Myofibrilla Protein Turnover. Subcellular Localization of the Protease in Porcine Skeletal Muscle. J. Cell Biol. 70:1-8; 1976.

Ringrose, P. S. Small Peptides as Carriers and Targets in Human Therapy. Biochem. Soc. Trans. 11:804-808; 1983.

Rosen-Leven, E. M., K. W. Smithson, and G. M. Gray. Complementary Role of Surface Hydrolysis and Intact Transport in the Intestinal Assimilation of Di- and Tripeptides. Biochim. Biophys. Acta 629:126-134; 1980.

Rozhin, J., D. Robinson, M. A. Stevens, T. T. Lah, K. V. Honn, R. E. Ryan, and B. F. Sloane. Properties of a Plasma Membrane-associated Cathepsin B-like Cysteine Proteinase in Metastatic B16 Melanoma Variants. Cancer Res. 47:6620-6628; 1987.

Santesson, L. Characteristics of Epithelial Mouse Tumor Cells in Vitro and Tumour Structures in Vivo. A Comparative Study. Acta. Pathol. Microbiol. Scand. Suppl. 24; 1935.

Schmidt, L. H., R. Fradkin, R. Sullivan, A. Flowers. Comparative Pharmacology of Alkylating Agents. Cancer Chemother. Rep. (Suppl 2): parts I-III; 1965.

Scriver, C. R., R. W. Chesney and R. R. McInnes. Genetic Aspects of Renal Tubular Transport: Diversity and Topology of Carriers. Kidney Int. 9:149-171; 1975.

Sheahan, K., S. Shuja, M. J. Murnane. Cysteine Protease Activities and Tumor Development in Human Colorectal Carcinoma. Cancer Res. 49:3809-3814; 1989.

Strauli, P. A Concept of Tumor Invasion. In Proteinases and Tumor Invasion, edited by P. Strauli, et al., Raven Press: New York, pp1-15; 1980.

Stewart, J. M., and J. D. Yong. Solid Phase Peptide Synthesis, second edition, Pierce Chemical Company, 1984.

Suzumiya, J., Y. Hasui, S. Kohaga, A. Sumiyoshi, S. Hashida, and E. Ishikawa. Comparative Study of Plasminogen Activator Antigens in Colonic Carcinomas and Adenomas. Int. J. Cancer 42:627-632; 1988.

Sweeney, D.J., N.H. Greig, and S.I. Rapoport. High-Performance Liquid Chromatograph Analysis of Melphalan in Plasma, Brain and Peripheral Tissue by *o*-phthalaldehyde Derivatization and Fluorescence Detection. J. Chromatogr. 339:434-439; 1985.

Sylven, B. and I. Bois-Svenssen. Protein Content and Enzymatic Assays of Interstial Fluid From Some Normal Tissue and Transplanted Mouse Tumors. Cancer Res. 20:831-836; 1960.

Sylven, B. Biochemical Factors Involved in the Cellular Detachment from Tumors. Schweiz. Med. Wochenschr. 104:258-261; 1974.

Takai, Y., M. Yamamoto, M. Inoue, A. Kishimoto, and Y. Nishizuka. A proenzyme of Cyclic Nucleotide-Independent Protein Kinase and its Activation by Calcium-Dependent Neutral Protease from Rat Liver. Biochem. Biophys. Res. Commun. 77:542-550; 1977.

Terranova, V. P. and R. N. Lyall. Chemotaxis of Human Gingival Epithelial Cells to Laminin. A Mechanism for Epithelial Cell Apical Migration. J. Periodot. 6:270-286; 1986.

Terranova, V. P., D. Maslow, and G. Markus. Directed Migration of Murine and Human Tumor Cells to Collagenases and Other Proteases. Cancer Res. 49:4835-4841; 1989.

Tiruppathi, C., V. Ganapathy, and F. H. Leibach. Evidence for Tripeptide-Proton Symport in Renal Brush Border Membrane Vesicles. J. Biol. Chem. 265:2048-2053; 1990.

Travis, J., J. Brown and R. Baugh. Human Alpha-1-Antichymotrypsin: Interaction with Chymotrypsin-like Proteases. Biochem. 17:5651-5656; 1978.

Trump, B. F. I., I. K. Berezesky, and A. R. Osorniavargas. Cell Death and the Disease Process. The Role of Calcium. In:Cell Death in Biology and

Pathology (I. D. Browen and R. A. Lockshin, eds.), pp209-242; 1981, Chapman and Hall, London/New york.

Tsavaris, N. B., P. A. Kosmidis, G. S. Delides, A. Delides, D. Papaioanou, E. Pavlakis, B. Lissaios, M. Zaharakis. Correlation of Histoenzymological Studies with the Response to Chemotherapy and Survival in Breast Cancer Patients. Cancer Lett. 42(3):225-230; 1988.

Tsay, B. L., and L. Wolfinbarger, Jr. Phase I study of Beta-alanyl-melphalan as a potent anticancer drug. Cancer Chemother. Pharmacol. 19:190-196; 1987.

Ugolev, A. M., N. M. Timofeeva, L. F. Smirnova, P. DeLavy, A. A. Gruzdkov, N. N. Iezuitova, N. M. Mityushova, G. M. Roschina, E.G. Gurman, V.M. Gurev, V.A. Tsuetkova, and G.G. Shcherbakov. Membrane and Intracellular Hydrolysis of Peptides: Differentiation, Role and Interrelations with Transport. In: Peptide Transport and Hydrolysis, New York: Elsevier, pp221-243; 1977.

Vistica, D. Cytotoxicity as an Indicator of Transport Mechanism: Evidence that Melphalan is Transported by Two Leucine-preferring Carrier Systems in the L1210 Murine Leukemia Cell. Biochim. Biophys. Acta. 550:309-317; 1979.

Vistica, D., J. Toal, and M. Rabinovitz. Characterization of Melphalan Transport and Correlation of Uptake with Cytotoxicity in Cultured L1210 Murine Leukemia Cells. Biochem. Pharmacol. 27:2865-2870; 1978.

von Figura, K., and A. Hasilik. Lysosomal Enzymes and their Receptors. Annu. Rev. Biochem. 55:167-193; 1986.

Watanable, Y., T. Kajima, and Y. Fujimoto. Deficiency of Membrane-bond Dipeptidyl Aminopeptidase IV in a certain Rat Strain. Experientia, 43(4):400-401; 1987.

Waterhouse, C., How Tumors Affect Host Metabolism. Ann. N.Y. Acad. Sci. 30:86-93; 1974.

Weber, M. J., P. K. Chakravarty, M. R. Bruesch, G. L. Johnson, J. A. Katzenellenbogen, and P. L. Carl. Ann. N. Y. Acad. Sci. 397:324-330; 1982.

Whitaker, J. N. and J. M. Seyer. The Sequential Limited Degradation of Bovine Myelin Basic Protein by Bovine Brain Cathepsin D. J. Bio. Chem. 254:6959-6963; 1979.

Wilson, D., J. A. Barry, and K. Ramaswamy. Characteristics of Tripeptide Transport in Human Jejunal Brush-border Membrane Vesicles. Biochim. Biophys. Acta 986:123-129; 1989.

Wolfinbarger, L. Jr. and G. A. Marzluf. Peptide Utilization by Amino Acid Auxotrophs of *Neurospora crassa*. J. Bacteriol. 119:371-378; 1974.

Wolfinbarger, L. Jr., F. Snyder, and J. Castellano. Peptide Utilization by Nitrogen-Starved *Neurospora crassa*. J. Bacteriol. 153:1567-1569; 1983.

Wolfinbarger, L. Jr. and G. A. Marzluf. Specificity and Regulation of Peptide Transport in *Neurospora crassa*. Arch. Biochem. Biophys. 171:637-644; 1975b.

Wolfinbarger, L. Jr. and G. A. Marzluf. Size Restriction on Utilization of Peptides by Amino Acid Auxotrophs of *Neurospora crassa*. J. Bacteriol. 122:949-956; 1975a.

Woolley, D. E., L. C. Tetlow, C. J. Mooney, and J. M. Evanson. Human Collagenase and its Extracellular Inhibitors in Relation to Tumor Invasiveness. In:Proteinases and Tumor Invasion, edited by P. Strauli et al., Raven Press, New York. pp97-115; 1980.

Yagi M.J., K.J. Scanlon, S.E. Chin, and J.G. Bekesi. Mammary Tumor and Melanoma Cell Transport of PTT.119, a Bis-(2-Cholorethyl)amino-L-Phenylalanine Derivative with Carrier Amino Acids. Chemotherapy 34:61-70; 1988a.

Yagi, M. J., J. G. Bekesi, M. D. Daniel, J. F. Holland, and A. De Barieri. Induced Cancerocidal Activity of PTT.119 a New Synthetic Bis-(-2-chloroethyl)amino-L-phenylalanine Derivative with Carrier Amino acids, I. In Vitro Cytotoxicity. Cancer Chemother. Pharmacol. 12:70-76; 1984a.

Yagi, M.J., K.J. Scanlon, S.E. Chin, J.F. Holland, J.G. Bekesi. Multiple Transport Pathways for L1210 Cells: Uptake of PTT.119, a Bifunctional Alkylator with Carrier Amino Acids. Chemotherapy 34:235-247; 1988b.

Yagi, M.J., M. Zanjani, J.F. Holland, and J.G. Bekesi. Increased Cancerocidal Activity of PTT.119; A New Synthetic Bis-(2-Chloroethyl)amino-L-Phenylalanine Derivative With Carrier Amino Acids II. In Vivo Bioassay. Cancer Chemother. Pharmacol. 12:77-82; 1984b.

Yang, L-Y., B. Drewinko. The stability of the Lethal Efficacy of Anti-Tumor Drugs. Proc. Am. Assoc. Cancer Res. 24:315; 1983.